

The role of phosphatidylinositol 3-kinases in autophagy regulation

Kelly Anne Devereaux

Submitted in partial fulfillment of the
requirements for the degree of
Doctor of Philosophy
under the Executive Committee
of the Graduate School of Arts and Sciences

COLUMBIA UNIVERSITY
2014

© 2014
Kelly Anne Devereaux
All rights reserved

Abstract

The role of phosphatidylinositol 3-kinases in autophagy regulation

Kelly Anne Devereaux

Autophagy requires the biogenesis of autophagosomes (APs), which are large multilamellar vesicles that sequester cytoplasmic substrates and undergo a maturation process that ultimately leads to their fusion with lysosomes. Previous studies have suggested that local production of phosphatidylinositol-3-phosphate (PI3P) by class III phosphatidylinositol 3-kinase (PI3K) (*i.e.*, Vps34) is required for AP biogenesis at specialized sites of the endoplasmic reticulum called "omegasomes". Although Vps34 is the sole source of PI3P in budding yeast, mammalian cells can produce PI3P through alternate pathways, including direct synthesis by the class II PI3Ks; however, the physiological relevance of these alternate pathways in the context of autophagy is unknown. To address this question, we generated Vps34 knock-out mouse embryonic fibroblasts (MEFs) and analyzed the impact of Vps34 deletion on autophagy in mammalian cells. Using a novel higher affinity 4x-FYVE finger PI3P-binding probe, we found a Vps34-independent pool of PI3P accounting for ~35% of the total amount of this lipid species by biochemical analysis. Importantly, WIPI-1, an autophagy-relevant PI3P probe, still formed some puncta upon starvation-induced autophagy in the Vps34 knock-out MEFs. Additional characterization of autophagy by electron microscopy as well as protein degradation assays showed that while Vps34 is important for starvation-induced autophagy there is a significant component of functional autophagy occurring in the absence of Vps34. Given these findings, class II PI3Ks (α and β isoforms) were examined

as potential positive regulators of autophagy. Depletion of class II PI3Ks reduced recruitment of WIPI-1 and LC3 to AP nucleation sites and caused an accumulation of the autophagy substrate, p62, which was exacerbated upon the concomitant ablation of Vps34. Our studies indicate that while Vps34 is the main PI3P source during autophagy, class II PI3Ks also significantly contribute to PI3P generation and regulate AP biogenesis.

In addition, we used a lipidomic approach to capture the lipid profile of cells in the presence and absence of Vps34 under steady-state and during starvation-induced autophagy. Lipidomics is an emerging powerful tool with the potential to identify new interconnected metabolic lipid networks as well as generate new hypotheses. Here, we identified a new relationship between Vps34 and cholesterol homeostasis. Additionally, we identified specific changes in lysolipids during autophagy.

Lastly, we investigated whether the retromer complex plays a role in autophagy. Retromer is a protein complex that binds PI3P on the endosomal membrane and mediates retrograde trafficking of transmembrane proteins from the endosome to the *trans*-Golgi network. Recent studies have shown a downregulation of this complex associated with sporadic Alzheimer's disease (AD) and have demonstrated aberrant trafficking and processing of APP, a pathological feature of AD, as a result of retromer deficiency. Because retromer is important for maintaining endo-lysosomal system function, we hypothesized that it promote efficient autophagy and may contribute to the dysfunctional autophagy observed in AD when impaired. Using standard autophagy assays, such as assessing LC3 conjugation and puncta formation, our preliminary studies suggest a negative regulatory role for retromer in autophagy. Additionally, we observed a strong

association of retromer with Atg9, an autophagy-related gene transmembrane protein that is believe to traffic lipids to the growing autophagosome membrane and recycle autophagy proteins from this compartment.

Table of Contents

List of Figures	v
List of Tables.....	vii
Abbreviations	viii
Chapter 1: Introduction	1
1.1 Autophagy in health and disease	1
1.1.1 Types of autophagy	2
1.1.2 Role of macroautophagy in cellular homeostasis.....	6
1.1.3 Autophagy dysfunction in disease	7
1.2 Autophagy process and machinery.....	9
1.2.1 Signaling and regulation of autophagy	10
1.2.2 Autophagosome biogenesis.....	13
1.2.2.1 <i>Origin of the AP membrane</i>	13
1.2.2.2 <i>Initiation step</i>	15
1.2.2.3 <i>Membrane elongation</i>	16
1.2.3.4 <i>Double-membrane vesicle closure</i>	19
1.2.3 Autophagosome maturation.....	20
1.2.4 Degradation of autophagosome cargo	22
1.2.5 Selective and nonselective autophagy	23
1.3 PI3P and autophagy.....	23
1.3.1 The role of PI3P and its effectors in autophagy	25
1.3.2 Sources of PI3P in autophagy	28
1.3.3 Regulation of PI3P levels during autophagy.....	29
1.4 Synthesis of PI3P by the class II and class III PI3K.....	30
1.4.1 Class III PI3K (Vps34)	31
1.4.1.1 Protein structure and catalytic activity of Vps34.....	32
1.4.1.2 Vps34 complexes	33
1.4.1.3 Vps34 and the endocytic pathway	35
1.4.1.4 Vps34 and mTOR signaling	37
1.4.1.5 Vps34 and autophagy	38
1.4.2 Class II PI3K (PI3KC2)	40

1.4.2.1 Protein structure and catalytic activity of PI3KC2	40
1.4.2.2 Isoform specific functions of the PI3KC2s	41
1.4.2.3 An emerging role for PI3KC2 in autophagy?.....	44
1.5 Objectives	45
Chapter 2: Regulation of mammalian autophagy by class II and III PI 3-kinases through PI3P synthesis.....	59
2.1 Results.....	59
2.1.1 Generation of <i>Vps34</i> knock-out MEFs.....	59
2.1.2 Characterization of <i>Vps34</i> KO MEFs and their autophagy machinery.	59
2.1.3 Steady-state and starvation-induced PI3P is detected in <i>Vps34</i> KO MEFs.....	61
2.1.4 Autophagosome formation is reduced, but not abolished in <i>Vps34</i> KO MEFs.....	63
2.1.5 <i>Vps34</i> mediates approximately half of autophagic protein degradation.	65
2.1.6 Class II PI3Ks contribute a pool of PI3P in MEFs.....	67
2.1.7 Class II PI3Ks positively regulate autophagy.	67
2.1.8 Initial characterization of the PI3K-C2 α and β in autophagy.....	69
2.2 Figures	72
2.3 Discussion.....	94
2.3.1 Mammalian <i>Vps34</i> and autophagy	95
2.3.2 An emerging role for class II and autophagy.....	96
2.3.3 PI3P sources in autophagy.....	100
2.3.4 Revisiting PI3K inhibitor specificity in the context of autophagy	101
2.3.5 Conclusion.....	102
2.4 Materials and Methods.....	102
2.4.1 Generation of <i>Vps34</i> KO MEFs.	102
2.4.2 Cell culture and transfection.....	103
2.4.3 Reagents and antibodies	104
2.4.4 Plasmids and RNAi.	106
2.4.5 SDS-PAGE and Western blotting.....	107
2.4.6 EGFR degradation assay.....	107
2.4.7 Immunofluorescence microscopy.....	108
2.4.8 Conventional electron microscopy and morphometric analysis.....	108
2.4.9 Immunoelectron microscopy.....	109
2.4.10 Intracellular protein turnover.	110

2.4.11 Quantification of phosphoinositide levels by HPLC analysis.....	111
2.3.12 Statistical analysis.....	111
Chapter 3: Lipidomic analysis of <i>Vps34</i> -deficient fibroblasts	112
3.1 Introduction.....	112
3.2 Results.....	117
3.2.1 Comparative lipid profiling of control and <i>Vps34</i> KO MEFs.....	117
3.2.2 <i>Vps34</i> ablation alters cholesterol homeostasis.....	119
3.2.3 Lipidomics of control and <i>Vps34</i> KO MEFs during starvation-induced autophagy.	120
3.3 Figures	121
3.4 Discussion.....	129
3.5 Materials and Methods.....	137
3.5.1 Generating <i>Vps34</i> KO MEFs.....	137
3.5.2 Annotation of Lipid Species	137
3.5.3 Analysis of Lipids Using High Performance Liquid Chromatography-Mass Spectrometry	137
3.5.4 Data Analysis and Presentation	138
Chapter 4: A novel role for retromer in autophagy.....	139
4.1 Introduction.....	139
4.2 Results.....	144
4.2.1 Knock-down of <i>Vps35</i> in HeLa and primary neurons enhances LC3 conjugation.	144
4.2.2 <i>Vps35</i> KO MEFs show an increase in basal and starvation-induced LC3 conjugation	146
4.2.3 <i>Vps35</i> minimally colocalizes with Atg16, a preautophagosomal marker, and LC3 during starvation-induced autophagy.....	147
4.2.4 <i>Vps35</i> strongly colocalizes with Atg9 during steady-state and starvation conditions.....	148
4.3 Figures	149
4.4 Discussion.....	155
4.5 Materials and Methods.....	162
4.5.1 Cell culture and transfection/infection.....	162
4.5.2 Generation of <i>Vps35</i> KO MEFs.....	163
4.5.3 shRNA and RNAi.....	163

4.5.4 Reagents and antibodies, SDS-PAGE and western blotting and immunofluorescence microscopy.....	164
Chapter 5: Concluding remarks and future directions.....	165
References	172

List of Figures

Figure 1.1 Cellular degradative processes	47
Figure 1.2 mTORC1 regulation of mammalian autophagy	48
Figure 1.3 Regulation of Atg1 complexes by TORC1.....	49
Figure 1.4 Schematic overview of the macroautophagy process	50
Figure 1.5 Schematic overview of autophagosome biogenesis	51
Figure 1.6 Atg12 and Atg8 ubiquitin-like conjugation systems in autophagy.....	52
Figure 1.7 Metabolism and distribution of phosphoinositides.....	53
Figure 1.8 Domain structure of mammalian phosphoinositide 3-kinases (PI3Ks).....	54
Figure 1.9 The major Vps34 complexes in yeast and mammals	55
Figure 2.1 Vps34 ablation in Vps34Flox/Flox MEFs infected with CRE lentivirus	72
Figure 2.2 Acute and chronic loss of Vps34 differentially affects the endo-lysosomal system	73
Figure 2.3 Ablation of Vps34 alters levels of Vps34 complex proteins	74
Figure 2.4 A higher affinity PI3P-binding probe, 4x-FYVEHrs, reveals a larger pool of intracellular PI3P in the absence of Vps34 compared to the conventional 2x-FYVEHrs probe.	75
Figure 2.5 Recruitment of WIPI-1, a PI3P-binding protein, to sites of AP biogenesis occurs in Vps34 KO MEFs but at diminished levels.....	76
Figure 2.6 Vps34 KO MEFs show a decrease in LC3 conjugation and LC3 puncta formation upon starvation	77
Figure 2.7 Lack of Vps34 decreases, but does not abolish the formation of autophagosomes and autophagolysosomes upon starvation	79
Figure 2.8 PI3K inhibitors 3-methyladenine and wortmannin block LC3-lipidation independently of Vps34.....	81
Figure 2.10 Prolonged ablation of Vps34 causes an increase in p62 levels.....	83
Figure 2.11 Silencing class II PI3Ks in control and Vps34 KO MEFs	84
Figure 2.12 Quantification of Vps34-dependent and independent sources of PI3P in MEFs	85
Figure 2.13 Silencing class II PI3Ks decreases autophagy in both control and Vps34 null MEFs.....	86
Figure 2.14 LC3 puncta formation during starvation-induced autophagy upon silencing class II PI3K in control and Vps34 KO MEFs	89
Figure 2.15 PI3K-C2 α and β only weakly interact with the Beclin-1 complex.....	90
Figure 2.16 Minimal co-localization was observed between PI3K-C2 α and β and various autophagy markers	92

Figure 2.17 PI3K-C2 α colocalizes with Atg9, a transmembrane marker of AP biogenesis, at the TGN under steady-state conditions and in the periphery during starvation-induced autophagy	93
Figure 3.1 Effects of acute and prolonged Vps34 ablation on lipid composition.....	122
Figure 3.2 Altered cholesterol homeostasis in <i>Vps34</i> KO MEFs.....	124
Figure 3.3 Effects of starvation-induced autophagy on lipid composition in control and <i>Vps34</i> KO MEFs	126
Figure 3.4 Comprehensive lipid profile of control and <i>Vps34</i> KO MEFs.....	127
Figure 4.1 The retromer complex.....	149
Figure 4.2 Vps35 ablation in HeLa cells and primary neurons causes an increase LC3 conjugation during basal and starvation-induced autophagy	150
Figure 4.3 <i>Vps35</i> KO MEFs show an increase in LC3 conjugation during basal and starvation-induced autophagy as well as larger LC3 puncta during starvation-induced autophagy	152
Figure 4.4 Vps35 minimally co-localizes with Atg16 and LC3 during starvation-induced autophagy	153
Figure 4.5 Vps35 strongly co-localizes with Atg9 under basal and starvation conditions..	154

List of Tables

Table 1.1 Glossary of PI3P autophagy effectors.	57
Table 1.2 Summary of autophagy findings in Vps34 conditional knock-out mouse models.....	58

Abbreviations

3-MA	3-methyladenine
A β	Amyloid β -peptide
ACAT	Acyl-CoA cholesterol acyltransferase
AD	Alzheimer's Disease
AMPK	AMP-activated protein kinase
AP	Autophagosome
APL	Autophagolysosomes
APP	Amyloid precursor protein
Atg	Autophagy-related gene
ATP	Adenosine triphosphate
Baf	Bafilomycin A1
BAR	Bin/Amphiphysin/Rvs-homology
CE	Cholesterol ester
CMA	Chaperone-mediated autophagy
CME	Clathrin mediated endocytosis
DFCP1	Double FYVE domain-containing protein 1
ESCRT	Endosomal Sorting Complexes Required for Transport
EGFR	Epidermal growth factor receptor
EM	Electron microscopy
ER	Endoplasmic reticulum
FC	Free cholesterol
FIP200	Focal adhesion kinase interacting protein of 200 kD
FYVE	Fab1, YOTB, Vac1 and EEA1
GABARAP	Gamma-aminobutyric acid receptor-associated protein
GFP	Green fluorescent protein
GWAS	Genome-wide association studies
HBSS	Hank's buffered salt solution
HeLa	Henrietta Lack's cervical cancer cell line
Hrs	Hepatocyte growth factor-regulated tyrosine kinase substrate
IF	Immunofluoresce

ILV	Intraluminal vesicle
IM	Isolation membrane
KO	Knock-out
LAL	Lysosomal acid lipases
LC3	MAP1 light chain 3
LDL	Low-density lipoprotein
LE	Late endosome
LOAD	Late-onset Alzheimer's Disease
LPE	Lysophosphatidylethanolamine
LPEp	Plasmalogens lysophosphatidylethanolamine
LY	Lysosome
M6PR	Mannose 6-phosphate receptor
MAM	Mitochondria-associated ER membrane
MEF	Mouse-embryonic fibroblasts
mTORC1	Mammalian target of rapamycin complex 1
MVB	Multivesicular body
NPC	Niemann Pick
PAS	Pre-autophagosomal structure or phagophore assembly site
PE	Phosphatidylethanolamine
PH	Pleckstrin homology
PI	Phosphatidylinositol
PI3K	Phosphatidylinositol 3- kinase
PI3KC2	Class II phosphatidylinositol 3- kinase
PI3P	Phosphatidylinositol 3-phosphate
PI(4,5)P2	Phosphatidylinositol 4,5-bisphosphate
PIKfyve	Phosphoinositide Kinase, FYVE Finger Containing
PKB	Protein kinase B
PX	Phox homology
siRNA	Short interfering RNA
shRNA	Short hairpin RNA
SNARE	Soluble N-ethylmaleimide-sensitive fusion attachment protein Receptor

SNX	Sorting nexin
TGN	Trans-Golgi Network
ULK	unc-51-like kinase (Atg1)
UPS	Ubiquitin proteasome system
UVRAG	Ultraviolet irradiation resistance-associated gene
Vps	Vacuolar protein sorting
WIPI	WD-repeat proteins interacting with phosphoinositides

Acknowledgements

First, I would like to thank my mentor Dr. Gilbert Di Paolo for the numerous opportunities he has given me for scientific growth during my graduate school training. He has always encouraged me to take on stimulating challenges and has continuously supported me as well as helped me to develop as an independent researcher. I appreciate his enthusiasm, passion and constant encouragement and value how he is always (yes always) available for insightful discussion and input.

I am also grateful for my amazing colleagues and friends in the Di Paolo lab. I would especially like to give great thanks Dr. Claudia Dall'Armi for her mentorship and support in life and in science over the years. She has been an incredible collaborator, teaching me in particular confocal microscopy and helping me take some of the pictures for my paper. She has also shared a tremendous amount of her autophagy and scientific knowledge. I would also like to thank Dr. Robin Chan and Bowen Zhou for their assistance with the lipidomic analysis and for educating me on lipids. Additionally, I would sincerely like to thank my other past and present lab members: Belle Chang, Tiago Oliveira, Dr. Samuel Frere, Dr. Akhil Bhalla, Kimberly Point Du Jour, Elizabeta Micevska, Jayson Bastien, Dr. Zofia Lasiecka, Dr. Sabrina Simoes, D.r. Catherine Marquer, Rebecca Williamson and Young Joo Yang for their energy, entertainment, collaboration and helpful scientific discussions. Lastly, I would like to acknowledge Bowen Zhou, Robin Chan and Rebecca Williamson for carefully reading chapters of this manuscript.

I would also like to thank the Columbia University Medical Scientist Training Program as well as Drs. Patrice Spitalnik, Ron Liem, and Michael Shelanski for all of

their support during my training. Additionally, I would like to thank the students in the M.D./Ph.D. and Graduate School Program for their input and discussions during student seminars and outside of school. I would like to acknowledge the coordinators of the Pathology Graduate School Program and M.D./Ph.D. program, Zaia Sivo and Jeffrey Brandt, for always keeping their students on track.

I am grateful to Drs. Fan Wang and Xiang Zhou for generating and generously sharing their mice used in this thesis work and to our collaborators Dr. Akitsugu Yamamoto and Yuta Ogasawara for providing us with the beautiful electron microscopy micrographs for our studies. I would also like to thank Drs. Pietro De Camilli and Abel Alcazar-Roman for enhancing the quality of this thesis work through their biochemical lipid studies and through ongoing discussion of the data. Lastly, I would also like to thank our collaborator Dr. Scott Small for generously sharing his mice for the retromer project studies and for Dr. Sabrina Simoes for providing us with the MEFs.

I would like to express my gratitude to my committee members, Drs. Richard Vallee, Liz Miller, and Ai Yamamoto, for their scientific discussions and intellectual contribution to this work. Also, I would like to thank the thesis committee members and Dr. Thomas Melia for participating in my thesis defense and reading this manuscript.

Lastly, I am indebted to my family and friends for their invaluable support and love. I must thank my mom for always encouraging me and being there for me. I would also like to thank Justin for his constant support and positive attitude each day (and for helping me format my thesis).

Chapter 1: Introduction

1.1 Autophagy in health and disease

All eukaryotic cells require constant surveillance and quality-control mechanisms in order to ensure that damaged proteins and organelles are eliminated. Additionally, efficient removal of excessive cellular components and the ability to synthesize new components in response to intra- and extracellular cues allows cells to continuously adapt and optimally function. Given the importance of degradative capacity in the health and viability of a cell, it is not surprising that multiple degradative pathways have evolved. While these pathways do provide some redundancy in function, it is clear they have also developed in specialized ways, which we are still only beginning to understand. The two most important modes of cellular degradation include the ubiquitin-proteasome and the lysosomal systems (Ciechanover, 2005; Goldberg, 2003). While the ubiquitin-proteasome system degrades proteins in a highly selective manner, the lysosomal system has a more diverse degradative capacity in its ability to degrade cytosolic and transmembrane proteins, organelles and foreign material by in-bulk, nonselective or selective mechanisms (Ciechanover, 2005; Yang and Klionsky, 2010). Greater understanding of such homeostatic, quality control processes is not only of basic science interest, but also of clinical interest since the misregulation of these pathways can cause various disease pathologies. In fact, identifying new therapeutic targets for degradation pathways is currently of high interest. This work focuses on better understanding the lysosomal form of degradation with a specific focus on the macroautophagy pathway.

1.1.1 Types of autophagy

The lysosome was originally believed to be an organelle dedicated to the degradation of products internalized by endocytosis or phagocytosis, however, first evidence that the lysosome was also responsible for degrading cytosolic content emerged over four decades ago. Two independent groups reported the presence of cytosolic content, specifically mitochondria and endoplasmic reticulum, within membrane-bound vesicles in rat kidney cells and hepatocytes (Ashford and Porter, 1962; Clark, 1957; Novikoff, 1959). Shortly after, it was discovered that these membrane bound vesicles also contained lysosomal hydrolases (Novikoff and Essner, 1962). In 1963, Christian de Duve, who previously discovered lysosomes, noted that the sequestering vesicles were related to lysosomes and coined this catabolic process "autophagy," meaning "self-eating." (De Duve and Wattiaux, 1966; Yang and Klionsky, 2010). Autophagy is broadly defined as a cellular degradative pathway that involves the delivery of cytoplasmic components to the lysosome (Deter et al., 1967; Klionsky, 2007; Mizushima, 2007). Once delivered to the lysosome, cytosolic components are digested by hydrolases and released back into the cytosol in the form of macromolecules for reuse by the cell (Klionsky, 2007; Mizushima, 2007; Singh and Cuervo, 2011; Yang and Klionsky, 2010). Future studies thereafter focused on understanding the mechanism by which the cytosolic content gets delivered to the lysosome. So far, three distinct modes of delivery have been observed and characterize the three types of autophagy: chaperone-mediated autophagy, microautophagy and macroautophagy (Fig. 1.1).

Chaperone-mediated autophagy (CMA) greatly differs from the other two forms of autophagy in both its method of cargo selection and lysosomal delivery. In

CMA, proteins containing a consensus motif (*e.g.*, KFERQ or sequences biochemically similar) are recognized by a specific CMA machinery, such as the heat shock-cognate chaperone of 70kDa (Hsc70) and lysosome-associated membrane protein type-2A (LAMP-2A) receptor, and are individually targeted to the lysosomal membrane where they are subsequently translocated into the lumen for degradation (Arias and Cuervo, 2011; Chiang et al., 1989; Dice, 1990; Kaushik and Cuervo, 2012). In CMA, protein degradation is regulated through the exposure of the targeting motif during protein misfolding, complex disassembly or post-translational modification (Kaushik and Cuervo, 2012; Lv et al., 2011; Thompson et al., 2009). The cytosolic chaperone protein, Hsc70, binds this motif, facilitates further protein unfolding and delivers the selected protein to the LAMP-2A receptor on the lysosomal membrane (Agarraberes and Dice, 2001; Arias and Cuervo, 2011; Chiang et al., 1989; Cuervo, 2010; Cuervo and Dice, 1996; Cuervo et al., 1995; Kaushik and Cuervo, 2012). At the lysosomal membrane, a subset of co-chaperones further assist in unfolding the substrate protein and LAMP-2A undergoes transient multimerization to form a pore through which the protein translocates (Agarraberes and Dice, 2001; Bandyopadhyay et al., 2008; Kaushik and Cuervo, 2012). Although CMA is, in part, similar to the ubiquitin-proteasome system in its ability to selectively degrade individual proteins, its regulation differs in that CMA degradation is determined by the accessibility of an intrinsic motif rather than the addition of a tag such as ubiquitin. Interestingly, it is a form of degradation that has so far only been observed in mammals, suggesting that this quality-control pathway has been adapted specifically for requirements of higher eukaryotes (Arias and Cuervo, 2011; Kaushik and Cuervo, 2012). Although CMA occurs constitutively, it becomes upregulated during prolonged

nutrient scarcity (Cuervo et al., 1995; Wing et al., 1991) and, particularly, in the presence of oxidative stress and denaturing conditions (Arias and Cuervo, 2011; Cuervo et al., 1999; Finn and Dice, 2005; Kaushik and Cuervo, 2012; Kiffin et al., 2004).

Microautophagy involves the direct delivery of cytoplasmic contents to the lysosome through the invagination of the limiting membrane of vacuoles (in plant and fungi) or lysosomes (in mammals) (Li et al., 2012; Mijaljica et al., 2011). In yeast, the vacuolar membrane undergoes inward tubular invaginations followed by scission at the tips to form luminal microautophagic vesicles, a process reminiscent of the biogenesis of multivesicular bodies (Li et al., 2012; Mijaljica et al., 2011). Microautophagy is capable of nonselective as well as the selective degradation of specific organelles, including mitochondria (micromitophagy), nucleus (piecemeal microautophagy) and peroxisomes (micropexophagy) (Li et al., 2012; Mijaljica et al., 2011). In mammals, the sequestration structure appears to have several forms, including arm-like projections around cytosolic content, lysosomal wrapping around the cytosol as well as intralysosomal vesicles (Li et al., 2012; Mijaljica et al., 2011). Microautophagy also appears to be both nonselective and selective in mammalian cells; however, only selectivity towards proteins has been observed so far (Mijaljica et al., 2011). Specifically, a microautophagy-like process named endosomal microautophagy was described which entailed the delivery of cytoplasmic cargo containing a KFERQ motif into intraluminal vesicles of late endosome/multivesicular bodies (MVBs) via a non-canonical ESCRT (Endosomal sorting complex required for transport)-pathway and its subsequent degradation in the lysosome (Ahlberg and Glaumann, 1985; Sahu et al., 2011). Like CMA, microautophagy is a constitutively active process that is upregulated during times of stress, such as

nutrient scarcity and oxidation (Li et al., 2012; Mijaljica et al., 2011). In addition, it has also been proposed that microautophagy plays a role in maintaining lysosome size and membrane homeostasis (Li et al., 2012). Microautophagy is by far the most understudied form of autophagy and much remains unknown about this process.

Macroautophagy, the best characterized autophagy pathway, requires the biogenesis of autophagosomes (APs), which are large double-membrane vesicles that sequester cytoplasmic substrates and ultimately fuse with the endolysosomal compartment, allowing for degradation of their cargo. Initially, macroautophagy was believed to be an in-bulk, non-specific degradative process; however, more recent studies have identified its role in selective degradation of specific proteins, organelles and foreign material, such as pathogens (Klionsky et al., 2007). The focus of this thesis work is to understand the regulation of macroautophagy, therefore, a more detailed overview of the role, regulation and mechanism of this key cellular process will be expanded upon in the sections below.

Although these three forms of autophagy coexist simultaneously in mammalian cells and all rely on lysosomal degradation, each has its own, distinct degradative role important for maintaining optimal cell function. In addition to better understanding the individual forms of autophagy, there is growing interest in understanding the signaling crosstalk between these different forms of autophagy. Recently, some studies have demonstrated bidirectional crosstalk and signaling between CMA and macroautophagy (Koga et al., 2011; Massey et al., 2006). For instance, when one pathway is impaired, the other may be upregulated to compensate (Koga et al., 2011; Massey et al., 2006). Less is known about the extent of compensation by microautophagy, however. Understanding

the mechanistic details that are shared or different among these pathways is key to developing novel ways to modulate cellular degradation in disease states.

1.1.2 Role of macroautophagy in cellular homeostasis

Macroautophagy, the “classical” form of autophagy (hereafter referred to as autophagy), is a homeostatic process that ensures cellular quality control through the efficient turnover of long-lived proteins and damaged organelles. Functional autophagy is essential for health and survival of all cells and plays a particularly critical role in maintaining the health of non-dividing cells, such as differentiated neurons and myocytes, which are unable to dilute any accumulated toxic structures by means of cell division and, therefore, largely rely on autophagic function (Mizushima et al., 2008; Singh and Cuervo, 2011; Yang and Klionsky, 2010). Under steady-state conditions, autophagy occurs at low, basal levels; however, it can be upregulated in response to cell stressors such as nutrient deprivation, free radicals, irradiation, accumulated misfolded proteins and microbial invasion (Mizushima and Komatsu, 2011; Mizushima et al., 2008; Rubinsztein et al., 2012b; Singh and Cuervo, 2011).

In addition to “housekeeping” and cleaning cellular waste, one of the major functions of autophagy is its contribution to energy homeostasis by helping maintain a balance between synthesis and turnover of cellular components. Bulk degradation of proteins and organelles by APs during autophagy enables rapid cellular adaptation in response to environmental changes (Levine and Kroemer, 2008; Mizushima et al., 2011; Singh and Cuervo, 2011). For instance, when energy deprivation and nutrient scarcity is sensed, autophagy is upregulated to promote the catabolism of proteins, organelles, membranes and, in some cases, lipid droplets, which provides metabolic substrates for

adenosine triphosphate (ATP) energy production and new protein synthesis almost immediately for the cell (Levine and Kroemer, 2008; Mizushima et al., 2011; Singh and Cuervo, 2011). Notably, autophagy not only plays a role in cellular survival, but also organismal survival through its ability to mobilize nutrients and energy during fasting periods (*e.g.*, in the early neonatal phase before breastfeeding is established) (Komatsu et al., 2005; Kuma et al., 2004; Singh and Cuervo, 2011).

1.1.3 Autophagy dysfunction in disease

The cytoprotective effects of autophagy are not only important for ensuring efficient cell functioning, but also in preventing a variety of disease states. Situations of insufficient as well as excessive levels of autophagy can be harmful for cells. For example, several neurodegenerative diseases, including Alzheimer's, Parkinson's and Huntington's disease, all exhibit toxic protein aggregates, a typical symptom of impaired autophagy (Levine and Kroemer, 2008; Mizushima et al., 2008; Mizushima et al., 2011; Yang and Klionsky, 2010). Insufficient autophagy and the build-up of toxic protein aggregates has also been linked to pathophysiologies in other, non-neuronal pathologies, including myopathies (*e.g.*, Danon disease, sporadic inclusion body myositis, limb girdle muscular dystrophy type B) and liver disease (*e.g.*, α 1-antitrypsin deficiency) (Levine and Kroemer, 2008; Mizushima et al., 2008; Mizushima et al., 2011; Yang and Klionsky, 2010). Lastly, it has been observed that cells defective in both autophagy and apoptosis are particularly susceptible to tumorigenesis. This finding can be explained by the fact that when there is decrease in the clearance of toxic proteins and organelles, DNA damage occurs and subsequent oncogene activation arises that can lead to uncontrolled growth and cause various cancers. On the contrary, enhanced autophagy can also promote

tumor survival in tumor microenvironments of high metabolic stress, such as hypoxia and nutrient deprivation (*e.g.*, in the core of the tumor) (Levine and Kroemer, 2008; Mizushima et al., 2008; Mizushima et al., 2011; Yang and Klionsky, 2010). Appropriate balance and regulation of autophagic activity is critical.

Interestingly, all aging cells display a progressive accumulation of damaged proteins and organelles, which correlates with a decline in macroautophagy and CMA function observed with age (Del Roso et al., 2003; Donati et al., 2001; Levine and Kroemer, 2008; Mizushima et al., 2011; Yang and Klionsky, 2010). Although the hierarchy of these hallmark features of aging cells remains unknown, they both certainly contribute to cellular dysfunction. In fact, caloric restriction, an inducer of autophagy, helps delay aging manifestations, likely through countering this stereotypical decline in autophagy and protein accumulation (Cavallini et al., 2008; Levine and Kroemer, 2008; Melendez et al., 2003; Mizushima et al., 2011; Yang and Klionsky, 2010).

Currently, there is growing interest in pharmacologically targeting the autophagy pathway to alleviate symptoms of impaired or misregulated cellular degradation pathways seen in aging and several diseases. For instance, stimulating autophagy in neurodegenerative diseases where there is a substantial accumulation of protein aggregates, such in as Huntington's disease, may not only improve symptoms, but overall disease outcome. Alternatively, inhibition of autophagy in cancers where autophagy promotes tumor growth under metabolic stress could be very beneficial. So far, most modulators of autophagy target this process through an indirect manner that also affects other pathways in the cell. For instance, lysosomal inhibitors (*e.g.*, chloroquine), which impair autophagic function, or mammalian target of rapamycin complex 1 (mTORC1)

pathway inhibitors (*e.g.*, rapamycin), which prevent growth signaling pathways and upregulate autophagy, are drugs commonly used in clinical trials to modulate autophagy (Harris and Rubinsztein, 2012; Rubinsztein et al., 2012a). In the future, it will be important to develop new autophagy-specific targeting strategies in order to more directly modulate this process.

1.2 Autophagy process and machinery

Although APs were initially discovered in mammalian cells by electron microscopy, it was not until 40 years later that significant progress was made in our molecular understanding of this process (Yang and Klionsky, 2010). In the late 1990's, Yoshinori Ohsumi's group showed that the morphology of APs in *S. cerevisiae* were similar to that in mammals and performed the first genetic screens for mutants defective in protein turnover (Takeshige et al., 1992; Tsukada and Ohsumi, 1993; Yang and Klionsky, 2010). In addition to the screens performed by Yoshinori's groups and others in the budding yeast *S. cerevisiae*, contemporaneous screens were also carried out in methylotrophic yeasts *Pichia pastoris* and *Hansenula polymorpha* for mutants defective in protein degradation, peroxisome degradation (pexophagy) and delivery of vacuolar hydrolases (the cytoplasm-to-vacuole targeting (Cvt) pathway) (Harding et al., 1996; Harding et al., 1995; Klionsky et al., 2003a; Sakai et al., 1998; Thumm et al., 1994; Titorenko et al., 1995). Atg1 was the first autophagy-related gene (Atg) identified, which was followed by the identification of over 30 Atgs (Klionsky et al., 2003a; Matsuura et al., 1997; Mizushima et al., 2011; Suzuki et al., 2007). Several, but not all, of the genes identified to be essential for macroautophagy are critical to the other degradative pathways as well (Harding et al., 1996; Klionsky et al., 2003a). Importantly however, most of the

autophagy genes identified in these screens possess a clear homolog in higher eukaryotes and several are well-defined orthologs (Mizushima et al., 2011). Among the Atg proteins identified, a core subset of proteins is required for AP formation and has been divided into four groups: 1) the Atg1-Atg13-Atg17 kinase complex; 2) the class III phosphatidylinositol 3-kinase (PI3K) complex, including Vps34, Vps15, Atg6/Vps30 and Atg14; 3) the Atg8 and Atg12 ubiquitin-like protein conjugation systems; and 4) the Atg9 transmembrane protein and its cycling system (Yang and Klionsky, 2010). Epistasis analysis in *S. cerevisiae* has demonstrated that the Atg proteins orchestrate AP biogenesis in a regulated, hierarchical manner that is largely conserved from yeast to mammals (Itakura and Mizushima, 2009; Suzuki et al., 2007; Yang and Klionsky, 2010).

1.2.1 Signaling and regulation of autophagy

Considering the diversity of autophagy inducers, the fact that there are multiple signaling pathways that regulate this process is expected. The best-characterized and most central pathway of autophagy regulation is the mammalian target of rapamycin complex 1 (mTORC1) pathway (Fig. 1.2). Apart from the classical mTORC1 pathway, several other mTOR-independent regulators of autophagy have been identified, including a cAMP-IP3 pathway, a Ca²⁺-calpain pathway, ceramide and other bioactive sphingolipids, reactive oxygen species as well as various apoptotic regulators (He and Klionsky, 2009; Ravikumar et al., 2010b); however, only regulation by mTORC1 will be discussed below.

mTORC1 is a nutrient and energy-sensing protein kinase that integrates multiple signaling inputs and promotes anabolic processes such as cell growth, cell-cycle progression and protein synthesis (Chen and Klionsky, 2011; Zoncu et al., 2011). Upon growth factor stimulation (*e.g.*, insulin), receptor tyrosine kinases undergo

autophosphorylation and activation and subsequently stimulate the PI3K-Akt/PKB (protein kinase B)-TOR pathway (also known as the Akt pathway) (Chen and Klionsky, 2011; Zoncu et al., 2011). Specifically, the class I PI3K phosphorylates PI(4,5)P₂ to PI(3,4,5)P₃ at the plasma membrane, which recruits both PKB (Akt) and its activator phosphoinositide-dependent kinase 1 (PDK1) (Chen and Klionsky, 2011; Zoncu et al., 2011). At the plasma membrane, PDK1 phosphorylates and activates PKB which, in turn, phosphorylates and inhibits the tuberous sclerosis complex 1/2 (TSC1-TSC2) (Chen and Klionsky, 2011; Inoki et al., 2002; Manning et al., 2002; Potter et al., 2002; Zoncu et al., 2011). During growth factor stimulation, the small GTPase Ras is also activated and stimulates both the PI3K-Akt/PKB-TOR and ERK pathways, which also phosphorylate and inhibit the TSC1-TSC2 complex (Ma et al., 2005; Zoncu et al., 2011). When active, the TSC1-2 complex acts as a GTPase-activating protein for Rheb (Ras homologue enriched in brain), a small GTP-binding protein that activates mTORC1 in its GTP-bound form (Chen and Klionsky, 2011; Garami et al., 2003; Huang and Manning, 2008; Inoki et al., 2003; Tee et al., 2003; Zhang et al., 2003a; Zoncu et al., 2011). Therefore, phosphorylation and inhibition of the TSC1/2 complex promotes Rheb-GTP binding and activation of mTORC1 (Chen and Klionsky, 2011; Garami et al., 2003; Huang and Manning, 2008; Inoki et al., 2003; Tee et al., 2003; Zhang et al., 2003a; Zoncu et al., 2011). Amino acids also play a critical role in mTORC1 activation, however, the mechanism by which amino acids are sensed and regulate mTORC1 is still under study (Zoncu et al., 2011). In the presence of amino acids, mTORC1 associates with an activated Rag (Ras-related GTPase) heterodimer and Raptor (regulatory-associate protein of mTOR) on the late endosome/lysosome membrane, increasing its proximity to Rheb

(Kim et al., 2008; Sancak et al., 2010; Sancak et al., 2008; Zoncu et al., 2011). Recent evidence indicates that relocalization of mTORC1 to the lysosome is indeed necessary for its regulation (Sancak et al., 2010; Saucedo et al., 2003; Stocker et al., 2003; Zoncu et al., 2011).

mTORC1 activation promotes cellular anabolism and restricts catabolic processes such as autophagy (Chen and Klionsky, 2011; Zoncu et al., 2011). Specifically, mTORC1 activates S6 kinase 1 (S6K1) and eIF4E-binding protein 1 (4E-BP1), which regulates translation initiation as well as translation rate to control protein synthesis (Ma and Blenis, 2009; Zoncu et al., 2011). mTORC1 also positively regulates synthesis of ribosomal RNAs and proteins through S6K1 (Mayer et al., 2004). Importantly, mTORC1 simultaneously inhibits autophagy by phosphorylating and inhibiting upstream autophagy activators like Atg13 in yeast or Atg13 and unc-51-like kinase (Ulk1/2, the mammalian homologue of Atg1) in mammals (Chen and Klionsky, 2011; Zoncu et al., 2011) (Fig. 3). However, autophagy is never either 'on' or 'off' (Musiwaro et al., 2013). Instead, a gradient activity level likely exists, ensuring that basal autophagy can still occur even during growth conditions. Although our current understanding of basal autophagy regulation is largely unknown, it was suggested that S6K1 downregulates growth factor receptor signaling to inactivate mTORC1 (Scott et al., 2004). In fact, this negative feedback loop may contribute to the basal level of autophagy observed under nutrient-rich conditions (Klionsky et al., 2005; Scott et al., 2004).

During nutrient scarcity and energy depletion, mTORC1 is inactivated to slow growth and stimulate 'recycling' programs such as autophagy (Chen and Klionsky, 2011; Zoncu et al., 2011). Specifically, mTORC1 is inactivated in response to situations of

growth factor withdrawal (PI3K-PKB-TOR pathway and Ras-ERK pathways), amino acid withdrawal and a decreased ATP/AMP ratio (AMPK pathway) (Chen and Klionsky, 2011; He and Klionsky, 2009; Zoncu et al., 2011). In yeast, TORC1 inactivation leads to dephosphorylation of Atg13, enabling it to form a complex with Atg1, Atg17, Atg31 and Atg29 to initiate autophagy (Fig. 1.3) (Kamada et al., 2000; Yang and Klionsky, 2010). In mammals, the autophagy initiation complex, which includes Ulk1/2, Atg13, FIP200 (focal adhesion kinase family interacting protein of 200 kD, also known as the mammalian homolog of Atg17) and Atg101, is constitutively stable and is regulated through mTORC1 binding and phosphorylation (Hara et al., 2008; Hosokawa et al., 2009a; Hosokawa et al., 2009b; Jung et al., 2009). During mTORC1 activation, mTORC1 associates with the autophagy initiation complex and phosphorylates Atg13 and Ulk1/2 to inhibit the complex. In contrast, mTORC1 inhibition causes its dissociation, leading to dephosphorylation of Atg13 and Ulk1/2 and complex activation (Chen and Klionsky, 2011; Hosokawa et al., 2009a; Jung et al., 2009; Zoncu et al., 2011). In both yeast and mammals, activated Atg1 complexes are targeted to pre-autophagosomal membranes to initiate autophagy (Chen and Klionsky, 2011; He and Klionsky, 2009).

1.2.2 Autophagosome biogenesis

1.2.2.1 Origin of the AP membrane

A key feature of autophagy is the biogenesis of large double membrane AP vesicles. Two models have been proposed to explain the source of AP membrane. The first model suggests that the membrane is formed by *de novo* lipid synthesis (Juhász and Neufeld, 2006; Kovacs et al., 2007), whereas the second, more popular model suggests that AP membrane is derived from pre-existing organelles. These two models, however, are not

mutually exclusive. Curiously, no organelle markers or transmembrane proteins have been observed on APs (Fengsrud et al., 2000; Stromhaug et al., 1998), suggesting that if AP membranes are, in fact, derived from other organelles, a significant amount of membrane reorganization and protein sorting and/or retrieval is required.

Although the source of membrane has yet to be defined, it is clear that the AP originates from different locations in yeast and higher eukaryotes. In yeast, all APs originate from a single site near the vacuole termed the preautophagosomal structure or the phagophore assembly site (PAS) (Suzuki et al., 2001). Specifically, Atg9-positive tubulo-vesicular structures derived from the secretory pathway are seen clustered near the vacuole and are believed to fuse to create the PAS and supply membrane to the growing APs (Mari et al., 2010; Rubinsztein et al., 2012b; Yamamoto et al., 2012). On the contrary, in mammals, there is no single site of AP formation. In fact, the origin of the AP membrane has been under intense debate in the field and evidence suggests that it is likely generated from multiple membrane sources, including the ER (Hayashi-Nishino et al., 2009; Yla-Anttila et al., 2009), mitochondria (Hailey et al., 2010), Golgi (Nishida et al., 2009), plasma membrane (Ravikumar et al., 2010a) and recycling endosome (Longatti et al., 2012). So far the ER is the most convincing and extensively studied site of AP formation, particularly during starvation-induced autophagy. Using live-cell microscopy and three-dimensional electron microscopy (EM) tomography, cup-shaped projections from the ER, termed omegasomes (for their Ω shape), have been observed (Axe et al., 2008; Hayashi-Nishino et al., 2009; Yla-Anttila et al., 2009). In fact, growing phagophores have been visualized by EM between juxtaposed ER membranes and in connection to the ER (Hayashi-Nishino et al., 2009; Ueno et al., 1991; Yla-Anttila et al.,

2009). More recently, AP biogenesis has been proposed to occur specifically at sites of contact between ER and mitochondria, or the mitochondria associated membrane (MAM) (Hamasaki et al., 2013). Additionally, there has been new evidence suggesting that Atg-positive (*e.g.*, Atg16 and Atg9) vesicles derived from the plasma membrane undergo heterotypic fusion and serve as AP precursors to promote AP biogenesis, a model reminiscent of the fusion between Atg9 vesicles to generate membrane for APs in yeast (Moreau et al., 2011; Puri et al., 2013).

Despite diversity in AP origin, AP formation universally requires: (i) an initiation step in which an isolation membrane (IM) cisterna begins to wrap around the cytoplasm; (ii) an elongation step during which the membrane increases in size; and (iii) a completion step in which the membrane fuses around a section of the cytoplasm to form a double membrane AP and its machinery is largely conserved between yeast and mammals (Fig. 1.4).

1.2.2.2 Initiation step

During autophagy stimulation, the activated Ulk1/2 (Atg1) autophagy complex relocates to the nucleation site on the IM (Fig. 1.5) (Weidberg et al., 2011). Following the recruitment of the Ulk1/2 (Atg1) complex, Atg14, a predominantly ER resident protein, clusters at the nucleation site and recruits the other members of the class III phosphatidylinositol 3-kinase (PI3K) complex (Vps34, Vps15, Beclin 1 (the mammalian homolog of Vps30/Atg6), and Atg14) (Sun et al., 2008; Zhong et al., 2009). Here, the class III PI3K, Vps34, plays a critical role in catalyzing the conversion of phosphatidylinositol to phosphatidylinositol 3-phosphate (PI3P) (Backer, 2008).

Localized production of the bioactive lipid, PI3P, is necessary for the recruitment of

several essential downstream effectors that orchestrate AP biogenesis (Dall'Armi et al., 2013; Knaevelsrud and Simonsen, 2012; Obara et al., 2006; Petiot et al., 2000; Sun et al., 2008). Historically, PI3P synthesis by Vps34 has been shown to be critical for regulating autophagy (Blommaert et al., 1997; Burman and Ktistakis, 2010; Dall'Armi et al., 2013; Itakura et al., 2008; Kihara et al., 2001b; Knaevelsrud and Simonsen, 2012; Matsunaga et al., 2010; Matsunaga et al., 2009; Noda et al., 2010; Obara et al., 2008a; Petiot et al., 2000; Zeng et al., 2006; Zhong et al., 2009); however, in this dissertation we sought to better understand the regulation of autophagy by PI3Ks and PI3P in mammalian autophagy. A more detailed discussion of PI3P and Vps34 will follow in the sections below.

1.2.2.3 Membrane elongation

After an IM is established, the membrane elongates around cytoplasmic content to form a functional AP. In yeast, the AP membrane undergoes expansion through the delivery of vesicles from the Atg9 compartment (Mari et al., 2010; Rubinsztein et al., 2012b; Yamamoto et al., 2012). In mammals, it appears that the membrane expansion largely occurs through continuous membrane input from organelle membranes of various origins, at least in the case of AP biosynthesis at the ER (Hayashi-Nishino et al., 2009; Yla-Anttila et al., 2009). Moreover, Atg9, the only transmembrane Atg protein, has been shown to constitutively cycle between the TGN and endosome during steady-state conditions and relocate to the recycling endosome (RE) during autophagy, where it has been proposed to shuttle membrane to the growing AP membrane via transient kiss-and-run fusion events (Orsi et al., 2012; Young et al., 2006; Zavodszky et al., 2013). As mentioned above, fusion of Atg16 and Atg9 positive vesicles derived from the plasma

membrane and trafficked to the recycling endosome may also be a way to provide membrane to the growing AP (Puri et al., 2013).

Both the Atg8 [the yeast homolog of microtubule-associated protein 1 light chain 3 in mammals (MAP1LC3, hereafter referred to as LC3)] and Atg12 ubiquitin-like conjugation systems have been shown to be particularly important for this elongation step (although one study suggested that AP-like structures can form independently of Atg ubiquitin-like conjugation in response to certain stimuli) (Fig. 1.6) (Geng and Klionsky, 2008; Ichimura et al., 2000; Mizushima et al., 1998; Nishida et al., 2009). During autophagy stimulation, Atg12 and Atg8 are activated by an E1-like enzyme (Atg7) and are conjugated by an E2-like enzyme (Atg10 and Atg3, respectively) to either Atg5 or phosphatidylethanolamine (PE), respectively (Geng and Klionsky, 2008; Mizushima et al., 1998; Ohsumi and Mizushima, 2004). Conjugated Atg5-12 is recruited to IM by Atg16 (the yeast homolog of Atg16L1 in mammals) to form an Atg5-12-16 complex (Mizushima et al., 2003), which subsequently recruits Atg8 and acts as an E3-like ubiquitin ligase facilitating the conjugation of Atg8 (LC3-I) to PE on the AP membrane (Fujita et al., 2008b; Geng and Klionsky, 2008; Hanada et al., 2007; Suzuki et al., 2007). The addition of the PE moiety to Atg8 (LC3-I) causes its conversion from a soluble Atg8 (LC3-I) form to a membrane bound Atg8-PE (LC3-II) form (Geng and Klionsky, 2008; Xie et al., 2008); however, recent work has shown that unlipidated LC3 can also be membrane-bound on the recycling endosome (Knaevelsrud et al., 2013). Both Atg8-PE (LC3-II) and the Atg5-Atg12-Atg16 complex localize to the expanding membrane until AP completion (Geng and Klionsky, 2008; Mizushima et al., 2001; Mizushima et al., 2003). Studies have demonstrated that members of the conjugation system are

particularly important for the expansion step (Mizushima et al., 2001; Sou et al., 2008; Xie and Klionsky, 2007). Yeast lacking Atg8 produce smaller APs (Abeliovich et al., 2000; Kirisako et al., 1999), whereas mammals lacking LC3 produce APs of inconsistent sizes (Weidberg et al., 2010). In fact, levels of Atg8 have been shown to be upregulated during autophagy stimulation in yeast (Huang et al., 2000; Nakatogawa et al., 2007).

In mammals, several homologues of yeast Atg8 have been identified, including LC3 (LC3A, LC3B, LC3B2, LC3C), Golgi-associated ATPase enhancer of 16kDa (GATE-16) and γ -amin-butyric acid receptor-associated protein (GABARAP, GABARAPL1) (Shpilka et al., 2011; Weidberg et al., 2011). Although GABARAP and GATE-16 were initially discovered for their roles in non-autophagy-related trafficking and SNARE-mediated fusion, each of these Atg8-related proteins undergo the same ubiquitin-like conjugation reaction described above and are found within APs during autophagy (Shpilka et al., 2011; Weidberg et al., 2011). A recent study has shown that the various Atg8 proteins may have specific functions in the autophagy process (Weidberg et al., 2010). For instance, LC3 may promote membrane elongation, whereas GABARAP/GATE-16 may act at the more downstream steps of AP closure and Atg5-Atg12-Atg16 complex (Weidberg et al., 2010). However, additional experiments will be required to understand why multiple Atg8 proteins have evolved in higher eukaryotes and their role(s) in autophagy.

In addition to membrane expansion, the growing AP must undergo a certain degree of curvature prior to its closure. It has been proposed that asymmetric distribution of lipids and proteins may induce membrane curvature; however, proteins with specialized, curvature inducing and stabilizing domains may also be required (Longatti

and Tooze, 2009). So far, BIF-1 (also known as endophilin B1) is a promising candidate given it contains a curvature sensing and driving N-BAR domain that has been shown to be required for AP formation (Reggiori and Klionsky, 2005; Takahashi et al., 2007). Additionally, mammalian Atg14L/Barkor, contains a Barkor/Atg14(L) AP targeting sequence (BATS)

domain that preferentially binds curved membranes containing PI3P; however, whether this domain promotes curvature has not been tested yet (Fan et al., 2011). Future studies are required to better elucidate how both AP curvature and, consequently, its size are established.

1.2.3.4 Double-membrane vesicle closure

Once the growing AP membrane has formed a cup-like structure, its ends must seal to form a double membrane vesicle. Since depletion of Atg8 homologues or blocking its lipidation results in “open” APs, it has been hypothesized that Atg8-PE/LC3-II promotes AP closure (Fujita et al., 2008a; Weidberg et al., 2010). Moreover, *in vitro* biochemical analysis has demonstrated that Atg8-PE/LC3-II can homo-oligomerize *in trans* on membranes, suggesting that Atg8 may play a tethering role between two membranes (Nakatogawa et al., 2007). Although Atg8/LC3 may serve as a tether factor, the mechanism of membrane fission still remains unknown. One study proposed a fusogenic role for Atg8 (Nakatogawa et al., 2007); however, another group demonstrated that this finding is largely attributable to the artificial lipid composition of the liposomes used (*i.e.*, high PE concentration) rather than the fusogenic capacity of Atg8/LC3 (Nair et al., 2011). A couple of hypotheses have been proposed to explain AP closure: 1) the lipid composition at the tips of the AP is energetically unstable, such that mere tethering by

Atg8 or another means promotes lipid mixing and fusion; or 2) fusogens [*e.g.*, SNAREs (soluble N-ethylmaleimide-sensitive factor-attachment protein receptor)] are recruited to the site of fusion either by Atg8 or by another means to promote fusion (Jotwani et al., 2012). In fact, several SNAREs were recently identified to be important for AP biogenesis, specifically in promoting homotypic fusion events between vesicles and membrane elongation during AP biogenesis in both yeast (*e.g.*, Sso2p, Tlg2, Sec9p, Sec22p, Ykt6p) (Nair et al., 2011) and mammals (*e.g.*, VAMP7, syntaxin-7, syntaxin-8, VTI1B) (Moreau et al., 2011); however, it has yet to be determined whether SNAREs are important for AP closure as well. Nevertheless, upon AP vesicle closure, the Atg5-Atg12-Atg16 complex dissociates from the vesicle and Atg4 proteolytically releases the Atg8-PE/LC3-II present on the external surface (Mizushima et al., 2001; Mizushima et al., 2003). Notably, some Atg8-PE/LC3-II still remains on the inner surface of the AP and is degraded only upon fusion of the AP with the lysosome, making it a reliable marker for APs (Geng and Klionsky, 2008; Jotwani et al., 2012; Kirisako et al., 1999; Tanida et al., 2008).

1.2.3 Autophagosome maturation

While APs are able to fuse directly with the vacuole in yeast, higher eukaryote APs require a maturation step prior to fusing with the lysosome (Eskelinen, 2005). During maturation, APs fuse with the endosomal system, including early endosomes, MVBs, and late endosomes, to become amphisomes (Fengsrud et al., 1995; Liou et al., 1997; Simonsen and Tooze, 2009; Tooze et al., 1990) (Figure 4). It has been hypothesized that fusion with these endocytic compartments allows APs to acquire machinery required for lysosomal fusion, such as fusogenic factors and proton pumps (Berg et al., 1998; Gordon

and Seglen, 1988; Kovacs et al., 1982; Simonsen and Tooze, 2009; Tooze et al., 1990; Yamamoto et al., 1998). Perturbation of endosome function, such as disruption of the ESCRT (endosomal sorting complex required for transport) pathway responsible for MVB formation, results in a massive accumulation of nascent APs that are unable to fuse with the endo-lysosomal system (Lee et al., 2007; Nara et al., 2002; Simonsen and Tooze, 2009)

Much of our understanding of AP fusion along the endo-lysosomal system is derived largely from other cellular membrane trafficking events, which rely on Rab GTPases, membrane-tethering complexes and SNAREs (soluble N-ethylmaleimide-sensitive factor (NSF)-attachment protein receptor) to mediate fusion. In both yeast and mammals, the small GTPase Rab7 (the yeast homolog of Ypt7) has been implicated in coordinating fusion of the AP with the vacuole or endo-lysosomal system, respectively (Jager et al., 2004; Mayer and Wickner, 1997). For instance, lipid synthesis of PI3P along the endosomal system is important for the activation of Rab7 and the recruitment of tethering complexes such as C-VPS/HOPS complex that mediate AP-endosomal fusion (Liang et al., 2008b). Since yeast APs do not undergo a maturation step, the SNARE proteins implicated in AP-vacuole fusion, include Vam3 (Darsow et al., 1997), the SNAP-25 homologue Vam7 (Sato et al., 1998), and the yeast orthologue of the NSF protein, Sec18 (Ishihara et al., 2001). Likewise, in mammals, SNARE proteins mediate AP-lysosome fusion and include SNAP-29, VAMP7, VAMP8 and VTI1B (Fader et al., 2009; Furuta et al., 2010). Recently, mammalian syntaxin 17 was the first SNARE protein identified that localizes to the AP membrane and mediates AP-lysosomal fusion through its interaction with lysosomal SNAREs (Itakura et al., 2012b).

In mammals, APs are formed at peripheral sites and require transportation to reach both the endosomal and lysosomal compartments, located in the perinuclear region near the microtubule-organizing center (MTOC) (Jahreiss et al., 2008; Monastyrska et al., 2009). In mammals, AP transport relies on microtubule- and dynein-dynactin motor complexes to facilitate fusion events with the endo-lysosomal system and delivery to the lysosome (Aplin et al., 1992; Fass et al., 2006; Jahreiss et al., 2008; Kimura et al., 2008a; Kimura et al., 2008b; Kochl et al., 2006; Kovacs et al., 1982; Maday et al., 2012; Ravikumar et al., 2005). On the contrary, in *S. cerevisiae*, AP motility does not rely on the microtubule network, but instead AP movement depends on the actin cytoskeleton (Kirisako et al., 1999; Monastyrska et al., 2008; Reggiori et al., 2005).

1.2.4 Degradation of autophagosome cargo

To complete the autophagy cycle, the AP contents are ultimately degraded within the lysosome. Upon fusion of the AP or amphisome with the vacuole or lysosome, respectively, the outer membrane becomes contiguous with the lysosomal membrane while the inner membrane and AP contents are delivered to the lysosome lumen where they are degraded by the lysosomal hydrolases. In mammals, these degrading structures are often called ‘autolysosomes’ (ALs) or ‘autophagolysosomes’ (APLs). Once macromolecules, such as nucleic acids, proteins, polysaccharides and lipids, have been degraded, the breakdown products are exported by lysosomal efflux transports and permeases into the cytosol for reuse by the cell.

Prolonged stimulated autophagy results in a pool of lysosomes that have all undergone fusion with AP (Yu et al., 2010). As a result, fewer and enlarged lysosomes exist as AL hybrid organelles (Chen and Yu, 2013; Yu et al., 2010). However, upon

mTORC1 reactivation, cells undergo autophagic lysosome recovery (ALR) to regenerate their lysosomal organelles again (Chen and Yu, 2013; Yu et al., 2010). During ALR, tubules form from ALs that subsequently bud-off from the tips and form vesicles (Chen and Yu, 2013; Yu et al., 2010). The budding vesicles consists of “proto-lysosomes” that then must re-acquire the proper protein pumps and hydrolases in order to become functional lysosomes (Chen and Yu, 2013; Yu et al., 2010).

1.2.5 Selective and nonselective autophagy

As mentioned above, APs can be both selective and non-selective when sequestering their cargo. In brief, non-selective autophagy entails the in-bulk envelopment of neighboring cytosolic content, whereas selective autophagy relies on the recognition of cargo by autophagy receptors. The different types of selective autophagy that have been described include: ubiquitinated proteins, excessive or damaged organelles such as peroxisomes (pexophagy) (Dunn et al., 2005), ribosomes (ribophagy) (Kraft et al., 2008), ER (reticulophagy) (Bernales et al., 2006), mitochondria (mitophagy) (Kim et al., 2007), secretory granules (crinophagy) and invading bacteria (xenophagy) (Weidberg et al., 2011). Specifically, autophagy receptors bind both to the cargo as well as to the LC3/Atg8 family of proteins via a specific LC3-interacting region (LIR), which links the cargo to autophagic membrane and targets it for degradation (Johansen and Lamark, 2011; Knaevelsrud and Simonsen, 2010; Noda et al., 2008). The best studied autophagy receptor is p62, which targets ubiquitinated cargo for autophagy (Bjorkoy et al., 2005; Pankiv et al., 2007).

1.3 PI3P and autophagy

Although autophagy, like most cellular processes, is predominantly understood from a

protein-centric point of view, the lipid biology underlying the formation, maturation and degradation of an AP is also fundamental to understanding how this process is regulated. In particular, phosphoinositides (PI), a low abundance subclass of glycerophospholipids, are important for acutely regulating membrane dynamics and protein flow in a variety of fundamental biological processes (Di Paolo and De Camilli, 2006; Kutateladze, 2010). Seven PIs have been identified and are defined by the phosphorylation state of the inositol headgroup at the 3'-, 4'- and 5'-position, which is regulated reversibly by several lipid kinases and phosphatases (Di Paolo and De Camilli, 2006; Kutateladze, 2010). The seven PIs include three monophosphorylated (PI3P, PI4P, PI5P), three bisphosphorylated (PI(3,4)P₂, PI(3,5)P₂, PI(4,5)P₂) and one triphosphorylated (PI(3,4,5)P₃) species (Figure 1.7). Notably, each of these lipids has a stereotypic spatial distribution within the cell and can serve as marker for various cell compartments. For example, PI(4,5)P₂ and PI(3,4,5)P₃ are concentrated at the plasma membrane, PI3P and PI(3,5)P₂ are localized to the endosomal compartment and PI4P is enriched on the TGN and secretory vesicles (Fig. 7) (Di Paolo and De Camilli, 2006; Kutateladze, 2010). While some PIs are constitutively present on membranes, others are transiently produced in a spatio-temporal manner in response to certain stimuli (Di Paolo and De Camilli, 2006; Kutateladze, 2010). PIs achieve direct signaling effects through their specific localization and their recruitment of proteins harboring a PI-binding module (Di Paolo and De Camilli, 2006; Kutateladze, 2010).

The importance of PI3P for autophagy regulation was first discovered in the late 1990s when Meijer's group discovered that PI3K inhibitors (*e.g.*, 3-methyladenine) block autophagy in mammalian cells under autophagy stimulating conditions (Blommaert et al.,

1997). At the time, this result was surprising given that the class I PI3K was the only known target of the PI 3-kinase inhibitors even though subsequent studies demonstrated that they broadly target the entire PI3K family (Backer, 2008; Falasca and Maffucci, 2007). A follow-up study was the first to demonstrate that PI3P specifically stimulates autophagy (Petiot et al., 2000). In *S. cerevisiae*, expression of a Vps34 kinase-dead mutant or ablation of Vps34, the sole PI3K and the only source of PI3P in budding yeast, showed that Vps34 synthesis of PI3P is essential for autophagy (Kihara et al., 2001b). Likewise, in higher eukaryotes, an important role for synthesis of PI3P by Vps34 in autophagy was confirmed in studies using molecular genetics (*e.g.*, siRNA against Vps34) (Itakura et al., 2008; Juhasz et al., 2008). Much of our understanding of the role of PI3P in autophagy has been learned through the discovery of autophagy-relevant PI3P effectors and the modulation of PI3P levels by modulating PI3P phosphatase activity, which is discussed in the following sections below (Dall'Armi et al., 2013).

1.3.1 The role of PI3P and its effectors in autophagy

Shortly after autophagy initiation by the Atg1 complex, PI3P is synthesized at the AP nucleation site. In yeast, PI3P is distributed on the inner (concave) surfaces of the IM as well as on uncharacterized organelles located in the vicinity of the IM, which have been hypothesized to supply a pool of PI3P necessary for the growth of the AP membrane (Obara et al., 2008a; Obara and Ohsumi, 2011). The asymmetric distribution of PI3P on the membrane has been postulated to intrinsically promote membrane curvature of the AP; however, whether the curvature of the AP is derived from intrinsic physiochemical properties of the lipid membrane, effector proteins or a combination of both is unclear (Obara and Ohsumi, 2011). Additionally, in mammals, PI3P has been observed along the

elongating tips of the IM, which may also facilitate curvature at this site or promote the expansion and/or sealing of the edges of this spherical structure (Obara and Ohsumi, 2011). The actions of PI3P are predominantly attributed to the effector proteins that harbor PI3P-binding modules, such as FYVE (for conserved in Fab1, YOTB, Vac1, EEA1), pleckstrin homology (PH), phox (PX) and a FRRG or LRRG motif (Di Paolo and De Camilli, 2006). In fact, the highly localized production of PI3P helps establish a membrane platform to concentrate and spatially coordinate such effectors and promote downstream signal transduction events necessary for AP biogenesis (Dall'Armi et al., 2013; Knaevelsrud and Simonsen, 2012; Obara and Ohsumi, 2011; Simonsen and Tooze, 2009). Currently, PI3P is known to regulate effectors required for AP biogenesis, cargo selection, maturation and intracellular transport, which will be discussed below (Table 1.1) (Dall'Armi et al., 2013).

Several PI3P effectors have been implicated in the initiation step of autophagy. In mammals, DFCP1, an ER-resident protein that contains two zinc-finger binding FYVE-domains, clusters at sites of AP nucleation along the ER membrane during starvation-induced autophagy (Axe et al., 2008; Ktistakis et al., 2009). Interestingly, knock-down studies of DFCP1 do not produce any overt phenotypes, making its function difficult to discern (Axe et al., 2008; Ktistakis et al., 2009). A better-characterized family of PI3P effector proteins includes the PROPPIN family or WD-repeat proteins interacting with phosphoinositide (WIPI-1–4) proteins (Dove et al., 2004; Krick et al., 2012; Watanabe et al., 2012). The PROPPIN family is defined by its WD40 repeats, which adopt a seven-bladed β -propeller fold containing two pseudo-equivalent PI3P-binding sites, and a FRRG motif, which binds PI3P, and are all required for the full autophagic function of

PROPPIN proteins (Baskaran et al., 2012). Three PROPPINs, WIPI-1, WIPI-2, and WIPI-4, are implicated in the initiation of mammalian autophagy. Specifically, WIPI-1 and WIPI-2 are recruited to omegasomes upon autophagy induction and play a role in the formation and maturation of the isolation membrane, respectively (Polson et al., 2010; Proikas-Cezanne et al., 2004). These two proteins are phylogenetically similar to yeast Atg18, which has also been indirectly implicated in the initiation step, specifically through shuttling Atg9 together with Atg2 during autophagy to the PAS (Krick et al., 2006; Nair et al., 2010; Obara et al., 2008b). While WIPI-4 has not been characterized in mammals, a *Caenorhabditis elegans* homolog of WIPI-4, EGF-6, is recruited to and controls the maturation of the omegasome. Importantly, unlike WIPI-2, EGF-6/WIPI-4 appears to have a negative regulatory role and restricts omegasome expansion and autophagosome size (Lu et al., 2011). In addition to their roles in autophagy initiation, these PI3P effectors also serve as important tools for visualizing PI3P-synthesis at the nucleation site.

In addition to its role in AP biogenesis, PI3P is important for recruiting effectors that promote selective cargo capture by the nascent AP. In particular, PI3P along the inner AP membrane serves as a docking site for the PI3P effector Alfy (autophagy-linked FYVE protein) to promote the selective engulfment of ubiquitinated protein aggregates (Filimonenko et al., 2010). Alfy is a nuclear scaffolding protein that interacts with Atg5 and the ubiquitin-binding adaptor protein p62 via its WD40 domain as well as with PI3P through its FYVE domain (Clausen et al., 2010; Filimonenko et al., 2010; Simonsen et al., 2004). Additionally, TECPR1 Tectonin Beta-Propeller Repeat Containing 1), which possesses a PI3P-binding PH domain has been implicated in binding PI3P on the nascent

AP to promote selective autophagy of intracellular bacteria (Ogawa et al., 2011).

PI3P also plays a prominent role in regulating membrane trafficking events along the endo-lysosomal system that are critical at the later stages of the autophagy pathway. For instance, in mammals, the PI3P-binding effector TECPR1 also serves as a tethering factor to promote AP–lysosome fusion (Chen et al., 2012; Ogawa et al., 2011). While evidence for an amphisome intermediate in yeast is still missing, there are PI3P effectors, such as Atg24 and Vam7, which are necessary for efficient autophagosome–vacuole fusion (Dall'Armi et al., 2013; Knaevelsrud and Simonsen, 2012; Obara and Ohsumi, 2011).

Lastly, PI3P has been shown to be important for AP motility. During starvation-induced autophagy, FYCO1 (FYVE and coiled-coil domain containing 1) is recruited to the outer membrane of an AP by its direct interaction with Rab7, LC3 and PI3P (Pankiv et al., 2010). FYCO1 mediates the microtubule plus-end directed transport of the AP toward the periphery of the cell (Pankiv et al., 2010).

In addition to the effectors highlighted in this section, there are likely to be more at various stages of the autophagy process that have yet to be identified. In the future, genetic screens for proteins that possess PI3P-binding domains will be helpful in identifying more PI3P effectors and, therefore, potentially more roles for PI3P in autophagy.

1.3.2 Sources of PI3P in autophagy

Although Vps34 and its lipid kinase activity are essential for autophagy in budding yeast, it is unclear whether this is the case in higher eukaryotes that possess alternate pathways to synthesize PI3P (Backer, 2008; Falasca and Maffucci, 2012; Hakim et al., 2012;

Vanhaesebroeck et al., 2001). For instance, in mammals, PI3P is also synthesized by the class II PI3Ks, which catalyze PI phosphorylation like Vps34, and inositol 4-phosphatase (Inpp4) type I and II, which dephosphorylate PI(3,4)P₂ to PI3P (Falasca and Maffucci, 2012; Norris et al., 1997; Norris and Majerus, 1994; Shin et al., 2005). Additionally, Sac1 family members, such Fig4 can dephosphorylate PI(3,5)P₂ to PI3P, accounting for yet another potential source of PI3P (Gary et al., 2002; Rudge et al., 2004). Previously, pharmacological and genetic studies have clearly demonstrated that Vps34 and its PI3K activity are important for autophagy in mammals, but whether Vps34 is essential for autophagy in mammals has not been determined. Recently, a Vps34 conditional genetic mouse model was generated which enabled the scientific community to address this question in a more qualitative way for the first time (see section 1.4.1.5). Identifying the sources of PI3P is critical to understanding autophagy regulation and a key question addressed in this thesis.

1.3.3 Regulation of PI3P levels during autophagy

During AP formation, tight control of PI3P levels through the coordination of PI3Ks and PI3P phosphatases at the site of AP formation is critical in determining both AP size and rate of production (Dall'Armi et al., 2013; Vergne and Deretic, 2010). In fact, the asymmetric distribution of PI3P along the isolation membrane may be achieved not only through spatially restricting synthesis of PI3P, but also through locally changing the metabolism of PI3P via the balance between kinases and phosphatases. In mammals, phosphoinositide 3-phosphatases, such as Jumpy (myotubularin-related protein 14, MTMR14) and MTMR3, have been implicated in dephosphorylation of a pool of PI3P synthesized for AP biogenesis (Dowling et al., 2010; Taguchi-Atarashi et al., 2010;

Vergne and Deretic, 2010; Vergne et al., 2009). Silencing of Jumpy resulted in an increase in WIPI-1 puncta and autophagic flux under both normal and starvation conditions (Vergne et al., 2009). Similarly, silencing of MTMR3 increases AP formation. On the contrary, overexpression of MTMR3 causes fewer and smaller AP (Taguchi-Atarashi et al., 2010). So far, phosphatases have not been implicated in the early autophagy steps in yeast; however, PI3P regulation by phosphatases is important for later steps of autophagy. In yeast, two phosphatases, Ymr1, the sole myotubularin ortholog, and synaptojanin-like protein 3, via its Sac1 phosphatase domain, have been shown to promote the AP-vacuole fusion step (Krick et al., 2008). Despite these initial studies concerning PI3P regulation in autophagy, this topic still remains poorly understood. In the future, it will be important to address the following questions: Are there additional PI3P phosphatases that regulate autophagy? Do the phosphatases act in a similar manner or do they have specialized roles in their regulation of autophagy? How are PI3P-phosphatases regulated? Is PI3P-phosphatase activity important for later, maturation steps of autophagy in mammals as in yeast?

1.4 Synthesis of PI3P by the class II and class III PI3K

All PI3Ks are defined by their ability to catalyze the phosphorylation of the 3-position of the inositol ring. In yeast, Vps34 is the sole PI3K; however, in mammals, Vps34 belongs to a family of PI3Ks that consists of eight isoforms grouped into three classes based on their substrate specificity and structure (Fig. 1.8) (Vanhaesebroeck et al., 2010).

Specifically, *in vitro*, the class I converts $PI(4,5)P_2$ to $PI(3,4,5)P_3$, class II converts PI and PI4P into PI3P and $PI(3,4)P_2$, respectively, and the class III converts PI to PI3P (Vanhaesebroeck et al., 2010). Each of the PI3K shares a kinase, helical and C2 domain

core in addition to possessing other, unique domains that define the function and cellular localization of each PI3K (Vanhaesebroeck et al., 2010). Given that PI3Ks share a structurally similar lipid kinase domain, it is unsurprising that PI3K inhibitors, such as 3-methyladenine and wortmannin, inadvertently target other members of the family as well, albeit at different rates. As mentioned in a previous section, the class I PI3K is a major regulator of cell growth and the mTOR pathway; however, it will not be discussed further in this section. Here, we focus on the class II and class III PI3Ks which are the only known lipid enzymes that synthesize PI3P from PI in mammalian cells. Although the class II and class III each play unique roles and have different physiological functions within the cell, it is unclear whether these two classes can also produce PI3P for a common cellular process. This thesis work is particularly important to the PI field because we determine the contribution of PI3P synthesized by the class III PI3K, Vps34, in the cell and for autophagy and address whether synthesis of PI3P by the class II PI3K is also important for this process.

1.4.1 Class III PI3K (Vps34)

Vps34 was first discovered in the early 1990's during genetic screen performed in *S. cerevisiae* to identify vps (vacuole protein sorting) genes important for endosomal trafficking to the vacuole (Herman and Emr, 1990). Stevens, Emr and their colleagues classified the vps mutants into five classes (A-E) based on the different phenotypes observed and placed both Vps34 and its regulator, Vps15, in the category of Class D mutants, which displayed improper sorting and trafficking of vacuolar hydrolases (e.g. carboxy peptidase Y) from the late-Golgi to the vacuole (Raymond et al., 1992), as well as the Class C mutants, which are sensitive to growth at high temperatures and osmotic

stress and have abnormal cytoplasmic membranous structure (Banta et al., 1988; Herman and Emr, 1990; Robinson et al., 1988). It was not until the discovery of the mammalian class IA PI3K p110 α and its lipid kinase activity that a homologous lipid kinase domain to *S. cerevisiae* Vps34 was identified (Backer, 2008; Hiles et al., 1992; Schu et al., 1993). Later studies in *S. cerevisiae* showed that the PI3K activity of Vps34 and its synthesis of PI3P were essential for regulating endo-lysosomal system trafficking events and autophagy (Kihara et al., 2001b). Vps34 is highly conserved with homologues in several species (*S. cerevisiae*, *C. albicans*, *C. elegans*, *Drosophila*, all vertebrates) (Eck et al., 2000; Herman and Emr, 1990; Linassier et al., 1997; Roggo et al., 2002; Volinia et al., 1995).

1.4.1.1 Protein structure and catalytic activity of Vps34

Notably, Vps34 is the only PI3K family member in *S. cerevisiae* and is the only class III PI3K isoform in mammals (Backer, 2008; Yan and Backer, 2007). As a member of the PI3K family, Vps34 possesses the characteristic core C2, helical and kinase domains. Although the C2 domain is more classically known for binding to calcium, the C2 domains in the PI3K family are believed to interact with acidic phospholipids. In the class I PI3Ks, the helical domain serves as a kinase regulatory domain via its interaction with regulatory factors, such as p85 subunit, however, its function in Vps34 still remains unknown (Backer, 2008; Vanhaesebroeck et al., 2010). Unlike the other PI3Ks, Vps34 specifically uses PI as a substrate and only produces the lipid product PI3P. The substrate specificity of Vps34 is largely attributed to its substrate recognition loop, which differs from that of the class I or II PI3K in that it is uncharged and, therefore, unable to accommodate negatively charged phosphate groups of phosphorylated PI headgroups

(Pirola et al., 2001). Although the helical domain does not appear to serve a regulatory function in Vps34, the catalytic activity of Vps34 is regulated by other means. Specifically, Vps34 is largely regulated through the binding of Vps15, a putative serine kinase, to its C-terminus (residues 837-864), which is believed to stabilize and appropriately target Vps34 to cellular membranes (Panaretou et al., 1997; Stack and Emr, 1994; Stack et al., 1993). Additionally, the 11 residues at the extreme end of the C-terminus of Vps34 required for lipid kinase activity independently of Vps15; however, the precise regulatory role of these residues is poorly understood (Budovskaya et al., 2002). Lastly, Vps34 possesses a highly unstructured N-terminal region, although its interactors and function is currently unknown (Backer, 2008).

So far, most of the studies on Vps34 have been focused on its lipid kinase activity; however, Vps34 is likely to have other important roles in the cell that are currently underappreciated. For instance, Vps34 has been shown to undergo autophosphorylation, suggesting that Vps34 may have protein kinase capabilities as well (Stack and Emr, 1994). Vps34 may also have kinase independent roles in the cell, including acting as a scaffold to organize complexes or to bring factors in close proximity to facilitate signaling events. Interestingly, in *Candida albicans*, the Vps34-null strain and the Vps34 kinase-dead strain display different osmotic and temperature responses, suggesting that other, noncatalytic domains of Vps34 have important functions as well (Gunther et al., 2005).

1.4.1.2 Vps34 complexes

Vps34 operates in several, largely conserved complexes that determine its different physiological roles and regulates its lipid kinase activity (Fig. 1.9). Vps34 forms a

constitutive heterodimer with Vps15, which promotes the recruitment of Vps34 to membranes as well as regulates its activity (Stack et al., 1995). In yeast, two major Vps34-Vps15 complexes exist: complex I (Vps34, Vps15, Vps30/Atg6, Atg14) and complex II (Vps34, Vps15, Vps30/Atg6, Vps38) (Kihara et al., 2001b). Vps34 complex I localizes to the PAS and functions in the initiation of autophagy (Obara et al., 2006; Suzuki et al., 2001), whereas complex II associates with the endosome and regulates endosomal trafficking events (Kihara et al., 2001b). In mammals, the Vps34 complexes are less clearly defined and more interactors regulate each complex. In brief, the mammalian equivalent of complex I consists of Vps34, Vps15, Beclin (the mammalian Vps30/Atg6 homolog) and Atg14 and also promotes the initiation step of autophagy (Itakura et al., 2008; Kihara et al., 2001a; Matsunaga et al., 2009; Zhong et al., 2009). Similar to yeast, the mammalian equivalent of complex II consists of Vps34, Vps15, Beclin and UVRAG (the mammalian Vps38 homolog) (Kihara et al., 2001a). In fact, Atg14 and UVRAG are mutually exclusive members of these complexes since they both bind the same site on Beclin (Matsunaga et al., 2009). Complex II in mammals is not well understood, but is thought to mainly participate in endo-lysosomal trafficking events, including autophagosome maturation, endocytic fusion, and multivesicular body formation. Additionally, this complex has been implicated in cytokinesis (Funderburk et al., 2010; Liang et al., 2008a; Thoresen et al., 2010; Zhong et al., 2009). Importantly, it is likely that Vps34 can also exist as a simple heterodimer with Vps15 at the endosome that interacts with myotubularin phosphatases, such as MTM1, to tightly regulate PI3P levels (Cao et al., 2007). Lastly, a third mammalian complex, Complex III, includes members of complex II plus Rubicon (Matsunaga et al., 2009). Complex III is primarily known for its

role in inhibiting fusion events along the endosome, including autophagosome maturation, by preventing the interaction between UVRAG and the C-VPS/HOPS tethering complex (Matsunaga et al., 2009; Sun et al., 2010; Tabata et al., 2010). In mammals, several accessory factors also associate with these complexes, such as BIF-1 and Ambra, and serve as additional modulators of autophagy (Fimia et al., 2007; Takahashi et al., 2007). So far, we are at the beginning stages of understanding post-translational modifications (e.g., phosphorylation) of Vps34 and how they regulate its localization, enzymatic activity and the stability of the various Vps34 complexes. The molecular basis governing the regulation and participation of these different Vps34 complexes and complex members in various cellular functions is still unclear, but is an area of active investigation. In fact, in yeast, Atg38 was recently identified as novel Vps34 complex I member that forms a homodimer to bridge the Vps15-Vps34 and Atg14-Atg30 complex (Araki et al., 2013).

1.4.1.3 Vps34 and the endocytic pathway

Since the discovery of Vps34 in the early 1990's, numerous studies have demonstrated that Vps34 and its synthesis of PI3P are important for multiple endocytic trafficking events, including homotypic fusion between early endosomes, phagocytosis, retrograde trafficking to the Golgi and MVB biogenesis (Backer, 2008; Lindmo and Stenmark, 2006).

Vps34 complexes are targeted to the early or late endosome via the direct interaction of Vps15 with Rab5 (Christoforidis et al., 1999; Stack et al., 1995) or Rab7 (Stein et al., 2003), respectively. In yeast and mammals, complex II or the homolog equivalent is primarily recruited to the endosomal membrane; however, the heterodimer

of Vps34 and Vps15 may also be recruited the membrane alone or as a complex with the myotubularin phosphatase, MTM1 (Cao et al., 2007). One of the major functions of Vps34 is to promote the homotypic fusion of endosomes. Specifically, PI3P synthesis on the endosome recruits the effectors EEA1 and Rabenosyn-5 through their PI3P-binding FYVE-domains, which regulate homotypic fusion (Simonsen et al., 1998). EEA1 regulates docking of membranes through the recruitment of SNARE proteins syntaxin 6 and syntaxin 13 (McBride et al., 1999; Simonsen et al., 1999), whereas Rabenosyn-5 binds Vps45, a negative regulator of SNAREs (Nielsen et al., 2000). Additionally, Vps34 plays an important role in the maturation and fusion step of phagocytosis. Nascent phagosomes contain activated Rab5, which likely facilitates the recruitment of Vps34, and transiently accumulate PI3P required for their subsequent maturation and fusion with the late endosomes/lysosomes.

As mentioned above, Vps34 was first identified in yeast for its essential role in the sorting and delivery of soluble hydrolases transported from the Golgi to the vacuole (Backer, 2008; Herman and Emr, 1990; Schu et al., 1993). This phenomenon was later attributed to the important role of Vps34 in regulating retrograde sorting and transport via the retromer complex. Retromer mediates the retrograde trafficking of Vps10p, the yeast homolog of the mannose 6-phosphate receptor that binds lysosomal hydrolases, from the endosome back to the TGN, which is important for its additional rounds of hydrolase sorting (Hurley and Emr, 2006; Lindmo and Stenmark, 2006; McGough and Cullen, 2011; Seaman, 2012; Seaman et al., 1998). The synthesis of PI3P by Vps34 is important for the recruitment of retromer complex members Vps5 and Vps17 (the mammalian

equivalent of SNX1, SNX2, SNX5, SNX6), which contain PI3P-binding PX domains (Bonifacino and Hurley, 2008; McGough and Cullen, 2011).

Lastly, the formation of intraluminal vesicle (ILVs) in multivesicular bodies (MVBs) is required for the degradation of endocytosed transmembrane proteins (*e.g.*, the EGF receptor) is also regulated by PI3P synthesis by Vps34 (Fernandez-Borja et al., 1999; Futter et al., 2001a; Schu et al., 1993). Specifically, PI3P recruits members of the ESCRT machinery, such as the FYVE-domain containing Vps27/HRS (ESCRT-0), and SNX3, via its PX domain, to promote the invagination and budding of endosomal membrane (Futter et al., 2001b; Katzmann et al., 2003; Raiborg and Stenmark, 2009; Saksena et al., 2007). Interestingly, PI3P not only participates in ILV formation, but is also sorted into ILVs and degraded upon reaching the late endosome and may be a means by which PI3P is physiologically downregulated (Gillooly et al., 2000).

Vps34 and its synthesis of PI3P are critical for maintaining homeostasis and proper functioning of the endo-lysosomal system. Importantly, the role of Vps34 in the endo-lysosomal system is also critical for efficient autophagy, which relies on APs fusing with endosomes and MVBs during maturation, at least in the mammalian system, and the lysosome for degradation.

1.4.1.4 Vps34 and mTOR signaling

Although Vps34 is important for the induction of autophagy in response to nutrient stressors, a paradoxical role for Vps34 in positively regulating mTORC1 signaling (and thus theoretically downregulating autophagy) has recently emerged in mammalian cells (Backer, 2008; Yan and Backer, 2007). Specifically, studies have shown Vps34 is required for insulin- and amino acid- stimulated activation of mTOR and its substrates,

S6K1 and 4EBP1 (Byfield et al., 2005). In fact, amino acid withdrawal and glucose starvation inhibit Vps34 activity (Byfield et al., 2005; Nobukuni et al., 2005). Currently, the mechanism by which insulin and amino acids regulate Vps34 is not well understood. In the case of amino acid stimulation, one model suggests that the activated Vps34 is recruited to the late endosome and lysosome where it stimulates PLD1 (phospholipase D1) to synthesize phosphatidic acid (PA), which subsequently contributes to the activation of mTORC1 (Dall'Armi et al., 2013; Wiczler and Thomas, 2012). PI3P-binding Phox homology (PX) domain of PLD1 was shown to be important for both its translocation to the late endosomes and lysosomes upon amino acid starvation as well as its activation (Yoon et al., 2011); however, another group reported Vps34 depletion had no effect on PLD1 activity, which may be explained by experimental differences (Xu et al., 2011). Importantly, the Vps34-PLD1 pathway is necessary but not sufficient to stimulate the mTORC1 and requires additional, parallel amino acids to drive mTORC1 signaling (Yoon et al., 2011). Additionally, activation of AMPK has also been shown to inhibit Vps34 to negatively regulate mTORC1 signaling (Byfield et al., 2005). Several studies have indicated that Vps34 does not mediate steady-state mTORC1 signaling, but rather mTORC1 signaling in response to acute cues (Jaber et al., 2012a; Juhasz et al., 2008; Xu et al., 2011). The requirement for Vps34 in both mTORC1 activation and autophagy seems contradictory given our current understanding of both pathways and will require further investigation to be reconciled.

1.4.1.5 Vps34 and autophagy

As described in previous sections, Vps34 and its synthesis of PI3P play an important role in the regulation of autophagy at the biogenesis, maturation and lysosomal fusion steps.

While Vps34 is the only source of PI3P and required for autophagy in budding yeast, whether this lipid kinase plays an essential role in mammalian autophagy has been an outstanding question in the field. Previous molecular genetic (*e.g.*, siRNA) and pharmacological studies using standard PI3K inhibitors, such as wortmannin or 3-methyladenine (3MA), have suggested that Vps34 is critical for starvation-induced autophagy but Vps34-independent pathways for PI3P synthesis have yet to be ruled out (Axe et al., 2008; Blommaart et al., 1997; Dall'Armi et al., 2013; Itakura et al., 2008; Petiot et al., 2000). In fact, genetic studies in *Drosophila* were the first to hint that Vps34 was not essential for AP biogenesis (Juhasz et al., 2008). Recently, several genetic mouse models have been generated to determine the role of mammalian Vps34 in autophagy and other physiological processes; however, conflicting conclusions have been drawn concerning its role in autophagy in particular (Table 2.2). For instance, studies in various conditional knockout (KO) mouse models have reported a spectrum of findings, ranging from no autophagy phenotypes in sensory neurons (Zhou et al., 2010) and T-lymphocytes (McLeod et al., 2011) to severe autophagy defects in the latter cell type (Parekh et al., 2013; Willinger and Flavell, 2012), fibroblasts, cardiomyocytes, hepatocytes (Jaber et al., 2012a), podocytes (Bechtel et al., 2013) and lens cells (Morishita et al., 2013) (See Table 2). The answer to whether Vps34 plays an essential role in mammalian autophagy is more complex than originally anticipated. In fact, differences in autophagy requirements may not only reflect cell type, but also genetic background, cell state and type of autophagy-inducing stimuli, continuing to raise the question of whether sources of PI3P besides Vps34, such as the class II PI3K, can regulate autophagy.

1.4.2 Class II PI3K (PI3KC2)

Of the three classes of PI3Ks, PI3KC2 is by far the most enigmatic. The PI3KC2 were first identified in *Drosophila* in which there is only one isoform, Pi3K68D (MacDougall et al., 1995). In mammals, three PI3KC2 isoforms have been identified, including the PI3KC2 α , PI3KC2 β , PI3KC2 γ ; however, the majority of the PI3KC2 studies have focused on the α and β isoforms which are the most ubiquitously expressed in tissues.

1.4.2.1 Protein structure and catalytic activity of PI3KC2

The PI3KC2s contain a helical, C2, and kinase domain core characteristic of the PI3K family. Like Vps34, the helical domain does not seem to possess any regulatory function and the C2 domain function is currently unknown for this class. The catalytic domain of PI3KC2 differs from Vps34 in that the substrate recognition loop of the PI3KC2 domain is similar to the class I PI3K in that it contains multiple basic charges allowing it to accommodate both unphosphorylated and phosphorylated PIs as their substrates. In fact, the PI3KC2 isoforms can use PI, PI4P and PI(4,5)P₂ as substrates to synthesize PI3P, PI(3,4)P₂ and PI(3,4,5)P₃ *in vitro*, respectively. However, PI appears to be the preferred substrate even for the α isoform, which has shown increased preference toward PI4P and PI(4,5)P₂ in the presence of clathrin and when participating in clathrin mediated endocytosis (CME) (Gaidarov et al., 2005; Posor et al., 2013). Although PI3KC2 does not possess a regulatory subunit like class I, there are several unique protein binding domains within the N- and C-terminus that likely control its localization and kinase activity. The N-terminus sequence of PI3KC2 defines each isoform and has the potential to regulate its lipid kinase activity by modulating protein conformation and/or regulating its localization (Arcaro et al., 1998). PI3KC2 α contains a clathrin-binding region

(Gaidarov et al., 2005), whereas PI3KC2 β contains proline-rich sequences (Wheeler and Domin, 2006). Additionally, similar to the class I isoform, the N-terminus of the PI3KC2 contains a Ras binding domain, although its binding to Ras family members remains untested. The C-terminus of PI3KC2 is quite distinct from Vps34 in that it contains a PX (phox homology) domain and a second C2 domain (Stahelin et al., 2006). The PX domain in the C-terminus binds PI(4,5)P₂ and may play a role in recruiting the PI3KC2 to the plasma membrane (Stahelin et al., 2006), whereas the second C2 domain possesses a nuclear localization motif that promotes the translocation PI3KC2 into the nucleus.

1.4.2.2 Isoform specific functions of the PI3KC2s

PI3KC2 α

Human PI3KC2 α is ubiquitously expressed, although it has highest expression in the heart, placenta and ovary (Domin et al., 1997; Falasca and Maffucci, 2012). The α isoform has been found at the plasma membrane, endosome and trans-Golgi network and has been implicated in a variety of cellular functions. The best understood role for PI3KC2 α is in the maturation and fission steps of clathrin mediated endocytosis (CME) (Posor et al., 2013). During CME, PI3KC2 α is recruited to the plasma membrane through its clathrin-binding domain as well as its PX domain, which binds PI(4,5)P₂ (Posor et al., 2013). The PI(4,5)P₂ here is initially synthesized during the nucleation step of endocytosis but is then subsequently dephosphorylated by 5-inositol phosphatase to PI4P and can be used as a substrate by PI3KC2 α (Posor et al., 2013). The catalysis of PI4P to PI(3,4)P₂ by PI3KC2 α leads to the recruitment of Snx9 and dynamin, the machinery required for the final vesicle fission step (Posor et al., 2013). PI3KC2 α has also been implicated in dynamin-independent endocytosis although its mechanism is currently

unknown. Importantly, this was the first cell-based instance of PI(3,4)P₂ synthesis by PI3KC2 α ; however, other roles for this isoform are still believed to depend on its synthesis of PI3P. PI3KC2 α has also been implicated in other trafficking events such as translocating GLUT4 to the plasma membrane to regulate glucose transport (Falasca et al., 2007; Maffucci et al., 2003), releasing insulin β -cells and releasing neurosecretory granules containing hcG (Meunier et al., 2005; Wen et al., 2008), and is thought to promote vesicle fusion. In addition to its role in trafficking, PI3KC2 α also seems to be important for several signaling pathways. PI3KC2 α has been found to regulate β -cell insulin secretion in part through the upregulation of β -GK (glucokinase) (Leibiger et al., 2010). Additionally, PI3KC2 α has also been shown to promote cell growth and survival, although through an unclear mechanism that likely involves regulation of apoptosis (Elis et al., 2008; Eun et al., 2010; Kang et al., 2005; Ng et al., 2009). Lastly, PI3KC2 α has been implicated in signaling muscle contraction via its stimulation of Rho (Wang et al., 2006; Yoshioka et al., 2007). The precise mechanism by which PI3KC2 α regulates this diverse set of pathways will require further investigation. The first conditional knock-out mouse model for PI3KC2 α provided some insights to the protein's function, however, it was not a bona fide knock-out because a kinase-dead, truncated form of the protein still remained (Harris et al., 2011). Nevertheless, this particular knock-out model showed the kinase activity of PI3KC2 α to be important for postnatal development given that a significant number of mutant mice died by 6 months of age (Harris et al., 2011). The early death of the PI3KC2 α knock-out mice was attributed to chronic renal failure (Harris et al., 2011). Since then, a second, a PI3KC2 α complete null conditional mouse model was generated (Yoshioka et al., 2012). Global knockout or endothelial-cell-specific

ablation of PI3KC2 α resulted in embryonic lethality due to abnormalities in multiple organs as well as severely impaired vascular formation (Yoshioka et al., 2012). Inducible deletion in endothelial cells demonstrated PI3KC2 α is critical for vascular formation, which requires efficient endothelial cell migration, proliferation and tube formation and cell junction assembly (Yoshioka et al., 2012). Notably, a decrease in PI3P enriched endosomes and impairment in endosomal trafficking and defective endothelial cell junction assembly is seen upon ablation of PI3KC2 α (Yoshioka et al., 2012).

PI3KC2 β

Similar to the PI3KC2 α , the PI3KC2 β is ubiquitously expressed, but shows increased expression in certain tissues, including the placenta and thymus (Arcaro et al., 1998; Brown et al., 1997). The PI3KC2 β has been found to localize to the plasma membrane and nucleus and regulate a wide range of cellular processes, including cell migration, K⁺ channel activation, cell growth and survival and cell-cycle progression (Falasca and Maffucci, 2007; Falasca and Maffucci, 2012). Specifically, PI3KC2 β has been shown to synthesize PI3P at the plasma membrane, which promotes motility by stimulating membrane ruffling and actin lamellipodia/fillipodia and decreasing adhesion (Domin et al., 2005; Katso et al., 2006; Maffucci et al., 2005). Notably, however, a role for PI3KC2 β in motility may be cell type specific given that other studies did not observe a role for PI3KC2 β in this process (Smith et al., 2007). Additionally, PI3KC2 β has been found to act downstream of TCR activation to regulate a K⁺ channel (KCa3.1) via its

PI3P synthesis (Srivastava et al., 2009). Mutations and misregulation of PI3KC2 β has been observed in several cancer cell lines. This finding corroborates with increased proliferation and protection from anoikis seen in cell lines overexpressing PI3KC2 β and suggests it positively regulates cell growth and survival (Katso et al., 2006). PI3KC2 β role in growth appears to be independent of Akt, but may instead help regulate a pathway that inhibits apoptosis (Das et al., 2007). Aside from its cytosolic roles, PI3KC2 β also localizes to the nucleus. During G2/M phase increased levels of PI3KC2 β are seen in the nucleus, suggesting it may have a role in cell cycle progression (Visnjic et al., 2003). PI3KC2 β and its synthesis of PI3P have been implicated in several cellular processes; however, its precise mechanism of action remains unknown. Further work will need to be done to identify novel interactors and place the PI3KC2 within signaling networks. Lastly, a conditional mouse knock-out was generated for PI3KC2 β , which showed no overt phenotype upon full body deletion (Harada et al., 2005). Given that there are three isoforms, it may be that PI3KC2 β is compensated for here. A multiple isoform knock-out study may be required to better understand the role of PI3KC2 (Harada et al., 2005).

PI3KC2 γ

Currently, very little is known about PI3KC2 γ isoform. PI3KC2 γ has a very limited expression pattern that includes the liver, prostate, breast and salivary glands with the liver being the major site of expression (Rozycka et al., 1998). Its function has yet to be studied (Falasca and Maffucci, 2012).

1.4.2.3 An emerging role for PI3KC2 in autophagy?

As mentioned previously, both Vps34 and PI3KC2 are the only enzymes in higher eukaryotes that catalyze the conversion of PI to PI3P. Whether the Vps34 and the

PI3KC2 can act together to both positively regulate the same function is unknown. Interestingly, *pi3c2α*, was recently identified as a "hit" in a large autophagy interaction network screen. Specifically, an interaction was detected between PI3KC2α and both Atg7 and MAP1LC3A (one of the six Atg8 orthologues in humans) (Behrends et al., 2010). Additionally, siRNA knock-down PI3KC2α suggested a decrease in autophagy flux, warranting a further exploration of PI3KC2α's potential regulatory role in autophagy (Behrends et al., 2010). A recent study in *C. elegans* reported the class II ortholog, PIK-1, produces a pool of PI3P on nascent phagosomes, which is then followed by sustained production of PI3P on these organelles (Lu et al., 2012). Here the production of PI3P by Vps34 depends on the initial production of PI3P by PIK-1 (Lu et al., 2012). In this model, PI3KC2 and Vps34 cooperate and act sequentially to regulate the autophagy process (Lu et al., 2012). Since mammalian cells have multiple isoforms it is uncertain which may participate in the autophagy process and, if so, whether they act in a hierarchical manner such as in *C. elegans* or whether they produce separate pools of PI3P.

1.5 Objectives

The main purpose of this dissertation is to better understand the role of PI3Ks in the regulation of autophagy. Given that the mammalian system has multiple ways to synthesize PI3P, we hypothesized that autophagy could still occur independently of Vps34 and that the class II PI3Ks synthesize PI3P during this process as well. The first part of this investigation was carried out using mouse embryonic fibroblasts (MEFs) from a *Vps34* conditional genetic mouse model to generate *Vps34* null cells. Using *Vps34* null MEFs, we assessed the contribution of Vps34 to levels of PI3P synthesis at steady-state

and during autophagy. Additionally, using several standard autophagy assays we quantitatively assessed autophagy in the absence of Vps34. In the second part of this work, we used a molecular RNA interference approach to determine whether the class II PI3K plays a positive role in regulating autophagy. We aimed to determine the contribution of PI3P by the class II PI3Ks as well as assess its role in autophagy by performing standard autophagy assays and colocalization studies with autophagy markers.

Additionally, the preliminary data from two side-projects are presented in the final chapters. The goal of the first project was to discover novel lipid interactions for Vps34 using a lipidomics approach. Since Vps34 and its synthesis of PI3P are responsible for numerous membrane trafficking events and maintaining endo-lysosomal homeostasis, we hypothesized that this lipid modifying enzyme may play a role in regulating lipid homeostasis in the cell. The aim of the second project was to determine whether the retromer complex, which is controlled by PI3P synthesis by Vps34, regulates autophagy. We hypothesized that the decline in retromer function observed in sporadic Alzheimer's disease cases may contribute to the breakdown of the endo-lysosomal system and subsequently cause a secondary impairment in the autophagy pathway.

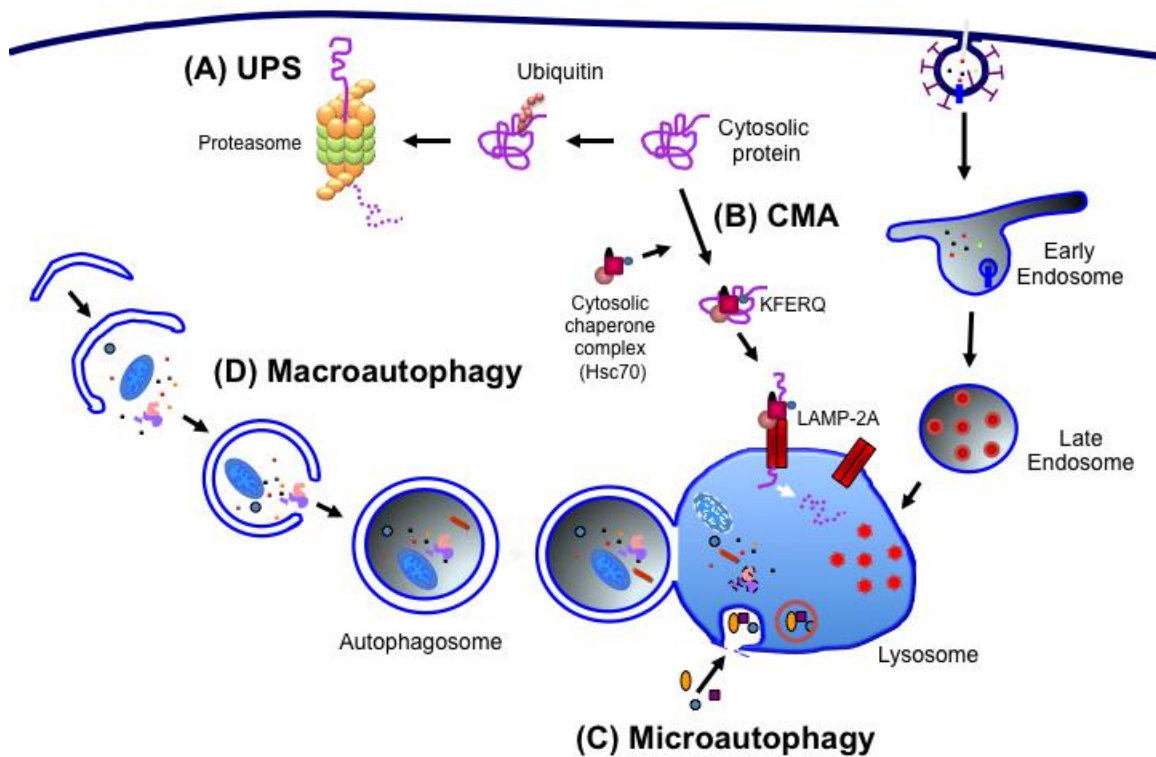


Figure 1.1 Cellular degradative processes. (A) The ubiquitin-proteasome system (UPS) is a cytosolic degradation pathway that consists of a proteasome that recognizes polyubiquitinated proteins and degrades them into small peptides. There are 3 modes of lysosomal degradation: chaperone-mediated autophagy (CMA), microautophagy and macroautophagy. (B) CMA occurs when soluble cytosolic proteins containing a targeting motif (*e.g.*, KFERQ) are recognized by the cytosolic heat shock cognate 70 (Hsc70) chaperone and translocated across the lysosomal membrane by LAMP-2A (lysosomal-associated protein type 2A) for degradation. (C) During microautophagy, the surface of the lysosome or late endosomes invaginates and engulfs the adjacent cytosolic material in a selective or nonselective manner into the lumen for degradation. (D) Macroautophagy is characterized by the sequestration of cytoplasmic proteins and organelles, either selectively or nonselectively, by a double-membrane vesicle termed the autophagosome. Autophagosomes fuse with the lysosome where its intraluminal contents are degraded.

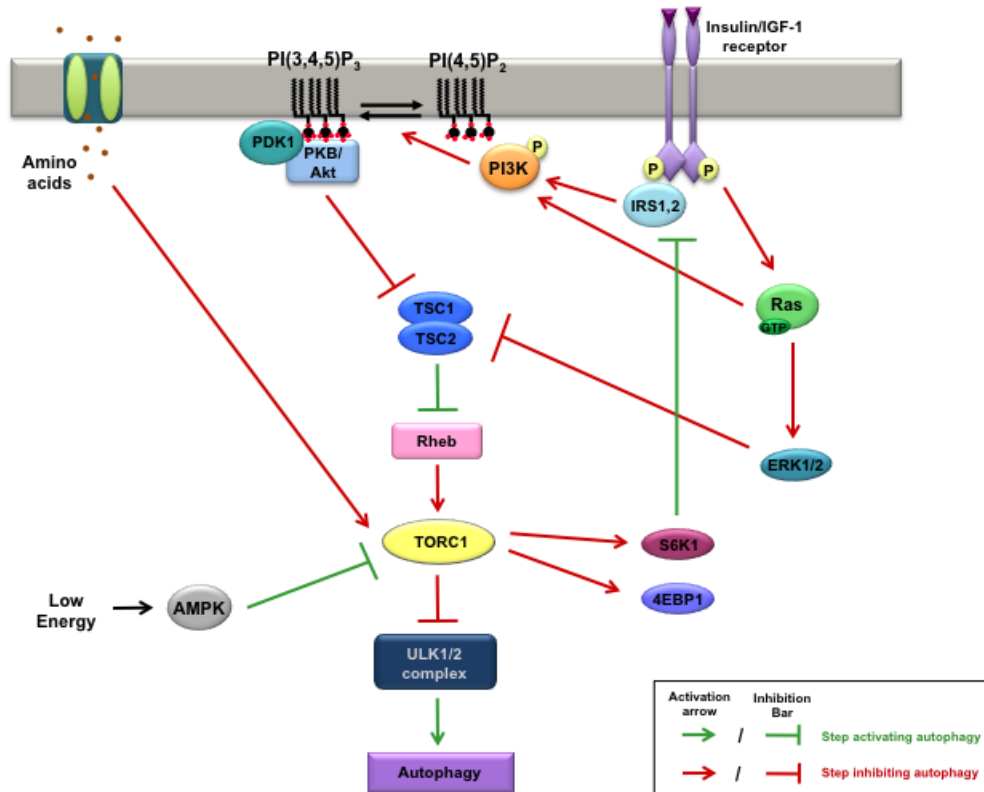


Figure 1.2 mTORC1 regulation of mammalian autophagy. Mammalian target of rapamycin complex 1 (mTORC1) plays a central role in autophagy by coordinating multiple signaling inputs, including the growth factor and hormone induced class I phosphatidylinositol 3-kinase (PI3K) and small GTPase Ras, amino acid and AMP-activated protein kinase (AMPK) signaling pathways. mTORC1 activation promotes cellular anabolism via phosphorylation of its downstream targets S6 kinase 1 (S6K1) and eIF4E-binding protein 1 (4E-BP1) and restricts catabolic processes such as autophagy by inhibiting the Ulk1/2 complex. When nutrient and energy supply is scarce, mTORC1 is inhibited and autophagy becomes activated. A negative feedback loop may exist whereby S6K1 downregulates growth factor receptor signaling to inactivate mTORC1. Adapted from (He and Klionsky, 2009; Yang and Klionsky, 2010).

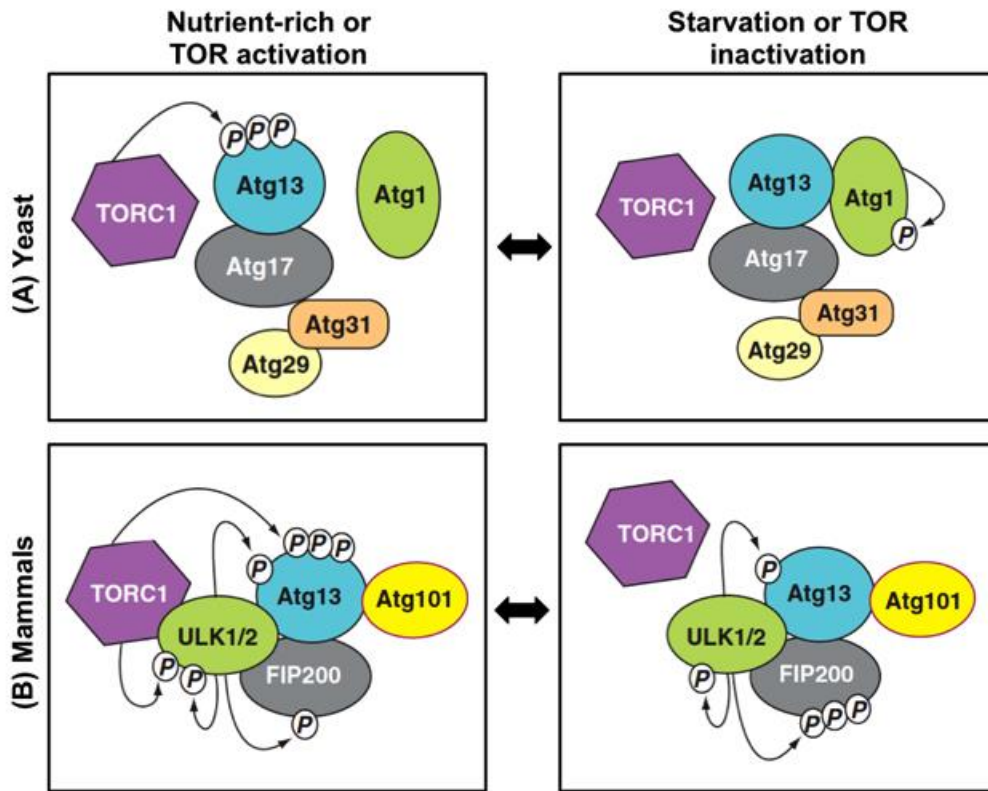


Figure 1.3 Regulation of Atg1 complexes by TORC1. (A) In yeast, the active target of rapamycin complex I (TORC1) hyperphosphorylates Atg13 and prevents the association of Atg1 with Atg13, Atg17, Atg31 and Atg29 to inhibit autophagy induction. Upon TOR inhibition, TORC1 no longer phosphorylates Atg13 and can associate with the Atg1 complex to promote autophagy. (B) In mammals, Ulk1/2 (the homologs of yeast Atg1) forms a stable, constitutive complex with Atg13, FIP200 (the mammalian homolog of Atg17) and Atg101. Activated mTORC1 associates with the ULK complex and phosphorylates ULK1 (or ULK2) and Atg13 to inhibit autophagy. Upon mTORC1 inhibition, mTORC1 dissociates from the ULK complex, leading to the dephosphorylation and activation of Atg13 and ULK1 (or ULK2) and autophagy induction. ULK1 (or ULK2) phosphorylates Atg13, FIP200 and itself at constant low levels and hyperphosphorylates FIP200 when activated. Taken and adapted from (Chen and Klionsky, 2011).

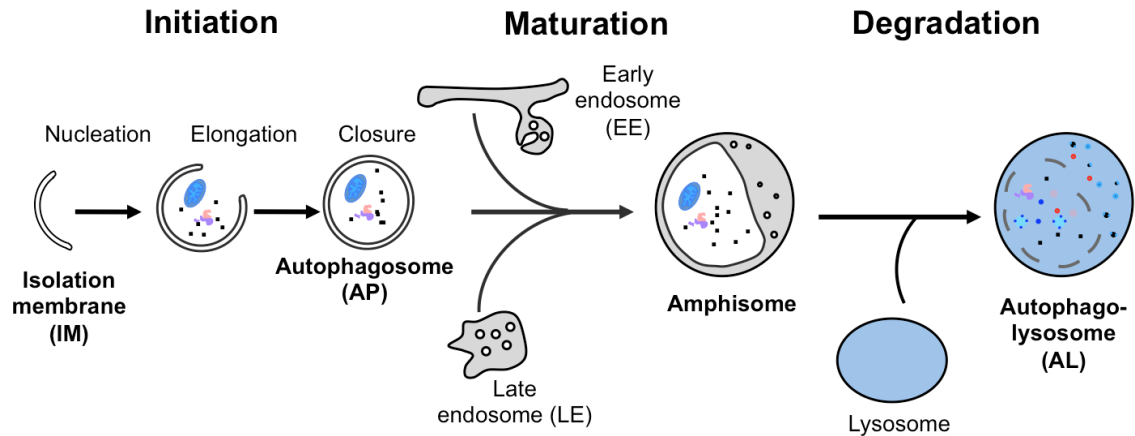


Figure 1.4 Schematic overview of the macroautophagy process. Autophagosome (AP) formation is a fundamental process in autophagy that depends on (i) an initiation step in which an isolation membrane (IM) cistern begins to wrap around the cytoplasm, (ii) an elongation step during which the membrane increases in size and (iii) a closure step in which the membrane seals around a section of the cytoplasm to form a double membrane AP. Unlike APs in yeast which directly fuse with the vacuole, APs of higher eukaryotes mature into amphisomes by fusing with endosomal organelles and then subsequently fuse with lysosomes to form autophagolysosomes (ALs). Once amphisomes have fused with the lysosomes, captured material is degraded by hydrolases and digested products are released into the cytosol for reuse by the cell.

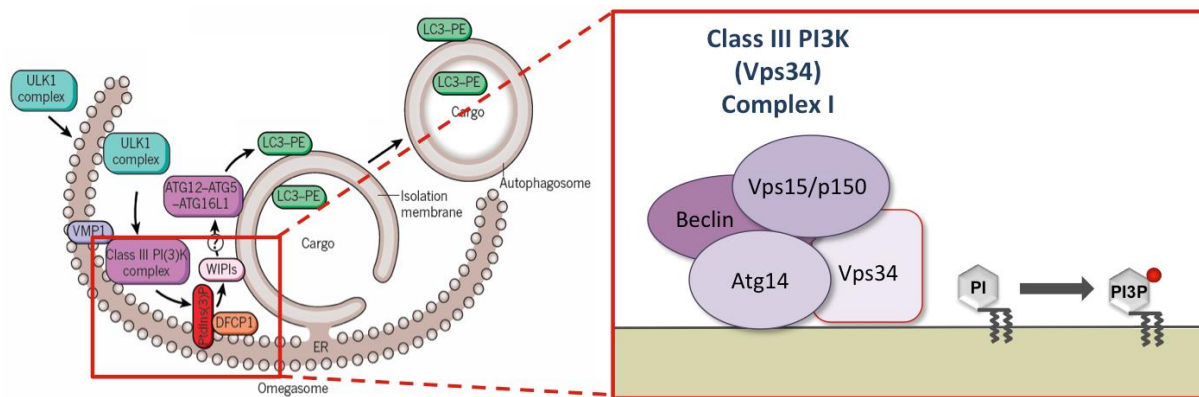
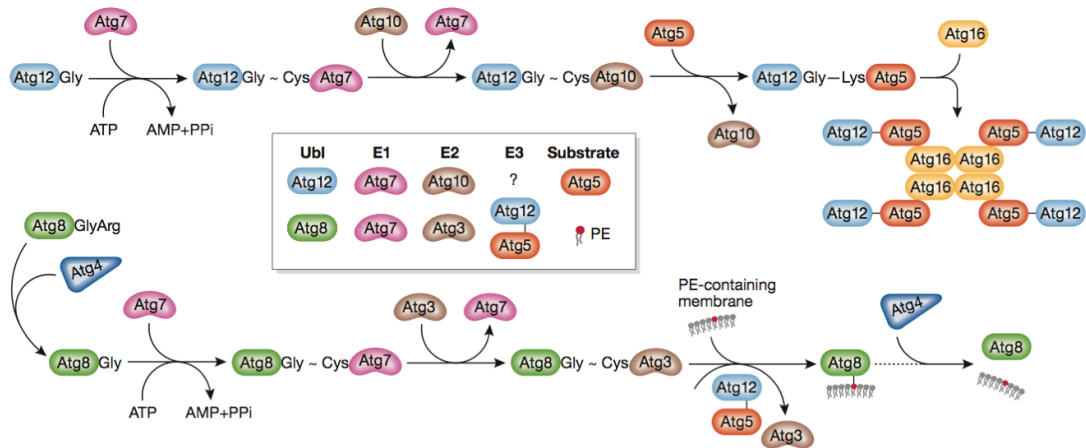


Figure 1.5 Schematic overview of autophagosome biogenesis. During mammalian autophagy, Ulk1/2 protein kinase complex (Ulk1/2, Atg13, FIP200) is activated and relocates to the site of AP nucleation. A core Vps34 complex consisting of Vps34, Beclin 1 (a homologue of yeast Vps30/Atg6), Vps15 and Atg14L is directed to the AP nucleation site along the ER membrane by Atg14L to promote local synthesis of PI3P and initiate AP biogenesis at subdomains of the endoplasmic reticulum (ER), termed “omegasomes” (for their omega-like shape). PI3P acts as a membrane platform to concentrate and spatially coordinate specific effectors, such as WIPI (the mammalian orthologue of Atg18) and DFCEP-1, which harbor PI3P-binding modules and are likely necessary for downstream signaling and the progression of autophagy. Taken and adapted from (Levine *et al.*, 2011).

(A)



(B)

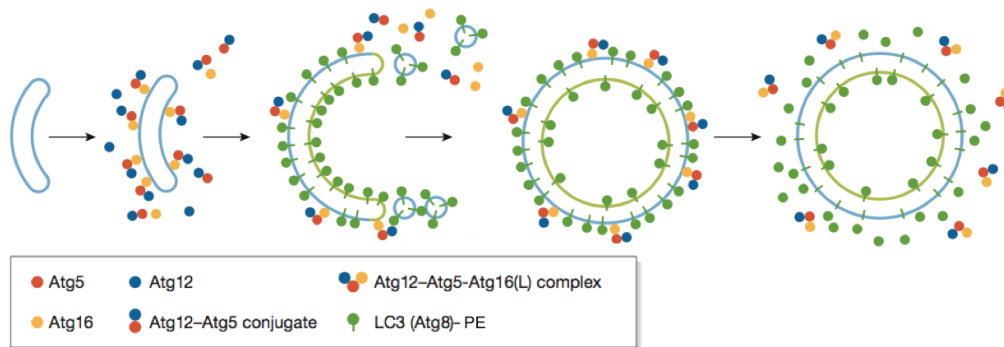


Figure 1.6 Atg12 and Atg8 ubiquitin-like conjugation systems in autophagy.

(A) Atg12 and Atg8 (the yeast homolog of mammalian LC3) are both ubiquitin-like proteins that undergo a series of enzymatic reactions similar to that of the ubiquitin system during autophagy. Atg12 possesses a C-terminal glycine residue required for conjugation; however, Atg8/LC3 must first undergo cleavage by Atg4 to expose its glycine residue prior to its conjugation. During autophagy, Atg12 and Atg8 are activated by an E1-like enzyme (Atg7) and are conjugated by an E2-like enzyme (Atg10 and Atg3, respectively) to either Atg5 or phosphatidylethanolamine (PE), respectively. Conjugated Atg5-12 interacts with Atg16L to form the Atg5-12-16 complex, which subsequently recruits Atg8 (LC3) and acts as an E3-like ubiquitin ligase that facilitates the conjugation of Atg8/LC3 to PE on the AP membrane. The addition of the PE moiety to Atg8/LC3 causes its conversion from a soluble Atg8/LC3-I form to a membrane bound Atg8-PE/LC3-II form. Atg4 proteolytically deconjugates Atg8/LC3 from PE to release it from the membrane. (B) Distribution of the Atg12 and Atg8 conjugation system on the AP during AP biogenesis. The Atg5-12-16 complex is recruited to the outer surface of the AP and directs Atg8 conjugation to phosphatidylethanolamine (PE) at this site. Atg8-PE/LC3-II? promotes the expansion of the AP membrane. Upon closure of the AP, the Atg5-12-16 complex dissociates and Atg4 proteolytically releases Atg8-PE from the external surface of the AP. Taken from (Geng and Klionsky, 2008).

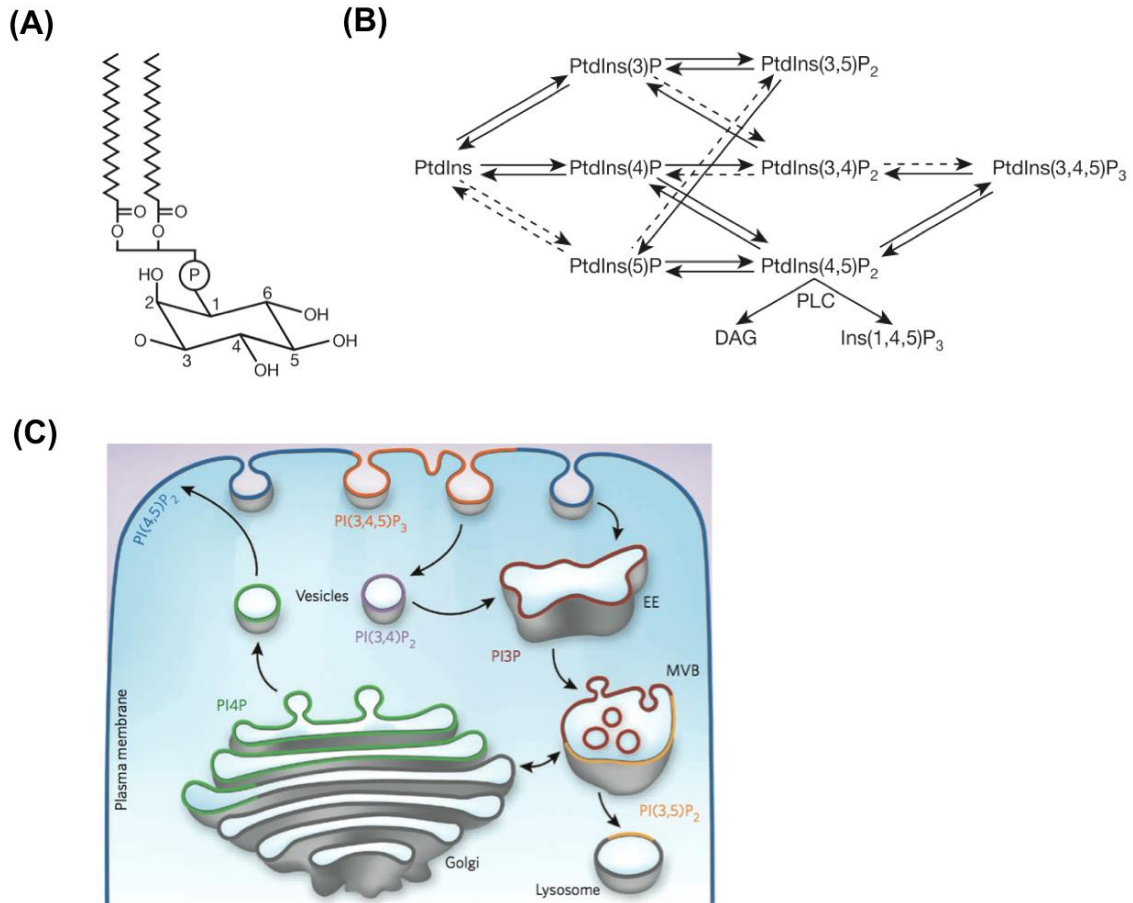


Figure 1.7 Metabolism and distribution of phosphoinositides. (A) Structure of phosphatidylinositol. (B) Metabolic reactions required to generate the seven phosphoinositide species. Reactions demonstrated *in vitro* are represented in broken arrows and their relevance in living cells still remains unclear. (C) Subcellular localization PI species. Taken from (Di Paolo and De Camilli, 2006; Kutateladze 2010).

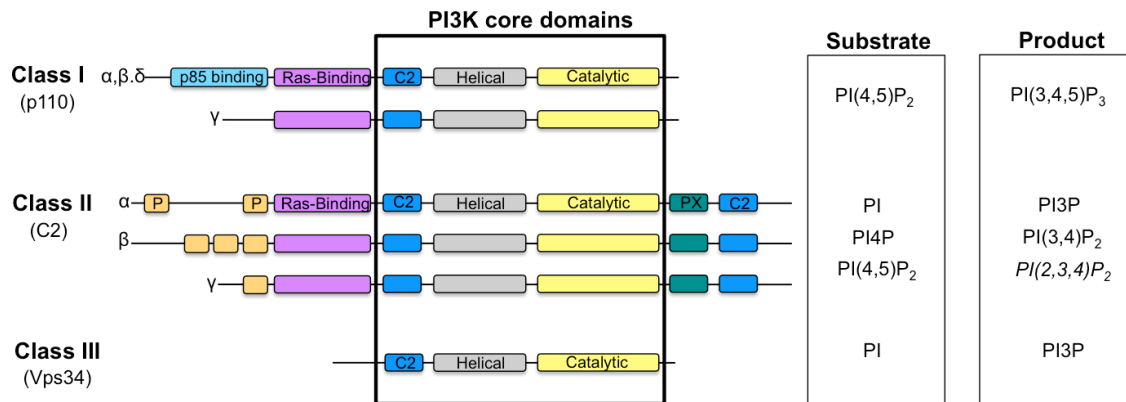


Figure 1.8 Domain structure of mammalian phosphoinositide 3-kinases (PI3Ks). All PI3Ks have a core structure consisting of a C2 domain, a helical domain and a catalytic domain and are grouped into three classes based on their substrate specificity and structure. Class I PI3Ks use PI(4,5)P₂ as a substrate and forms heterodimer with a regulatory subunit. Class II PI3Ks use PI as a primary substrate; however, the α isoform can also use PI4P in cells for certain functions. Both the class I and class II PI3Ks have N- extensions, which likely mediate protein-protein interactions. Additionally, the class II PI3K possesses a unique C-terminal extension that contains a second C2 domain and a phox homology (PX) domain. Class III PI3K (Vps34) uses PI as a substrate and requires binding to Vps15 for activation. Reactions in italics have only been demonstrated *in vitro*. Adapted from (Vanhaesebroeck et al., 2010).

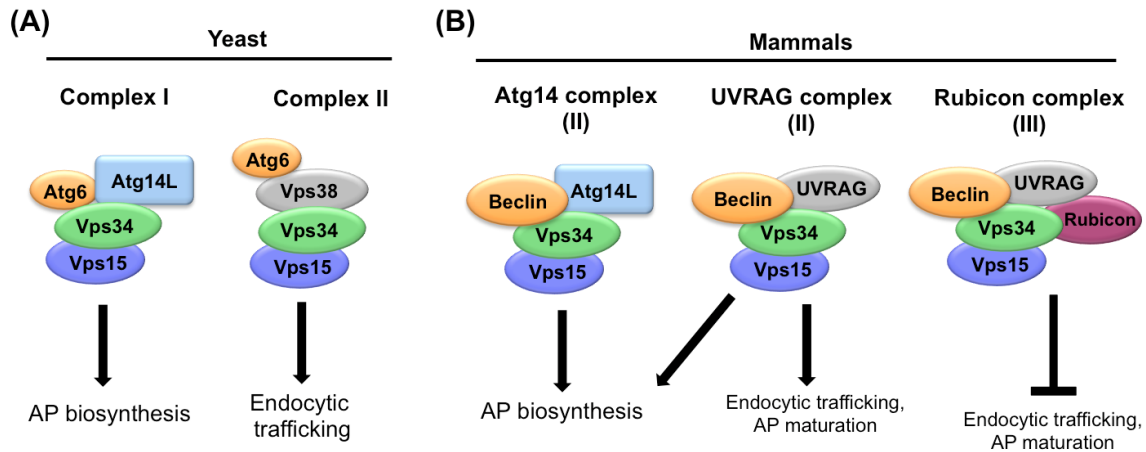


Figure 1.9 The major Vps34 complexes in yeast and mammals. (A) In yeast, complex I and II regulate autophagy and endocytic system, respectively. (B) In mammals, multiple complexes act at different stages of the autophagy process as well as in endocytic trafficking. Atg14L associates with the core Beclin1-Vps34-Vps15 to promote autophagosome formation (the mammalian equivalent of complex I). UVRAG binds Beclin in a mutually exclusive manner with Atg14 to form a complex with Beclin1-Vps34-Vps15 (the mammalian equivalent of complex II). The UVRAG complex is required for endosome function and AP maturation, although it has also been implicated in AP biogenesis as well. Lastly, a third major complex consists the UVRAG complex bound to Rubicon, which has been shown to inhibit autophagosome maturation. Adapted from (Funderbunk *et al.*, 2010).

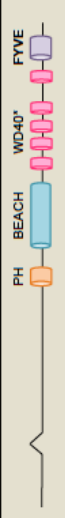






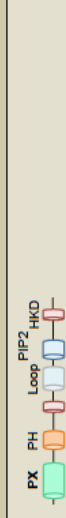







PI3P Effector	Interacting sequence	Autophagy-related function	Structure	Organism
Atfy	FYVE domain	Mediates selective degradation of protein aggregates and is not involved in starvation induced autophagy		Mammals
Atg14/Barkor	BATS domain	Required for AP formation during both basal and inducible autophagy; ATG14/Barkor forms a complex with Vps34, Vps15/p150 and Beclin		Mammals
Atg18/AUT10, CVT18/ SVP1	FRRG motif	Involved in the retrograde movement of Atg9 away from the PAS together with Atg2 and is required for AP formation		Yeast
Atg21	FRRG motif	Required for vacuole formation in the Cvt pathway		Yeast
Atg24/Snx4/ Cvt13p	PX domain	Required for Cvt and pexophagy		Yeast
DFCP1/ ZFYVE1	FYVE domain	ER resident protein that forms PI3P-dependent puncta during starvation-induced autophagy, although it is not essential for autophagy		Mammals
FYCO1/ ZFYVE7	FYVE domain	Mediates plus-end microtubule transport of APs to late endosomes/lysosomes and interacts with LC3 and Rab7		Mammals
Plkfyve	FYVE domain	PI3P 5-kinase that synthesizes PI(3,5)P2 and is required for the homeostasis of the endosomal system through membrane recycling; involved in the maturation of APs		Mammals
PLD1	PX domain	Involved in the biogenesis and maturation of APs; also mediates mTOR reactivation by amino acids after nutrient deprivation.		Mammals
TECPR1	PH domain	Tethering factor that binds to conjugated Atg5-12 and PI3P to promote AP-lysosome fusion; involved in selective autophagy of bacterial pathogens at the AP biogenesis and maturation steps		Mammals
Vam7	PX domain	t-SNARE targeted to vacuoles and involved in Cvt vesicle fusion		Yeast
WIPI1/WIPI149	FRRG motif	Recruited to omegasome to mediate the biogenesis of APs		Mammals
WIPI2	FRRG motif	Positively regulates the maturation of preautophagosomal structures into APs		Mammals
WIPI4/epg-5/ WDR45	LRRG motif	Negatively regulates the maturation of preautophagosomal structures into APs		C. elegans
Ygr223/HSV2	FRRG motif	Involved in piecemeal autophagy of the nucleus		Yeast

Table 1.1 Glossary of PI3P autophagy effectors. PI3P-binding modules/motifs (shown in bold) include: **BATS**, **Barkor/Atg14(L)** autophagosome targeting sequence; **FYVE**, protein present in **Fab1**, **YOTB**, **Vac1**, and **EEA1**; **PH**, pleckstrin homology domain; **PX**, **Phox** homology domain; **WD40**, defined as a core unit of approximately 40 amino acids ending with the residues tryptophan and aspartic acid which adopts a 7-bladed beta propeller fold containing a PI3P-binding **FRRG** or **LRRG** motif. In the case of **Alfy**, however, the individual **WD40** regions are shown (**WD40***) because it is unclear whether they adopt a beta propeller fold. Taken from (Dall'Armi et al., 2012).

Vps34 exon targeted	CRE	Cell/ Tissue KO	Genetic background	Autophagy type		Autophagy assays and results			PIP levels	Other	Lab of mouse origin	Ref.	
				Autophagy type	Aggregates	LCS puncta by IF	LCS-II by WB	PDA					EM
17-18 (ATP binding domain)	Adillin	Sensory neurons	Mixed	Basal	Increased ubiquitin	Increased LCS-GFP	Increased flux (chloroquine)	n.d.	AFs present	n.d.	Wang	Zhou et al., 2010.	
17-18 (ATP binding domain)	Lck	T-lymphocyte	n.m.	TCR complex stimulation with anti-CD3 and anti-CD28 (48hrs); Serum or amino acid starvation for 18hrs	Slight increase in p62	Unchanged	Unchanged	n.d.	AFs present	No change in ROS or mitochondria	Wang	McLeod et al., 2011.	
4	Adenovirus-CRE	MIEFs	C57BL/6	Starvation - serum free (6hrs)	Increased p62	Increased LCS-GFP puncta	LC3-II conversion, decreased flux (EGAD +PepA)	Total protein degradation decreased	EM not quantified, cytosolic LC3-GFP immuno-EM	Minimal DFCP1-RFP puncta	Decreased Atg12 recruitment		
	Alb	Hepatocytes		Basal and Fasted (24hrs)	Increased p62, ubiquitinated proteins	Increased LCS-GFP puncta	No flux assay, but increased LC3-I and II	n.d.	n.d.	n.d.	Increased mitochondria	Zong	Isaber et al., 2011
	Mck	Cardiomyocytes		Basal	Increased p62, ubiquitinated proteins	Increased LCS-GFP puncta	No flux assay, but increased LC3-I and II	n.d.	n.d.	n.d.	Increased mitochondria		
4	Cd4	T-lymphocyte	C57BL/6	TCR stimulation (24hrs)	Slight increase in p62	n.d.	LC3-II conversion, decreased flux (Bafilomycin)	n.d.	n.d.	n.d.	Flavell	Willinger et al., 2012	
4	Cd4	T-lymphocyte	C57BL/6	Basal; TCR stimulation (36hrs)	Increased p62	Increased	Increased LC3-II, but no autophagy by flux (EGAD)	n.d.	Cytosolic LC3B immuno-EM	n.d.	LC3 lipidation insensitive to wortmannin treatment	Zong	Parakh et al., 2013.
20-21 (kinase domain)	MDR1D	Lens	C57BL/6	Basal	Increased p62, ubiquitinated proteins	None observed	No flux assay, but increased LC3-I and II	n.d.	---	n.d.	Sasaki	Morishita et al., 2013	
17-18 (ATP binding domain)	Nphc2	Podocytes	n.m.	Basal	Increased p62	n.d.	No flux assay, but increased LC3-I and II	n.d.	Cytosolic LC3B immuno-EM	n.d.	Wang	Bechtel et al., 2013	
17-18 (ATP binding domain)	Lentivirus-CRE	MIEFs	Mixed	Starvation - HBSS/complete nutrient withdrawl (90mins)	Slightly increased, enhanced with prolonged KO	Decreased	Decreased flux (Bafilomycin)	50% decrease in macroautophagy	APs/ALs present, but fewer	Some WIPI-1-GFP puncta; 65% decrease in P13P by HPLC analysis	Wang	Dovergow et al., 2013; this thesis	

Table 1.2 Summary of autophagy findings in Vps34 conditional knock-out mouse models. Abbreviation include: n.d., not determined; n.m., not mentioned; IF, immunofluorescence; EM, electron microscopy; PDA, protein degradation assay.

Table 1.2 Summary of autophagy findings in Vps34 conditional knock-out mouse models

Chapter 2: Regulation of mammalian autophagy by class II and III PI 3-kinases through PI3P synthesis

2.1 Results

2.1.1 Generation of Vps34 knock-out MEFs.

To investigate the contribution of Vps34 to starvation-induced autophagy, $Vps34^{Flox/Flox}$ MEFs were generated and characterized. $Vps34^{Flox/Flox}$ MEFs were immortalized by multiple passages and infected with lentiviruses expressing either a catalytically-inactive or active, nuclear Cre recombinase fused to eGFP (green) or tdTomato fluorescent protein (red) to generate control and $Vps34$ KO cells, respectively (see Materials and Methods). Expression of active Cre, but not inactive Cre, resulted in the progressive loss of Vps34 immunoreactivity by Western blot analyses over the course of several days with complete loss of expression reproducibly achieved by 9 to 10 days (Fig. 2.1A,B).

Importantly, although exons 17 and 18 were targeted, antibodies directed to the very NH₂-terminus of Vps34 (*i.e.*, amino acids 1-40) did not reveal any truncated fragments of Vps34 at day 10 post-infection (Fig. 2.1C). This finding together with the original analysis of $Vps34$ mRNA in Cre-expressing $Vps34^{Flox/Flox}$ tissue (Zhou et al., 2010) confirms that this targeting strategy successfully produces a *null* mutant.

2.1.2 Characterization of Vps34 KO MEFs and their autophagy machinery.

To begin to characterize the $Vps34$ KO MEFs, various cellular compartments and levels of relevant autophagy and endosomal proteins were assessed. When membranous organelles were examined by immunofluorescence, no major alterations of the ER, Golgi

complex and lysosomes were found at day 10 post-infection based on the immunofluorescent analysis of protein disulfide isomerase (PDI), giantin, and LAMP1, respectively (Fig. 2.2A). There was, however, an enlargement of the EEA1-positive early endosomal compartment, consistent with other studies (Futter et al., 2001a; Johnson et al., 2006; Morel et al., 2013; Zhou et al., 2010) (Fig. 2.2A). Notably, prolonged ablation of Vps34 for an additional 4-5 days (day 14-15 post-infection) consistently resulted in cell vacuolization (Fig. 2.2B), a breakdown of the lysosomal compartment (as evidenced by an aberrant LAMP1 compartment) (Fig. 2.2B) and impaired lysosomal degradation of the EGF receptor in response to EGF stimulation (Fig. 2.2C). These features, which have been reported elsewhere (Jaber et al., 2012a; Johnson et al., 2006), reflect the reduced viability resulting from the chronic loss of Vps34, a factor potentially confounding the analysis of the physiological function of Vps34 in autophagy. We thus focused our analysis at 10 days post-infection prior to the breakdown of the endolysosomal system.

Additionally, we examined levels of relevant autophagy and endosomal proteins in *Vps34* KO MEFs. Ablation of Vps34 resulted in a significant decrease in levels of Vps34 complex members, including Vps15/p150 and Beclin-1, as previously reported (Willinger and Flavell, 2012), as well as Atg14L and UVRAG. In contrast, Rubicon, a negative regulator of Vps34 (Matsunaga et al., 2009; Zhong et al., 2009), showed increased levels in the KO. Levels of proteins operating in the endosomal pathway were also assessed and no changes were found in the expression levels of the retromer subunits Vps26 and Vps35 or Rab5, although EEA1 levels were slightly decreased (Fig. 2.3). These data indicate that Vps34 ablation results in the destabilization of molecular

components previously reported to associate with Vps34 complexes as well as the endosomal PI3P effector, EEA1.

2.1.3 Steady-state and starvation-induced PI3P is detected in *Vps34* KO MEFs.

To quantitatively determine the amount of PI3P produced by Vps34, phosphoinositides were measured in control and *Vps34* KO MEFs. For such large scale biochemical studies, control and *Vps34* KO cells were generated from *Vps34*^{Flox/Flox} Cre-ER MEFs (see Materials and Methods). Specifically, cells were radiolabeled with [³H] *myo*-inositol, high performance liquid chromatography (HPLC) was performed and phosphoinositide levels were detected by radioactivity. We found a ~65% decrease in PI3P levels in *Vps34* KO MEFs relative to controls and no obvious alterations in other inositol lipids levels detected by the assay, such as PI, PI4P and PI(4,5)P₂ (see also Fig. 2.12). Therefore, we conclude that in our fibroblasts, Vps34 accounts for the majority of cellular PI3P levels and that ~35% of this lipid can be synthesized through alternate pathways.

Additionally, we detected intracellular PI3P using fluorescence microscopy. Historically, the detection and localization of intracellular PI3P has relied on the use of the FYVE domain (*i.e.*, a zinc finger originally identified in **F**ab1, **Y**OTB, **V**ac1p, **E**EA1) as a genetically-encoded or purified PI3P-binding probe (Raiborg et al., 2013; Stenmark and Aasland, 1999; Stenmark et al., 1996). The first of these biosensors consisted of a tandem FYVE domain from Hrs (2xFYVE^{Hrs}) which showed PI3P concentrated on the limiting and intraluminal membranes of endosomes (Gillooly et al., 2000). Here control and *Vps34* KO MEFs were transiently transfected with RFP-2x-FYVE^{Hrs}. In control MEFs, RFP-2x-FYVE^{Hrs} localized to vesicular structures, consistent with previous studies showing PI3P on endosomes (Gillooly et al., 2000). In contrast, the RFP-2x-

FYVE^{Hrs} fluorescent signal was largely diffuse in *Vps34* KO MEFs, which is also observed upon treatment with wortmannin and in MEFs where *Vps15*, the lipid kinase regulator of *Vps34*, is knocked out (Gillooly et al., 2000; Nemazanyy et al., 2013). In order to improve the sensitivity and threshold of PI3P detection knowing that other pathways synthesize ~35% of the total PI3P, a high affinity 4xFYVE^{Hrs} probe was generated, based on the work of others suggesting that combining multiple FYVE domains may enhance PI3P detection or sequestration through an avidity effect (Bohdanowicz et al., 2010). In fact, transfection with the GFP-4x-FYVE^{Hrs} probe produced a more robust signal and revealed a pool of PI3P underestimated by the traditional 2x-FYVE probes in *Vps34* KO MEFs. Importantly, the 4x-FYVE^{Hrs} clearly confirmed PI3P synthesis occurs via other pathways (Fig. 2.4).

Next, we wanted to assess whether PI3P synthesis still occurred during starvation-induced autophagy in *Vps34* KO MEFs. As mentioned previously, PI3P plays an important role in recruiting PI3P effectors to the site of AP biogenesis. WD repeat domain phosphoinositide-interacting proteins (WIPI-1 and 2), mammalian orthologues of yeast Atg18, are a major family of PI3P-binding effectors that localize to the site of nucleation and promote AP formation; therefore, they are often used to monitor PI3P synthesis during autophagy (Proikas-Cezanne et al., 2007; Proikas-Cezanne et al., 2004). Here, GFP-WIPI-1 was transiently transfected in control and *Vps34* KO MEFs and its localization examined under normal media and starvation conditions (HBSS for 90min). As previously observed, GFP-WIPI-1 remained largely soluble under normal media, basal autophagy conditions (data not shown) and formed punctate structures in control

cells during starvation (Proikas-Cezanne et al., 2007) (Fig. 2.5). In *Vps34* KO MEFs, an ~80% and ~30% reduction in the number and size of GFP-WIPI-1 puncta was observed during starvation compared to control MEFs, respectively (Fig. 2.5). Importantly, however, some WIPI-1 recruitment still occurred in the absence of *Vps34*, suggesting that PI3P production during autophagy may occur through other synthesis pathways, such as the class II PI3Ks.

2.1.4 Autophagosome formation is reduced, but not abolished in *Vps34* KO MEFs.

Since PI3P still formed in the absence of *Vps34*, we investigated the ability of *Vps34*-deficient cells to form and clear APs in response to nutrient deprivation by measuring LC3 lipidation. Activation of autophagy results in the conversion of LC3-I to its lipidated form LC3-II, a process that can be monitored by Western blot analysis. Experiments are typically performed under normal media and starvation conditions in the presence or absence of proton pump blocker Bafilomycin A1 (Baf), which blocks the acidification of lysosomes and thus the clearance of APs and enables the assessment of autophagic flux. Levels of LC3-II were similarly low in both control and *Vps34* KO cells under basal conditions (Nm), although more LC3-II was apparent in control cells after the addition of Baf (Nm+B), suggesting a slightly higher rate of basal autophagy. While LC3-II levels remained low with no genotype-specific differences after nutrient deprivation (St) for 90 min, changes in autophagic flux were observed after the addition of Baf into the starvation media (St+B). Specifically, a more robust increase in the levels of LC3-II was seen in control cells (~3.3-fold) compared to *Vps34* KO cells (~2.5-fold), suggesting a decline in the rate of AP biogenesis in the absence of *Vps34* in response to starvation

(Fig. 2.6A). This result suggests that while Vps34 may be an important modulator of autophagy, it is not essential for starvation-induced autophagy.

Additionally, endogenous LC3 localization was examined by confocal microscopy during starvation-induced autophagy. Under normal media conditions, LC3 immunofluorescence displayed a predominantly diffuse distribution with few basal LC3-positive compartments in control and Vps34-deficient cells. After 30 min starvation, LC3 was recruited to APs and an ~8-fold increase in the average number of fluorescent LC3 puncta was observed in control MEFs, whereas a less robust, ~4-fold increase was observed in *Vps34* KO MEFs. A more prolonged, 90 min starvation produced comparable results (Fig. 2.6B,C). Levels of p62, an AP cargo, as well as its relationship with the LC3 compartment were also examined by immunofluorescence. In control MEFs, the baseline number of p62 puncta was low under normal media conditions, transiently increased by ~2.5-fold after 30 min of starvation, but then returned back to basal levels by 90 min. Likewise, the amount of co-localization between LC3 and p62 increased at 30 min and then returned to basal levels at 90 min as clearance of p62 by APs occurred over time. In contrast, the number of p62 puncta was 2.5-fold higher in *Vps34* KO MEFs under normal media compared to control cells and remained largely unaffected by starvation. Although the co-localization between p62 and LC3 significantly increased in the *Vps34* KO cells after 30 min starvation, the higher co-localization persisted after 90 min (Fig. 2.6B,C). Altogether, our results suggest that LC3 can still be mobilized in response to autophagy stimulation in Vps34-deficient MEFs, but not as efficiently as in control MEFs. Also, given the persistent increase in p62 observed in the *Vps34* KO MEFs, it seems that

although autophagy may be occurring in the absence of Vps34, levels are suboptimal for the efficient clearance of this cargo.

To more quantitatively compare APs and autophagolysosomes (ALs) in control and Vps34-deficient cells, standard electron microscopy (EM) was performed. Under basal conditions, APs and ALs were rarely observed, and no genotype-specific differences were found (Fig. 2.7A-C). Starving cells for 30 min caused an increase both in the number and total surface area covered by APs and ALs with no genotype-specific differences. The number and surface area of APs and ALs further increased after 90 min, but not as robustly in *Vps34* KO MEFs. The average size of APs and ALs also continued to increase with prolonged starvation, but was not affected by the genotype (Fig. 2.7B,C). Finally, immunogold-EM using an anti-LC3 revealed that APs observed upon starvation in Vps34-deficient cells are decorated with gold particles indistinguishably from control cells (Fig. 2.7D), indicating that LC3 is normally recruited to the AP membranes in the absence of Vps34. These data confirm that ablation of Vps34 does not prevent the formation of APs and ALs, but does result in the generation of fewer autophagic vacuoles in response to nutrient deprivation, consistent with the light microscopic observations.

2.1.5 Vps34 mediates approximately half of autophagic protein degradation.

Given that LC3 conjugation and APs and ALs were still observed in *Vps34* KO cells, it was important to assess the functionality of the remaining autophagy. A [¹⁴C]-valine-labeled long-lived protein assay was performed in the presence of PI3K inhibitors (3MA or wortmannin) to inhibit autophagy, or the weak base ammonium chloride to inhibit lysosomal degradation, allowing us to determine the contribution of (macro)autophagy to

the overall lysosomal degradation (see Materials and Methods). Since 3MA and wortmannin are generally thought to block autophagy by targeting Vps34, it was first necessary to determine whether this was, in fact, the case. Both 3MA and wortmannin dramatically reduced the lipidation of LC3 during starvation in both control and *Vps34* KO MEFs in the presence and absence of Baf (Fig. 2.8A,B). This finding demonstrated that these drugs have additional autophagy-relevant targets besides Vps34 and can, therefore, still be used to effectively block (macro)autophagy in *Vps34* KO MEFs. Here, we observed a 50% decrease in total starvation-induced proteolysis in *Vps34* KO MEFs by protein degradation assay (Fig. 2.9A). Importantly, the 3MA-inhibitable component of lysosomal protein degradation, which corresponds to (macro)autophagy, was reduced by ~50% in *Vps34*-deficient MEFs upon nutrient deprivation, accounting for this significant decrease in total lysosomal protein degradation (Fig. 2.9B). In contrast, *Vps34* ablation only caused a decreasing trend in protein degradation through the microautophagy and/or chaperone-mediated autophagy pathways, suggesting that these lysosomal functions are not affected by the lack of *Vps34* at this time-point of study (Fig. 2.9B). Therefore, the reduction in autophagy function upon acute deletion of *Vps34*, most likely reflects a decrease in overall autophagosome number at Day 10 rather than impaired autophagosome clearance. However, prolonged ablation of *Vps34* results in the progressive accumulation of p62 by Western blot analysis and immunofluorescence, possibly due to both reduced autophagy efficacy and a progressive decline in lysosomal function (Fig. 2.10A,B).

2.1.6 Class II PI3Ks contribute a pool of PI3P in MEFs.

After establishing that functional autophagy still occurs in *Vps34* KO MEFs, we determined the contribution of PI3P synthesis by class II PI3Ks. Phosphoinositide levels were measured as described above (see Materials and Methods). Control and *Vps34* KO cells were treated with mock siRNA or both PI3K-C2 α and β siRNAs (the third isoform, PI3K-C2 γ , appears to be mostly expressed in the liver (Falasca and Maffucci, 2012)). PI3K-C2 α and β expression was consistently abolished after 48hrs of PI3K-C2 α/β siRNA treatment with no major impact on *Vps34* levels (Fig. 2.11). Interestingly, silencing of class II PI3Ks in control and *Vps34* KO cells caused a comparable relative decrease in the overall levels of PI3P. Specifically, we observed a ~20% decrease in PI3P levels in control cells treated with PI3K-C2 α/β siRNA as compared to mock siRNA (Fig. 2.12). Likewise, an additional ~15% reduction in PI3P levels was observed when the class II PI3Ks were silenced in the *Vps34* KO background (Fig. 2.12). Taken together, we conclude that the contributions of *Vps34* and class II PI3Ks to total PI3P levels are additive and non-compensatory. Additionally, we observed that class II PI3Ks produces approximately half of the amount of PI3P produced in *Vps34* KO MEFs.

2.1.7 Class II PI3Ks positively regulate autophagy.

Since lack of *Vps34* did not abolish autophagy and PI3P production, we next tested whether class II PI3Ks could be an additional source of PI3P required to promote AP biogenesis. To determine whether PI3K-C2 α/β may be regulating autophagy through PI3P production, we examined GFP-WIPI-1 puncta formation upon silencing of the PI3K-C2 α/β isoforms in starved control cells (Fig. 2.13A). Silencing of PI3K-C2 α/β

caused a ~30% decrease in the number of GFP-WIPI-1 puncta (Fig. 2.13A), compared to the ~80% decrease observed in the *Vps34*-deficient cells (Fig. 2.5), which seemingly accounts for the totality of WIPI-1 puncta in response to starvation. Thus, although the contribution of the class II PI3Ks to the formation of WIPI-1 puncta is quantitatively minor relative to that of *Vps34*, they appear to be significant modulators of autophagy through production of PI3P. We next examined the effect of the class II PI3Ks on LC3 localization during starvation-induced autophagy by siRNA silencing of PI3K-C2 α / β isoforms in control and *Vps34* KO MEFs (Fig. 2.11). Under normal media conditions, a trend for a decrease in LC3 puncta number was observed upon siPI3K-C2 α / β -treatment of control MEFs (Fig. 2.13B). While minor differences were observed during starvation for 30 min, changes in autophagic flux became more apparent in the presence of Baf (Fig. 2.13B, 2.14). Indeed, knocking down class II PI3Ks in control MEFs produced a ~40% decrease in the number of LC3-positive puncta in response to a 30 min starvation period in the presence of Baf, a decrease of the same magnitude as that achieved by knocking out *Vps34* (Fig. 2.13B). When *Vps34*-deficient cells were treated with PI3K-C2 α / β siRNAs, the number of LC3 puncta was further decreased relative to siPI3K-C2 α / β -treated control or *Vps34* KO MEFs (Fig. 2.13B). We also observed a decrease in LC3 puncta size in siPI3K-C2 α / β -treated control MEFs that was exacerbated by the absence of *Vps34* (Fig. 2.13B). While silencing of class II PI3Ks in control and *Vps34* KO MEFs did not prevent LC3 lipidation in response to starvation, an increase in p62 was observed in *Vps34* KO MEFs treated with PI3K-C2 α / β siRNA, suggesting class II PI3Ks may be

playing a positive regulatory role in autophagy (Fig. 2.13C). Importantly, these results indicate that PI3K-C2 α/β positively regulate autophagy in addition to Vps34.

2.1.8 Initial characterization of the PI3K-C2 α and β in autophagy.

After establishing a role for PI3P synthesis by the class II PI3K in autophagy, our goal was to determine how the PI3K-C2 α and β fit into the autophagy signaling network.

Given that Vps34 and PI3K-C2 α and β are in the same PI3K family, they possess structural homology and may share common interactors important for their regulation of autophagy (Falasca and Maffucci, 2012; Vanhaesebroeck et al., 2010). The conserved C2 domain of Vps34 has been shown to directly interact with the central coil-coil domain (CCD) and evolutionarily conserved domain (ECD) domains of Beclin 1 (Funderburk et al., 2010; Furuya et al., 2005); therefore, we tested whether PI3K-C2 α and β could also form a complex with Beclin 1. An immunoprecipitation experiment using an anti-Beclin 1 antibody was performed in control MEFs. Consistent with previous observations (Furuya et al., 2005; Kihara et al., 2001b), Vps34 was efficiently coimmunoprecipitated with Beclin-1 (Fig. 2.15). In contrast, only a trace amount of PI3K-C2 α and β was coimmunoprecipitated with Beclin-1. These results indicate that while Vps34 binds to and forms a complex with Beclin-1 in a near stoichiometric manner, PI3K-C2 α and β do not significantly interact with Beclin-1 and are thus likely to modulate autophagy in a different complex from that of Vps34.

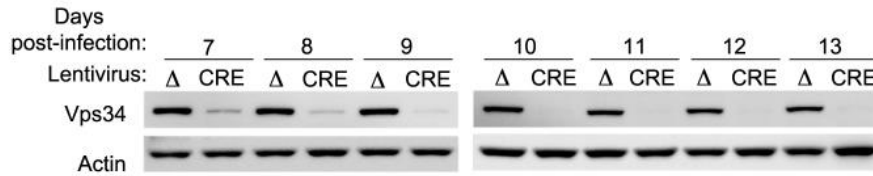
Next, co-localization studies were performed between PI3K-C2 α and β and markers of autophagy. Due to antibody limitations, PI3K-C2 α -HA or PI3K-C2 β -MYC constructs were transiently transfected into MEFs in order to assess their localization with

anti-tag antibodies. Cells were cultured under normal media or starvation conditions (St; HBSS for 90min), fixed and immunostained with the appropriate antibodies. By confocal microscopy, a partial co-localization was observed between PI3K-C2 α -HA or PI3K-C2 β -MYC and LC3 under starvation conditions (Fig. 2.16). Interestingly, very little co-localization was observed between PI3K-C2 α -HA and Beclin-1-FLAG, while higher levels of co-localization was seen between PI3K-C2 β -MYC and Beclin-1-FLAG upon starvation-induced autophagy, suggesting that there may be isoform differences in autophagy regulation (Fig. 2.16). Notably, we observed a striking redistribution of PI3K-C2 α -HA from a juxtannuclear to a more peripheral position when autophagy was induced. This pattern of PI3K-C2 α re-localization during autophagy is reminiscent of that of Atg9, a transmembrane protein that predominately localizes to the *trans*-Golgi network (TGN) under basal conditions, but redistributes to the peripheral endosomal system during autophagy (Webber and Tooze, 2010b; Young et al., 2006). Therefore, we examined the co-localization between PI3K-C2 α -HA, Atg9 and Giantin (a marker of the TGN) under normal media and 90 min of starvation condition (Fig. 2.17). In fact, we observed some co-localization between PI3K-C2 α -HA, Atg9 and Giantin under normal media conditions. During starvation, co-localization of PI3K-C2 α -HA and Atg9 with Giantin diminished as both proteins moved to peripheral sites, whereas co-localization between PI3K-C2 α -HA and Atg9 persisted (Fig. 2.17). These preliminary data indicate that although Vps34 and the class II PI3K both synthesize PI3P during autophagy, they likely act in mechanistically different ways. In fact, there may be isoform specific differences in how PI3K-C2 α and β are regulated and participate in autophagy. Further investigation is

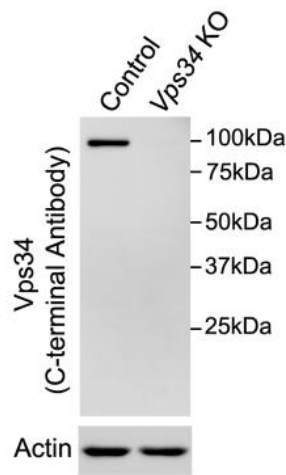
still required however to elucidate the role(s) of PI3K-C2 α and β in the autophagy pathway.

2.2 Figures

A



B



C

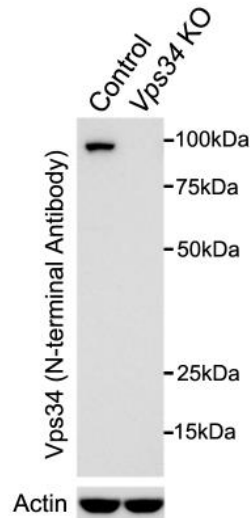


Figure 2.1 Vps34 ablation in $Vps34^{Fllox/Fllox}$ MEFs infected with CRE lentivirus. (A) Western blot analysis showing a time-course of Vps34 protein levels in $Vps34^{Fllox/Fllox}$ MEFs infected with lentiviruses expressing either an inactive Cre (Δ) or active (CRE) full-length Cre recombinase for 7-13 days. (B) Western blot using antibodies directed to the COOH-terminus of Vps34 in control and $Vps34$ KO cell extracts. (C) Western blot using an antibody directed to the NH2-terminus of Vps34 in control and $Vps34$ KO cell extracts.

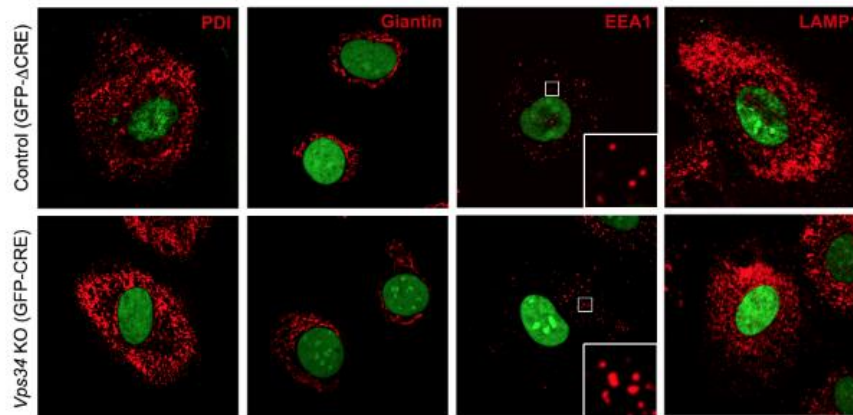
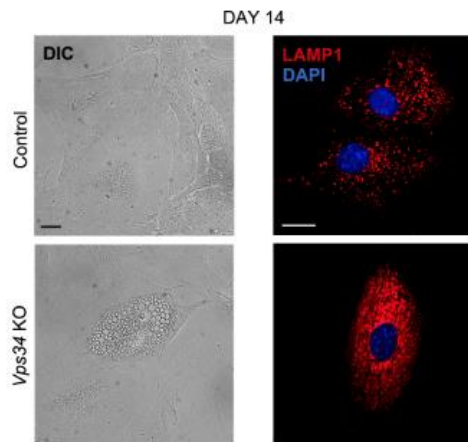
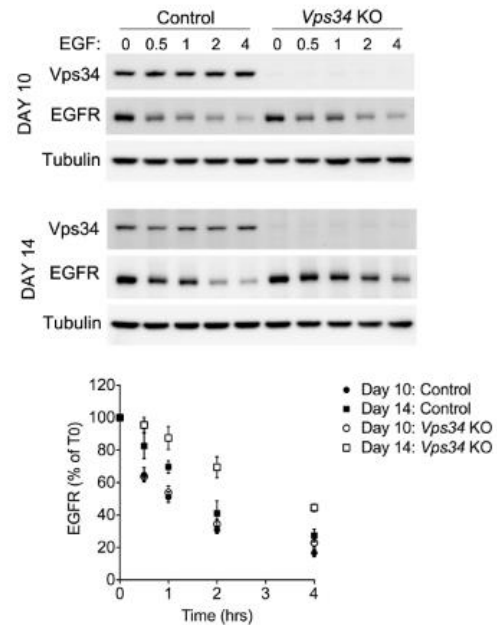
A**B****C**

Figure 2.2 Acute and chronic loss of Vps34 differentially affects the endo-lysosomal system. (A) Confocal analysis of control and *Vps34* KO MEFs immunostained for the following organelle markers: PDI, Giantin, EEA1 and LAMP1 (red). Nuclear inactive and active GFP-CRE is shown in green. Scale bar: 10 μ m. (B) Right: DIC image of control and *Vps34* KO cells on day 14 post-infection. Left: Confocal analysis of LAMP1, a late endosomal/lysosomal marker, immunostaining (red) in control and *Vps34* KO MEFs on day 14 post-infection. DAPI is shown in blue. Scale bar: 10 μ m. (C) Western blot analysis of Epidermal Growth Factor Receptor (EGFR) degradation in control and *Vps34* KO MEFs on day 10 and day 14 post-infection. MEFs were serum starved overnight and stimulated with EGF (100ng/ml) for the indicated times. EGFR protein level is quantified relative to tubulin and represented as a percent EGFR at time 0 (n=4 and 3 for day 10 and 14, resp.).

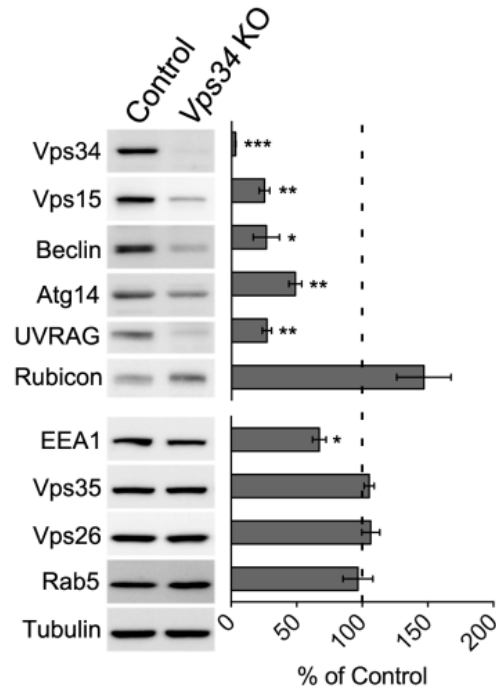


Figure 2.3 Ablation of Vps34 alters levels of Vps34 complex proteins. Western blot analysis of Vps34 complex components and endosomal protein levels in control and *Vps34* KO MEF lysates. Quantification of protein levels after normalization to tubulin (n=3).

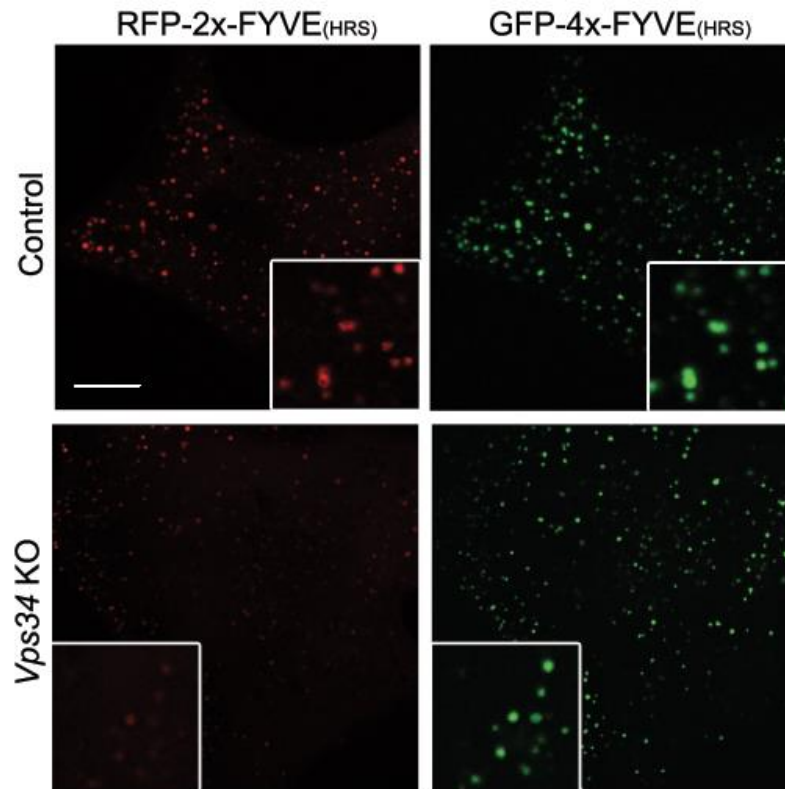


Figure 2.4 A higher affinity PI3P-binding probe, 4x-FYVEHrs, reveals a larger pool of intracellular PI3P in the absence of Vps34 compared to the conventional 2x-FYVEHrs probe. Control and *Vps34* KO MEFs were transiently transfected with both RFP-2x-FYVEHrs and GFP- 4x-FYVEHrs PI3P-binding constructs for 24hr, grown in normal media and fixed. Confocal microscopy analysis of RFP-2x-FYVEHrs (red) and GFP-4x-FYVEHrs (green) is shown. Scale bar: 10 μ m.

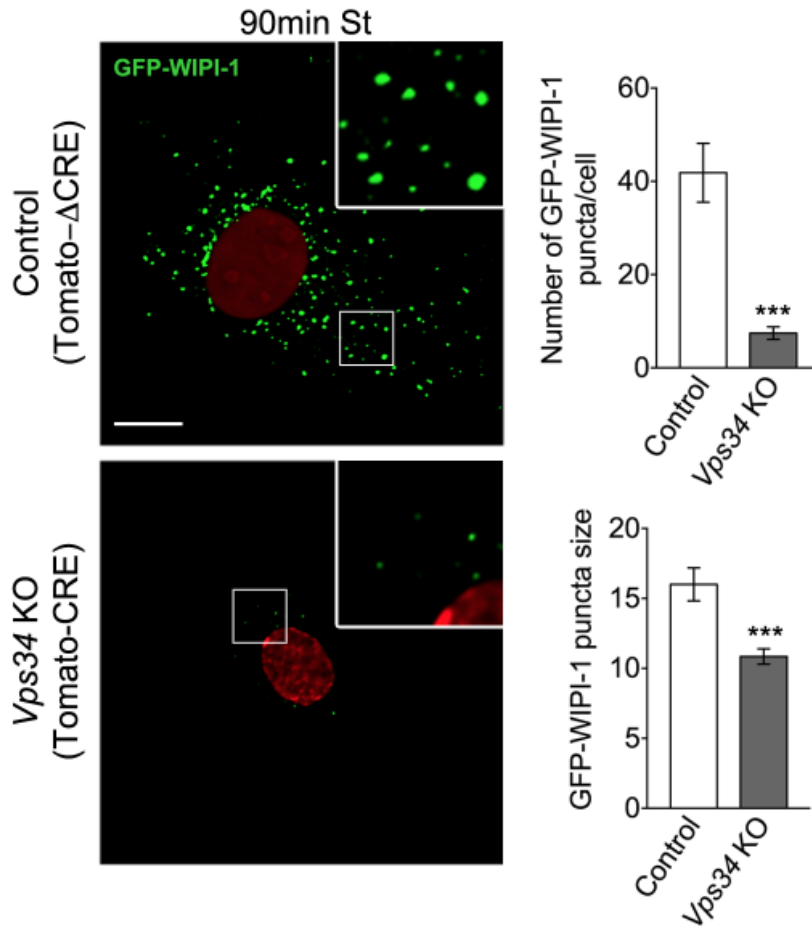


Figure 2.5 Recruitment of WIPI-1, a PI3P-binding protein, to sites of AP biogenesis occurs in *Vps34* KO MEFs but at diminished levels. Control and *Vps34* KO MEFs were transiently transfected with GFP-WIPI-1 for 24 hrs, cultured in HBSS for 90 min (90 min St) and fixed. Left: Confocal microscopy analysis of GFP-WIPI-1 fluorescence (green). Nuclear inactive and active Tomato-Cre is shown in red. The contrast was enhanced to reveal the WIPI puncta over the cytosolic background fluorescence. Right: Quantification of the number of GFP-WIPI-1 puncta (n=13-15 cells). Scale bar: 10 μ m.

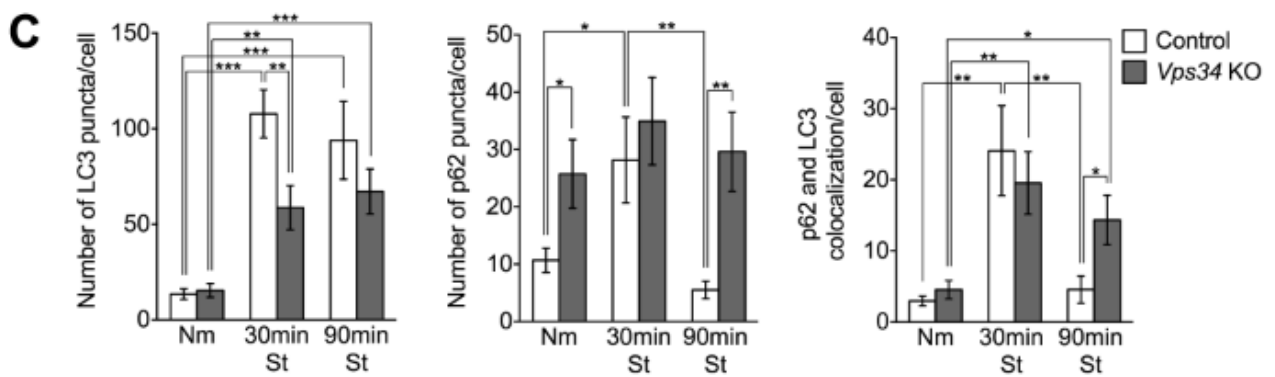
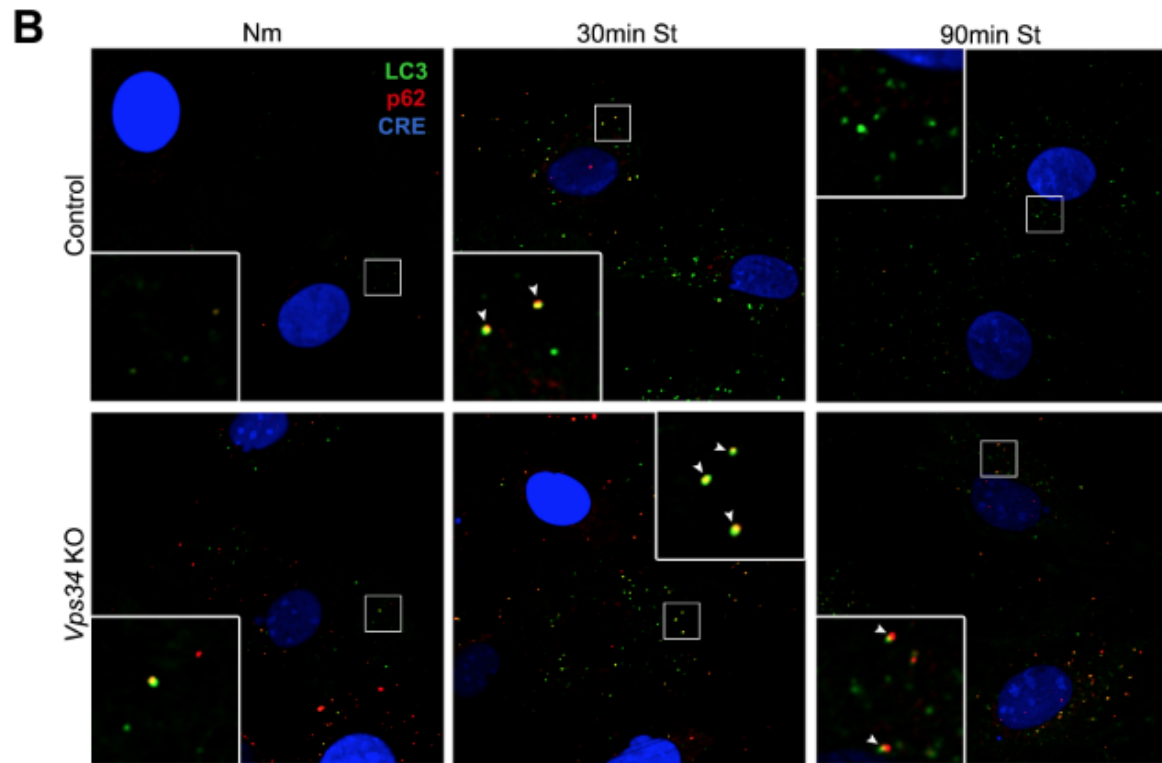
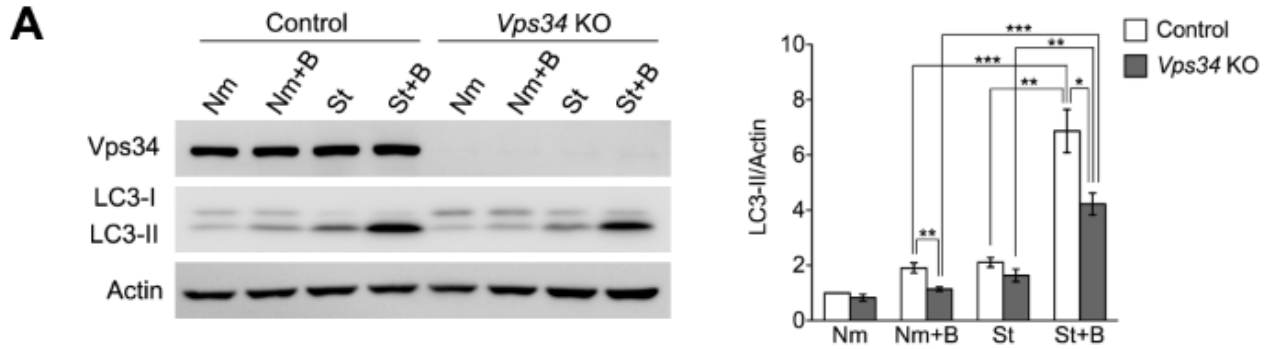


Figure 2.6 *Vps34* KO MEFs show a decrease in LC3 conjugation and LC3 puncta formation upon starvation. (A) Control and *Vps34* KO MEFs were cultured in normal medium (N) or HBSS (St) in the presence or absence of 50nM Bafilomycin (Nm+B or St+B, respectively) for 90 min. Right: Lysates were analyzed by immunoblotting using the indicated antibodies. Left: Relative LC3-II levels normalized to actin (n=4). **(B)** Control and *Vps34* KO MEFs were cultured in normal media (Nm) or HBSS (St) for 30 and 90 min, fixed and immunostained. Confocal analysis of LC3, p62 and GFP-Cre fluorescence, which is artificially shown in green, red and blue colors, respectively. Arrowheads indicate LC3 and p62 colocalization (yellow). Scale bar: 10 μ m. **(C)** Quantification of the number of LC3 (left panel) and p62 puncta (middle panel) per cell. Colocalization of p62 with LC3 puncta is also shown (right panel) (colocalization was defined as the number of pixels overlapping in the p62 and LC3 channels normalized per cell) (n=35-45 cells).

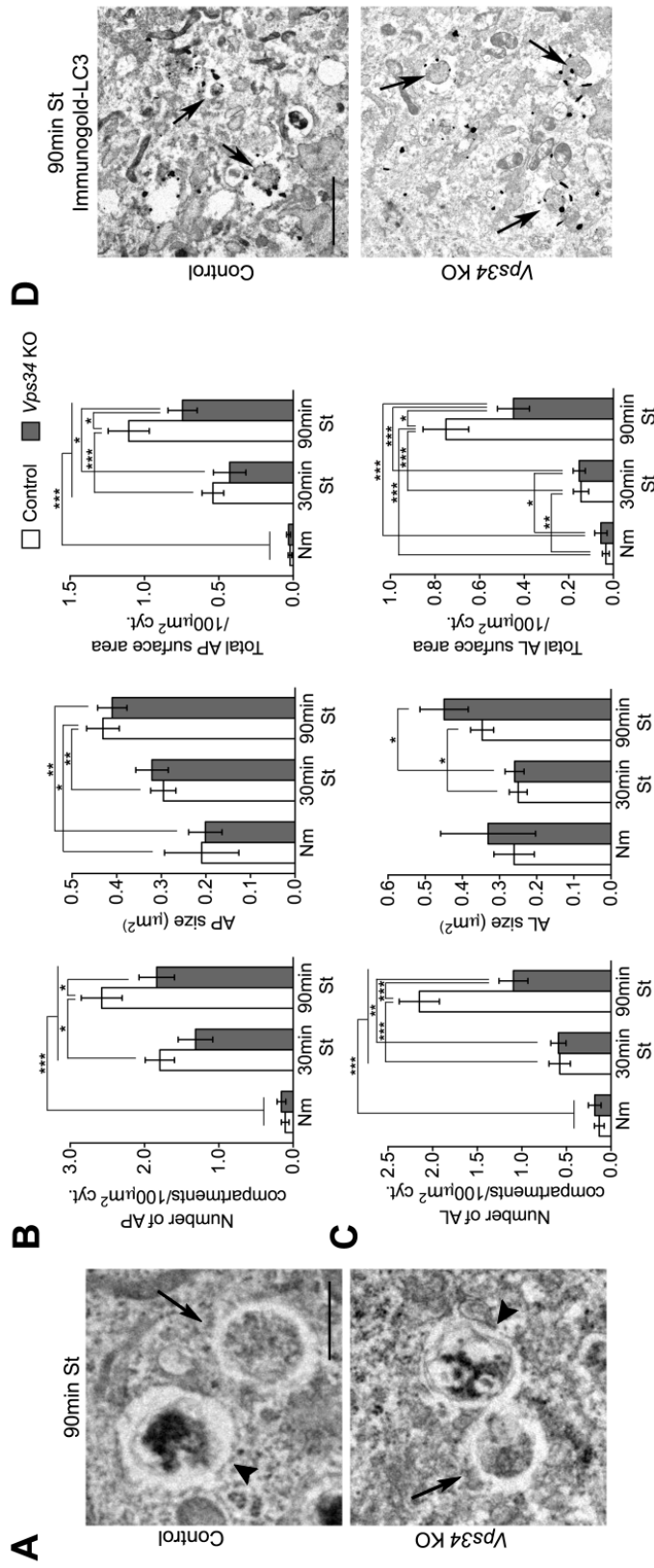


Figure 2.7 Lack of Vps34 decreases, but does not abolish the formation of autophagosomes and autophagolysosomes upon starvation. (A) Electron micrographs of control and *Vps34* KO MEFs cultured in normal media or after 30 and 90 min (shown) of HBSS starvation. Arrows, autophagosomes. Arrowheads, autophagolysosomes. Scale bar: 1 μm . (B) Quantification of average number of autophagosomes (AP), average size (μm^2) of APs and the total AP surface area/ $100\mu\text{m}^2$ of cytoplasm. (C) Quantification of average number of autophagolysosomes (AL), average size (μm^2) of ALs and the total AL surface area/ $100\mu\text{m}^2$ of cytoplasm. In both AP and AL quantifications, 30 cells were analyzed. (D) Immuno-gold electron microscopic analysis of endogenous LC3 in control and *Vps34* KO MEFs. Arrows, LC3 immunoreactive APs. Scale bar: 1 μm .

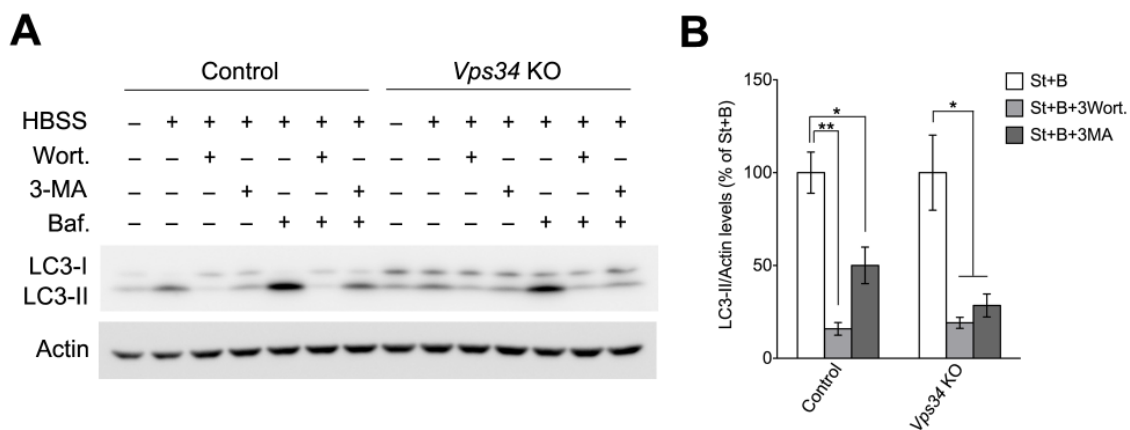


Figure 2.8 PI3K inhibitors 3-methyladenine and wortmannin block LC3-lipidation independently of *Vps34*. (A) Western blot analysis showing LC3-II levels in WT and *Vps34* KO MEFs upon 90 min of HBSS starvation alone or in the presence of wortmannin (Wort, 100 nM) or 3-methyladenine (3MA, 10 mM) and with or without Bafilomycin (Baf or simply B, 50 nM). (B) Quantification of the percent inhibition of LC3 conversion by each PI3K inhibitor during starvation in control and *Vps34* KO MEFs compared to starvation alone for Bafilomycin-treated conditions (n=3).

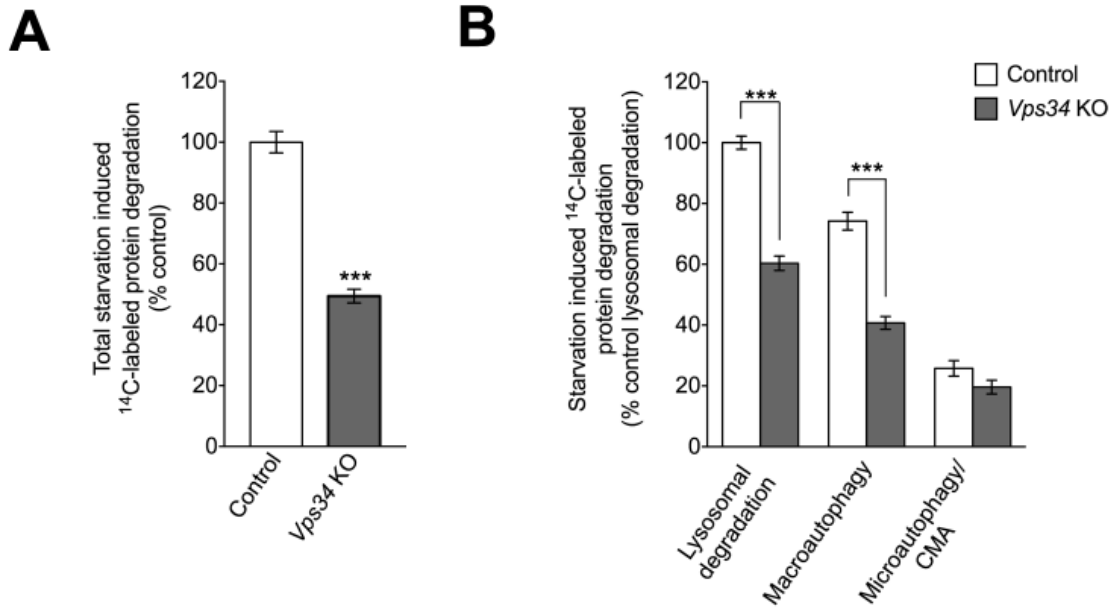


Figure 2.9 Macroautophagy-mediated protein degradation is partially impaired in *Vps34* null MEFs. (A) Quantification of total [¹⁴C]-valine long-lived protein degradation induced by nutrient deprivation (HBSS) in control and *Vps34* KO MEFs. (B) Assessment of autophagy efficiency in control and *Vps34* KO MEFs by ¹⁴C-valine long-lived protein degradation under starvation (HBSS), starvation with 3MA or starvation with NH₄Cl conditions (see Methods) (n=8 for both A and B).

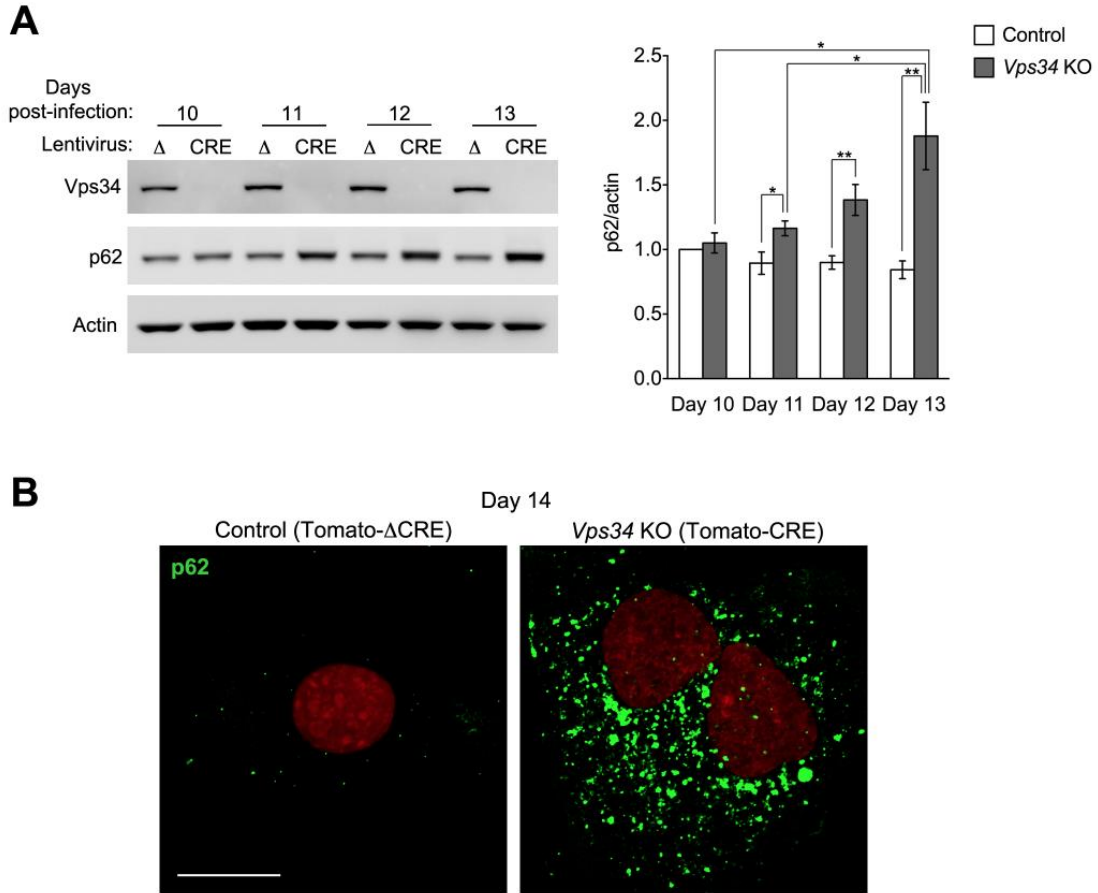


Figure 2.10 Prolonged ablation of Vps34 causes an increase in p62 levels. (A) Right: Western blot analysis of p62 levels in control and *Vps34* KO cells 10 to 13 days post-infection with either inactive (Δ) or active (CRE) CRE-lentiviruses, respectively. Left: Quantification of protein signal intensities showing relative p62 levels normalized to actin (n=5). (B) Immunofluorescence showing endogenous p62 (green) in control and *Vps34* KO MEFs on day 14 post-infection. Nuclear inactive and active tomato-CRE are shown in red. Scale bar: 10 μ m.

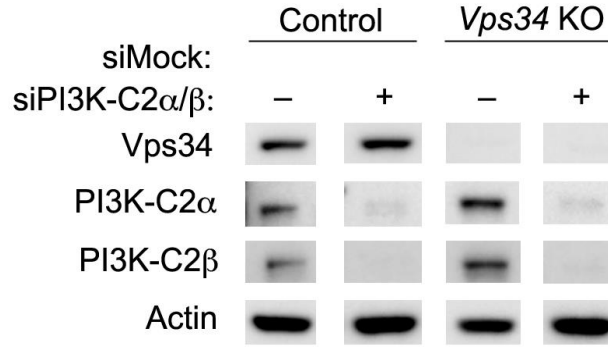


Figure 2.11 Silencing class II PI3Ks in control and *Vps34* KO MEFs. Western blot analysis demonstrating protein levels in control and *Vps34* KO MEFs transfected for 48 hrs with mock or PI3K-C2 α/β siRNA. Efficiency of *Vps34* ablation obtained by 4-HT or CRE lentivirus treatment was consistent. Silencing of PI3K-C2 α/β in either KO model was achieved with comparable efficiency.

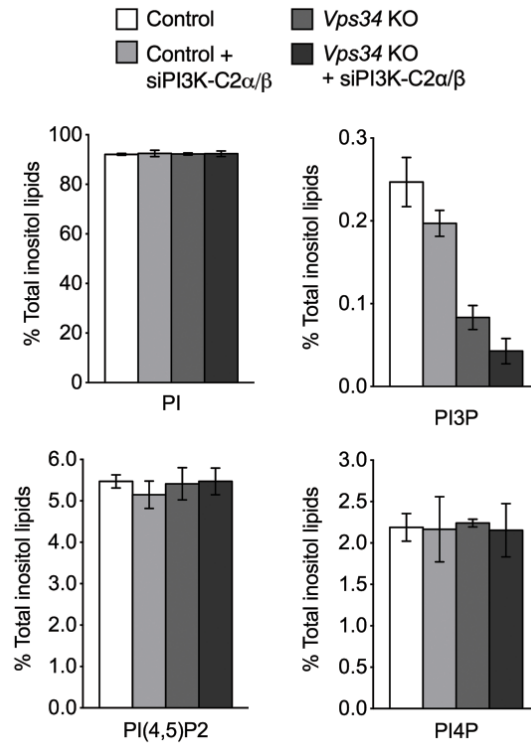
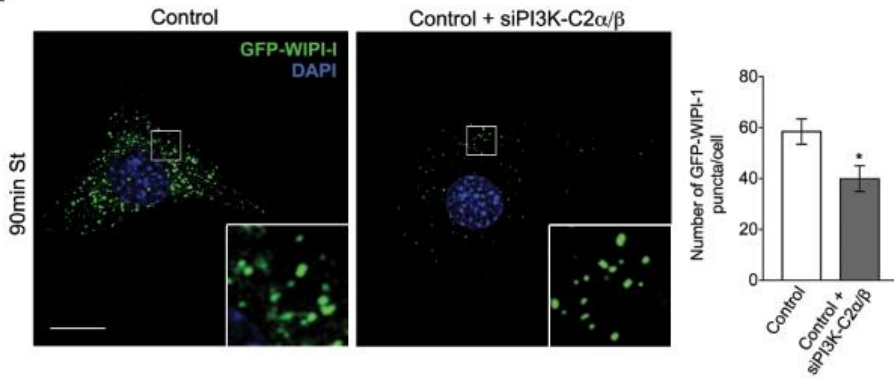
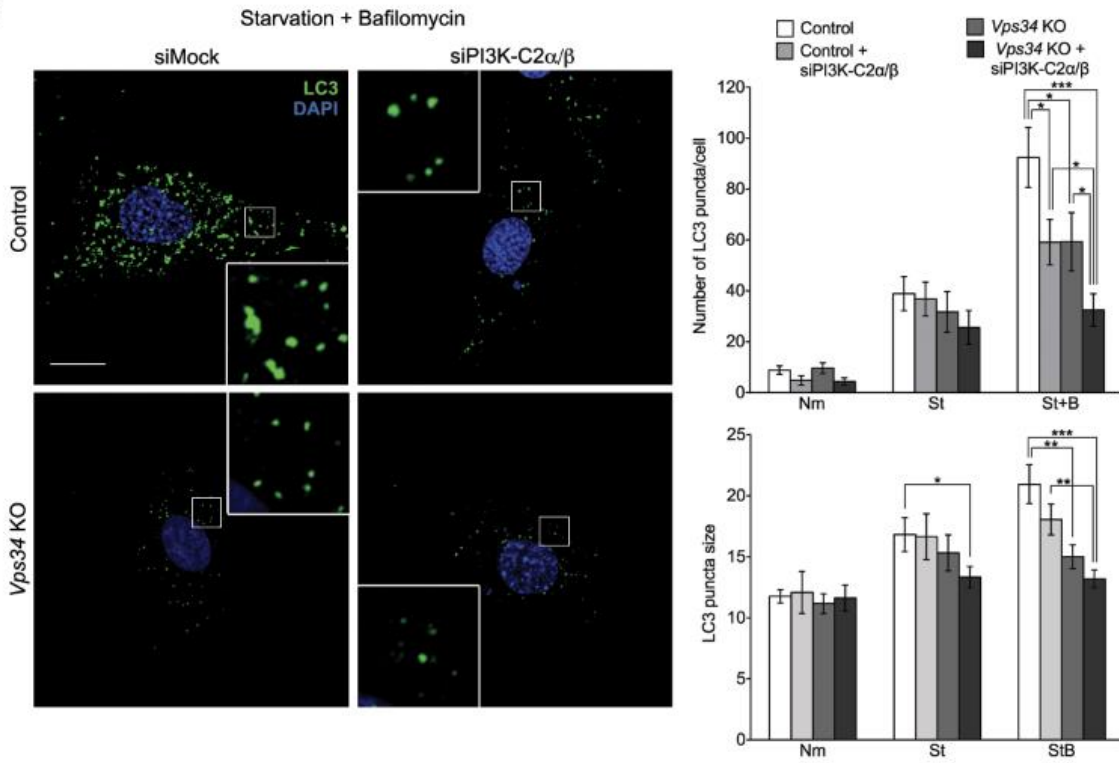


Figure 2.12 Quantification of Vps34-dependent and independent sources of PI3P in MEFs. *Vps34* KO MEFs alone or transfected with mock or PI3K-C2α/β siRNA for 48 hrs grown in normal medium supplemented with [³H] *myo*-inositol. [³H]-labeled phosphoinositides were extracted, deacylated and analyzed by HPLC and scintillation detection. Graph indicates relative levels of phosphatidylinositol (PI), phosphatidylinositol 3-phosphate (PI3P), phosphatidylinositol 4-phosphate (PI4P), phosphatidylinositol 4,5-bisphosphate (PI(4,5)P2), as a percentage of total inositol lipid abundance (n=3).

A



B



C

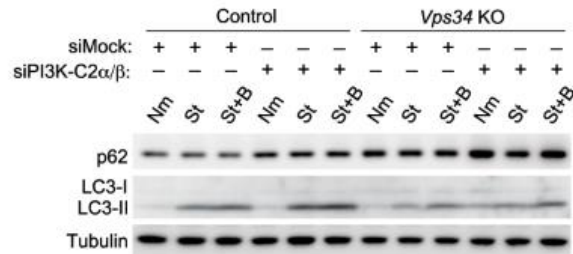


Figure 2.13 Silencing class II PI3Ks decreases autophagy in both control and *Vps34* null MEFs. (A) Control MEFs were transfected with mock or PI3K-C2 α/β siRNA as well as GFP-WIPI-1 for 48 hrs, cultured in normal media or HBSS for 90 min and fixed. Right: Confocal microscopy images of GFP-WIPI-1 fluorescence in mock or PI3K-C2 α/β siRNA-treated control cells after HBSS starvation for 90 min. Scale bar: 10 μ m. Left: Quantification of the number and size (arbitrary units) of GFP-WIPI-1 puncta observed after 90 min HBSS starvation (n=11-15 cells). (B) Cells prepared as in (A) were fixed and immunostained. Right: Confocal microscopy images showing endogenous LC3 (green) in cells cultured in HBSS in the presence of 50 nM Bafilomycin (St+B) for 30 min. DAPI is shown in blue. Scale bar: 10 μ m. Left: Quantification of the number and size (arbitrary units) of LC3 puncta observed under normal media (Nm), HBSS (St) and HBSS in the presence of Bafilomycin (St+B) conditions (n=12-19, 23-40 and 26-53 cells for Nm, St and St+B conditions, respectively). Scale bars: 10 μ m. (C) Control and *Vps34* KO MEFs were transfected for 48 hrs with mock or PI3K-C2 α/β siRNA, cultured in normal medium (N), HBSS (St) or HBSS with 50 nM Bafilomycin (St+B) for 30 min, lysed and analyzed by immunoblotting using the indicated antibodies (n=3).

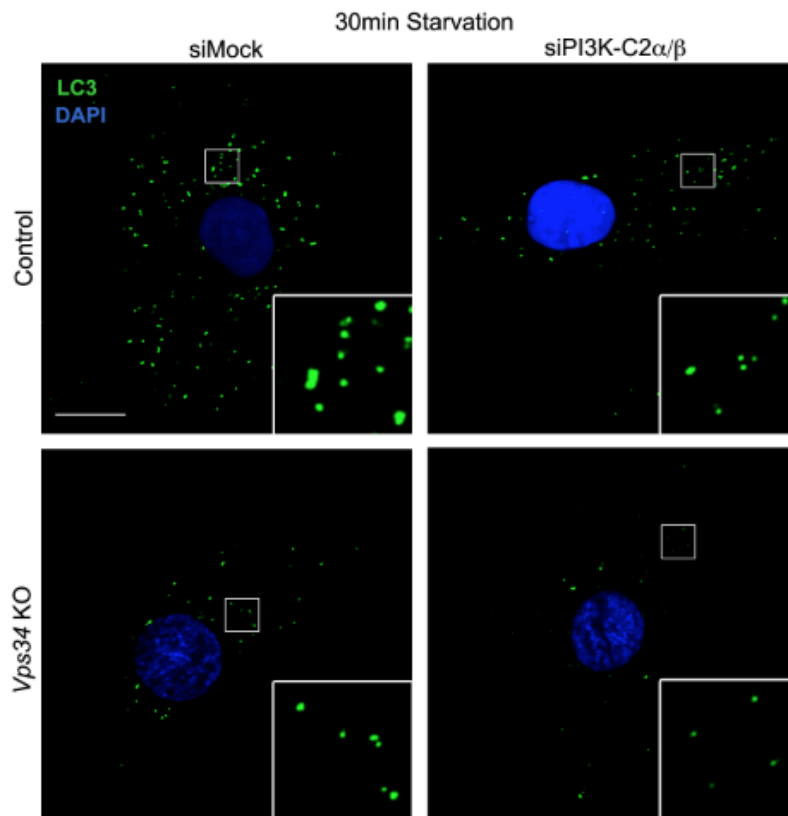
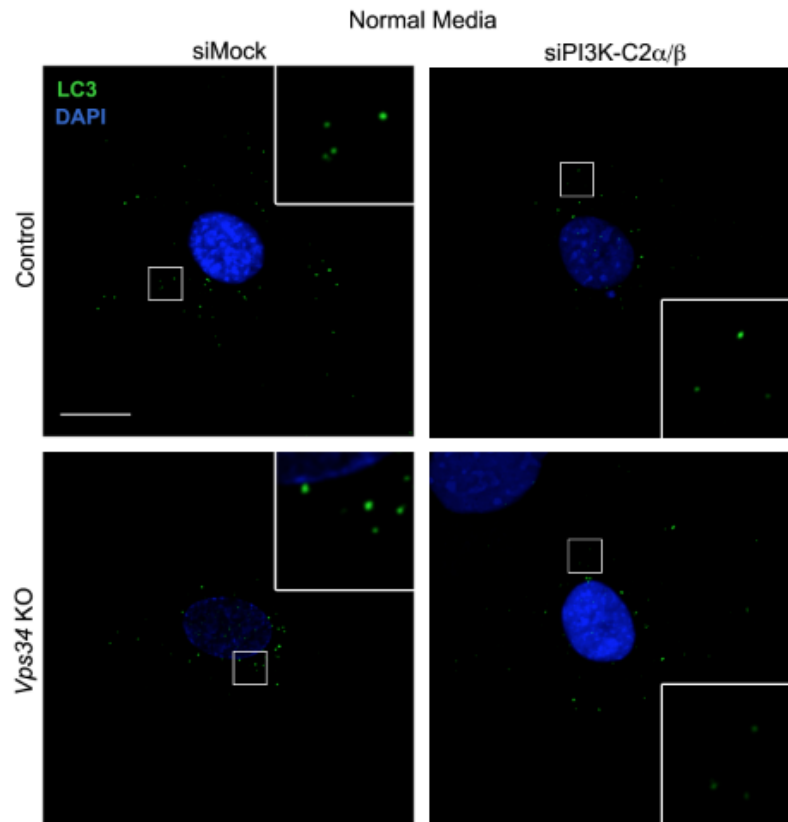


Figure 2.14 LC3 puncta formation during starvation-induced autophagy upon silencing class II PI3K in control and Vps34 KO MEFs. Control and Vps34 KO MEFs were transfected for 48 hrs with mock or PI3K-C2 α/β siRNA, cultured in normal medium (N) or HBSS (St) for 30 min, fixed and immunostained. Representative confocal microscopy images showing endogenous LC3 (green) in cells cultured in normal media (top) or HBSS starvation conditions for 30min (bottom). DAPI is shown in blue. Scale bar: 10 μ m.

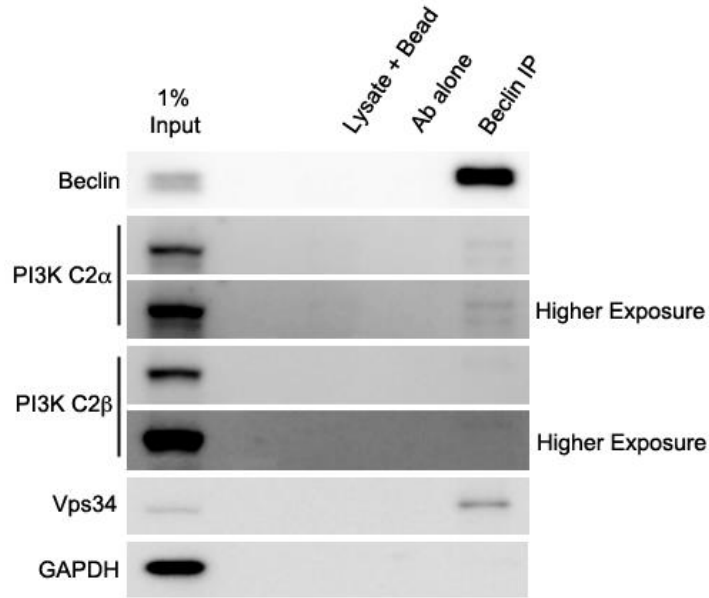


Figure 2.15 PI3K-C2 α and β only weakly interact with the Beclin-1 complex. Uninfected *Vps34*^{flox/flox} MEFs lysates were immunoprecipitated (IP) with anti-Beclin1 antibodies. The resulting immune complexes were analyzed by Western blot using the indicated antibodies.

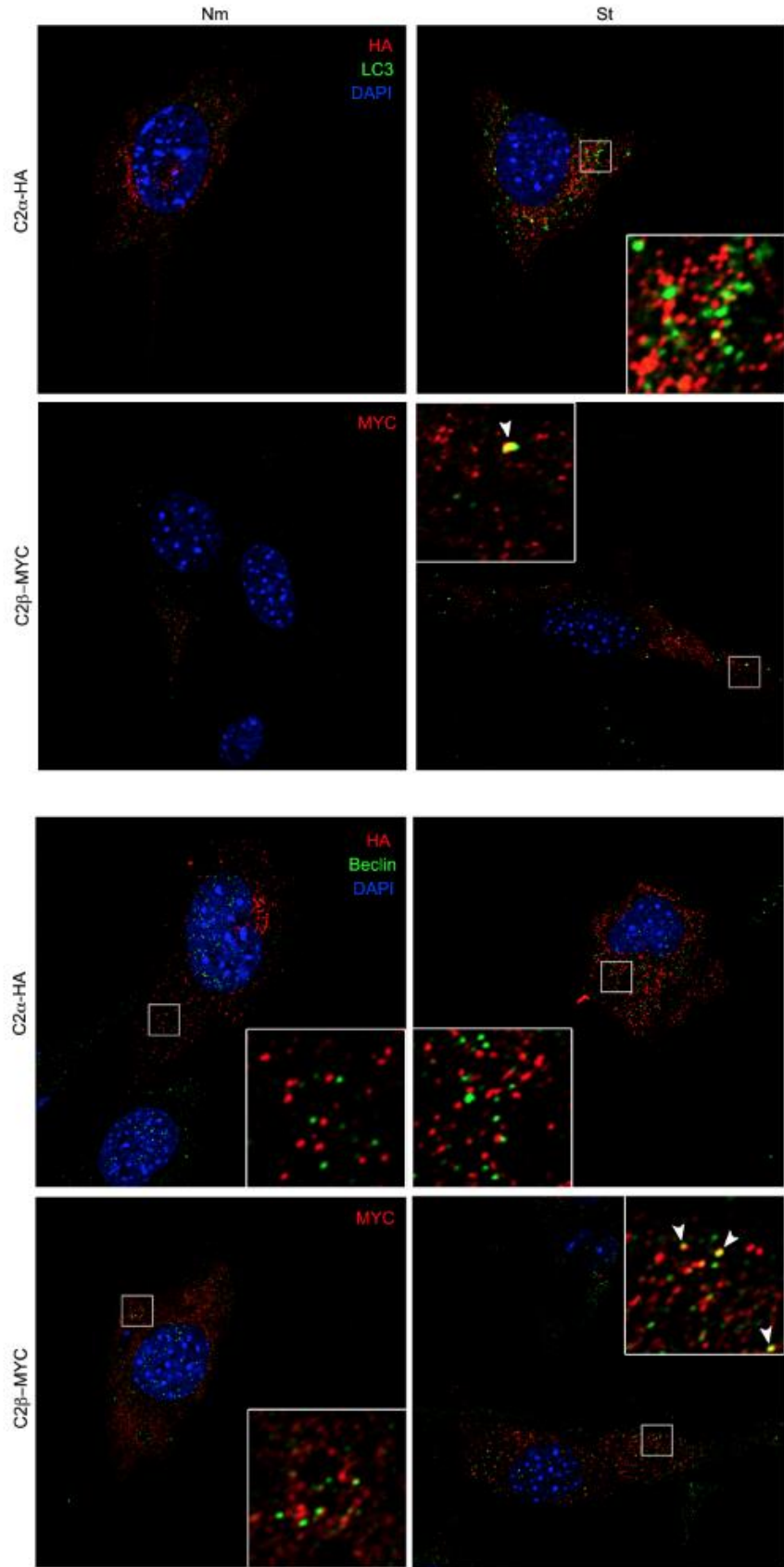


Figure 2.16 Minimal co-localization was observed between PI3K-C2 α and β and various autophagy markers. Uninfected *Vps34*^{fllox/fllox} MEFs were transiently transfected with either PI3K-C2 α -HA or PI3K-C2 β -MYC alone or co-transfected with a Beclin-1-FLAG construct for 24 hrs, cultured in HBSS for 90 min (90 min St) and fixed. Confocal microscopy images showing endogenous LC3 (MAP1LC3B isoform) (green) or exogenous Beclin-1-FLAG (green) colocalization with PI3K-C2 α -HA (red) or PI3K-C2 β -MYC (red). Scale bar: 1 μ m.

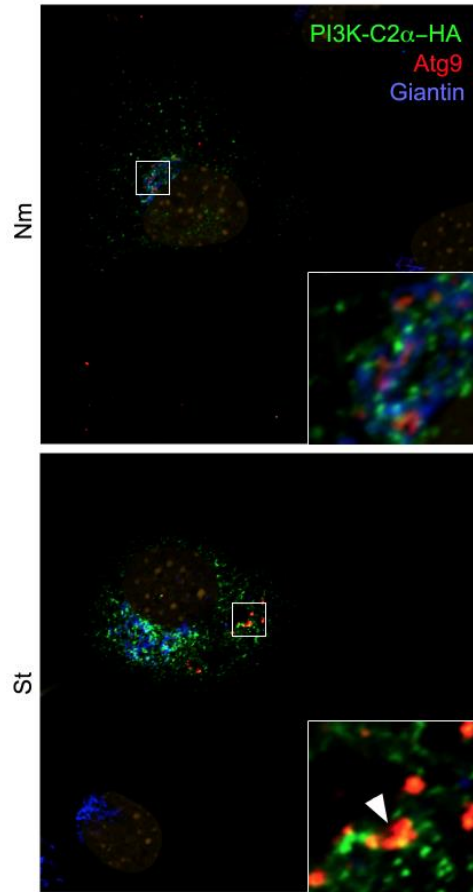


Figure 2.17 PI3K-C2 α colocalizes with Atg9, a transmembrane marker of AP biogenesis, at the TGN under steady-state conditions and in the periphery during starvation-induced autophagy. Uninfected *Vps34*^{flox/flox} MEFs were transiently transfected with PI3K-C2 α -HA for 24 hrs, cultured in normal media or HBSS for 90 min (90 min St) and fixed. Confocal microscopy images showing endogenous Atg9 (red) colocalization with PI3K-C2 α -HA (green). Scale bar: 1 μ m.

2.3 Discussion

Determining the lipid signaling events required for AP formation is critical to our understanding of the regulation of autophagy. PI3P is known to play a critical role in orchestrating AP formation during starvation-induced autophagy (Burman and Ktistakis, 2010; Dall'Armi et al., 2013; Knaevelsrud and Simonsen, 2012; Noda et al., 2010; Simonsen and Tooze, 2009), however, unlike lower eukaryotes, such as budding yeast, where Vps34 is the only source of PI3P, other pathways of PI3P synthesis have been described in higher eukaryotes, and mammalian cells in particular (Falasca and Maffucci, 2012; Hakim et al., 2012; Vanhaesebroeck et al., 2001). These include generation of PI3P by class II PI3Ks, which catalyze a PI phosphorylation like Vps34, and inositol 4-phosphatase (Inpp4) type I and II, which dephosphorylate PI(3,4)P₂ to PI3P (Norris et al., 1997; Norris and Majerus, 1994; Shin et al., 2005). Additionally, Sac1 family members, such Fig4 can dephosphorylate PI(3,5)P₂ to PI3P, accounting for yet another potential source of PI3P (Gary et al., 2002; Rudge et al., 2004). Evidence that an alternative source of PI3P could potentially regulate mammalian autophagy originated from reports on conditional KO mice showing that APs can form in Vps34-deficient sensory neurons (Zhou et al., 2010) and T lymphocytes (McLeod et al., 2011). Additionally, the class II PI3K isoform, *PIK3C2α*, was identified as a 'hit' in a recent autophagy interaction network screen (Behrends et al., 2010). Therefore, we aimed to assess the extent of autophagy occurring in the absence of Vps34 and determine whether the class II PI3K family contributes to autophagy regulation. Here we performed a comprehensive series of autophagy assays using *Vps34* KO MEFs which confirmed that while Vps34 is important for autophagy, it is not the sole source of PI3P synthesis during autophagy. Importantly,

we showed that in addition to Vps34, the class II PI3Ks contribute a pool of PI3P that positively regulates AP biogenesis.

2.3.1 Mammalian Vps34 and autophagy

Several conditional *Vps34* KO mouse models have been generated recently, with selective deletions in sensory neurons (Zhou et al., 2010), T-lymphocytes (McLeod et al., 2011; Parekh et al., 2013; Willinger and Flavell, 2012), podocytes (Bechtel et al., 2013), fibroblasts, cardiomyocytes and hepatocytes (Jaber et al., 2012b) as well as lens cells (Morishita et al., 2013); however, the requirement for Vps34 in autophagy remains highly debated. Potential explanations for phenotype discrepancies include differential gene targeting strategies (*e.g.*, deletion of proximal vs. distal exons), mouse genetic backgrounds, cell types and age-dependency of phenotypes. In our mouse model, we have confirmed by Western blot analysis using antibodies to both the NH₂- and COOH-terminus of Vps34 that no residual, truncated forms of the protein remain expressed in the KO despite the fact that our strategy targets distal exons in the catalytic domain (*i.e.*, exons 17-18) (Zhou et al., 2010). Complete loss of Vps34 is important to ensure in KO models, considering truncated forms of the protein can in some cases provide partial function or even cause dominant negative effects. We note that Jaber *et al.* also characterized *Vps34* KO MEFs and found a more robust defect in autophagy (Jaber et al., 2012b). In addition to this apparent discrepancy perhaps due to differences in targeting strategy (*e.g.*, proximal exon 4 targeting was targeted in Jaber *et al.*), it may be that differences in genetic background influence the regulation of the various PI3P synthesis pathways. Similarly, distinct cell types may differentially rely on the Vps34-dependent and -independent pathways. For instance, PI3P measurements showed that it is PI3KC2 α

that contributes to the majority of steady-state PI3P in endothelial cells, demonstrating such cellular differences (Yoshioka et al., 2012). By identifying the class II PI3Ks as an additional source of PI3P during autophagy, our study provides a potential explanation for the difference in phenotypes observed among the various Vps34 conditional KO models (Yoshioka et al., 2012). Lastly, we noticed that prolonged Vps34 ablation caused a progressive breakdown of the endolysosomal function. In a recent study where Vps15 (*i.e.*, a key subunit of the Vps34 complex) was ablated in skeletal muscle, which subsequently caused a secondary loss of Vps34, similar findings were reported and reminiscent of the lysosomal storage disorders such as Pompe's disease (Nemazany et al., 2013). Importantly, like in our *Vps34* KO MEFs, AP biogenesis was still evident in *Vps15* KO skeletal muscle cells by EM; however, an accumulation of APs and ALs was also observed due to secondary endolysosomal dysfunction, likely as a result of defects in AP maturation and clearance. Because endolysosomal dysfunction impacts the functionality of autophagy, it can potentially confound the analysis and interpretation of the early autophagic role of Vps34. By performing our studies upon acute Vps34 ablation and prior to a collapse of the endolysosomal system, we aimed to more accurately delineate the specific requirements for Vps34 in the autophagy process.

2.3.2 An emerging role for class II and autophagy

Synthesis of PI3P by both class II and III PI3Ks during the same physiological process may be an emerging theme. In fact, a recent study in *C. elegans* reported the class II ortholog, PIK-1, produces an initial pool of PI3P on nascent phagosomes prior to that of Vps34, which is responsible for the sustained production of PI3P on these organelles (Lu et al., 2012). While the *C. elegans* data indicates that PIK-1 and Vps34 act sequentially,

we propose that in the mammalian system the effects of Vps34 and class II PI3Ks are additive, demonstrated by p62 accumulation, LC3 puncta formation and WIPI-1 recruitment, suggesting they act in parallel pathways. The class II PI3Ks are an understudied class of PI3Ks and currently there is growing interest in determining whether they cooperate or function redundantly with Vps34. The α isoform has been implicated in processes such as glucose transport, insulin secretion and endocytosis, whereas the β isoform has been shown to promote cell migration, cell-cycle progression, growth and survival (Falasca and Maffucci, 2012; Posor et al., 2013; Yoshioka et al., 2012). Less is known about the PI3KC2 γ isoform, whose expression may be limited to the liver (Falasca and Maffucci, 2012). While class II isoforms can synthesize PI3P, PI(3,4)P₂ and PI(3,4,5)P₃ *in vitro*, PI appears to be the preferential substrate; however, the α isoform increases its activity toward PI4P and PI(4,5)P₂ substrates in the presence of clathrin (Falasca and Maffucci, 2012; Gaidarov et al., 2005). The majority of studies in intact cells have reported PI3P synthesis by the class II PI3Ks at the plasma membrane, in the nucleus, the Golgi complex, phagosomes and endosomes, although a recent study revealed a role for the α isoform in PI(3,4)P₂ synthesis at the plasma membrane to promote clathrin-mediated endocytosis (Falasca and Maffucci, 2012; Posor et al., 2013). Here we provide novel evidence that class II PI3K α and β isoforms also supply a pool of PI3P during AP biogenesis, based on the partial loss of WIPI-1 puncta upon their silencing. Because WIPI-like proteins, such as Atg18, do not bind efficiently to PI(3,4)P₂ (Stromhaug et al., 2004), we conclude that the class II PI3Ks synthesize PI3P in the context of autophagy. Although the pool of PI3P produced by the class II PI3Ks during autophagy is smaller than that produced by Vps34 as assessed by WIPI-I recruitment,

knocking down PI3K-C2 α/β reduces LC3 puncta formation to the same extent as knocking out Vps34, indicating class II PI3Ks still plays a significant role in starvation-induced autophagy. Importantly, although the class II PI3K α isoform was identified as a "hit" in a genome wide screen looking for new components of the autophagy network and a potential interactor of Atg7 and MAP1LC3A in U2OS cells (Behrends et al., 2010), the same isoform was not identified as a hit in an independent study aiming to identify new regulators of autophagy among genes harboring FYVE and PX domains in 293T cells (Knaevelsrud et al., 2013). In our study, silencing of both class II PI3K α and β isoforms was required to cause an autophagy phenotype, suggesting there is some level of redundancy within the class II PI3K family.

The precise molecular details concerning the class II PI3K α and β isoforms in regulating autophagy still remain unknown. Preliminary evidence suggests that Vps34 and the class II PI3K have different mechanisms of action in regulating AP biogenesis. For instance, despite structural homology in the PI3K family, such as the core helical, C2 and kinase domains (Falasca and Maffucci, 2012; Funderburk et al., 2010; Furuya et al., 2005; Vanhaesebroeck et al., 2010), the C2 domain of Vps34 directly interacts with Beclin-1 whereas the class II PI3K shows a very weak interaction with Beclin-1 that is likely to be indirect. When co-localization was examined, very little overlap was observed between class II PI3K α and Beclin-1; however, some Beclin-1 did appear to co-localize with class II PI3K β . Together the weak coimmunoprecipitation and minimal co-localization indicate that any association between the class II PI3K and Beclin-1 is likely to be indirect. In the future, it will be important to identify autophagy relevant interactors for the class II PI3Ks in order to better understand how they fit into the

autophagy pathway. Although the genome wide screen identified promising interactor hits, such as Atg7 and MAP1LC3A, for the class II PI3K α isoform, these interaction still need confirmation (Behrends et al., 2010). Here we observed low levels of co-localization between class II PI3K α and β and the MAP1LC3B isoform of the mammalian Atg8 family of ubiquitin-like conjugation proteins during autophagy. Co-localization between other isoforms of the Atg8 family, particularly MAP1LC3A, still needs to be tested. Interestingly, we noticed that specifically the class II PI3K α isoform moves from a juxtannuclear to peripheral localization during starvation-induced autophagy, which is a similar to the redistribution pattern of Atg9 seen during autophagy (Webber and Tooze, 2010b; Young et al., 2006). In fact, we observed some co-localization between Atg9 and class II PI3K α during steady-state conditions that continued during starvation-induced autophagy. Future studies will need to be performed to determine whether Atg9 and class II PI3K α interact and how the redistribution of the class II PI3K α is regulated. These findings are a first step in providing insight into the mechanism of class II PI3K α and β isoforms in autophagy; however, more rigorous studies of the class II PI3K will be required to understand their role in the autophagy signaling network (see Future directions and concluding remarks).

As mentioned above, the class II PI3K α isoform can synthesize PI(3,4)P₂ in certain biological contexts, such as clathrin mediated endocytosis (CME) (Posor et al., 2013). In this study, we show that the class II PI3Ks synthesizes PI3P to positively regulate autophagy; however, whether class II PI3K α isoform also synthesizes PI(3,4)P₂ during this process has yet to be ruled out since only WIPI-I recruitment, a PI3P-binding protein, was assessed in our study. In CME, vesicle scission by dynamin is regulated by

Class II PI3K α synthesis of PI(3,4)P₂ and the recruitment of SNX9, which contains a PI(3,4)P₂-binding PX-BAR module (Posor et al., 2013). Interestingly, SNX9 is functionally redundant to SNX18, a recently identified positive regulator of autophagy (Knaevelsrud et al., 2013; Park et al., 2010). Specifically, SNX18 binds LC3 and Atg16 as well as facilitates the tubulation of the recycling endosome, which has been shown to provide membrane to the growing autophagosome (Knaevelsrud et al., 2013). Given that SNX18 and SNX9 are functionally similar, a role for class II PI3K α synthesis of PI(3,4)P₂ at this step in AP biogenesis should be investigated, although alternative roles for PI(3,4)P₂ in autophagy may also exist.

2.3.3 PI3P sources in autophagy

Our studies indicate that together Vps34 and the class II contribute to the majority of PI3P synthesis during autophagy. Notably, we observed few LC3 puncta in *Vps34* KO MEFs upon concomitant knockdown of the class II PI3Ks, suggesting a small amount of autophagy may still be occurring in the absence of Vps34 and the class II PI3Ks. Whether PI3P can be produced via a third pathway, such as dephosphorylation of PI(3,4,5)P₃ by PI 5-phosphatases and PI 4-phosphatases (Inpp4 I and II) will require further investigation (Shin et al., 2005). As mentioned above, contribution of these different PI3P synthesis pathways to autophagy may be largely determined by cell type and genetic background. It will be important to determine whether the physiological context of autophagy stimulation, site of AP biogenesis and type of cargo dictate which pathways of PI3P synthesis are used.

2.3.4 Revisiting PI3K inhibitor specificity in the context of autophagy

As previously shown in other studies, including in yeast (Itakura et al., 2008; Obara et al., 2008a), our results indicate that Vps34 is not essential for LC3 lipidation *per se*. In fact, the *Vps34* conditional KO models have reported findings that range from decreased LC3-II levels (Willinger and Flavell, 2012); see also Fig. 4A), no change (McLeod et al., 2011) or even an increase in LC3-II levels (Bechtel et al., 2013; Jaber et al., 2012a; Morishita et al., 2013; Parekh et al., 2013; Zhou et al., 2010). The findings are consistent with the view that Vps34 and more generally, PI3P, are involved in spatially restricting where LC3 lipidation (and AP biogenesis) occur, rather than controlling the enzymatic conjugation reaction itself. Importantly, our work suggests that pharmacological experiments utilizing wortmannin or 3MA should be interpreted with caution, as the robust effects these drugs typically exert on autophagy are likely to be caused in part by targets distinct from Vps34. We found that LC3-II levels were drastically reduced during starvation in both control and *Vps34* KO MEFs treated with wortmannin and 3MA. Although class I PI3K are known to be susceptible to these inhibitors and may effect the production of PI(3,4,5)P₃ and its subsequent dephosphorylation by 4- and 5-phosphatases to PI3P, the alternate targets of wortmannin are unlikely to be class II PI3Ks, as these enzymes (particularly the α isoform) are less sensitive to wortmannin (Falasca and Maffucci, 2007) and silencing of class II PI3Ks does not alter LC3-II levels (Fig. 8C). Future studies identifying the additional targets of wortmannin and 3MA will be helpful to our understanding the regulation of LC3 conjugation during autophagy as well as to potentially discover new targets for modulating autophagy.

2.3.5 Conclusion

Overall our study highlights the complexity and plasticity of PI3P metabolism in mammalian cells and provides strong impetus for future studies exploring the precise role of Vps34-independent sources of PI3P in autophagy, including class II PI3Ks and potentially, the Inpp4 pathway, and their regulation during this essential process. Additionally, reports of noncanonical autophagy in the field have suggested that autophagy can occur independently of known factors, such as Beclin 1, Atg5 and Atg7 for example (Codogno et al., 2012). The extent to which autophagy can occur without PI3P synthesis altogether remains undetermined. A better understanding of the lipid biology in autophagy, including key lipid species and their roles in regulating autophagy, is of both basic science and clinical significance since lipid enzymes serve as promising targets for modulating autophagy.

2.4 Materials and Methods

2.4.1 Generation of *Vps34* KO MEFs.

Primary mouse embryonic fibroblasts (MEFs) were generated from embryonic day 13.5 *Vps34* (*pik3c3*) *Flox/Flox* mouse embryos in which exons 17/18, encoding the catalytic domain, were flanked by *loxP* sites, as described previously (Zhou et al., 2010). MEFs were immortalized by multiple passaging and were used for experiments after 25 passages. Control $Vps34^{Flox/Flox}$ (Control) and $Vps34^{-/-}$ (KO) cells were generated by infecting cells with a lentivirus carrying either a catalytically active Cre recombinase or catalytically-dead Cre recombinase (control), respectively. Both Cre recombinases encoded two nuclear localization sequences (NLS) and were fused to either eGFP or Tomato moieties containing a third NLS for enhanced nuclear targeting. Lentivirus was

produced in human embryonic kidney 293T cells according to Ho *et al.* with slight modifications (Ho et al., 2006). Virus-containing media was harvested 72 hrs after transfection, centrifuged at 2,800xg for 5 min, filtered through a 0.45mm filter (Millipore) and supplemented with 10ug/ml polybrene (Sigma-Aldrich) prior to adding to MEFs. Infection rate was estimated by determining the percentage of cells with nuclear EGFP or Tomato-fluorescent positivity. In addition, *Vps34^{Flox/Flox}*; Cre-ER MEFs were generated for experiments requiring larger amounts of cells such as HPLC biochemistry studies using the protocol mentioned above. MEFs contain a Cre-estrogen receptor (Cre-ER) fusion protein whereby Cre activity is inducible by tamoxifen (Hayashi and McMahon, 2002). To generate *Vps34* KO and control cells, *Vps34^{Flox/Flox}*; Cre-ER MEFs were incubated with either 3μM 4-hydroxytamoxifen (4-HT) (Sigma-Aldrich) diluted in ethanol or vector alone for 72hrs followed by culturing in normal growth media. In both MEF cell lines, KO efficiency was monitored by Western blot analysis using antibodies to the NH₂- and COOH-termini of Vps34. A minimum of 10 days post-infection or tamoxifen treatment was required to abolish the expression of Vps34, therefore, all experiments were performed upon acute gene ablation 10 days after infection, unless indicated otherwise

2.4.2 Cell culture and transfection.

MEFs were cultured in DMEM-Glutamax (Invitrogen) supplemented with 10% fetal bovine serum (FBS), penicillin (200 units/mL)/streptomycin (200 μg/mL) (Invitrogen) at 37 °C under 5% CO₂. For starvation assays, MEFs were cultured in Hanks' buffer (Invitrogen) for the indicated times. MEFs were transiently transfected using the Lipofectamine RNAiMAX (Invitrogen) and/or AMAXA MEF I Nucleofector Kit

(Lonza) according to the manufacturer's instructions. Cells were incubated with siRNA for 48 hrs and efficient silencing was confirmed by Western blot for each experiment. Plasmids were transiently expressed for 24 hrs when transfected alone or 48 hrs when co-transfected with siRNA.

2.4.3 Reagents and antibodies.

The following compounds were used in autophagy assays: Bafilomycin A1 (50nm, Wako), 3-methyladenine (10mM, Sigma), wortmannin (100nM, Billerica). Primary antibodies used for Western blotting include: anti-pan-actin mouse polyclonal antibody (1:4000 dil., Novus), anti-Atg5 rabbit polyclonal antibody (1:500 dil., Abgent; to detect free form), anti-Atg5 rabbit polyclonal antibody (1:1,000 dil., Sigma; to detect conjugated form), anti-Atg9 armenian hamster polyclonal antibody (1:100 dil., generous gift from Sharon Tooze) anti-Atg14 rabbit polyclonal antibody (1:500 dil., generous gift from Dr. Zhenyu Yue), anti-Beclin mouse polyclonal antibody (1:1000 dil., BD Biosciences), anti-EEA1 mouse polyclonal antibody (1:500 dil., ThermoFisher), anti-EGFR rabbit polyclonal antibody (1:1000 dil., Millipore), anti-FLAG mouse monoclonal (M2, Sigma), anti-LC3 rabbit polyclonal antibody (1:1000 dil., Novus), anti-HA rat monoclonal antibody (3F10, Sigma), anti-MYC mouse monoclonal (9E10, Sigma), anti-p62/SQSTM1 mouse monoclonal antibody (2C11; 1:2000 dil., Abnova), anti-PI3KC2 α rabbit polyclonal antibody (1:1000 dil.; Santa Cruz), anti-PI3KC2 β mouse polyclonal antibody (1:1000 dil., BD Biosciences), anti-Rab5 621.3 mouse monoclonal antibody (1:500 dil., Synaptic Systems), anti-Rubicon rabbit polyclonal antibody (1:500 dil., generous gift from Dr. Zhenyu Yue), anti- β -tubulin mouse polyclonal antibody (1:4000 dil., Sigma), anti-UVRAG mouse monoclonal antibody (1H4, 1:500 dil., MBL), anti-

Vps15/p150 mouse monoclonal antibody (M02, 1:1000 dil., Abnova), anti-Vps26 rabbit polyclonal antibody (1:1000 dil., Abcam), anti-Vps34/PI3KC3 rabbit monoclonal antibody (D4E4, 1:1,000 dil., Cell Signaling Technology; to amino terminal sequence), anti-Vps34/PI3KC3 rabbit monoclonal antibody (D9A5; 1:1,000 dil.; Cell Signaling Technology; to C-terminal sequence) and anti-Vps35 mouse polyclonal antibody (1:1000 dil., Abcam). Secondary antibodies used for western blot include HRP conjugated anti-guinea pig (1:3000 dil., Santa Cruz), anti-mouse (1:3000 dil., Biorad), and anti-rabbit (1:3000 dil., Biorad). Immunofluorescence experiments were conducted using the following primary antibodies: anti-Atg16L1 rabbit polyclonal antibody (1:200 dil., Cosmo), anti-EEA1 goat polyclonal antibody (1:200 dil., Santa Cruz), anti-Giantin rabbit polyclonal antibody (1:1000 dil., Covance), anti-LAMP1 rabbit polyclonal antibody (1:500 dil., Abcam), anti-LC3 mouse monoclonal antibody (4E12, 1:100 dil., MBL), anti-myc mouse monoclonal antibody (9E10, 1:400 dil., Roche), anti-p62/SQSTM1 guinea pig polyclonal antibody (1:1000 dil., Progen) and anti-PDI mouse monoclonal antibody (1D3; 1:50 dil., Stressgen). Fluorescent secondary antibodies used include: Alexa Fluor 647 donkey anti-goat (1:100 dil., Jackson ImmunoResearch), Alexa Fluor 647 donkey anti-guinea pig (1:100 dil., Jackson ImmunoResearch), Alexa Fluor 488 donkey anti-mouse (1:200 dil., Molecular Probes), Alexa Fluor 555 donkey anti-mouse (1:200 dil., Molecular Probes), Alexa Fluor 647 donkey anti-mouse (1:100 dil., Jackson ImmunoResearch), Alexa Fluor 488 donkey anti-rabbit (1:200 dil., Molecular Probes), Alexa Fluor 555 donkey anti-rabbit (1:200 dil., Molecular Probes) and Alexa Fluor 647 donkey anti-rabbit (1:100 dil., Jackson ImmunoResearch).

2.4.4 Plasmids and RNAi.

RFP-2x-FYVE^{HRS} and GFP-2x-FYVE^{HRS} plasmids were gifts from Harald Stenmark (University of Oslo, Norway). To generate GFP-4x-FYVE^{HRS}, the FYVE domain of HRS was amplified with XhoI/SalI sites and cloned twice into the XhoI site of the GFP-2x-FYVE^{HRS} plasmid. GFP-WIPI-1 was a gift from Sharon Tooze (Cancer Research UK). Beclin-1-FLAG was a gift from Beth Levine (UT Southwestern). MYC-DDK-PIK3C2 β – HA-PIK3C2 α was a gift from Volker Hauke (Leibniz-Institut für Molekulare Pharmakologie, Berlin). Second generation lentiviral packaging plasmids VSVg and Δ 8.9 were gifts from Peter Scheiffele (University of Basel), whereas the EGFP-tagged active, full-length Cre recombinase and catalytically inactive, truncated Cre FUGW lentiviral constructs were a gift from Thomas Sudhof (Stanford University, California) (Kaeser et al., 2011). Active and inactive Tomato-tagged Cre FUGW lentiviral constructs were generated by EcoRI/BsrGI replacement of EGFP in the CRE FUGW vector with a PCR-amplified Tomato sequence that included EcoRI/BsrGI overhangs and retained the third N-terminal NLS by using the following primers: forward, 5'-AAATAAGAATTCACAACCATGGTGAAGCGACCAGCAGCAACAAAGAAGGCA GGACAAGCAAAGAAGAAGAAGCTCGTGAGCAAGGGCGAGGAGG -3' and reverse, 5'- AAATAATGTACAGCTCGTCCATGCC-3'. Gene silencing was achieved using pre-designed siRNA sequences against murine *pik3c2 α* (5'-TTGGCAGAAATTATAAACTTA-3'; SI02671011) and murine *pik3c2 β* (5'-CTGGCTCTGATCCCACCCTAA-3'; SI00935928) (Qiagen). As a negative control, an siRNA scramble sequence (5'-AATTCTCCGAACGTGTCACGT-3'; 1027310) was used.

2.4.5 SDS-PAGE and Western blotting.

MEFs cultured in 60 or 100mm plates were lysed in lysis buffer (50 mM Tris–HCl (pH 7.2), 250 mM NaCl, 0.1% NP-40, 2 mM EDTA, 10% glycerol) containing protease (Complete Mini, EDTA-Free, Protease Inhibitor Cocktail; Roche) and phosphatase (phosSTOP; Roche) inhibitors. For immunoprecipitation, cells were lysed in RIPA lysis Buffer (0.025M Tris, 0.15M NaCl, 0.001M EDTA, 1% NP-40, 5% glycerol, pH 7.4 (Pierce)) containing containing protease (Complete Mini, EDTA-Free, Protease Inhibitor Cocktail; Roche) and phosphatase (phosSTOP; Roche) inhibitors. The Pierce Co-immunoprecipitation (Co-IP) Kit (ThermoScientific) was used according to the protocol using the indicated antibodies. Extracts were centrifuged at 16,000xg for 30 min at 4 °C and the protein concentration was measured using the Coomassie Plus Protein Assay Kit (Thermo-Scientific). Proteins were separated by SDS–PAGE and transferred to PVDF (Immobilon-P; Millipore) or nitrocellulose membranes (iBlot Transfer Stack; Invitrogen). Specifically, immunoprecipitations were performed from 1mg of protein extract and 1% of the initial extract (input) and half of the eluate were analyzed. Membranes were probed with the indicated primary antibodies and the appropriate HRP-conjugated secondary antibodies. Immunoreactive protein bands were visualized and imaged using a chemiluminescent HRP substrate kit (Immobilon Western; Millipore) and the Fuji LAS4000 Imaging unit (GE Healthcare), respectively. Densitometric quantification was performed using the ImageJ software (NIH).

2.4.6 EGFR degradation assay.

MEFs were grown in 60mm dishes and serum-starved overnight in DMEM-Glutamax (Invitrogen). Cells were then stimulated with 100 ng/mL EGF (Millipore) in serum-free

medium and harvested at the indicated time points.

2.4.7 Immunofluorescence microscopy.

MEFs grown on coverslips were fixed with 4% paraformaldehyde for 20 min at room temperature. After permeabilization with 200 µg/ml digitonin (Invitrogen) in PBS for 10 min, cells were incubated with the specified primary antibodies for 1 hr at room temperature. Subsequently, cells were incubated with the appropriate Alexa-Fluor or Cy5-conjugated secondary antibodies for 1 hr at room temperature and coverslips were mounted in DAPI Fluoromount G (Southern Biotech). Images were acquired by confocal laser scanning microscopy (Zeiss LSM-700) and analyzed with Zeiss Zen and Image J Software (NIH). The number of LC3-positive compartments and their surface areas (expressed as number of pixels per field) were normalized to the number of cells in each field. The average size was obtained by dividing the surface area of the LC3-positive compartment (in pixel²) by the number of LC3 puncta. Similar measurements were made for Atg16L1- and p62-positive compartments. The colocalization between p62 and LC3 was calculated as the number of pixels overlapping in the two channels per cell.

2.4.8 Conventional electron microscopy and morphometric analysis.

MEFs cultured on plastic coverslips (LF1, Sumitomo Bakelite, Tokyo, Japan) were fixed in 2.5% glutaraldehyde (Electron Microscopy Sciences) in 0.1 M sodium phosphate buffer (PB) (pH 7.4) for 2 hrs at room temperature. After washing with PB, the cells were post-fixed in 1% OsO₄ in PB for 60 min at room temperature and washed with distilled water before being dehydrated in a series of graded ethanol solutions and embedded in epoxy resin. Ultra-thin sections were doubly stained with uranyl acetate and lead citrate and observed under an H7600 electron microscope (Hitachi, Tokyo, Japan). Electron

micrographs were taken of thin sections from three different parts of the plastic cover slips using a H7600 electron microscope (Hitachi, Tokyo, Japan) equipped with ORIUS™ SC200W 2k x 2k TEM CCD camera (Gatan Inc.CA) at a magnification of 8,000. Thirty electron micrographs were taken per condition and analyzed by morphometry. The number and surface area of autophagosomes/amphisomes (AP) and autolysosomes/ lysosomes (AL) were measured using the software MacSCOPE 2.5 (Mitani Corporation, Fukui, Japan). The surface area of APs and ALs was normalized to the cytoplasmic area.

2.4.9 Immunoelectron microscopy.

The pre-embedding gold enhancement immunogold method was used for immunoelectron microscopy as described previously (Dall'Armi et al., 2010) with slight modifications. Briefly, MEFs cells were cultured on plastic coverslips (LF1, Sumitomo Bakelite, Tokyo, Japan) and fixed in 4% paraformaldehyde in PB for 2 hrs at room temperature. After permeabilizing in 0.25% saponin diluted in PB for 30 min and blocking in 0.1% saponin, 10% bovine serum albumin, 10% normal goat serum and 0.1% cold water fish skin gelatin diluted in PB for 30 min, cells were incubated overnight in mouse monoclonal anti-LC3 antibody (Itakura et al., 2012a; Velikkakath et al., 2012) (clone LC3 1703, Cosmo Bio. Co. LTD Tokoyo, Japan) diluted in blocking solution. Subsequently, MEFs were incubated with colloidal gold (1.4 nm in diameter, Nanoprobes, New York, NY)-conjugated anti-mouse IgG Fab fragments diluted in the blocking solution for 2 hrs. The signal was intensified using a gold enhancement kit (GoldEnhance EM, Nanoprobes) for 2 min at room temperature. Cells were post-fixed in 1% OsO₄ containing 1.5% potassium ferrocyanide at room temperature and processed as

described above for conventional EM.

2.4.10 Intracellular protein turnover.

The long-lived protein degradation assay was adapted from previously reported protocol (Martinez-Vicente et al., 2010; Yamamoto et al., 2006). Control and *Vps34* KO MEFs were plated in 6-well plates. The following day, MEFs were labeled with [¹⁴C]Valine (0.1uCi/ml, Perkin-Elmer) for 18 hrs at 37 °C. Cells were washed three times with PBS before chasing with radioactivity-free medium containing an excess of unlabeled valine (10mM, Sigma) for 3 hrs to allow for short-lived protein degradation. Again, cells were washed three times with PBS and cultured in complete medium or in serum-free medium (HBSS) either alone or in the presence of 3-methyladenine (10mM, Sigma) or NH₄Cl (15mM, Sigma). A fraction of the medium was taken at different time points and precipitated with trichloroacetic acid (final concentration 15%, v/v, Sigma) in order to separate [¹⁴C]Valine incorporated into secreted proteins from that of free [¹⁴C]Valine released after intracellular proteolysis. After 4 hrs, cells were washed three times in PBS, lysed (0.1M NaOH, 0.1% Na deoxycholate) and TCA-precipitated. TCA-soluble and total cell radioactivity were measured by liquid scintillation counting. Proteolysis was estimated as the ratio of TCA-soluble radioactivity to the total cell radioactivity. Specifically, total lysosomal degradation was calculated as a percentage of protein degradation sensitive to NH₄Cl. Contribution of macroautophagy calculated as a percentage of lysosomal protein degradation sensitive to 3MA. Microautophagy and/or chaperone-mediated autophagy (CMA) account(s) for the difference between total lysosomal degradation and macroautophagy-associated protein degradation.

2.4.11 Quantification of phosphoinositide levels by HPLC analysis.

Control and *Vps34* KO cells produced via the Cre-ER system were incubated with inositol-free DMEM (MP Biomedicals) supplemented with 10% dialyzed FBS (Invitrogen), L-glutamine, glucose and 5 $\mu\text{Ci/ml}$ ^3H -myo-inositol (MP Biomedicals) 24 hrs before transfection with siRNA duplexes. After transfection, cells were again incubated with 5 $\mu\text{Ci/ml}$ ^3H -myo-inositol (MP Biomedicals) in inositol-free DMEM (MP Biomedicals) for an additional 48hrs. Prior to lipid extraction, cells were washed twice with PBS and incubated 15 minutes in inositol-free DMEM (MP Biomedicals) supplemented with 10% dialyzed FBS, glutamine and glucose. Cells were treated with 0.7 ml 4.5% perchloric acid in ice for 15 mins, scraped and centrifuged. Pellets were washed twice with ice-cold 1 ml 0.1 M EDTA, and deacylated as described (Kirk, 1990). Deacylated phosphoinositides were then separated using high performance liquid chromatography (Shimadzu Scientific Instruments). Peaks were identified using deacylated ^{32}P -standards and detected by an online flow scintillation analyzer (B-RAM, IN/US) (Cremona et al., 1999).

2.3.12 Statistical analysis.

Quantitative results represent three independent experiments (unless indicated otherwise) and values denote mean \pm s.e.m, as indicated in each figure. Statistical analysis was performed using a two-tailed, equal variance Student's *t*-test, except for data shown in Figure 1C, where the one-sample *t*-test was used. *P*-values of < 0.05 (*), < 0.01 (**), < 0.001 (***) were determined to be statistically significant. All statistical data were calculated with the GraphPad Prism software.

Chapter 3: Lipidomic analysis of Vps34-deficient fibroblasts

3.1 Introduction

In comparison to our current understanding of the genome and proteome, the lipidome remains largely enigmatic. For many years, lipids were simply viewed as membrane structural units and sources of energy within the cell; however, in 1979, platelet-activating factor was identified as the first biologically active lipid (Demopoulos et al., 1979; Pinckard et al., 1979). Following studies revealed several additional lipid species endowed with bioactive properties in trafficking processes, the recruitment and regulation of membrane proteins, and cellular signaling (van Meer et al., 2008). Given the wide range of functions for lipids, it is not surprising that such a diverse set of chemically distinct molecules exists. The structural variation among lipids is derived from the numerous combinations of different fatty acid chains, which vary in length and saturation, and functional headgroups typically linked by a carbon based backbone (*e.g.*, glycerol) (Fahy et al., 2005; Fahy et al., 2009; van Meer et al., 2008; Wenk, 2005). Eight major classes of lipids have been identified in mammalian cells: fatty acyls, glycerolipids, glycerophospholipids, sphingolipids, sterol lipids, prenol lipids, saccharolipids, and polyketides. Each is further divided into subclasses that are predicted to comprise over 100,000 lipid species (Fahy et al., 2005; Fahy et al., 2009; Yetukuri et al., 2008). However, glycerolipids, glycerophospholipids, sphingolipids and sterol lipids are the most abundant classes in higher eukaryotes and together they probably account for less than 1,500 species. Since lipids are not genetically encoded, most functional knowledge comes from genetic and biochemical studies on lipid synthesis and modifying enzymes. Additionally, many diseases, such as cancer, lysosomal storage diseases, and infectious

diseases, that involve the disruption of lipid metabolic pathways have helped improve our understanding of lipids. However, we are still left with many unanswered questions in the field, including: How do cells synthesize such a diverse set of lipid species and what are their roles in the cell? How do lipids regulate and respond to changes in cellular physiology and pathophysiology? How do different lipids impact membrane structure and function? How are lipids distributed among various organelle membranes, and what is the relevance of this distribution? Through what effectors do lipids signal or change physiological outcomes? Finally, what metabolic crosstalks exist between the various lipid families?

Technological advancements, especially in mass spectrometry and bioinformatics, in the past decade have been critical in the development of a systems-based approach to study lipids, termed lipidomics. Specifically, developments in mass spectrometry and liquid chromatography have allowed for a multitude of individual lipid species to be distinguished and accurately quantified from minute amounts of cell sample (Blanksby and Mitchell, 2010; Wenk, 2005; Wenk, 2010). Like its other sister "-omics," genomics and proteomics, lipidomics enables broad biochemical characterization of lipids in cells, tissues, and organisms. By capturing the lipid profiles of cells in different physiological states and genetic backgrounds, new insight into lipid metabolism, regulation, and function can be gained. Additionally, a systems based approach to studying lipids, such as lipidomics, is important because of the potential for discovery of new lipid networks and relationships between different parts of biological systems. Although lipidomics is still emerging as a field, its findings are of both basic bioscience and biomedical interest, and its use is becoming more widespread in an effort to better understand lipid biology.

Since Vps34 is a phosphatidylinositol 3-kinase (PI3K) that synthesizes the bioactive lipid phosphatidylinositol 3-phosphate (PI3P) and plays an important role in endo-/lysosomal trafficking, it is likely that Vps34 also interacts with other lipid networks besides that of the phosphoinositide subclass, which can be tested using a lipidomic approach. As mentioned in previous chapters, Vps34 was first identified in yeast for its essential role in the sorting and delivery of soluble hydrolases transported from the Golgi to the vacuole (the yeast equivalent of the mammalian lysosome) (Backer, 2008; Herman and Emr, 1990; Schu et al., 1993). Later studies using PI3K inhibitors (*e.g.*, wortmannin and LY294002) and siRNA approaches demonstrated this conserved role for Vps34 in higher eukaryotes and showed defects in maturation of the lysosomal hydrolase cathepsin D and the appearance of large, cytoplasmic vacuoles in the absence of Vps34's PI3K activity (Brown et al., 1995; Davidson, 1995; Johnson et al., 2006). As predicted, both Vps34 siRNA knock-down and genetic knock-out mouse models have demonstrated impairment in lysosomal degradation (*e.g.*, of EGFR) upon ablation of Vps34 (chapter 2; (Devereaux et al., 2013; Jaber et al., 2012a)). Likewise, knocking out Vps15, an interactor and activator of Vps34, produced a secondary downregulation of Vps34 in cells and subsequently resulted in lysosomal dysfunction and storage defects in the muscle (Nemazanyy et al., 2013). Failure to properly traffic and deliver hydrolases to the lysosome in the absence of Vps34 is largely attributed to the diminished recruitment of PI3P-binding effectors that mediate the retrieval and recycling of the hydrolase receptors from the endosomal system back to the TGN (*e.g.*, Snx1-3). However, failure to recruit other key PI3P-binding effectors (*e.g.*, EEA1, Rabenosyn-5, Hrs, Snx1-3, and KIF16B) that mediate vesicular transport, fusion and sorting at the endosomal system

likely impair endo-/lysosomal system function as well (Lindmo and Stenmark, 2006; Raiborg et al., 2013). However, it is important to note that PI3P also serves as a unique substrate for phosphatidylinositol 3,5-bisphosphate, PI(3,5)P₂, synthesis by the PI3P 5-kinase PIKfyve (the mammalian homolog of yeast Fab1) (Ho et al., 2012). In fact, PI(3,5)P₂ is important for maintaining lysosomal morphology, trafficking, membrane recycling, and lysosomal acidification, and, when ablated, enlarged endosomes and endolysosomal dysfunction occur (Efe et al., 2005; Gary et al., 1998; Ho et al., 2012; Ikononov et al., 2003; Ikononov et al., 2001; Nicot et al., 2006; Rusten et al., 2006; Rutherford et al., 2006). Therefore, the breakdown of the endolysosomal system seen upon Vps34 ablation and the subsequent loss of PI3P likely reflect a secondary decline in PI(3,5)P₂ levels as well. It is well known that the lysosome serves as a major catabolic site for lipids; therefore, the deletion of Vps34 would disrupt endolysosomal function, which in turn could result in altered lipid turnover and homeostasis in the cell.

In addition to regulating the endo-/lysosomal system trafficking required for efficient delivery of hydrolases to the lysosome, PI3P synthesis by Vps34 promotes formation of intraluminal vesicles (ILVs) (Fernandez-Borja et al., 1999; Futter et al., 2001a; Schu et al., 1993). ILVs are formed through the invagination and budding of endosomal membrane and serve as an important pathway for the degradation of transmembrane proteins. Although the heterogeneity in ILVs formation and composition is only beginning to be understood (Babst, 2011; Kobayashi et al., 2002; van der Goot and Gruenberg, 2006), it is known that PI3P synthesis by Vps34 is required to form ILVs via the Endosomal Sorting Complexes Required for Transport (ESCRT-0, I, II, III) pathway (Raiborg and Stenmark, 2009; Saksena et al., 2007) (see section 1.4.1.3 for

details). The primary fate of ILVs formed via the canonical ESCRT pathway appears to be lysosomal degradation, which is regulated by the fusion of multivesicular bodies (MVBs), an endosomal intermediate that contains multiples ILVs, with the lysosome (Babst, 2011; de Gassart et al., 2004; Hurley, 2010; Hurley and Hanson, 2010; Raiborg and Stenmark, 2009). So far, ILVs have been studied predominately in the context of transmembrane protein degradation; however, ILVs appear to have an important role in membrane and lipid turnover as well (Gillooly et al., 2000; Hurley, 2010; Mobius et al., 2003; van der Goot and Gruenberg, 2006). Interestingly, PI3P not only participates in ILV formation but is also sorted into ILVs and degraded upon reaching the late endosome (Gillooly et al., 2000). Likewise, ILVs are also enriched in cholesterol early in the endosomal pathway; however, it is currently unclear whether cholesterol promotes ILV formation or whether it is incorporated once ILVs have formed (Gillooly et al., 2000; Hurley, 2010; Kobayashi et al., 1999; Mobius et al., 2003; van der Goot and Gruenberg, 2006). In addition to PI3P and cholesterol, it is likely that the metabolism of other lipids are regulated through a Vps34-dependent ILV pathway.

Lastly, PI3P synthesis by Vps34 is also important for regulating autophagy. At the site of autophagosome (AP) nucleation, PI3P is synthesized and recruits downstream PI3P-binding autophagy effectors (*e.g.*, WIPI, DFPCP) that promote membrane expansion and curvature during AP biogenesis (Axe et al., 2008; F et al., 2013; Obara and Ohsumi, 2008; Proikas-Cezanne et al., 2004). Given that an autophagosome is a transient organelle that is formed *de novo* during autophagy stimulation, a significant amount of membrane remodeling and lipid content is required to construct this large, double-membraned organelle. Additionally, Vps34 regulates AP maturation steps and fusion

with the endo-lysosomal system. Importantly, autophagy is an important pathway not only for the bulk degradation of proteins but also for the turnover and degradation of organelles and lipids (He and Klionsky, 2009). Although phosphoinositide species such as PI3P have been the major subclass of lipids implicated in autophagy, other lipid subclasses likely participate in the regulation of or change during autophagy as well. Since Vps34 is an important regulator of this catalytic cellular process, it likely to interact, either directly or indirectly, with the lipid networks important this process.

Here, we performed lipidomic analysis on control and *Vps34* KO MEFs in order to determine the effects Vps34 and its synthesis of PI3P on lipid metabolism. The effects of both acute and prolonged ablation of Vps34 on the lipidome were analyzed, since endolysosomal breakdown and dysfunction occurs over time (data presented in Chapter 2, Fig. 2.2B,C) and may differentially affect the lipid network. Lipidomic analysis is also ideal for identifying important lipid changes due to autophagy under normal circumstances and during impairment caused by absence of Vps34; therefore, we also analyzed changes in the lipidome and lipid metabolism during autophagy in both control cells and in *Vps34* KO MEFs.

3.2 Results

3.2.1 Comparative lipid profiling of control and *Vps34* KO MEFs.

Vps34^{Flox/Flox} MEFs were infected with lentiviruses expressing either a catalytically-inactive or active, nuclear CRE in order to generate control and *Vps34* KO MEFs, respectively. Successful gene deletion of Vps34 reproducibly occurred 10 days after infection with lentivirus and was confirmed by Western blot analysis (previously shown in Fig. 2.1). In order to determine differences in the lipidome of control and *Vps34* KO

MEFs, cells were harvested and lipids were extracted for analysis by mass-spectrometry either 10 or 14 days post-infection with lentivirus. Non-infected MEFs were also analyzed to control for the effects of lentivirus infection on lipid metabolism. Importantly, we found no significant differences between the lipid profiles of uninfected MEFs compared to lentivirus infected, control MEFs (data not shown). When the lipidome of control and *Vps34* KO MEFs were analyzed, we observed a trend for an increase in free cholesterol (FC) and a significant decrease in cholesterol esters (CE) upon acute ablation of *Vps34* (Day 10) (Fig. 3.1A). With prolonged ablation of *Vps34* (Day 14) an even further reduction in CE was seen (Fig. 3.1B). Notably, changes in other lipid subclasses were also observed in the absence of *Vps34* over time. Specifically, an increase in sphingomyelin (SM), dihydrosphingomyelin (dhSM), ceramide (Cer), ceramide-lactose-N-acetylneuraminic acid (GM3), phosphatidylcholine (PC), plasmalogens phosphatidylethanolamine (PEp) was observed in *Vps34* KO MEFs 14 days post-infection (Day 14) (Fig. 3.1B). Within each subclass of lipid, several lipid species that varied in fatty acid chain length and saturation were also measured for each genotype, and relative levels are displayed in a heat map (Fig. 3.4). In fact, many of the changes in specific species occurred within the subclasses observed to change in the *Vps34* KO MEFs mentioned above; however, the heat map also revealed changes in several specific lipid species within a subclass that did not significantly change. For example, a decrease in bis(monoacylglycero)phosphate (BMP) species with a 36 carbon chain length and high saturation was observed (Fig. 3.4). In summary, lipidomic analysis of *Vps34* KO MEFs revealed a novel relationship between *Vps34* and cholesterol homeostasis and demonstrated that lipid dysregulation occurs with prolonged *Vps34*

ablation.

3.2.2 Vps34 ablation alters cholesterol homeostasis.

Cholesterol is an essential structural lipid that can be acquired through cell uptake or synthesized endogenously. Although cholesterol resides predominately at the plasma membrane where it forms lipid rafts, it is also found in the TGN, recycling endosomes, and multivesicular bodies (Maxfield and Tabas, 2005; Mobius et al., 2003). Because of its importance and toxicity at high levels to cells, cholesterol levels are tightly regulated by enzymes that interconvert FC and CE (Maxfield and Tabas, 2005; Tabas, 2002). Excess FC is esterified and stored within lipid droplets as CEs. In order to better understand the relationship between the increase in FC and decrease in CE observed in the *Vps34* KO MEFs, we examined the ratio of these two lipid subclasses. The ratio of CE to FC was significantly decreased upon ablation of *Vps34* and demonstrated a further decrease over time (Fig. 3.2A). In particular, continual decrease in CE over time in *Vps34* KO MEFs suggests that FC to CE metabolism is impaired. In order to confirm the increase in FC seen by lipidomic analysis as well as determine its localization in *Vps34* KO MEFs, cells were immunostained with filipin. Filipin is a polyene macrolide antibiotic and antifungal that fluoresces and can be used to detect unesterified free cholesterol (Bornig and Geyer, 1974; Lefevre, 1988). As expected, acute ablation of *Vps34* produced an increase in filipin staining compared to control cells, a finding consistent with higher FC levels measured by lipidomic analysis (Day 10) (Fig. 3.2B). With prolonged ablation of *Vps34*, more and larger filipin-positive puncta were observed (Day 14) (Fig. 3.2B). These results further confirm that *Vps34* is important for the regulation FC and CE levels in the MEFs.

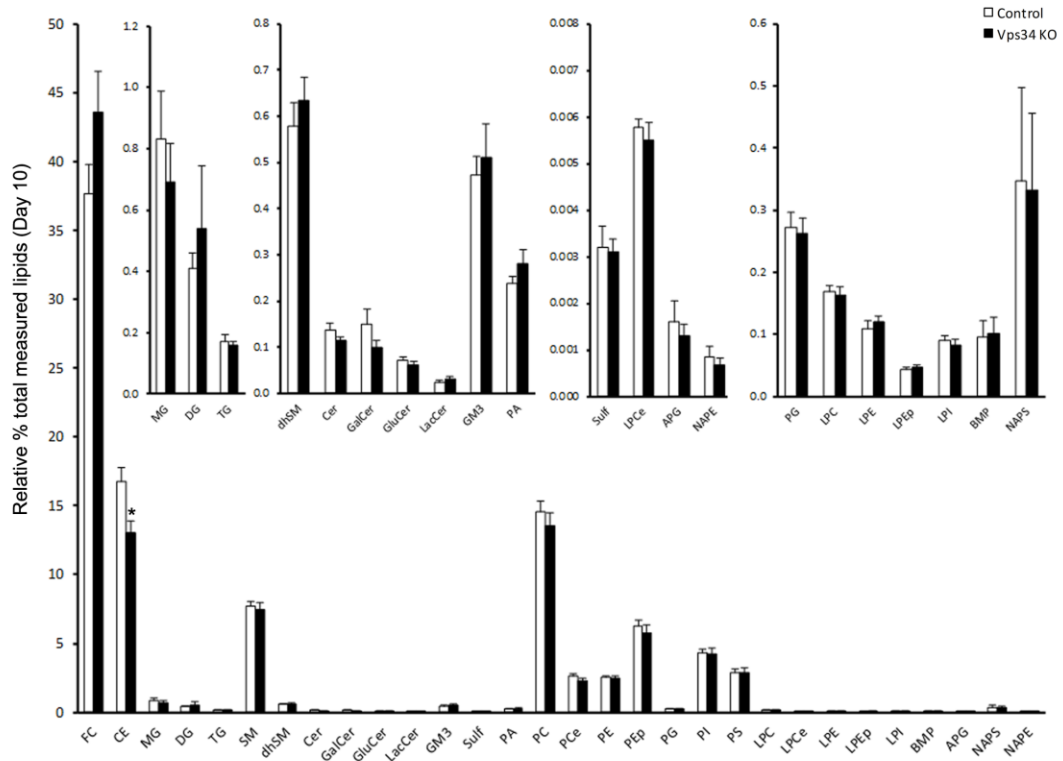
3.2.3 Lipidomics of control and *Vps34* KO MEFs during starvation-induced autophagy.

In order to identify novel lipids and lipid metabolic networks implicated in autophagy, we examined the lipidome of control and *Vps34* KO MEFs during starvation-induced autophagy. Control and *Vps34* KO MEFs were cultured in normal media or starved for 30min or 90min in HBSS prior to lipid extraction and mass-spectrometry analysis. When control cells were starved for 30 and 90mins, only plasmalogens lysophosphatidylethanolamine (LPEp) increased significantly compared to steady state levels. Additionally, a trend for an increase in FC and a decrease in CEs was observed in control MEFs (Fig. 3.3). Interestingly, analysis of the lipidome in the absence of *Vps34* revealed changes only in CE upon autophagy induction when compared to control levels. Although there was a trend for a decrease in CEs in both genotypes during starvation-induced autophagy, CE levels were significantly reduced in the *Vps34* KO MEFs compared to the control MEFs at steady-state and during both 30 and 90 min of starvation. Similar to the control MEFs, *Vps34* KO MEFs showed an increase LPEp in response to 30 and 90mins of starvation when compared to its own steady-state levels (Fig. 3.3). Additionally, increase in lysophosphatidylethanolamine (LPE) was also observed after 30 and 90mins of starvation in *Vps34* KO MEFs (Fig. 3.3). Most changes in molecular species occurred in subclasses that changed as a whole. In particular, we observed a decline in many cholesteryl ester species during 30 and 90mins of starvation, as was observed under steady-state conditions in *Vps34* KO MEFs (Fig. 3.4). Interestingly, short chained, unsaturated LPEp appeared to increase in control MEFs during autophagy, whereas both short and medium chained LPEs increased in the *Vps34*

KO MEFs. Additionally, the increase in these LPE species appears early at 30mins and further increases by 90mins, whereas there appears to be a delay in the Vps34 KO MEFs, as the increase is only observed at 90mins (Fig. 3.4).

3.3 Figures

A



B

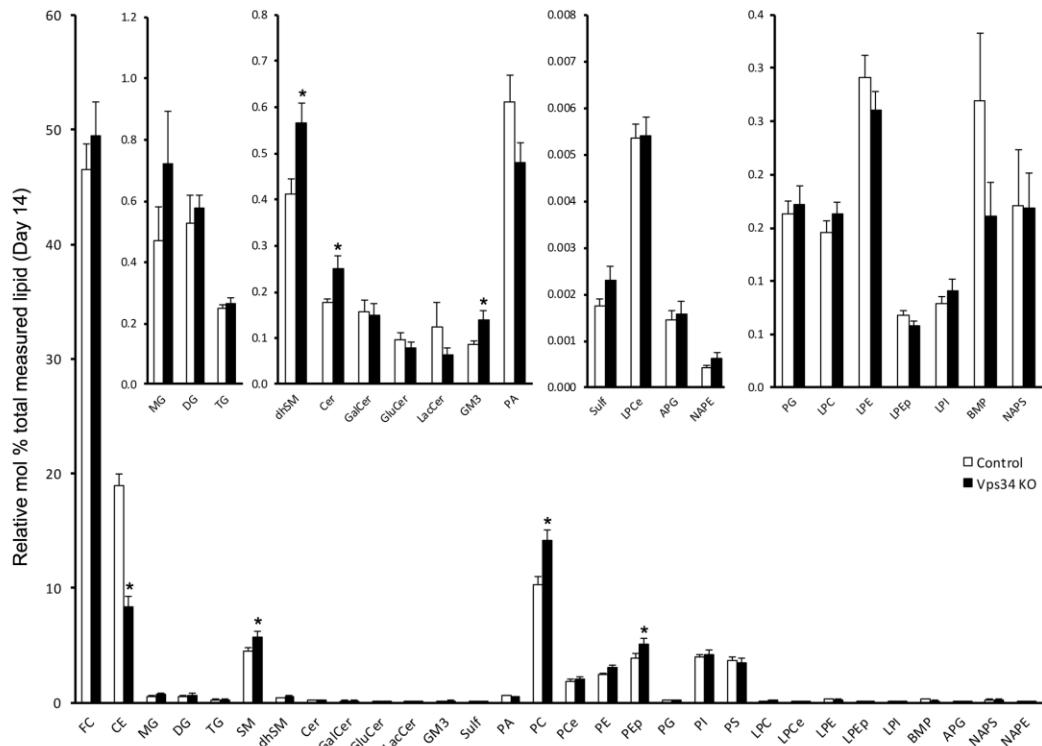


Figure 3.1 Effects of acute and prolonged Vps34 ablation on lipid composition. *Vps34^{Flox/Flox}* MEFs were infected with lentiviruses expressing either an inactive Cre (Δ) or active (CRE) full-length Cre recombinase for 10 or 14 days prior to harvesting cells and extracting lipids for analysis. **(A)** Levels of various lipid subclasses in control and *Vps34* KO MEFs after 10 days of lentiviral infection. **(B)** Levels of lipid subclasses in control and *Vps34* KO MEFs after 14 days of lentiviral infection. Values expressed as mean relative mol % of total lipid species measured and error bars indicate S.E.M. (n=7).

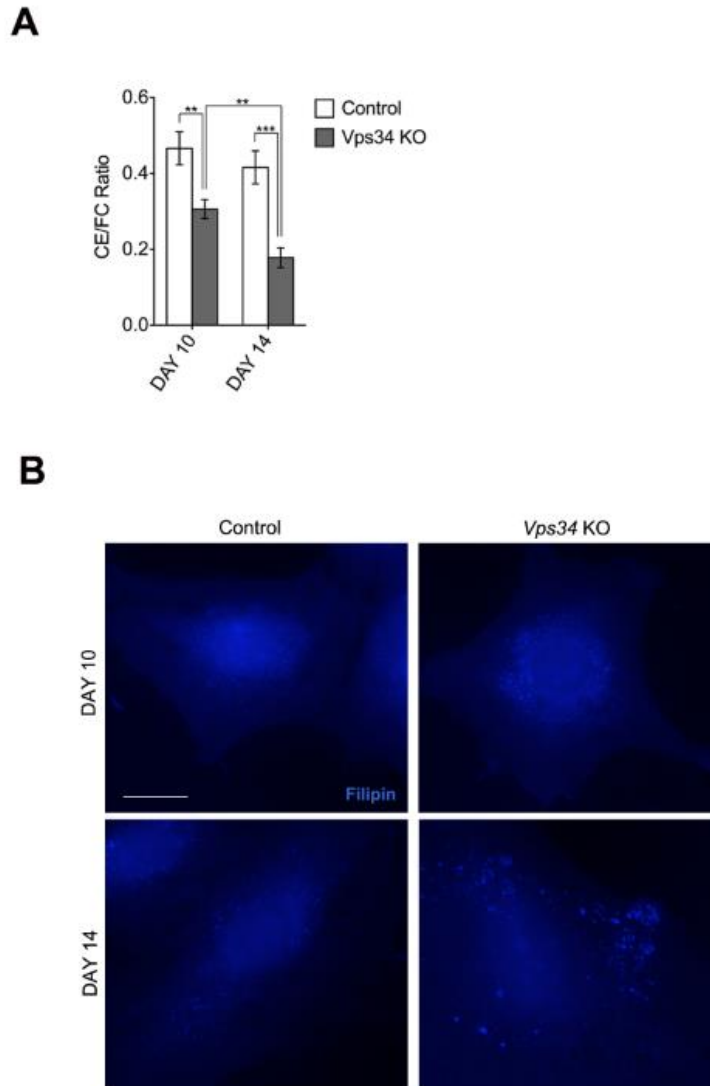


Figure 3.2 Altered cholesterol homeostasis in *Vps34* KO MEFs. (A) Mean ratio of total cholesteryl esters to free cholesterol in control and *Vps34* KO MEFs after 10 and 14 days of lentivirus infection (n=7). (B) Confocal analysis of control and *Vps34* KO MEFs immunostained with filipin on days 10 and 14 post-infection.

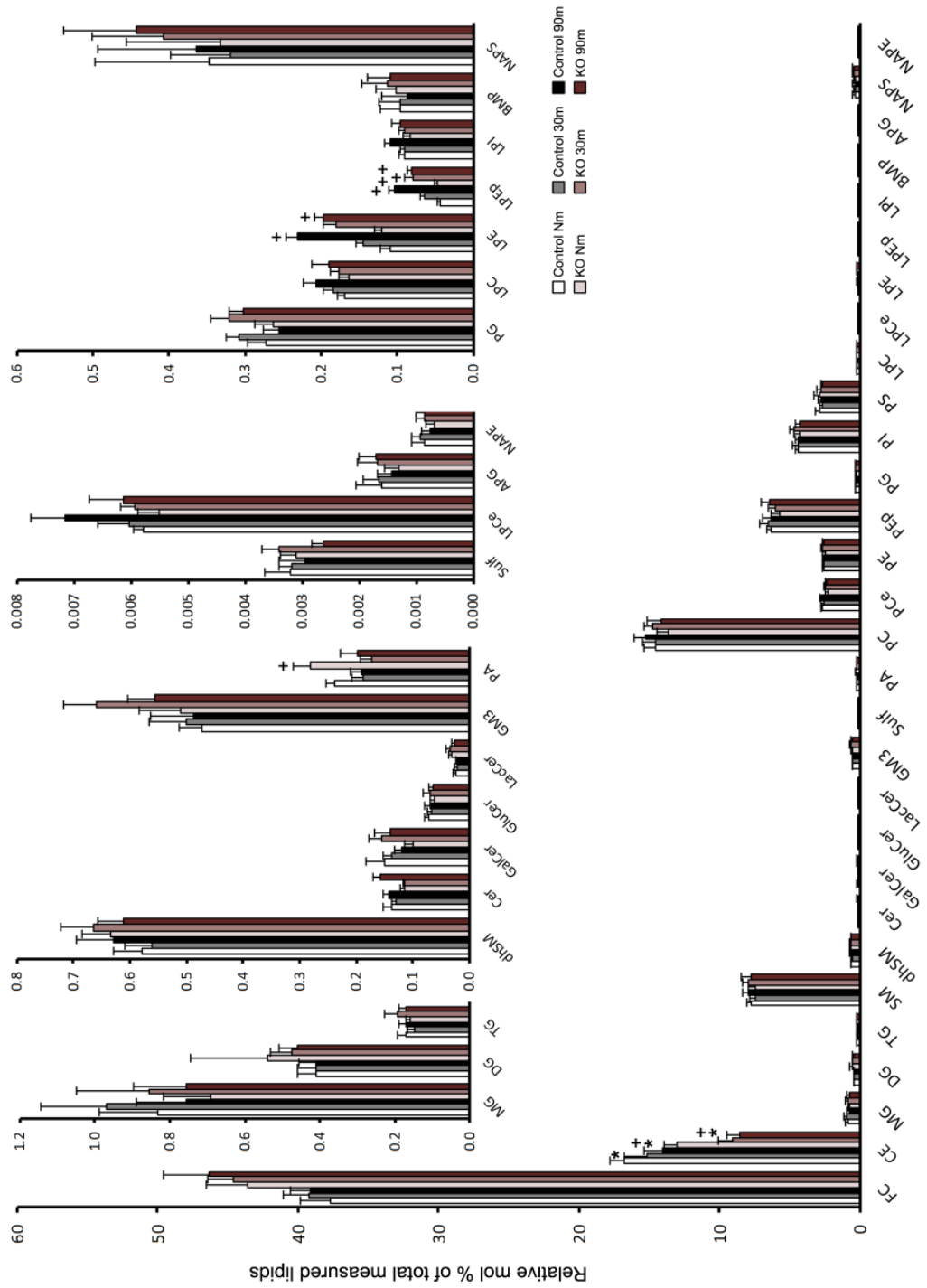


Figure 3.3 Effects of starvation-induced autophagy on lipid composition in control and Vps34 KO MEFs. Control and *Vps34* KO MEFs infected for 10 days with lentivirus were cultured in normal media (Control Nm; KO Nm) or starved for 30mins (Control 30m; KO 30m) or 90mins (Control 90m; KO 90m) in HBSS prior to harvesting and extracting lipids for analysis. Levels of various lipid subclasses in control and *Vps34* KO MEFs after 10 days of lentiviral infection. Values expressed as mean relative mol % of total lipid species measured and error bars indicate s.e.m. (n=7). Statistical analysis was performed using two-way ANOVA followed by two-way unpaired Student's t-test, with additional Bonferroni correction for within-genotype comparisons. *P-value* < 0.05 was indicated as (*) when representing changes within a genotype when compared to normal media conditions and (+) when representing changes between genotypes at a given timepoint.

Figure 3.4 Comprehensive lipid profile of control and *Vps34* KO MEFs. Heatmap shows changes in lipid species organized by subclass. The first four columns compare the relative mol % of total lipid for each species in *Vps34* KO MEFs (KO) to control (C) MEFs when cultured in normal media conditions 10-days post-infection (Nm), normal media conditions 10-days post-infection (Nm_{d14}), or starved for 30mins (30 m) or 90mins (90 m). The last four columns compare the relative mol % of total lipid for each species after 30mins or 90mins to normal media conditions within the control (C) and *Vps34* KO (KO) MEF genotypes. Color bars represent the log₂ ratio of mean relative mol% between two genotypes or conditions.

3.4 Discussion

In the first part of this study, we aimed to identify novel interactions between the class III PI3K, Vps34, and the lipidome using a lipidomic approach. Our analysis revealed a previously unrecognized relationship between Vps34 and cholesterol homeostasis in cells. Specifically, an increase in FC levels and a decrease in CE were observed upon ablation of Vps34. These findings raise several hypotheses discussed below and will require future studies to better understand how Vps34 regulates cholesterol metabolism.

Cholesterol levels and its distribution within cells are tightly regulated through a combination of trafficking and enzymatic processes in the mammalian cells (Ioannou, 2001; Maxfield and Tabas, 2005; Maxfield and van Meer, 2010; Maxfield and Wustner, 2002). Intracellular cholesterol is derived either through its endogenous biosynthesis by the 3-hydroxy-3-methylglutaryl-coenzyme (HMG-CoA) reductase pathway or through the uptake of circulating plasma lipoproteins via the low-density lipoprotein (LDL) receptor pathway (Ioannou, 2001; Maxfield and Tabas, 2005; Maxfield and van Meer, 2010; Maxfield and Wustner, 2002). In the uptake pathway, cholesterol is endocytosed as LDL-associated CE, which is trafficked to the late endosomes (LE) and lysosomes (LY) (Ioannou, 2001; Maxfield and Tabas, 2005; Maxfield and van Meer, 2010; Maxfield and Wustner, 2002). In the LE/LY, CE is hydrolyzed by lysosomal acid lipases (LAL) into FC and fatty acids. The liberated FC is first transferred to Niemann Pick type C2 (NPC2), a soluble protein within the lumen, and then to Niemann Pick type C1 (NPC1), a transmembrane protein within the limiting membrane of the LE/LY (Infante et al., 2008; Kwon et al., 2009). Importantly, BMP, a lipid that resides mainly in the ILVs of late endosomes, has been shown to enhance LAL and NPC2 activity as well as enhance the

cholesterol storage capacity of LEs (Kobayashi et al., 1999; Xu et al., 2008). Once FC is delivered to NPC1 it is transferred to the limiting membrane of the LE/LY and transported via vesicles or carrier proteins to other membrane sites within the cell (Kwon et al., 2009; Maxfield and Wustner, 2002; Soccio and Breslow, 2004; Yang, 2006). FC may be transported to membranes, such as the plasma membrane, endosomes or TGN, where it plays a critical role in lipid raft functions (Mesmin and Maxfield, 2009). Alternatively, FC may be trafficked to the ER and undergo esterification by acyl-CoA cholesterol acyltransferase (ACAT) and stored in lipid droplets (Buhman et al., 2000; Chang et al., 1997). When levels of FC become too high, a "reverse cholesterol transport" program is upregulated through the activation of liver X/retinoid X receptors (LXR/RXR) to promote cholesterol efflux out of the cell via transporters (*e.g.*, ABCA1) at the plasma membrane (Chawla et al., 2001; Costet et al., 2003; Oram, 2002; Stefkova et al., 2004). Conversely, if levels of FC become too low, sterol regulatory element-binding proteins (SREBP) undergo cleavage to allow for transcription factor release and upregulation of sterol-synthesizing genes (*e.g.*, HMG CoA reductase, LDL receptor) (Brown and Goldstein, 1999). Cholesterol regulation is a complex pathway that makes the increase in FC and decrease in CE observed in *Vps34* KO cells more challenging to understand due to the fact that perturbations could occur multiple steps.

At this stage, it is unclear whether an upregulation in uptake and/or synthesis of cholesterol or a decline in efficient efflux and trafficking is causing the FC accumulation in *Vps34* KO MEFs. First, it will be important to localize the excess FC in the *Vps34* KO MEFs. In this study, filipin was used to confirm the increase in FC levels seen by lipidomic analysis in *Vps34* KO MEFs; however, filipin colocalization studies with

various organellar markers also need to be performed in order to determine whether filipin puncta observed upon Vps34 ablation represent an accumulation of FC in LE/LYs. Additionally, determining whether FC accumulates on the luminal versus limiting membrane will likely be helpful in identifying whether cholesterol transfer to or efflux from the limiting membrane is impaired. For instance, when NPC1/2 is impaired FC accumulates in the lumen of the LE/LY; however, when cholesterol carrier proteins, such as the oxysterol-binding protein related protein 5 (ORP5), are impaired, FC accumulates within the limiting membrane (Du et al., 2011). Additionally, levels and localization of major regulators of the cholesterol metabolic pathway should be characterized in the *Vps34* KO MEFs in order to better understand the cause(s) of FC accumulation. Major regulators that should be examined in the *Vps34* KO MEFs include: LXR/RXR and SREBP transcription factors, HMGCoA reductase, LDL receptor, ACAT-1/2 (ACAT-2 expression is limited to intestinal cells), ABCA transporters (*e.g.*, ABCA1) and cytosolic nonvesicular transporters (*e.g.*, MLN64, OSBPs, START proteins, Hrs). Interestingly, a recent study showed that Hrs, a PI3P-binding protein implicated in ESCRT-dependent MVB formation, plays a role in LDL-derived cholesterol trafficking from the endosome to the ER (Du et al., 2012; Petiot et al., 2003). Specifically, Hrs is thought to recruit lipid carriers, such as ORP5 (an OSBP family member), that facilitate cholesterol removal from the limiting membrane (Du et al., 2012). Additionally, Hrs is important for ILV formation, which plays a critical role in the storage and trafficking of luminal cholesterol (Du et al., 2012; Gruenberg and Stenmark, 2004). In previous studies, PI3P production by Vps34 has been shown to be important for recruiting Hrs to the endosomal membrane as well as promote ILV formation via the ESCRT-pathway, making this

process a likely candidate to be affected by *Vps34* ablation (Fernandez-Borja et al., 1999; Futter et al., 2001a; Komada and Soriano, 1999; Petiot et al., 2003; Raiborg et al., 2001; Reaves et al., 1996; Urbe et al., 2000)

In addition to studying FC in *Vps34* KO MEFs, further investigation will be required to understand the progressive decrease in CE observed with prolonged ablation of *Vps34*. The studies proposed above will help determine whether ACAT is misregulated or mislocalized in *Vps34* KO MEFs; however, its activity may need to be tested as well. ACAT is an ER resident enzyme that localizes to mitochondria-associated ER membranes (MAM), a subcompartment of the ER that is physically and biochemically connected to the mitochondria (Hayashi et al., 2009; Lewin et al., 2002; Rusinol et al., 1994). ACAT plays an important role in preventing an accumulation of FC cholesterol by converting FC to CE for lipid droplet storage. CEs in lipid droplets can be mobilized by cholesterol ester hydrolases residing in the cytoplasm or the lysosome, although lysosomal hydrolysis requires that lipid droplets first be delivered to the lysosome via autophagy (termed lipophagy) (Thiam et al., 2013; Walther and Farese, 2012). In order to prevent excess conversion of FC into CE, the activity of ACAT is allosterically regulated by cholesterol (Tabas, 2002; Zhang et al., 2003b). ACAT activity can be assessed using a standard cholesterol esterification assay, whereby radioactive cholesteryl oleate is added to cells and its conversion to CE is measured. If localization and levels of ACAT are normal, but its activity declines, it may reflect two scenarios. Simply, there may be a kinetic delay in FC efflux and/or trafficking from the LE/LY to the ER. Alternatively, ACAT activity may be impaired due to a disruption of the MAM. ACAT activity and CE synthesis has been correlated with MAM function (Area-Gomez

et al., 2012). Specifically, MAM integrity can be examined by electron microscopy and ultrastructural analysis of the membrane as well as isolation of MAMs and checking for the presence of known markers. Recently, it was discovered that Vps34 associates with the MAM during starvation-induced autophagy to promote autophagosome biogenesis at this site (Hamasaki et al., 2013). Whether Vps34 has additional roles at the MAM that could be affecting ACAT activity at this site is currently unclear.

Interestingly, a trend for an increase in FC and significant decrease in CE observed in *Vps34* KO MEFs is reminiscent of an NPC disease phenotype. In NPC disease, mutations in NPC1 and 2 lead to accumulation of LDL-derived FC in the lumen of the LE/LY, which subsequently triggers upregulation of pathways that favor endogenous cholesterol synthesis and further uptake (Rosenbaum and Maxfield, 2011). Also, a decline in CE synthesis is observed and may reflect slowed FC efflux and trafficking to the ER from the LE/LY (Liscum, 2000; Pentchev et al., 1985; Rosenbaum and Maxfield, 2011). Importantly, in addition to the changes in FC and CE observed in NPC, there is a multitude of other lipid species that also accumulate in NPC, including sphingomyelin, sphingosine, GM2, GM3 and BMP (Lloyd-Evans and Platt, 2010; Walkley and Vanier, 2009; Zervas et al., 2001). Likewise, in the *Vps34* KO MEFs there is an accumulation of specific lipid species, including dhSM, SM, Cer, GM3, PC, and PEp, with more prolonged ablation. Notably, BMP levels have been shown to correlate with an increase in FC level, as in NPC (Chevallier et al., 2008; Kobayashi et al., 1999); however, its overall level does not change in *Vps34* KO MEFs and may reflect the fact that the increased in FC observed in the knock-out is not significant enough. Given that

Vps34 plays a major role in hydrolase trafficking to the lysosome, an accumulation in lipids is expected and may be secondary to insufficient lysosomal hydrolase activity.

In the second part of this study, lipidomics was used to identify new lipid networks related to starvation-induced autophagy. In our analysis, we found a specific increase in LPEp in control and *Vps34* KO MEFs as well as an increase in LPE in *Vps34* KO MEFs during starvation-induced autophagy. LPE is a lysolipid subclass derived from PE through hydrolysis by lysosomal phospholipase A2 (PLA2) (Library; Makide et al., 2009), although its role is currently unknown. LPEp and its purported precursor PEP are structurally similar, though as plasmalogens they contain a vinyl-ether bond at the sn-1 position, rather than the typical ester linkage (Lohner, 1996). Although all plasmalogen biosynthesis begins in the peroxisome, very little is known about LPEp specifically in terms of its synthesis, function and localization. Although a physiological explanation for an increase in these lipids unclear at this stage, PE is known to be important lipid subclass for AP biogenesis. During autophagy, LC3 (the mammalian homolog of Atg8) is conjugated to PE on the inner and outer leaflets of AP membrane by a ubiquitin-like conjugation system. Given that APs ultimately undergo fusion with the lysosome for degradation, PE may be delivered to the lysosome at a higher rate during this process and subsequently be metabolized to LPE, for example. Previous studies in yeast have demonstrated that Atg8 is conjugated to PE in yeast (Ichimura et al., 2000), but whether mammalian LC3 is conjugated solely to PE or to other PE-related lipids, such as PEP, has not been determined. Given that an increase in LPEp is observed in starved control and *Vps34* KO MEFs, it would be interesting to test whether LC3-PEp conjugation could also occur in mammals. So far, it is unclear why an increase in LPE

is observed in *Vps34* KO and not in control MEFs. Notably, the increase in LPE during autophagy is delayed in the *Vps34* KO MEFs, which may reflect impaired kinetics in AP flux. However, in future studies, it will be important to determine whether the LPEp and LPE changes are, in fact, due to downstream maturation and degradation steps and not autophagy initiation. In order to distinguish between these scenarios, the lipidome of a mutant cells defective in AP biogenesis (*e.g.*, *Atg5*) should be compared to cells in which fusion and lysosomal degradation is impaired (*e.g.*, chloroquine).

In addition, we observed a trend for an increase in FC and a decrease in CE during autophagy stimulation in MEFs of both genotypes. Recent studies have shown that during autophagy, lipid droplets, which are single membrane organelles that store CE and TGs, are engulfed by APs and taken to the lysosome where LAL enzymes hydrolyze CE into FC and fatty acids (Singh and Cuervo, 2012; Singh et al., 2009). Notably, a trend for an increase in FC and a significant decrease in CE was observed under starvation conditions in the *Vps34* KO MEFs compared to control MEFs, reflecting the dysregulation in cholesterol homeostasis discussed above. Taken together, lipidomic analysis revealed fewer lipid changes than expected, considering the amount of membrane remodeling and cellular degradation that occurs during this process. In the future it would be interesting to analyze the lipid composition of various membranes in the cell by through subcellular fractionation, which may reveal important localized changes that were not observed during whole cell analysis.

Lipidomics is instrumental in identifying and understanding lipids. Not only is lipidomics of basic science relevance, but also it is powerful technology that holds promise for identifying new biomarkers in disease and identifying and addressing lipid

dysregulation in numerous diseases. Recent advances in analytical technologies have enhanced our ability to detect a wide array of lipids; however, continuous efforts are required to improve detection capabilities and more comprehensively catalog the wide range of lipids. Combining lipidomics with genomics and proteomics is an emerging concept in the biological sciences that will be important for discovering new relationships between genes, proteins, and lipids.

3.5 Materials and Methods.

3.5.1 Generating *Vps34* KO MEFs.

See Chapter 2 Materials and Methods.

3.5.2 Annotation of Lipid Species

Lipids were annotated in bar graphs and heat maps as follows:

APG, acyl phosphatidylglycerol; BMP, bis(monoacylglycerol)phosphate; CE, cholesteryl ester; Cer, ceramide; DG, diacylglycerol; LPC, lysophosphatidylcholine; LPCe, ether lysophosphatidylcholine; LPE, lysophosphatidylethanolamine; LPEp, plasmalogens lysophosphatidylethanolamine; LPI, lysophosphatidylinositol; FC, free cholesterol; GalCer, galactosylceramide; GluCer, glucosylceramide; GM3, ceramide-lactose-N-acetylneuraminic acid; LacCer, lactosylceramide; MG, monoacylglycerol; NAPS, N-acyl phosphatidylserine; NAPE, N-acyl phosphatidylethanolamine; SM, sphingomyelin; dhSM, dihydrosphingomyelin; Sulf, sulfatide; PA, phosphatidic acid; PC, phosphatidylcholine; PCe, ether phosphatidylcholine; PE, phosphatidylethanolamine; PEp, plasmalogens phosphatidylethanolamine; PG, phosphatidylglycerol; PI, phosphatidylinositol; PS, phosphatidylserine; TG, triacylglycerol.

3.5.3 Analysis of Lipids Using High Performance Liquid Chromatography-Mass Spectrometry

Cell lipid extracts were prepared using a modified Bligh/Dyer procedure (Bligh and Dyer). Samples were spiked with an internal standard cocktail and analyzed using a 6490 Triple Quadrupole LC/MS system (Agilent Technologies, Santa Clara, CA).

Glycerophospholipids and sphingolipids were separated with normal-phase HPLC as before (Chan et al., 2012), with a few changes. An Agilent Zorbax Rx-Sil column (inner

diameter 2.1 x 100 mm) was used under the following conditions: mobile phase A (chloroform:methanol:1 M ammonium hydroxide, 89.9:10:0.1, v/v) and mobile phase B (chloroform:methanol:water:ammonium hydroxide, 55:39:5.9:0.1, v/v); 95% A for 2 min, linear gradient to 30% A over 18 min and held for 3 min, and linear gradient to 95% A over 2 min and held for 6 min. FC, CEs, and glycerophospholipids (GLs) were separated with reverse-phase HPLC using an isocratic mobile phase as before (Chan et al., 2012) with an Agilent Zorbax Eclipse XDB-C18 column (4.6 x 100 mm). GLs and sphingolipids were analyzed using both positive and negative mode ionization, while FC, CE and GLs were analyzed using only positive mode ionization.

3.5.4 Data Analysis and Presentation

Lipid levels were represented as relative mol %, which was calculated by normalizing individual lipid subclasses or species to the total lipids measured in all three LC-MS methodologies. The final data are presented as mean with error bars showing mean \pm s.e.m. Statistical analysis was performed using a two-way ANOVA followed by two-tailed unpaired Student's t-test for each comparison with an additional Bonferoni correction as appropriate. *P-value* < 0.05 indicated as (*).

Chapter 4: A novel role for retromer in autophagy

4.1 Introduction

Alzheimer's disease (AD), the most common form of age-related dementia, is a devastating neurodegenerative disorder that results in the progressive loss of memory function and cognition (Blennow et al., 2006; Querfurth and LaFerla, 2010; Thies and Bleiler, 2013). In an effort to better understand the molecular mechanisms underlying both familial and sporadic (or late-onset) AD, linkage analyses as well as genome-wide association studies (GWAS) have been performed in recent years and have revealed multiple genetic variants as risk factors (Elias-Sonnenschein et al., 2012). Although AD is a genetically complex disorder, two hallmark pathological features observed in the hippocampus and cerebral cortex regions of all AD patient brains include: 1) intracellular neurofibrillary tangles, which consist of hyperphosphorylated and aggregated forms of the microtubule-associated protein tau, and 2) extracellular amyloid plaques, which are composed of fibrillar aggregates of β -amyloid peptide (primarily A β 42) derived from the proteolysis of amyloid precursor protein (APP) (De Strooper, 2010; Delacourte, 2008; Glenner and Wong, 2012; Mandelkow and Mandelkow, 2012; Masters and Beyreuther, 2006). In addition to these findings, however, ultrastructural analysis of AD brains has consistently revealed less characterized features of pathogenesis, including enlarged endosomes (Cataldo et al., 1997; Cataldo et al., 2004; Cataldo et al., 2000) and the progressive appearance of swollen neurites filled with vacuolar structures, which were later identified as autophagosomes (APs) and autophagolysosomes (ALs), and lysosomal dense-bodies (Nixon et al., 2005; Suzuki and Terry, 1967; Terry et al., 1964). These findings, together with studies on fetuses with Down syndrome showing endosomal

anomalies preceding A β plaques and tangles by several decades (Cataldo et al., 2000), support a hypothesis in which endo-lysosomal system dysfunction may be a major factor underlying many of the pathogenic features of AD (Nixon, 2007; Nixon and Yang, 2011).

Currently, the precise cause of this breakdown in the endo-lysosomal system that appears to occur in AD is unknown. However, several recent GWAS studies have identified important gene ‘hits’ encoding members of the retromer complex and its cargo, the vacuolar protein sorting 10 (Vps10) family of receptors, as significant risk factors for several neurodegenerative diseases, including late-onset AD (LOAD), Parkinson’s disease and frontotemporal dementia (Lane et al., 2012; Small, 2008; Small and Gandy, 2006; Willnow and Andersen, 2013) and are likely contributory factors. In brief, retromer was first discovered in yeast for its role in recycling Vps10 (the yeast ortholog of the mannose 6-phosphate receptor (M6PR)) from the endosomal pathway to the TGN, which is essential for maintaining proper delivery of acidic hydrolases to the vacuole (the yeast equivalent of the lysosome) and lysosomal function (Bonifacino and Hurley, 2008; Seaman, 2005). Later studies showed that retromer is a highly conserved complex in mammals and is required for the retrograde endosome-to-TGN trafficking of M6PR, which is responsible for trafficking mammalian lysosomal hydrolases (Seaman, 2012), and of a subset of the Vps10 receptor family members (including sortilin, sorL1, SorCS1, SorCS2 and SorC2), which all contains a conserved Vps10-recognition domain and bind to a variety of ligands, including some lysosomal hydrolases and APP (Brulke and Bonifacino, 2009; Lane et al., 2012; Willnow et al., 2008). In mammals, the retromer complex consists of a cargo recognition domain (Vps35/26/19) and a membrane association domain composed of a dimer of the sorting nexin proteins SNX1 or SNX2

with either SNX5 or SNX6 (or possibly SNX32) (Bonifacino and Hurley, 2008; Haft et al., 2000; McGough and Cullen, 2011; Seaman, 2004; Seaman, 2005) (Fig. 4.1) The SNX proteins contains an N-terminal phox homology (PX) domain, shown to bind phosphatidylinositol-3-phosphate (PI3P) on the early endosomes (although the PX domain can also associate with other phosphoinositides such as phosphatidylinositol-3,5-bisphosphate (PI(3,5)P₂)) as well as a BAR domain, believed to sense and drive membrane curvature facilitating membrane evagination in the form of tubules (Carlton and Cullen, 2005; Cullen and Korswagen, 2012; Seet and Hong, 2006; Worby and Dixon, 2002). Together, the components of the retromer complex facilitate cargo sorting and tubulation of the endosomes whereby vesicles can bud off and traffic to the TGN or other compartments, such as the cell surface (McGough and Cullen, 2011; Seaman, 2005; Seaman, 2012). The retromer was first implicated in AD when a study found deficiencies in Vps35 and Vps26 in the hippocampus of LOAD patients (Small et al., 2005). More recently, members of the Vps10 family of receptors (*e.g.* SorLA, SorCS1) (Lane et al., 2012; Willnow and Andersen, 2013) as well as SNX1, SNX3 and RAB7A (Vardarajan et al., 2012), which all regulate the membrane association of retromer, were also identified as risk genes in LOAD. Further investigation is required to determine how risk factors implicated in retrograde trafficking may contribute to the pathogenesis of AD.

So far, several studies have shown that the ablation of retromer complex members, including Vps35 (Muhammad et al., 2008; Small et al., 2005) and Vps26 (Rogaeva et al., 2007), or members of the Vps10 receptor family, including SorL1 (Andersen et al., 2005; Dodson et al., 2006; Rogaeva et al., 2007) and SorCS1 (Lane et al., 2010), causes an increase in A β production. In fact, it has been hypothesized that

efficient retrieval of APP from the endosome by retromer reduces its retention time in the endosome, where evidence suggests APP processing by BACE1 and cleavage into A β takes place (Lane et al., 2010; Small, 2008; Small and Gandy, 2006; Willnow and Andersen, 2013).

In addition to an increase in A β 42 production, the dysfunctional endo-lysosomal trafficking caused by retromer impairment is likely to contribute to other pathological features observed in LOAD. Previous studies have shown that retromer depletion results in a failure to recycle M6PR from the endosome back to the TGN, which leads to an accumulation of pre-mature hydrolases in the Golgi as well as mistrafficking of hydrolases into the secretory pathway and subsequent secretion extracellularly (Seaman, 2004; Seaman, 2005). However, whether impaired retromer trafficking causes a decline in delivery of lysosomal hydrolases to the lysosome and compromised lysosomal function in AD has not been addressed. Interestingly, an immature form of cathepsin D, a hydrolase recognized and trafficked by the M6PR, was shown to be elevated in the cerebral spinal fluid of AD patients, which would be an expected consequence of a deficiency in retromer (Cataldo et al., 1995). Additionally, a concomitant upregulation of many lysosomal system components has been observed in AD and likely reflects a compensatory attempt by neuronal cells to try to rescue lysosomal system dysfunction (Cataldo et al., 1995; Cataldo et al., 1991; Cataldo et al., 1990). If retromer is, in fact, important for maintaining proper lysosomal function, its impairment likely would contribute to the formation of lysosomal dense bodies and an accumulation of AP and AVs observed in LOAD. Interestingly, presenilin 1 (PS1), a component of the gamma-secretase and one of the most commonly mutated genes in familial AD (FAD), was

recently implicated in promoting the maturation and targeting of the vacuolar [H⁺] ATPase V0a1 subunit to the lysosome required for acidification (Lee et al., 2010). Acidification of lysosomes is not only necessary for endo-lysosomal trafficking and fusion events (Huotari and Helenius, 2011), but also for proper proteolytic maturation and activation of lysosomal hydrolases (Kokkonen et al., 2004). In fact, impairment in PS1 resulted in a defect in lysosomal acidification and cathepsin D maturation, which led to a decline in autophagic flux and an accumulation of APs and AVs as seen in AD (Lee et al., 2010). As mentioned in previous chapters, autophagy is largely responsible for clearing cells of protein aggregates; therefore, a defect in this process is likely to exacerbate the accumulation of intracellular tau aggregates observed in AD (Wong and Cuervo, 2010). Although mutations in PS1 are well known for causing aberrant APP and contributing to elevated levels of amyloidogenic A β 42 in AD (Duff et al., 1996; Scheuner et al., 1996), this particular study demonstrates how a single hit can potentially cause multiple features of AD as well as provides an explanation for the endo-lysosomal dysfunction observed in FAD. Like PS1, retromer also holds the potential to contribute to multiple features of AD, specifically in sporadic AD cases; therefore, we hypothesized that in addition to its known role in APP trafficking, retromer is required for maintaining lysosomal homeostasis and autophagy.

Identifying genes associated with familial and sporadic AD that cause common AD pathological features is important for advancing our understanding of disease progression and therapeutic intervention strategies. We hypothesize that genetic risk factors associated with retromer complex in LOAD not only contribute to an increase in A β production and tau aggregation, but also contribute more broadly to other cellular

pathologies observed in AD. As mentioned in Chapter 2, lysosomal function is particularly important for maintaining homeostasis in non-dividing cells, such as neurons, which rely on autophagy for the removal of accumulated organelles and aggregates (Mizushima et al., 2008). In fact, much attention has been placed on the idea of modulating autophagy in proteinopathies such as AD in order to clear intracellular tau and A β protein aggregates and to promote neuronal survival (Wong and Cuervo, 2010). Importantly, the impairment in autophagy observed in AD is likely to be the result of lysosomal dysfunction rather than an inherent problem in the process itself, making it critical to determine and target the cause of the autophagy defect in order to improve its overall function. Here, we specifically focused on and tested whether Vps35 regulates autophagy in a variety of cell types, including HeLa cells, primary neurons and mouse embryonic fibroblasts (MEFs). Our results show that retromer is a negative regulator of autophagy by LC3 conjugation and immunofluorescence. Additionally, there is a strong colocalization between Vps35 and Atg9, the only transmembrane autophagy protein identified, suggesting a functional link between these two proteins.

4.2 Results

4.2.1 Knock-down of Vps35 in HeLa and primary neurons enhances LC3 conjugation.

In order to test our hypothesis that Vps35 plays a role in regulating autophagy, we first monitored the lipidation of LC3 upon Vps35 depletion. During AP formation, a ubiquitin-like enzymatic reaction occurs whereby LC3-I is conjugated to phosphatidylethanolamine PE to yield LC3-II, which can be monitored by a shift in protein migration on a Western blot. HeLa cells were transfected with mock and *Vps35*

siRNAs for 144 hrs to generate control and Vps35-depleted cells, respectively. Interestingly, an increase in the basal (Nm) levels of LC3-II was observed in Vps35 depleted cells (~3-fold) compared to control cells (Fig. 4.2A). The addition of Bafilomycin (Nm+B), a proton pump inhibitor that prevents lysosomal acidification and thus the clearance of APs, produced an increase in LC3-II levels of a similar scale in both control (~2-fold) and *Vps35* depleted (~2-fold) cells compared to their respective basal LC3-II levels. This result indicates that siRNA-depletion of Vps35 causes an increase in autophagic flux rather than an impairment in AP clearance. Likewise, LC3-II levels were higher in Vps35 depleted cells (~2.5-fold) compared to control cells after 3hrs of starvation (St) (Fig. 4.2A). Again, this increase in LC3-II observed in the Vps35 depleted cells is predominately due to an increase in autophagic flux since LC3-II levels were greatly enhanced upon Bafilomycin treatment (St+B). Notably, the addition of Baf caused a similar increase in LC3-II levels in both control (~2.5-fold) and Vps35 depleted (~2-fold) compared starvation alone (Fig. 4.2A). Levels of p62, an AP cargo, were also measured by Western blot in control and Vps35 depleted HeLa cells (Fig. 4.2B). A decrease in p62 levels is apparent in all conditions (Nm, Nm+B, St, St+B) upon Vps35 depletion, reflecting an overall increase in autophagy. As expected, p62 levels were reduced in control and Vps35-depleted cells during starvation-induced autophagy. Additionally, in the presence of Bafilomycin, degradation of p62 was impaired in both conditions (Fig. 4.2B). Taken together, the enhanced LC3 conjugation and decreased p62 levels in the Vps35 depleted cells suggest that Vps35 is a negative regulator of autophagy.

To test whether this phenomenon also occurs in another cell type, we examined LC3 conjugation in primary neurons treated with either mock or *Vps35* shRNA lentivirus. Our neuronal studies showed an increase in LC3 lipidation under steady-state or basal conditions in *Vps35* depleted compared to control neurons, which is consistent with our findings in HeLa cells (Fig. 4.2C). Since bafilomycin was not added to the media in this experiment, whether this finding also reflects an increase in flux rather than a decrease in AP clearance has not yet been determined. Additionally, we have yet to test whether induced autophagy is affected by *Vps35* ablation in neurons.

4.2.2 *Vps35* KO MEFs show an increase in basal and starvation-induced LC3 conjugation.

Next, *Vps35*^{Flox/Flox} mouse embryonic fibroblasts (MEFs) were generated from a *Vps35* conditional mouse model in order to verify these findings in a third cell type as well as employ a strategy that would enable a more efficient depletion of *Vps35* in future experimentation. *Vps35*^{Flox/Flox} MEFs were immortalized by multiple passages and infected with lentiviruses encoding either a catalytically-inactive or active, nuclear Cre recombinase fused to eGFP (green) fluorescent protein to generate control and *Vps35* KO cells, respectively (see Materials and Methods). Expression of active Cre, but not inactive Cre, resulted in the progressive loss of *Vps35* immunoreactivity by Western blot analyses over the course of several days with complete loss of expression achieved by 9 to 10 days (Fig. 4.3A).

In order to compare autophagy in control and *Vps35* KO MEFs, we monitored LC3 lipidation by Western blot as well as examined endogenous LC3 by confocal microscopy. *Vps35* KO MEFs showed similar Western blot results to that of HeLa cells

treated with *Vps35* siRNA (Fig. 4.3B). Specifically, LC3 conjugation increased under steady-state conditions (Nm) and after 3hrs of starvation (St) in *Vps35* KO MEFs. Additionally, an increase in LC3-II levels was observed after treatment of *Vps35* KO MEFs with Baf (Nm+B, St+B), indicating enhanced autophagic flux. Endogenous LC3 was also examined in control and *Vps35* KO MEFs by confocal microscopy during starvation-induced autophagy (Fig. 4.3C). After 90 minutes of starvation, a trend for an increase in LC3 puncta was observed in the *Vps35* KO MEFs compared to control MEFs. Notably, the size of the LC3 puncta in the *Vps35* KO MEFs was significantly larger, which may reflect larger APs or tightly clustered APs (Fig. 4.3C). Both an increase in LC3 conjugation as well as an increase in LC3 puncta and puncta size seen in the *Vps35* KO MEFs corroborate with the findings observed in HeLa cells and again suggests that *Vps35* is a negative regulator of autophagy.

4.2.3 *Vps35* minimally colocalizes with Atg16, a preautophagosomal marker, and LC3 during starvation-induced autophagy.

To better understand the role of *Vps35* in the autophagy process, we examined the localization of *Vps35* compared to autophagosome precursors and autophagosomes. Control MEFs were immunostained for endogenous *Vps35* and LC3 or Atg16 after 90 minutes of starvation (Fig. 4.4). Atg16, a preautophagosomal marker, is recruited to the AP nucleation site in a complex with Atg5 and 12 and facilitates LC3 conjugation during AP biogenesis. Here we observed very minimal colocalization between *Vps35* and Atg16 upon starvation-induced autophagy (Fig. 4.4). Additionally, the colocalization between *Vps35* and LC3, a marker of both immature and mature APs, was also minimal (Fig. 4.4). Taken together, these findings suggest that *Vps35* does not participate in autophagy at the

site of AP biogenesis in a stable manner, but instead may transiently interact with APs or play an indirect role in autophagy perhaps by regulation of autophagy machinery or signaling pathways.

4.2.4 Vps35 strongly colocalizes with Atg9 during steady-state and starvation conditions.

Interestingly, Atg9, an integral membrane protein that is essential for autophagosome formation (Mari et al., 2010; Puri et al., 2013; Webber and Tooze, 2010b), displays a similar trafficking pattern to CI-M6PR, a retromer cargo (Arighi et al., 2004; Seaman, 2004; Seaman, 2005). Specifically, mammalian Atg9 predominately localizes to the trans-golgi network (TGN) during steady-state conditions; however, it re-distributes peripherally to the recycling endosome during autophagy induction (Puri et al., 2013; Webber and Tooze, 2010b; Young et al., 2006). Similarly, CI-M6PR, traffics between the TGN and endosomes and redistributes to peripheral endosome compartments during starvation (Orsi et al., 2012; Young et al., 2006). Given these similarities, we further explored the potential interaction between retromer and Atg9. Control MEFs were cultured in normal media or starved for 90 min and immunostained for endogenous Vps35 and Atg9 (Fig. 4.5). A strong colocalization was observed between retromer and Atg9 at the TGN under steady-state conditions. Colocalization persisted after starvation-induced autophagy and Vps35 re-distributed with Atg9 in the periphery (Fig. 4.5). The high levels of colocalization observed between Atg9 and Vps35 under basal and starvation-induced autophagy is suggestive of a functional association, which is further discussed below.

4.3 Figures

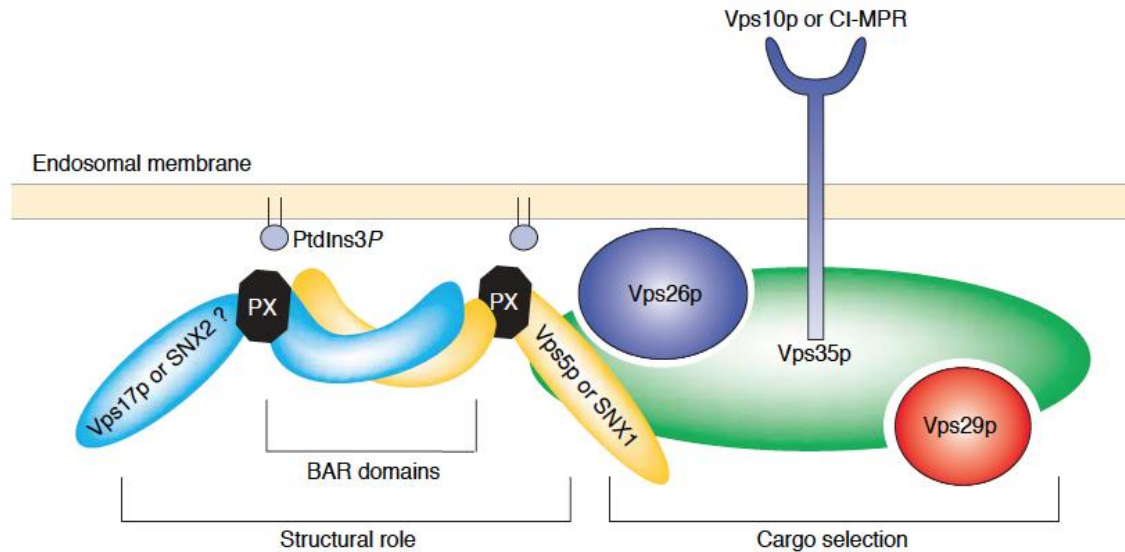


Figure 4.1 The retromer complex. The mammalian retromer complex consists of a cargo selection domain (Vps35/26/19) and a membrane association domain composed of a dimer of the sorting nexin proteins SNX1 or SNX2 (the mammalian homologs of the yeast Vps5) with either SNX5 or SNX6 (or possibly SNX32) (the mammalian homologs of the yeast Vps17). The SNX proteins contains a N-terminal phox homology (PX) domain that binds phosphatidylinositol-3-phosphate (PI3P) on the early endosomes as well as a BAR domain, believed to sense and drive membrane curvature. Taken from (Seaman, 2005).

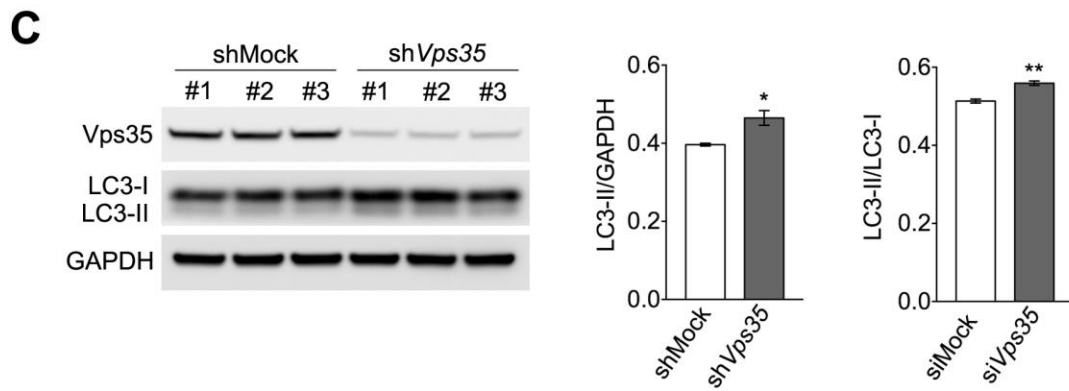
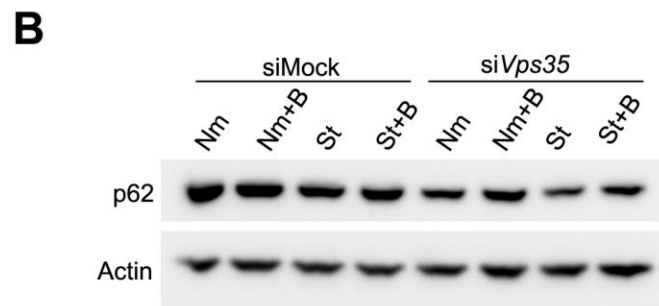
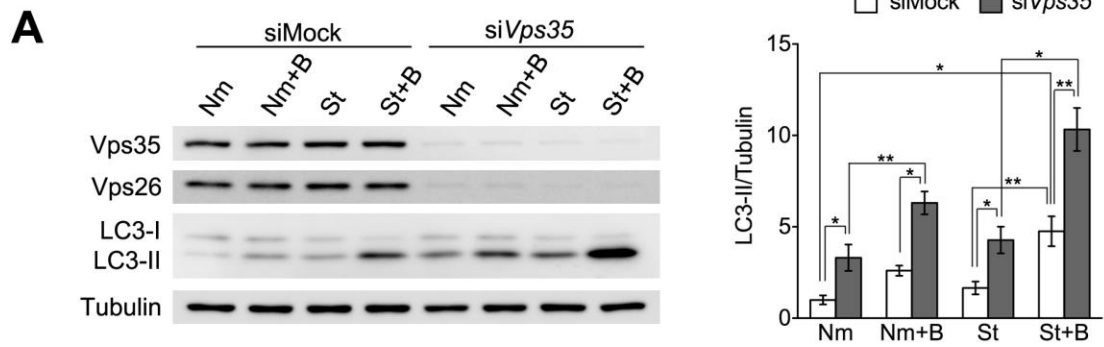


Figure 4.2 Vps35 ablation in HeLa cells and primary neurons causes an increase LC3 conjugation during basal and starvation-induced autophagy. (A) HeLa cells treated with mock or *Vps35* siRNA were cultured in normal media (N) or HBSS (St) in the presence or absence of 50nM Bafilomycin (Nm+B or St+B, respectively) for 3hrs. Right: Lysates were analyzed by immunoblotting using the indicated antibodies. Left: Relative LC3-II levels normalized to tubulin (n=4). (B) Western blot analysis of p62 levels in HeLa cells treated with mock and *Vps35* siRNA and cultured in normal media (N) or HBSS (St) in the presence or absence of 50nM Bafilomycin (Nm+B or St+B, respectively) for 3hrs (n=1) (C) Primary hippocampal neurons treated with mock or *Vps35* shRNA lentivirus and cultured in normal media. Right: Lysates were analyzed by immunoblotting using the indicated antibodies. Left: Quantification of the relative levels of LC3-II normalized to GAPDH and the ratio of LC3-II to LC3-I (n=3).

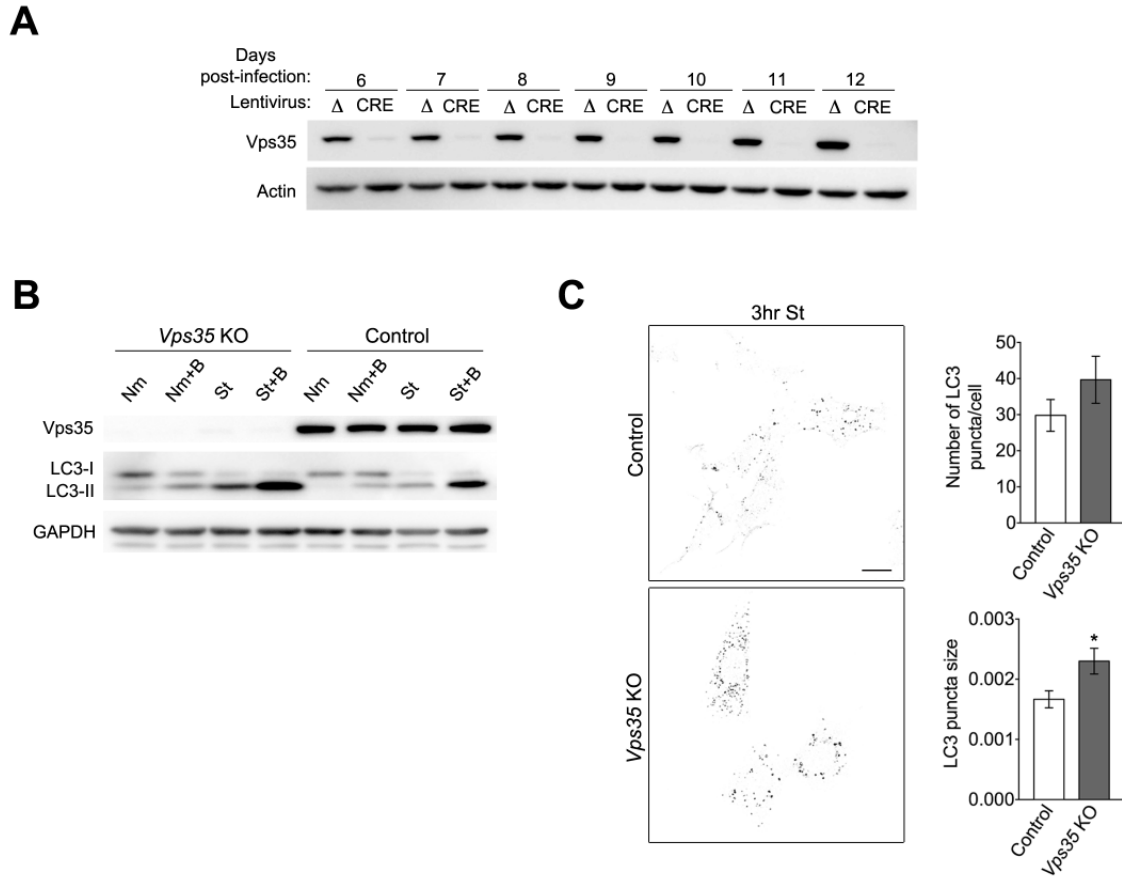


Figure 4.3 *Vps35* KO MEFs show an increase in LC3 conjugation during basal and starvation-induced autophagy as well as larger LC3 puncta during starvation-induced autophagy. (A) Western blot analysis showing a time-course of Vps35 protein levels in *Vps35^{Flox/Flox}* MEFs after infection with lentiviruses expressing either an inactive Cre (Δ) or active (CRE) full-length Cre recombinase for 6-12 days. (B) Control and *Vps35* KO MEFs were cultured in normal media (N) or HBSS (St) in the presence or absence of 50nM Bafilomycin (Nm+B or St+B, respectively) for 90 min. Lysates were analyzed by immunoblotting using the indicated antibodies. (n=1). (C) Control and *Vps35* KO MEFs were cultured in HBSS (St) for 90 min, fixed and immunostained. Right: Confocal microscopy images show endogenous LC3 (black). The image was inverted to allow for better visualization of LC3-positive structures. Scale bar: 10 μ m. Left: Quantification of the average number and size of LC3 puncta per cell. Puncta size given in arbitrary units (a.u.). (n=30-45 cells).

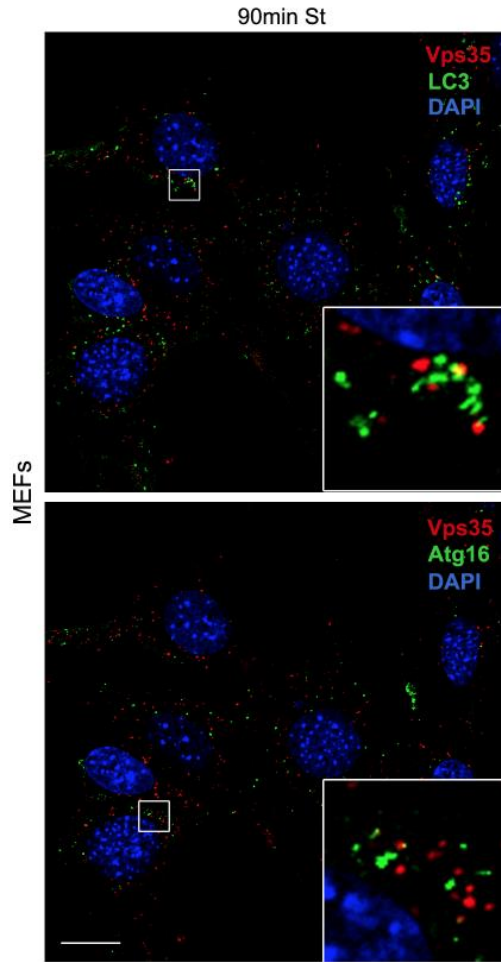


Figure 4.4 Vps35 minimally co-localizes with Atg16 and LC3 during starvation-induced autophagy. Uninfected *Vps35^{Flox/Flox}* MEFs cells were cultured in HBSS for 90min (90min St) and fixed. Confocal microscopy images show endogenous Vps35 (red) and Atg16 or LC3 (green). Scale bar: 10 μ m.

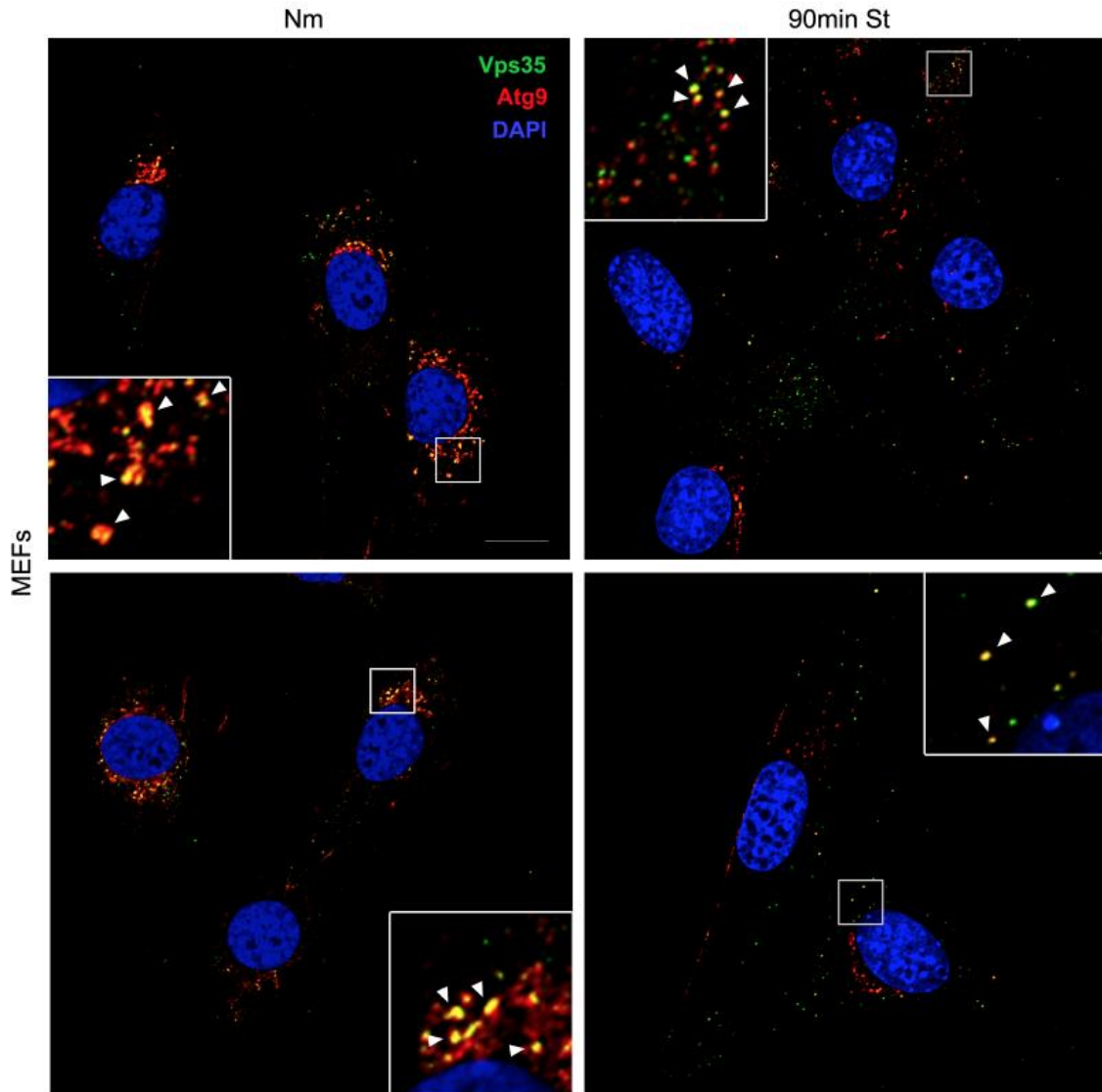


Figure 4.5 Vps35 strongly co-localizes with Atg9 under basal and starvation conditions. Uninfected *Vps35^{Flox/Flox}* MEFs cells were cultured in normal media or HBSS for 90min (90min St) and fixed. Confocal microscopy images show endogenous Vps35 (green) and Atg9 (red). Scale bar: 10 μ m

4.4 Discussion

Given that retromer plays an important role in delivering hydrolases to the lysosome, we hypothesized that retromer depletion would cause lysosomal dysfunction and consequently impair autophagy. However, preliminary results showed minimal, if any, lysosomal impairment upon Vps35 depletion, and an unexpected role for retromer in the negative regulation of autophagy. Specifically, LC3 conjugation was increased upon Vps35 depletion both under basal conditions and during starvation, which clearly reflected enhanced autophagy rather than impaired AP turnover according to the Bafilomycin flux test. Additionally, Vps35 was found to strongly colocalize with Atg9, a transmembrane protein implicated in AP biogenesis that cycles between the TGN and the endosome in a similar manner to its well-known cargo, M6PR. Here we discuss potential reasons for the absence of lysosomal impairment observed upon Vps35 depletion as well as follow up studies that will be important for confirming and better understanding the role of Vps35 in autophagy.

As described in the introduction, retromer has been shown to play an essential role in the trafficking of hydrolases to the lysosome, which we hypothesized to cause the impaired endo-lysosomal trafficking observed in sporadic AD cases displaying genetic variations in retromer complex members. Although lysosomal activity was not directly measured in this study, results from our autophagy flux assays suggest that sufficient levels of hydrolases are delivered to the lysosome since APs are still efficiently cleared upon Vps35 depletion. Retromer-independent pathways for lysosomal hydrolase trafficking have been described, such as the lysosomal integral membrane protein type 2 (LIMP-2) receptor that targets β -glucocerebrosidase to the lysosome, which may be a

mechanism by which hydrolases are still delivered to the lysosome in retromer depleted cells and therefore, can still clear APs (Braulke and Bonifacino, 2009; Reczek et al., 2007; Saftig and Klumperman, 2009). In fact, we speculate that these alternate pathways may be upregulated in Vps35 -depleted cells. Currently, it is unclear whether the M6PR can undergo retrograde transport independently of retromer; however, studies have demonstrated that ablation of Vps35 results in the impaired retrieval and subsequent lysosomal degradation of the M6PR, suggesting little redundancy in this retrograde pathway, at least in the cell type analyzed (Arighi et al., 2004; Seaman, 2004). Interestingly, in yeast, there is an alternate pathway for delivery of hydrolases to the vacuole, termed the cytoplasm-to-vacuole targeting (Cvt) pathway (Khalfan and Klionsky, 2002; Teter and Klionsky, 2000). Specifically, the Cvt pathway sequesters the precursor hydrolases (*e.g.*, α -mannosidase and aminopeptidase I) into a vesicle using much of the same machinery as autophagy and delivers them to the vacuole (Khalfan and Klionsky, 2002; Teter and Klionsky, 2000). Although selective autophagy for hydrolases has yet to be described in mammals, it is plausible that autophagy could facilitate the delivery of hydrolases through its bulk degradation of organelles, such as the ER, trans-Golgi and endosomes, that these enzymes typically traffic through to reach the lysosome. It is important to note that in our cursory studies, more minor changes in lysosomal function upon Vps35 depletion have not been ruled out and lysosomal function should be tested more rigorously in the future. In fact, the *Vps35* KO MEFs are an ideal tool for studying the pathways required for Vps35-independent lysosomal hydrolase trafficking, which are currently poorly understood.

Although a couple of groups have examined the role of retromer in autophagy,

disparate findings have been reported which can be explained by potential differences in the model system and/or experimental design. For instance, Dengjel *et al.* reported a decrease in autophagy in cells null for the retromer components (e.g. $\Delta vps5$, $\Delta vps17$, $\Delta vps29$, $\Delta vps35$) in yeast; however, a single autophagy assay was used in this study (e.g. alkaline phosphatase (ALP) activity) and its readout does not exclude the possibility of a confounding impairment in lysosomal degradation (Dengjel *et al.*, 2012). Additionally, if retromer modulates autophagy through an interaction with Atg9 function in mammals, this functional interaction is not necessarily conserved in yeast. For instance, cytoplasmic N- and C-terminal domains of Atg9 vary significantly between yeast and mammals and they likely display different interactions and behaviors, demonstrated by differences in their trafficking patterns (Young *et al.*, 2006). In a more relevant study performed by Orsi *et al.* in mammalian HEK cells, siRNA knock-down of *Vps26* did not appear to affect LC3 conjugation or localization of Atg9 (Orsi *et al.*, 2012). Although a change in LC3 conjugation was not observed in their study, knock-down of *Vps26* was suboptimal in these studies (~50%) and may not be sufficient to detect the same phenotype seen in our studies (Orsi *et al.*, 2012). Additionally, since there are two isoforms of *Vps26*, *Vps26a* and *Vps26b*, compensation can occur when only one is ablated, leading to minimal impairment of retromer function in their experiments (Collins *et al.*, 2008; Kerr *et al.*, 2005). Here we have efficiently knocked-down *Vps35* in HeLa cells and neurons to effectively inhibit the function of the retromer complex. Additionally, we generated *Vps35* KO MEFs that are null for *Vps35* to test autophagy.

Our preliminary data suggests that *Vps35* plays a negative role in regulating autophagy; however, further studies are required to better understand how *Vps35* fits into

the autophagy pathway. In addition to assessing LC3 conjugation and localization upon Vps35 ablation, other standard autophagy assays should be performed in order to more quantitatively assess autophagy. Specifically, long-lived protein degradation should be tested to assess autophagy efficiency in Vps35 depleted cells. Additionally, electron microscopy analysis and morphometry should be performed to compare the size and shape as well as the number of APs and ALs in Vps35 depleted cells relative to control cells. Although the bafilomycin flux assay did not show any overt defects in AP clearance in the Vps35 depleted cells, it may be that Vps35 depletion causes more minor changes in lysosomal function and requires a more sensitive assay for its detection. For instance, monitoring the ratio of autophagosomes to autophagolysosomes by electron microscopy or using a tandem GFP-RFP-LC3, whereby the GFP fluorescence is quenched upon delivery to an acidic, lysosomal environment, are considered more sensitive read-outs of autophagy flux that should also be performed. Since lysosomal function and nutrient recycling is an important regulator of mTOR activity (Zoncu et al., 2011), it will also be important to test mTORC1 activity in Vps35 depleted cells in order to ensure mTORC1 is not misregulated. For instance, if lysosomal function is impaired in Vps35 depleted cells, mTORC1 may be inhibited, resulting in autophagy stimulation. Lastly, it will be important to characterize Vps35 in relation to additional autophagy and organelle markers by performing immunostainings under steady-state and autophagy stimulation in order to better understand the role of Vps35 in the autophagy pathway. In our preliminary studies, little colocalization was observed between Vps35 and Atg16 (early AP marker) or LC3 (early and late AP marker); however, we did notice significant co-localization between Vps35 and Atg9 (early AP marker), which is discussed below.

Given the strong colocalization between Vps35 and Atg9, it is possible that these two proteins may functionally interact during autophagy. Atg9 is the only integral membrane protein in autophagy and is essential for AP biogenesis in yeast and mammals (Lang et al., 2000; Noda et al., 2000; Webber and Tooze, 2010b; Young et al., 2006). In mammals, Atg9 resides in the TGN during steady-state conditions and re-localizes to the early endosomes and recycling endosomes upon autophagy induction (Webber and Tooze, 2010b). Atg9 redistribution is one of the first events observed during autophagy and requires both Ulk1 activation and PI3K activity (Young et al., 2006). Notably, Atg9 minimally colocalizes with other Atgs, similar to Vps35, since it is a highly dynamic protein that transiently delivers lipid and membrane to the growing autophagosome (Orsi et al., 2012). Interestingly, CI-M6PR, a known retromer cargo, and Atg9 have also been previously shown to colocalize and display a similar pattern of redistribution to the periphery during autophagy (Orsi et al., 2012). Additionally, the PI3P effector WIPI protein (the yeast homolog of Atg18) has been shown to be important for the trafficking of both Atg9 and M6PR (Jeffries et al., 2004), which may reflect a functional link between these two proteins. In a recent study, it was proposed that Atg9 localizes to the plasma membrane during autophagy and undergoes clathrin-mediated endocytosis and trafficking to the early and recycling endosome, where it heterotypically fuses with endocytosed Atg16-positive vesicles to generate autophagic precursors (Puri et al., 2013). Notably, little colocalization was observed between Vps35 and Atg16, suggesting that Atg9 may interact with Vps35 in a different compartment. Although mechanisms of Atg9 trafficking are still being understood, a recent study showed that ablation of p38 α MAPK causes a redistribution of Atg9 to the periphery and increases autophagy in both fed and

starved conditions (Webber and Tooze, 2010a). Although this phenotype is similar to that observed upon Vps35 depletion, whether Atg9 is mislocalized to the periphery in this case is unclear. In future studies, it will be important to characterize Atg9 localization and determine whether the retromer machinery is required for its endosome-to-TGN trafficking.

If retromer controls autophagy, a fundamental question is the type of factor mediating its recruitment to membranes in this specific context. There is a growing role for the sorting nexin (SNX) family of proteins in autophagy (Knaevelsrud et al., 2013). SNX proteins possess a characteristic BAR domain that can sense membrane curvature and induce tubule formation as well as a PX domain that binds phosphatidylinositol 3-phosphate (PI3P) (Carlton and Cullen, 2005; Cullen and Korswagen, 2012; Worby and Dixon, 2002). Recently, a screen using a single knock-down approach was used to identify SNX18 as a positive regulator of autophagy that promotes LC3 lipidation and tubulation of recycling endosomes to provide membrane during autophagosome biogenesis (Knaevelsrud et al., 2013). Although the SNX proteins of the retromer complex (SNX 1, 2, 5, 6, 27) were not identified in these screens, they cannot be ruled out as regulators of autophagy since SNX1 and SNX2 as well as SNX 5 and SNX6 (and possibly SNX37) act redundantly (Rojas et al., 2007; Schwarz et al., 2002; Wassmer et al., 2007; Wassmer et al., 2009). Additionally, SNX3, a non-BAR containing that directly associates with and recruits retromer to PI3P positive membranes independently of the other SNXs, also possesses redundant functions to another SNX, SNX12, and may be implicated in autophagy (Cullen and Korswagen, 2012; Pons et al., 2012). In order to more thoroughly assess whether the SNX proteins of the retromer complex and SNX

proteins in general regulate autophagy, double knock-down experiments may be required. Mammalian SNX proteins have been shown to have cellular roles independent from retromer; therefore, they may also participate in autophagy separately from the retromer complex (Nisar et al., 2010; Prosser et al., 2010).

In addition to understanding how retromer regulates autophagy, it will also be important to more generally characterize how retrograde transport is regulated during autophagy. Since endosome-to-TGN recycling of M6PR and Atg9 changes during autophagy, retrograde trafficking does not appear to be constitutive pathway but rather one controlled by certain stimuli. In future studies, it would be interesting to determine the signaling pathways and mechanism regulating retrograde transport. For instance, it is possible that cargoes undergo a conformation change or a post-translational modification to reduce their affinity for recycling machinery. Conversely, the recycling machinery may be inhibited and unable to bind the cargo during certain stimuli. Additionally, it may be that intracellular trafficking and motors are regulated differently under autophagy stimulating conditions and subsequently slow retrograde transport by the retromer.

Identifying retromer as a novel regulator of autophagy is not only of basic science interest but also of disease relevance. In AD, the progressive appearance of swollen neurites filled with APs and ALs is commonly observed; however, the underlying cause is unknown (Nixon et al., 2005; Suzuki and Terry, 1967; Terry et al., 1964). Genetic mouse models for AD have suggested that both an increase in autophagy as well as an impairment in clearance underlies the observed increase in APs and ALs (Nixon et al., 2005; Yu et al., 2005). Our preliminary data suggests that retromer deficiencies may in fact be contributing to an increase in AP structures seen in LOAD; however, determining

whether these retromer deficiencies also impair AP clearance will require additional experimentation. Although many risk factors have been associated with LOAD, it will be important to try to understand which factors cause common pathological features in all AD cases in order to improve therapeutic intervention and disease outcome.

4.5 Materials and Methods

4.5.1 Cell culture and transfection/infection.

HeLa cells were cultured at 37°C in a 5% CO₂ incubator in DMEM-Glutamax (Invitrogen) supplemented with 10% fetal bovine serum (FBS) (Invitrogen) and penicillin (200 units/mL)/streptomycin (200 µg/mL) (Invitrogen). HeLa cells were siRNA transfected twice at a 72 hr interval using Lipofectamine 2000 (Invitrogen) according to the manufacturer's instructions and experiments were performed 144 hrs after the initial transfection.

Hippocampal neurons were dissected from postnatal day 0 wild type mice, trypsinized for 30 minutes at 37°C, dissociated by passing through a Pasteur pipette and finally plated on 6 well plates (ELISA) at a density of 40,000-50,000 cells/cm². Media was changed 24 hours after plating. Neurons were cultured for 14 days in Neurobasal-A media supplemented with B-27, Glutamax and u-FDU, in a 5% CO₂ incubator. shRNA Vps35 lentivirus was generated by transfecting control or a combination of two Vps35 shRNA vectors and pPACK-H1 packaging mix (System Biosciences) into HEK-293T cells using Lipofectamine 2000 according to the manufacturer's protocol. Media was collected 72 hours post-transfection and spun in an ultracentrifuge at 22,000xg for 1.5 hours. The lentiviral pellet was re-suspended in Neurobasal-A media and added to cells at 7 days *in vitro*. Vps35 ablation occurred consistently at 7 days post-infection (methods

cited in (Bhalla et al., 2012)).

4.5.2 Generation of *Vps35* KO MEFs.

Primary mouse embryonic fibroblasts (MEFs) were generated from embryonic day 13.5 *Vps35^{Flox/Flox}* mouse embryos in which exons 3-5 were flanked by *loxP* sites (a kind gift from collaborator, Dr. Scott Small, Columbia University). MEFs were cultured at 37°C in a 5% CO₂ incubator in DMEM-Glutamax (Invitrogen) supplemented with 10% fetal bovine serum (FBS) (Invitrogen) and penicillin (200 units/mL)/streptomycin (200 µg/mL) (Invitrogen). MEFs were immortalized by multiple passaging and were used for experiments after 25 passages. *Vps35^{Flox/Flox}* (Control) and *Vps35^{-/-}* (KO) cells were generated by infecting cells with a lentivirus carrying either a catalytically active Cre recombinase or catalytically-dead Cre recombinase (control) (see Chapter 2 Materials and Methods for more detail). A minimum of 9 days post-infection was required to abolish the expression of *Vps35* by Western blot.

4.5.3 shRNA and RNAi.

shRNA vectors were generated using the lentivector pSIH-H1 shRNA (System Biosciences). A control, pSIH1-H1-copGFP Luciferase shRNA lentivector and two h*Vps35* pSIH-H1 shRNA lentivectors were designed and used to make the lentivirus. The target sequences for the two h*Vps35* shRNA lentivectors include:

vps35-1 shRNA, 50TCAGAGGATGTTGTATCTTTACAAGTCTC-30 ; *vps35*-2 shRNA, 50-GCTTCACACTGCCACCTTTGGTATTTGCA-30.

RNAi gene silencing was achieved using two pre-designed sequences against human *Vps35* (5'-CACCATACTCCTTTCCATGTA-3', S104268131; 5'-AGCACTTATCTTGGCTACTAA-3', S104279296) (Qiagen). As a negative control, an

siRNA scramble sequence (5'-AATTCTCCGAACGTGTCACGT-3'; 1027310) was used.

4.5.4 Reagents and antibodies, SDS-PAGE and western blotting and immunofluorescence microscopy.

See Chapter 2 Materials and Methods section. Additional primary antibodies used in this chapter include: anti-Vps35 mouse monoclonal antibody (1:1000 dil., Abnova) and anti-Vps26 rabbit polyclonal (1:1000 dil., Abnova).

Chapter 5: Concluding remarks and future directions

The goal of this thesis work was to better understand the regulation of autophagy from a lipid biology perspective. So far, the majority of our knowledge concerning AP biogenesis has been largely derived from genetic screens in *S. cerevisiae* which have identified several key protein players in this process, namely a subset of the factors encoded by ATGs (Harding et al., 1996; Klionsky et al., 2003b; Thumm et al., 1994; Tsukada and Ohsumi, 1993). Interestingly, the class III PI3K, Vps34, did not appear as a hit in these initial screens and it was not until later autophagy studies, which identified Vps34 as a regulator of autophagy in the yeast *Hanensula polymorpha* and human cells, that its synthesis of PI3P was found to be essential for autophagy in *S. cerevisiae* (Kiel et al., 1999; Kihara et al., 2001b; Petiot et al., 2000). Due to limitations in genetic screens and the fact that higher eukaryotes have multiple PI3P synthesis pathways, we questioned whether Vps34 was the sole source of PI3P during autophagy in the mammalian system. Here we discovered that in addition to Vps34, the class II PI3K α and β isoforms synthesize PI3P to positively regulate autophagy. In this final section, some of the major outstanding questions that still remain surrounding regulation of autophagy by the class II PI3K and by other lipids in general will be discussed that were not discussed in the chapter discussions.

In the phosphoinositide field, there has been growing interest in determining whether the class II and class III PI3Ks can synthesize PI3P for the same process (Falasca and Maffucci, 2012). Recent evidence in mammalian cells has shown that in addition to Vps34, the class II PI3K α can also synthesize PI3P at the endosome (Yoshioka et al., 2012). However, whether Vps34 and the class II PI3K α contribute to the same or distinct

subdomains of PI3P or whether the source dictates a specific role for the PI3P at the endosome will require further investigation. Additionally, in *C. elegans*, the homologs of the class II and class III PI3K produce PI3P at the site of phagosome biogenesis. In this case, it is clear that each class plays a distinct roles and act in a hierarchical and sequential manner to promote phagocytosis (Lu et al., 2012). Interestingly, the roles of Vps34 and the class II PI3Ks in the mammalian system appear different from that of *C. elegans*. Our work is the first to demonstrate that the class II and class III PI3K synthesize PI3P independently of one another and in an additive manner during mammalian autophagy (Devereaux et al., 2013). Although we have demonstrated here that synthesis of PI3P by class II PI3K α and β isoforms positively regulate autophagy, it still unknown how the class II PI3K fit into the larger autophagy pathway and their relationship to Vps34 during this process. Key questions that remain include: Are the Vps34 and the class II PI3Ks regulated differently during autophagy? Do they all share downstream effectors and, if not, what effectors are specific to the class II PI3K? Are there multiple sites of PI3P synthesis during AP biogenesis? Where do Vps34 and the class II PI3K synthesize PI3P during autophagy? Lastly, is the pool of PI3P synthesized by each class differentially regulated by phosphatases?

Despite the fact that the class II and III PI3Ks are in the same lipid kinase family and synthesize PI3P during autophagy, preliminary studies suggest that they may operate in distinct pathways from one another. For instance, the class II PI3K α and β isoforms did not appear to strongly interact or co-localize with Beclin-1, a core complex member of multiple Vps34 complexes. To better characterize the class II PI3Ks in the autophagy pathway, immunoprecipitation and mass-spectrometry proteomic analysis can be

performed to identify novel autophagy-relevant interactors of the class II PI3K. Additionally, a more comprehensive study of the class II PI3K in relation to various autophagy markers should be performed to better understand where they fit into the hierarchical autophagy network. As mentioned in previous chapters, an autophagy interaction network screen hinted of an interaction between PI3KC2 α and both Atg7 and MAP1LC3A (one of the six Atg8 orthologues in humans) (Behrends et al., 2010); however, further confirmation of this interaction is still required. Interestingly, in our preliminary characterization studies we observed that PI3KC2 α displays a similar distribution pattern to and co-localized with Atg9. In future studies, it will be interesting to determine how the redistribution of the class II PI3K α is regulated and whether it interacts with Atg9. Notably, the class II PI3K β did not possess the same cellular distribution pattern as the class II PI3K α , which suggests that there may even be isoform differences in autophagy regulation.

So far, PI3P synthesis has only been observed at the ER during autophagy; however, other organelles have also been shown to contribute to AP formation (Axe et al., 2008). In future studies, it would be interesting to determine where Vps34 and the class II PI3K synthesize PI3P and whether they regulate different membrane sources required for AP biogenesis in the cell. Differences in the classes of PI3K have already been suggested by the fact that the PI3KC2 α redistributes from a juxtannuclear location to the periphery during starvation, whereas Vps34 has been seen in close proximity to the ER, particularly at MAM sites, during autophagy (Hamasaki et al., 2013; Webber and Tooze, 2010b; Young et al., 2006). However, the function of the class II α isoform and whether it is catalytically active at these peripheral, Atg9 positive sites still needs to be

determined. Interestingly, different autophagy stimuli have been shown to induce non-canonical autophagy pathways, which do not require core autophagy machinery. For instance, when proapoptotic compounds and resveratrol are used to stimulate autophagy, autophagosomes are still able to form in the absence of Beclin-1 (Grishchuk et al., 2011; Proikas-Cezanne and Codogno, 2011; Scarlatti et al., 2008; Tian et al., 2010; Zhu et al., 2007). Likewise, autophagosome have been shown to form independently of Atg5, Atg7 and LC3 when autophagy is induced by staurosporine, etoposide or starvation (Nishida et al., 2009). The fact that different autophagy machinery regulates autophagy in response to particular types of autophagy stimulation is intriguing when considering the relationship between Vps34 and the class II PI3K in autophagy. In the future, it will be interesting to determine whether Vps34 and the class II PI3Ks synthesis PI3P at different membranes to promote AP biogenesis and whether they differentially respond to various autophagy stimuli.

At the site of AP biogenesis, PI3P levels are tightly regulated through the coordination of PI 3-kinases and phosphatases. Prior to the discovery that the class II PI3K could also synthesis PI3P during autophagy, the phosphatases implicated in autophagy, including Jumpy (myotubularin-related protein 14, MTMR14) and MTMR3, were believed to act on Vps34 derived PI3P (Dowling et al., 2010; Taguchi-Atarashi et al., 2010; Vergne and Deretic, 2010; Vergne et al., 2009). Currently, it is unknown whether PI3P phosphatases have specificity for those pools of PI3P synthesized by Vps34 the class II versus the class II PI3Ks during autophagy. Studies have shown that the phosphatase MTM1 can directly associate with Vps34 and Vps15 in a mutually exclusive manner with Rab GTPases to control endosomal levels (Cao et al., 2007). MTM1 has

also been linked to the regulation of PI3P generated by the PI3K-C2 β isoform, although it is unclear whether they form a complex as well (Razidlo et al., 2011). A more careful investigation of the relationship between Vps34 and the class II PI3Ks and PI3P phosphatases is not only required to fully understanding PI3P metabolism during autophagy, but also PI3P regulation more generally in the cell.

In addition to PI3P, other PIs are beginning to emerge as important regulators of autophagy. For instance, in *S. cerevisiae*, two PI 4-kinases that synthesize phosphatidylinositol 4-phosphate (PI4P) at either the TGN or the plasma membrane have been shown to positive regulate of autophagy in an Atg9-dependent and independent manner, respectively (Wang et al., 2012). Additionally, in higher eukaryotes, synthesis of PI(3,5)P₂ by the PI3P 5-kinase Fab1/PIKfyve has been shown to play an important role in the maturation step of autophagy, although it is unclear whether its role in autophagy is secondary to its more homeostatic role in maintaining endo-lysosomal function (Dall'Armi et al., 2013; de Lartigue et al., 2009; Dove et al., 2009; Ferguson et al., 2012; Ferguson et al., 2009; Ferguson et al., 2010; Rusten et al., 2007). Lastly, the class II PI3K α isoform has been shown to synthesize PI(3,4)P₂ in certain biological contexts, such as clathrin mediated endocytosis (CME) (Posor et al., 2013); however, whether the class II PI3K produces PI(3,4)P₂ during autophagy should be tested in the future. Specifically, we showed that knockdown of the class II PI3K in our experiments produced a decrease in autophagy by decreased LC3 conjugation and p62 which was largely attributed to the decline in PI3P synthesis and subsequent recruitment of the PI3P-binding autophagy effector WIPI-I, but did not address PI(3,4)P₂ synthesis. Because antibody detection of PIs is limited, PI effectors and/or their PI-binding domains are

widely used as lipid probes in the phosphoinositide field when studying the localization and crudely quantifying a particular lipid species (Rusten and Stenmark, 2006). While additional PIs are starting to be appreciated for their role in autophagy, determining their precise role becomes challenging until effectors are identified. Additionally, it is difficult to know whether the synthesis or conversion of a PI species is responsible for mediating a cellular action. More extensive screens are required to identify the lipid kinases and phosphatases as well as the autophagy-relevant lipid effectors.

Although PIs are critical in mediating acute membrane signals important for orchestrating processes such as autophagy, other lipid classes and subclasses have been shown to be important for autophagy as well (Dall'Armi et al., 2013; Di Paolo and De Camilli, 2006; Knaevelsrud and Simonsen, 2012). For instance, our lab has shown that phospholipase D1 (PLD1) hydrolyzes phosphatidylcholine (PC) to produce phosphatidic acid (PA), a 'cone' shaped lipid with negative curvature-inducing properties that positively regulates both AP biogenesis and maturation likely through its structural properties (Dall'Armi et al., 2010). Given the extent of membrane remodeling that occurs during autophagy there is likely to be additional, previously unrecognized lipids that regulate this process. Recent advances in large-scale lipid analysis have opened up an entirely new field termed lipidomics, which will be critical for constructing a map of the lipidome and expanding our current understanding lipids in various biological, including autophagy. In our studies, we compared the lipidomic profiles of cells under steady-state and starvation conditions in hopes of identifying new lipids relevant for autophagy. Although few lipid changes were observed during autophagy, such as an increase in LPE, it is important to note that analysis was performed on a more global, cellular level. In

fact, it may be that there are important, local changes in the lipid composition of various organelle membranes during autophagy; therefore, purification and lipidomic analysis of different membranes should be performed in the future. In fact, there continues to be great interest in understanding the protein and lipid composition of an autophagosome in the field; however, analyzing purified APs is complicated by the fact that APs contain cytoplasmic protein and organelle cargo and are constantly in a state of transition as they fuse with the endolysosomal system during maturation. Although technological advancements have improved our lipid identification and quantification capabilities over the past few years, there are still limitations in lipid detection due to the large structural diversity and chemical composition among lipids (Lam and Shui, 2013; Wenk, 2005; Wenk, 2010). Improvements in lipid analytics will not only enhance our detection capabilities but will also provide a more comprehensive picture of the lipidome and will be critical to fully understand lipid dynamics and how various lipid networks interact within the cell.

Detailed molecular insight into the regulation of autophagy is invaluable due the numerous disease states, such as neurodegenerative diseases, cancer, infectious disease, that display impaired autophagy and the consequential pathologies.

Modulating autophagy is now widely viewed as a promising approach to alleviate symptoms of, if not, treat diseases where autophagy is misregulated. Understanding the molecular mechanisms underlying autophagy regulation from both a protein and lipid perspective is imperative for identifying new therapies for disease.

References

- Abeliovich, H., W.A. Dunn, Jr., J. Kim, and D.J. Klionsky. 2000. Dissection of autophagosome biogenesis into distinct nucleation and expansion steps. *J Cell Biol.* 151:1025-1034.
- Agarraberes, F.A., and J.F. Dice. 2001. Protein translocation across membranes. *Biochim Biophys Acta.* 1513:1-24.
- Ahlberg, J., and H. Glaumann. 1985. Uptake--microautophagy--and degradation of exogenous proteins by isolated rat liver lysosomes. Effects of pH, ATP, and inhibitors of proteolysis. *Experimental and molecular pathology.* 42:78-88.
- Andersen, O.M., J. Reiche, V. Schmidt, M. Gotthardt, R. Spoelgen, J. Behlke, C.A. von Arnim, T. Breiderhoff, P. Jansen, X. Wu, K.R. Bales, R. Cappai, C.L. Masters, J. Gliemann, E.J. Mufson, B.T. Hyman, S.M. Paul, A. Nykjaer, and T.E. Willnow. 2005. Neuronal sorting protein-related receptor sorLA/LR11 regulates processing of the amyloid precursor protein. *Proc Natl Acad Sci U S A.* 102:13461-13466.
- Aplin, A., T. Jasionowski, D.L. Tuttle, S.E. Lenk, and W.A. Dunn, Jr. 1992. Cytoskeletal elements are required for the formation and maturation of autophagic vacuoles. *Journal of cellular physiology.* 152:458-466.
- Araki, Y., W.C. Ku, M. Akioka, A.I. May, Y. Hayashi, F. Arisaka, Y. Ishihama, and Y. Ohsumi. 2013. Atg38 is required for autophagy-specific phosphatidylinositol 3-kinase complex integrity. *J Cell Biol.* 203:299-313.
- Arcaro, A., S. Volinia, M.J. Zvelebil, R. Stein, S.J. Watton, M.J. Layton, I. Gout, K. Ahmadi, J. Downward, and M.D. Waterfield. 1998. Human phosphoinositide 3-kinase C2beta, the role of calcium and the C2 domain in enzyme activity. *J Biol Chem.* 273:33082-33090.
- Area-Gomez, E., M. Del Carmen Lara Castillo, M.D. Tambini, C. Guardia-Laguarta, A.J. de Groof, M. Madra, J. Ikenouchi, M. Umeda, T.D. Bird, S.L. Sturley, and E.A. Schon. 2012. Upregulated function of mitochondria-associated ER membranes in Alzheimer disease. *EMBO J.* 31:4106-4123.
- Arias, E., and A.M. Cuervo. 2011. Chaperone-mediated autophagy in protein quality control. *Curr Opin Cell Biol.* 23:184-189.
- Arighi, C.N., L.M. Hartnell, R.C. Aguilar, C.R. Haft, and J.S. Bonifacino. 2004. Role of the mammalian retromer in sorting of the cation-independent mannose 6-phosphate receptor. *J Cell Biol.* 165:123-133.
- Ashford, T.P., and K.R. Porter. 1962. Cytoplasmic components in hepatic cell lysosomes. *J Cell Biol.* 12:198-202.
- Axe, E.L., S.A. Walker, M. Manifava, P. Chandra, H.L. Roderick, A. Habermann, G. Griffiths, and N.T. Ktistakis. 2008. Autophagosome formation from membrane compartments enriched in phosphatidylinositol 3-phosphate and dynamically connected to the endoplasmic reticulum. *J Cell Biol.* 182:685-701.
- Babst, M. 2011. MVB vesicle formation: ESCRT-dependent, ESCRT-independent and everything in between. *Curr Opin Cell Biol.* 23:452-457.

- Backer, J.M. 2008. The regulation and function of Class III PI3Ks: novel roles for Vps34. *Biochem J.* 410:1-17.
- Bandyopadhyay, U., S. Kaushik, L. Varticovski, and A.M. Cuervo. 2008. The chaperone-mediated autophagy receptor organizes in dynamic protein complexes at the lysosomal membrane. *Mol Cell Biol.* 28:5747-5763.
- Banta, L.M., J.S. Robinson, D.J. Klionsky, and S.D. Emr. 1988. Organelle assembly in yeast: characterization of yeast mutants defective in vacuolar biogenesis and protein sorting. *J Cell Biol.* 107:1369-1383.
- Baskaran, S., M.J. Ragusa, E. Boura, and J.H. Hurley. 2012. Two-Site Recognition of Phosphatidylinositol 3-Phosphate by PROPPINs in Autophagy. *Mol Cell.*
- Bechtel, W., M. Helmstadter, J. Balica, B. Hartleben, C. Schell, and T.B. Huber. 2013. The class III phosphatidylinositol 3-kinase PIK3C3/VPS34 regulates endocytosis and autophagosome-autolysosome formation in podocytes. *Autophagy.* 9.
- Behrends, C., M.E. Sowa, S.P. Gygi, and J.W. Harper. 2010. Network organization of the human autophagy system. *Nature.* 466:68-76.
- Berg, T.O., M. Fengsrud, P.E. Stromhaug, T. Berg, and P.O. Seglen. 1998. Isolation and characterization of rat liver amphisomes. Evidence for fusion of autophagosomes with both early and late endosomes. *J Biol Chem.* 273:21883-21892.
- Bernales, S., K.L. McDonald, and P. Walter. 2006. Autophagy counterbalances endoplasmic reticulum expansion during the unfolded protein response. *PLoS Biol.* 4:e423.
- Bhalla, A., C.P. Vetanovetz, E. Morel, Z. Chamoun, G. Di Paolo, and S.A. Small. 2012. The location and trafficking routes of the neuronal retromer and its role in amyloid precursor protein transport. *Neurobiol Dis.* 47:126-134.
- Bjorkoy, G., T. Lamark, A. Brech, H. Outzen, M. Perander, A. Overvatn, H. Stenmark, and T. Johansen. 2005. p62/SQSTM1 forms protein aggregates degraded by autophagy and has a protective effect on huntingtin-induced cell death. *J Cell Biol.* 171:603-614.
- Blanksby, S.J., and T.W. Mitchell. 2010. Advances in mass spectrometry for lipidomics. *Annual review of analytical chemistry.* 3:433-465.
- Blennow, K., M.J. de Leon, and H. Zetterberg. 2006. Alzheimer's disease. *Lancet.* 368:387-403.
- Bligh, E.G., and W.J. Dyer. 1959. A rapid method of total lipid extraction and purification. *Canadian journal of biochemistry and physiology.* 37:911-917.
- Blommaart, E.F., U. Krause, J.P. Schellens, H. Vreeling-Sindelarova, and A.J. Meijer. 1997. The phosphatidylinositol 3-kinase inhibitors wortmannin and LY294002 inhibit autophagy in isolated rat hepatocytes. *Eur J Biochem.* 243:240-246.
- Bohdanowicz, M., G. Cosio, J.M. Backer, and S. Grinstein. 2010. Class I and class III phosphoinositide 3-kinases are required for actin polymerization that propels phagosomes. *J Cell Biol.* 191:999-1012.
- Bonifacino, J.S., and J.H. Hurley. 2008. Retromer. *Curr Opin Cell Biol.* 20:427-436.
- Bornig, H., and G. Geyer. 1974. Staining of cholesterol with the fluorescent antibiotic "filipin". *Acta histochemica.* 50:110-115.

- Braulke, T., and J.S. Bonifacino. 2009. Sorting of lysosomal proteins. *Biochim Biophys Acta*. 1793:605-614.
- Brown, M.S., and J.L. Goldstein. 1999. A proteolytic pathway that controls the cholesterol content of membranes, cells, and blood. *Proc Natl Acad Sci U S A*. 96:11041-11048.
- Brown, R.A., L.K. Ho, S.J. Weber-Hall, J.M. Shipley, and M.J. Fry. 1997. Identification and cDNA cloning of a novel mammalian C2 domain-containing phosphoinositide 3-kinase, HsC2-PI3K. *Biochemical and biophysical research communications*. 233:537-544.
- Brown, W.J., D.B. DeWald, S.D. Emr, H. Plutner, and W.E. Balch. 1995. Role for phosphatidylinositol 3-kinase in the sorting and transport of newly synthesized lysosomal enzymes in mammalian cells. *J Cell Biol*. 130:781-796.
- Budovskaya, Y.V., H. Hama, D.B. DeWald, and P.K. Herman. 2002. The C terminus of the Vps34p phosphoinositide 3-kinase is necessary and sufficient for the interaction with the Vps15p protein kinase. *J Biol Chem*. 277:287-294.
- Buhman, K.F., M. Accad, and R.V. Farese. 2000. Mammalian acyl-CoA:cholesterol acyltransferases. *Biochim Biophys Acta*. 1529:142-154.
- Burman, C., and N.T. Ktistakis. 2010. Regulation of autophagy by phosphatidylinositol 3-phosphate. *FEBS Lett*. 584:1302-1312.
- Byfield, M.P., J.T. Murray, and J.M. Backer. 2005. hVps34 is a nutrient-regulated lipid kinase required for activation of p70 S6 kinase. *J Biol Chem*. 280:33076-33082.
- Cao, C., J. Laporte, J.M. Backer, A. Wandinger-Ness, and M.P. Stein. 2007. Myotubularin lipid phosphatase binds the hVPS15/hVPS34 lipid kinase complex on endosomes. *Traffic*. 8:1052-1067.
- Carlton, J.G., and P.J. Cullen. 2005. Sorting nexins. *Curr Biol*. 15:R819-820.
- Cataldo, A.M., J.L. Barnett, S.A. Berman, J. Li, S. Quarless, S. Bursztajn, C. Lippa, and R.A. Nixon. 1995. Gene expression and cellular content of cathepsin D in Alzheimer's disease brain: evidence for early up-regulation of the endosomal-lysosomal system. *Neuron*. 14:671-680.
- Cataldo, A.M., J.L. Barnett, C. Pieroni, and R.A. Nixon. 1997. Increased neuronal endocytosis and protease delivery to early endosomes in sporadic Alzheimer's disease: neuropathologic evidence for a mechanism of increased beta-amyloidogenesis. *J Neurosci*. 17:6142-6151.
- Cataldo, A.M., P.A. Paskevich, E. Kominami, and R.A. Nixon. 1991. Lysosomal hydrolases of different classes are abnormally distributed in brains of patients with Alzheimer disease. *Proc Natl Acad Sci U S A*. 88:10998-11002.
- Cataldo, A.M., S. Petanceska, N.B. Terio, C.M. Peterhoff, R. Durham, M. Mercken, P.D. Mehta, J. Buxbaum, V. Haroutunian, and R.A. Nixon. 2004. Abeta localization in abnormal endosomes: association with earliest Abeta elevations in AD and Down syndrome. *Neurobiology of aging*. 25:1263-1272.
- Cataldo, A.M., C.M. Peterhoff, J.C. Troncoso, T. Gomez-Isla, B.T. Hyman, and R.A. Nixon. 2000. Endocytic pathway abnormalities precede amyloid beta deposition in sporadic Alzheimer's disease and Down syndrome: differential effects of APOE genotype and presenilin mutations. *Am J Pathol*. 157:277-286.

- Cataldo, A.M., C.Y. Thayer, E.D. Bird, T.R. Wheelock, and R.A. Nixon. 1990. Lysosomal proteinase antigens are prominently localized within senile plaques of Alzheimer's disease: evidence for a neuronal origin. *Brain research*. 513:181-192.
- Cavallini, G., A. Donati, Z. Gori, and E. Bergamini. 2008. Towards an understanding of the anti-aging mechanism of caloric restriction. *Current aging science*. 1:4-9.
- Chan, R.B., T.G. Oliveira, E.P. Cortes, L.S. Honig, K.E. Duff, S.A. Small, M.R. Wenk, G. Shui, and G. Di Paolo. 2012. Comparative lipidomic analysis of mouse and human brain with Alzheimer disease. *J Biol Chem*. 287:2678-2688.
- Chang, T.Y., C.C. Chang, and D. Cheng. 1997. Acyl-coenzyme A:cholesterol acyltransferase. *Annu Rev Biochem*. 66:613-638.
- Chawla, A., J.J. Repa, R.M. Evans, and D.J. Mangelsdorf. 2001. Nuclear receptors and lipid physiology: opening the X-files. *Science*. 294:1866-1870.
- Chen, D., W. Fan, Y. Lu, X. Ding, S. Chen, and Q. Zhong. 2012. A mammalian autophagosome maturation mechanism mediated by TECPR1 and the Atg12-Atg5 conjugate. *Mol Cell*. 45:629-641.
- Chen, Y., and D.J. Klionsky. 2011. The regulation of autophagy - unanswered questions. *J Cell Sci*. 124:161-170.
- Chen, Y., and L. Yu. 2013. Autophagic lysosome reformation. *Experimental cell research*. 319:142-146.
- Chevallier, J., Z. Chamoun, G. Jiang, G. Prestwich, N. Sakai, S. Matile, R.G. Parton, and J. Gruenberg. 2008. Lysobisphosphatidic acid controls endosomal cholesterol levels. *J Biol Chem*. 283:27871-27880.
- Chiang, H.L., S.R. Terlecky, C.P. Plant, and J.F. Dice. 1989. A role for a 70-kilodalton heat shock protein in lysosomal degradation of intracellular proteins. *Science*. 246:382-385.
- Christoforidis, S., M. Miaczynska, K. Ashman, M. Wilm, L. Zhao, S.C. Yip, M.D. Waterfield, J.M. Backer, and M. Zerial. 1999. Phosphatidylinositol-3-OH kinases are Rab5 effectors. *Nat Cell Biol*. 1:249-252.
- Ciechanover, A. 2005. Proteolysis: from the lysosome to ubiquitin and the proteasome. *Nat Rev Mol Cell Biol*. 6:79-87.
- Clark, S.L., Jr. 1957. Cellular differentiation in the kidneys of newborn mice studies with the electron microscope. *The Journal of biophysical and biochemical cytology*. 3:349-362.
- Clausen, T.H., T. Lamark, P. Isakson, K. Finley, K.B. Larsen, A. Brech, A. Overvatn, H. Stenmark, G. Bjorkoy, A. Simonsen, and T. Johansen. 2010. p62/SQSTM1 and ALFY interact to facilitate the formation of p62 bodies/ALIS and their degradation by autophagy. *Autophagy*. 6:330-344.
- Codogno, P., M. Mehrpour, and T. Proikas-Cezanne. 2012. Canonical and non-canonical autophagy: variations on a common theme of self-eating? *Nat Rev Mol Cell Biol*. 13:7-12.
- Collins, B.M., S.J. Norwood, M.C. Kerr, D. Mahony, M.N. Seaman, R.D. Teasdale, and D.J. Owen. 2008. Structure of Vps26B and mapping of its interaction with the retromer protein complex. *Traffic*. 9:366-379.

- Costet, P., F. Lalanne, M.C. Gerbod-Giannone, J.R. Molina, X. Fu, E.G. Lund, L.J. Gudas, and A.R. Tall. 2003. Retinoic acid receptor-mediated induction of ABCA1 in macrophages. *Mol Cell Biol.* 23:7756-7766.
- Cremona, O., G. Di Paolo, M.R. Wenk, A. Luthi, W.T. Kim, K. Takei, L. Daniell, Y. Nemoto, S.B. Shears, R.A. Flavell, D.A. McCormick, and P. De Camilli. 1999. Essential role of phosphoinositide metabolism in synaptic vesicle recycling. *Cell.* 99:179-188.
- Cuervo, A.M. 2010. Chaperone-mediated autophagy: selectivity pays off. *Trends in endocrinology and metabolism: TEM.* 21:142-150.
- Cuervo, A.M., and J.F. Dice. 1996. A receptor for the selective uptake and degradation of proteins by lysosomes. *Science.* 273:501-503.
- Cuervo, A.M., H. Hildebrand, E.M. Bomhard, and J.F. Dice. 1999. Direct lysosomal uptake of alpha 2-microglobulin contributes to chemically induced nephropathy. *Kidney international.* 55:529-545.
- Cuervo, A.M., A. Palmer, A.J. Rivett, and E. Knecht. 1995. Degradation of proteasomes by lysosomes in rat liver. *Eur J Biochem.* 227:792-800.
- Cullen, P.J., and H.C. Korswagen. 2012. Sorting nexins provide diversity for retromer-dependent trafficking events. *Nat Cell Biol.* 14:29-37.
- Dall'Armi, C., K.A. Devereaux, and G. Di Paolo. 2013. The role of lipids in the control of autophagy. *Curr Biol.* 23:R33-45.
- Dall'Armi, C., A. Hurtado-Lorenzo, H. Tian, E. Morel, A. Nezu, R.B. Chan, W.H. Yu, K.S. Robinson, O. Yeku, S.A. Small, K. Duff, M.A. Frohman, M.R. Wenk, A. Yamamoto, and G. Di Paolo. 2010. The phospholipase D1 pathway modulates macroautophagy. *Nat Commun.* 1:142.
- Darsow, T., S.E. Rieder, and S.D. Emr. 1997. A multispecificity syntaxin homologue, Vam3p, essential for autophagic and biosynthetic protein transport to the vacuole. *J Cell Biol.* 138:517-529.
- Das, M., E. Scappini, N.P. Martin, K.A. Wong, S. Dunn, Y.J. Chen, S.L. Miller, J. Domin, and J.P. O'Bryan. 2007. Regulation of neuron survival through an intersectin-phosphoinositide 3'-kinase C2beta-AKT pathway. *Mol Cell Biol.* 27:7906-7917.
- Davidson, H.W. 1995. Wortmannin causes mistargeting of procathepsin D. evidence for the involvement of a phosphatidylinositol 3-kinase in vesicular transport to lysosomes. *J Cell Biol.* 130:797-805.
- De Duve, C., and R. Wattiaux. 1966. Functions of lysosomes. *Annual review of physiology.* 28:435-492.
- de Gassart, A., C. Geminard, D. Hoekstra, and M. Vidal. 2004. Exosome secretion: the art of reutilizing nonrecycled proteins? *Traffic.* 5:896-903.
- de Lartigue, J., H. Polson, M. Feldman, K. Shokat, S.A. Tooze, S. Urbe, and M.J. Clague. 2009. PIKfyve regulation of endosome-linked pathways. *Traffic.* 10:883-893.
- De Strooper, B. 2010. Proteases and proteolysis in Alzheimer disease: a multifactorial view on the disease process. *Physiological reviews.* 90:465-494.
- Del Roso, A., S. Vittorini, G. Cavallini, A. Donati, Z. Gori, M. Masini, M. Pollera, and E. Bergamini. 2003. Ageing-related changes in the in vivo function of rat liver macroautophagy and proteolysis. *Experimental gerontology.* 38:519-527.

- Delacourte, A. 2008. Tau pathology and neurodegeneration: an obvious but misunderstood link. *Journal of Alzheimer's disease : JAD*. 14:437-440.
- Demopoulos, C.A., R.N. Pinckard, and D.J. Hanahan. 1979. Platelet-activating factor. Evidence for 1-O-alkyl-2-acetyl-sn-glycerol-3-phosphorylcholine as the active component (a new class of lipid chemical mediators). *J Biol Chem*. 254:9355-9358.
- Dengjel, J., M. Hoyer-Hansen, M.O. Nielsen, T. Eisenberg, L.M. Harder, S. Schandorff, T. Farkas, T. Kirkegaard, A.C. Becker, S. Schroeder, K. Vanselow, E. Lundberg, M.M. Nielsen, A.R. Kristensen, V. Akimov, J. Bunkenborg, F. Madeo, M. Jaattela, and J.S. Andersen. 2012. Identification of autophagosome-associated proteins and regulators by quantitative proteomic analysis and genetic screens. *Molecular & cellular proteomics : MCP*. 11:M111 014035.
- Deter, R.L., P. Baudhuin, and C. De Duve. 1967. Participation of lysosomes in cellular autophagy induced in rat liver by glucagon. *J Cell Biol*. 35:C11-16.
- Devereaux, K., C. Dall'armi, A. Alcazar-Roman, Y. Ogasawara, X. Zhou, F. Wang, A. Yamamoto, P. De Camilli, and G. Di Paolo. 2013. Regulation of Mammalian Autophagy by Class II and III PI 3-Kinases through PI3P Synthesis. *PLoS One*. 8:e76405.
- Di Paolo, G., and P. De Camilli. 2006. Phosphoinositides in cell regulation and membrane dynamics. *Nature*. 443:651-657.
- Dice, J.F. 1990. Peptide sequences that target cytosolic proteins for lysosomal proteolysis. *Trends in biochemical sciences*. 15:305-309.
- Dodson, S.E., M. Gearing, C.F. Lippa, T.J. Montine, A.I. Levey, and J.J. Lah. 2006. LR11/SorLA expression is reduced in sporadic Alzheimer disease but not in familial Alzheimer disease. *J Neuropathol Exp Neurol*. 65:866-872.
- Domin, J., L. Harper, D. Aubyn, M. Wheeler, O. Florey, D. Haskard, M. Yuan, and D. Zicha. 2005. The class II phosphoinositide 3-kinase PI3K-C2beta regulates cell migration by a PtdIns3P dependent mechanism. *Journal of cellular physiology*. 205:452-462.
- Domin, J., F. Pages, S. Volinia, S.E. Rittenhouse, M.J. Zvelebil, R.C. Stein, and M.D. Waterfield. 1997. Cloning of a human phosphoinositide 3-kinase with a C2 domain that displays reduced sensitivity to the inhibitor wortmannin. *Biochem J*. 326 (Pt 1):139-147.
- Donati, A., G. Cavallini, C. Paradiso, S. Vittorini, M. Pollera, Z. Gori, and E. Bergamini. 2001. Age-related changes in the autophagic proteolysis of rat isolated liver cells: effects of antiaging dietary restrictions. *The journals of gerontology. Series A, Biological sciences and medical sciences*. 56:B375-383.
- Dove, S.K., K. Dong, T. Kobayashi, F.K. Williams, and R.H. Michell. 2009. Phosphatidylinositol 3,5-bisphosphate and Fab1p/PIKfyve underpin endolysosome function. *The Biochemical journal*. 419:1-13.
- Dove, S.K., R.C. Piper, R.K. McEwen, J.W. Yu, M.C. King, D.C. Hughes, J. Thuring, A.B. Holmes, F.T. Cooke, R.H. Michell, P.J. Parker, and M.A. Lemmon. 2004. Svp1p defines a family of phosphatidylinositol 3,5-bisphosphate effectors. *Embo J*. 23:1922-1933.

- Dowling, J.J., S.E. Low, A.S. Busta, and E.L. Feldman. 2010. Zebrafish MTMR14 is required for excitation-contraction coupling, developmental motor function and the regulation of autophagy. *Hum Mol Genet.* 19:2668-2681.
- Du, X., A.S. Kazim, A.J. Brown, and H. Yang. 2012. An essential role of Hrs/Vps27 in endosomal cholesterol trafficking. *Cell reports.* 1:29-35.
- Du, X., J. Kumar, C. Ferguson, T.A. Schulz, Y.S. Ong, W. Hong, W.A. Prinz, R.G. Parton, A.J. Brown, and H. Yang. 2011. A role for oxysterol-binding protein-related protein 5 in endosomal cholesterol trafficking. *J Cell Biol.* 192:121-135.
- Duff, K., C. Eckman, C. Zehr, X. Yu, C.M. Prada, J. Perez-tur, M. Hutton, L. Buee, Y. Harigaya, D. Yager, D. Morgan, M.N. Gordon, L. Holcomb, L. Refolo, B. Zenk, J. Hardy, and S. Younkin. 1996. Increased amyloid-beta42(43) in brains of mice expressing mutant presenilin 1. *Nature.* 383:710-713.
- Dunn, W.A., Jr., J.M. Cregg, J.A. Kiel, I.J. van der Klei, M. Oku, Y. Sakai, A.A. Sibirny, O.V. Stasyk, and M. Veenhuis. 2005. Pexophagy: the selective autophagy of peroxisomes. *Autophagy.* 1:75-83.
- Eck, R., A. Bruckmann, R. Wetzker, and W. Kunkel. 2000. A phosphatidylinositol 3-kinase of *Candida albicans*: molecular cloning and characterization. *Yeast.* 16:933-944.
- Efe, J.A., R.J. Botelho, and S.D. Emr. 2005. The Fab1 phosphatidylinositol kinase pathway in the regulation of vacuole morphology. *Curr Opin Cell Biol.* 17:402-408.
- Elias-Sonnenschein, L.S., L. Bertram, and P.J. Visser. 2012. Relationship between genetic risk factors and markers for Alzheimer's disease pathology. *Biomarkers in medicine.* 6:477-495.
- Elis, W., E. Triantafellow, N.M. Wolters, K.R. Sian, G. Caponigro, J. Borawski, L.A. Gaither, L.O. Murphy, P.M. Finan, and J.P. Mackeigan. 2008. Down-regulation of class II phosphoinositide 3-kinase alpha expression below a critical threshold induces apoptotic cell death. *Molecular cancer research : MCR.* 6:614-623.
- Eskelinen, E.L. 2005. Maturation of autophagic vacuoles in Mammalian cells. *Autophagy.* 1:1-10.
- Eun, L.Y., B.W. Song, M.J. Cha, H. Song, I.K. Kim, E. Choi, W. Chang, S. Lim, E.J. Choi, O. Ham, S.Y. Lee, K.H. Byun, Y. Jang, and K.C. Hwang. 2010. Overexpression of phosphoinositide-3-kinase class II alpha enhances mesenchymal stem cell survival in infarcted myocardium. *Biochemical and biophysical research communications.* 402:272-279.
- F, O.F., T.E. Rusten, and H. Stenmark. 2013. Phosphoinositide 3-kinases as accelerators and brakes of autophagy. *The FEBS journal.*
- Fader, C.M., D.G. Sanchez, M.B. Mestre, and M.I. Colombo. 2009. TI-VAMP/VAMP7 and VAMP3/cellubrevin: two v-SNARE proteins involved in specific steps of the autophagy/multivesicular body pathways. *Biochim Biophys Acta.* 1793:1901-1916.
- Fahy, E., S. Subramaniam, H.A. Brown, C.K. Glass, A.H. Merrill, Jr., R.C. Murphy, C.R. Raetz, D.W. Russell, Y. Seyama, W. Shaw, T. Shimizu, F. Spener, G. van Meer, M.S. VanNieuwenhze, S.H. White, J.L. Witztum, and E.A. Dennis. 2005. A

- comprehensive classification system for lipids. *Journal of lipid research*. 46:839-861.
- Fahy, E., S. Subramaniam, R.C. Murphy, M. Nishijima, C.R. Raetz, T. Shimizu, F. Spener, G. van Meer, M.J. Wakelam, and E.A. Dennis. 2009. Update of the LIPID MAPS comprehensive classification system for lipids. *Journal of lipid research*. 50 Suppl:S9-14.
- Falasca, M., W.E. Hughes, V. Dominguez, G. Sala, F. Fostira, M.Q. Fang, R. Cazzoli, P.R. Shepherd, D.E. James, and T. Maffucci. 2007. The role of phosphoinositide 3-kinase C2alpha in insulin signaling. *J Biol Chem*. 282:28226-28236.
- Falasca, M., and T. Maffucci. 2007. Role of class II phosphoinositide 3-kinase in cell signalling. *Biochem Soc Trans*. 35:211-214.
- Falasca, M., and T. Maffucci. 2012. Regulation and cellular functions of class II phosphoinositide 3-kinases. *The Biochemical journal*. 443:587-601.
- Fan, W., A. Nassiri, and Q. Zhong. 2011. Autophagosome targeting and membrane curvature sensing by Barkor/Atg14(L). *Proc Natl Acad Sci U S A*. 108:7769-7774.
- Fass, E., E. Shvets, I. Degani, K. Hirschberg, and Z. Elazar. 2006. Microtubules support production of starvation-induced autophagosomes but not their targeting and fusion with lysosomes. *J Biol Chem*. 281:36303-36316.
- Fengsrud, M., E.S. Erichsen, T.O. Berg, C. Raiborg, and P.O. Seglen. 2000. Ultrastructural characterization of the delimiting membranes of isolated autophagosomes and amphisomes by freeze-fracture electron microscopy. *Eur J Cell Biol*. 79:871-882.
- Fengsrud, M., N. Roos, T. Berg, W. Liou, J.W. Slot, and P.O. Seglen. 1995. Ultrastructural and immunocytochemical characterization of autophagic vacuoles in isolated hepatocytes: effects of vinblastine and asparagine on vacuole distributions. *Experimental cell research*. 221:504-519.
- Ferguson, C.J., G.M. Lenk, J.M. Jones, A.E. Grant, J.J. Winters, J.J. Dowling, R.J. Giger, and M.H. Meisler. 2012. Neuronal expression of Fig4 is both necessary and sufficient to prevent spongiform neurodegeneration. *Hum Mol Genet*. 21:3525-3534.
- Ferguson, C.J., G.M. Lenk, and M.H. Meisler. 2009. Defective autophagy in neurons and astrocytes from mice deficient in PI(3,5)P2. *Hum Mol Genet*. 18:4868-4878.
- Ferguson, C.J., G.M. Lenk, and M.H. Meisler. 2010. PtdIns(3,5)P2 and autophagy in mouse models of neurodegeneration. *Autophagy*. 6:170-171.
- Fernandez-Borja, M., R. Wubbolts, J. Calafat, H. Janssen, N. Divecha, S. Dusseljee, and J. Neefjes. 1999. Multivesicular body morphogenesis requires phosphatidylinositol 3-kinase activity. *Curr Biol*. 9:55-58.
- Filimonenko, M., P. Isakson, K.D. Finley, M. Anderson, H. Jeong, T.J. Melia, B.J. Bartlett, K.M. Myers, H.C. Birkeland, T. Lamark, D. Krainc, A. Brech, H. Stenmark, A. Simonsen, and A. Yamamoto. 2010. The selective macroautophagic degradation of aggregated proteins requires the PI3P-binding protein Alfy. *Mol Cell*. 38:265-279.
- Fimia, G.M., A. Stoykova, A. Romagnoli, L. Giunta, S. Di Bartolomeo, R. Nardacci, M. Corazzari, C. Fuoco, A. Ucar, P. Schwartz, P. Gruss, M. Piacentini, K.

- Chowdhury, and F. Cecconi. 2007. Ambra1 regulates autophagy and development of the nervous system. *Nature*. 447:1121-1125.
- Finn, P.F., and J.F. Dice. 2005. Ketone bodies stimulate chaperone-mediated autophagy. *J Biol Chem*. 280:25864-25870.
- Fujita, N., M. Hayashi-Nishino, H. Fukumoto, H. Omori, A. Yamamoto, T. Noda, and T. Yoshimori. 2008a. An Atg4B mutant hampers the lipidation of LC3 paralogues and causes defects in autophagosome closure. *Mol Biol Cell*. 19:4651-4659.
- Fujita, N., T. Itoh, H. Omori, M. Fukuda, T. Noda, and T. Yoshimori. 2008b. The Atg16L complex specifies the site of LC3 lipidation for membrane biogenesis in autophagy. *Mol Biol Cell*. 19:2092-2100.
- Funderburk, S.F., Q.J. Wang, and Z. Yue. 2010. The Beclin 1-VPS34 complex--at the crossroads of autophagy and beyond. *Trends in cell biology*. 20:355-362.
- Furuta, N., N. Fujita, T. Noda, T. Yoshimori, and A. Amano. 2010. Combinational soluble N-ethylmaleimide-sensitive factor attachment protein receptor proteins VAMP8 and Vti1b mediate fusion of antimicrobial and canonical autophagosomes with lysosomes. *Mol Biol Cell*. 21:1001-1010.
- Furuya, N., J. Yu, M. Byfield, S. Pattingre, and B. Levine. 2005. The evolutionarily conserved domain of Beclin 1 is required for Vps34 binding, autophagy and tumor suppressor function. *Autophagy*. 1:46-52.
- Futter, C.E., L.M. Collinson, J.M. Backer, and C.R. Hopkins. 2001a. Human VPS34 is required for internal vesicle formation within multivesicular endosomes. *J Cell Biol*. 155:1251-1264.
- Futter, C.E., L.M. Collinson, J.M. Backer, and C.R. Hopkins. 2001b. Human VPS34 is required for internal vesicle formation within multivesicular endosomes. *J Cell Biol*. 155:1251-1264.
- Gaidarov, I., Y. Zhao, and J.H. Keen. 2005. Individual phosphoinositide 3-kinase C2alpha domain activities independently regulate clathrin function. *J Biol Chem*. 280:40766-40772.
- Garami, A., F.J. Zwartkruis, T. Nobukuni, M. Joaquin, M. Rocco, H. Stocker, S.C. Kozma, E. Hafen, J.L. Bos, and G. Thomas. 2003. Insulin activation of Rheb, a mediator of mTOR/S6K/4E-BP signaling, is inhibited by TSC1 and 2. *Mol Cell*. 11:1457-1466.
- Gary, J.D., T.K. Sato, C.J. Stefan, C.J. Bonangelino, L.S. Weisman, and S.D. Emr. 2002. Regulation of Fab1 phosphatidylinositol 3-phosphate 5-kinase pathway by Vac7 protein and Fig4, a polyphosphoinositide phosphatase family member. *Mol Biol Cell*. 13:1238-1251.
- Gary, J.D., A.E. Wurmser, C.J. Bonangelino, L.S. Weisman, and S.D. Emr. 1998. Fab1p is essential for PtdIns(3)P 5-kinase activity and the maintenance of vacuolar size and membrane homeostasis. *J Cell Biol*. 143:65-79.
- Geng, J., and D.J. Klionsky. 2008. The Atg8 and Atg12 ubiquitin-like conjugation systems in macroautophagy. 'Protein modifications: beyond the usual suspects' review series. *EMBO Rep*. 9:859-864.
- Gilooly, D.J., I.C. Morrow, M. Lindsay, R. Gould, N.J. Bryant, J.M. Gaullier, R.G. Parton, and H. Stenmark. 2000. Localization of phosphatidylinositol 3-phosphate in yeast and mammalian cells. *Embo J*. 19:4577-4588.

- Glenner, G.G., and C.W. Wong. 2012. Alzheimer's disease: initial report of the purification and characterization of a novel cerebrovascular amyloid protein. 1984. *Biochemical and biophysical research communications*. 425:534-539.
- Goldberg, A.L. 2003. Protein degradation and protection against misfolded or damaged proteins. *Nature*. 426:895-899.
- Gordon, P.B., and P.O. Seglen. 1988. Prelysosomal convergence of autophagic and endocytic pathways. *Biochemical and biophysical research communications*. 151:40-47.
- Grishchuk, Y., V. Ginet, A.C. Truttmann, P.G. Clarke, and J. Puyal. 2011. Beclin 1-independent autophagy contributes to apoptosis in cortical neurons. *Autophagy*. 7:1115-1131.
- Gruenberg, J., and H. Stenmark. 2004. The biogenesis of multivesicular endosomes. *Nat Rev Mol Cell Biol*. 5:317-323.
- Gunther, J., M. Nguyen, A. Hartl, W. Kunkel, P.F. Zipfel, and R. Eck. 2005. Generation and functional in vivo characterization of a lipid kinase defective phosphatidylinositol 3-kinase Vps34p of *Candida albicans*. *Microbiology*. 151:81-89.
- Haft, C.R., M. de la Luz Sierra, R. Bafford, M.A. Lesniak, V.A. Barr, and S.I. Taylor. 2000. Human orthologs of yeast vacuolar protein sorting proteins Vps26, 29, and 35: assembly into multimeric complexes. *Mol Biol Cell*. 11:4105-4116.
- Hailey, D.W., A.S. Rambold, P. Satpute-Krishnan, K. Mitra, R. Sougrat, P.K. Kim, and J. Lippincott-Schwartz. 2010. Mitochondria supply membranes for autophagosome biogenesis during starvation. *Cell*. 141:656-667.
- Hakim, S., M.C. Bertucci, S.E. Conduit, D.L. Vuong, and C.A. Mitchell. 2012. Inositol polyphosphate phosphatases in human disease. *Current topics in microbiology and immunology*. 362:247-314.
- Hamasaki, M., N. Furuta, A. Matsuda, A. Nezu, A. Yamamoto, N. Fujita, H. Oomori, T. Noda, T. Haraguchi, Y. Hiraoka, A. Amano, and T. Yoshimori. 2013. Autophagosomes form at ER-mitochondria contact sites. *Nature*. 495:389-393.
- Hanada, T., N.N. Noda, Y. Satomi, Y. Ichimura, Y. Fujioka, T. Takao, F. Inagaki, and Y. Ohsumi. 2007. The Atg12-Atg5 conjugate has a novel E3-like activity for protein lipidation in autophagy. *J Biol Chem*. 282:37298-37302.
- Hara, T., A. Takamura, C. Kishi, S. Iemura, T. Natsume, J.L. Guan, and N. Mizushima. 2008. FIP200, a ULK-interacting protein, is required for autophagosome formation in mammalian cells. *J Cell Biol*. 181:497-510.
- Harada, K., A.B. Truong, T. Cai, and P.A. Khavari. 2005. The class II phosphoinositide 3-kinase C2beta is not essential for epidermal differentiation. *Mol Cell Biol*. 25:11122-11130.
- Harding, T.M., A. Hefner-Gravink, M. Thumm, and D.J. Klionsky. 1996. Genetic and phenotypic overlap between autophagy and the cytoplasm to vacuole protein targeting pathway. *J Biol Chem*. 271:17621-17624.
- Harding, T.M., K.A. Morano, S.V. Scott, and D.J. Klionsky. 1995. Isolation and characterization of yeast mutants in the cytoplasm to vacuole protein targeting pathway. *J Cell Biol*. 131:591-602.

- Harris, D.P., P. Vogel, M. Wims, K. Moberg, J. Humphries, K.G. Jhaver, C.M. DaCosta, M.K. Shadoan, N. Xu, G.M. Hansen, S. Balakrishnan, J. Domin, D.R. Powell, and T. Oravec. 2011. Requirement for class II phosphoinositide 3-kinase C2alpha in maintenance of glomerular structure and function. *Mol Cell Biol.* 31:63-80.
- Harris, H., and D.C. Rubinsztein. 2012. Control of autophagy as a therapy for neurodegenerative disease. *Nature reviews. Neurology.* 8:108-117.
- Hayashi, S., and A.P. McMahon. 2002. Efficient recombination in diverse tissues by a tamoxifen-inducible form of Cre: a tool for temporally regulated gene activation/inactivation in the mouse. *Developmental biology.* 244:305-318.
- Hayashi, T., R. Rizzuto, G. Hajnoczky, and T.P. Su. 2009. MAM: more than just a housekeeper. *Trends Cell Biol.* 19:81-88.
- Hayashi-Nishino, M., N. Fujita, T. Noda, A. Yamaguchi, T. Yoshimori, and A. Yamamoto. 2009. A subdomain of the endoplasmic reticulum forms a cradle for autophagosome formation. *Nat Cell Biol.* 11:1433-1437.
- He, C., and D.J. Klionsky. 2009. Regulation mechanisms and signaling pathways of autophagy. *Annual review of genetics.* 43:67-93.
- Herman, P.K., and S.D. Emr. 1990. Characterization of VPS34, a gene required for vacuolar protein sorting and vacuole segregation in *Saccharomyces cerevisiae*. *Mol Cell Biol.* 10:6742-6754.
- Hiles, I.D., M. Otsu, S. Volinia, M.J. Fry, I. Gout, R. Dhand, G. Panayotou, F. Ruiz-Larrea, A. Thompson, N.F. Totty, and et al. 1992. Phosphatidylinositol 3-kinase: structure and expression of the 110 kd catalytic subunit. *Cell.* 70:419-429.
- Ho, A., W. Morishita, D. Atasoy, X. Liu, K. Tabuchi, R.E. Hammer, R.C. Malenka, and T.C. Sudhof. 2006. Genetic analysis of Mint/X11 proteins: essential presynaptic functions of a neuronal adaptor protein family. *J Neurosci.* 26:13089-13101.
- Ho, C.Y., T.A. Alghamdi, and R.J. Botelho. 2012. Phosphatidylinositol-3,5-bisphosphate: no longer the poor PIP2. *Traffic.* 13:1-8.
- Hosokawa, N., T. Hara, T. Kaizuka, C. Kishi, A. Takamura, Y. Miura, S. Iemura, T. Natsume, K. Takehana, N. Yamada, J.L. Guan, N. Oshiro, and N. Mizushima. 2009a. Nutrient-dependent mTORC1 association with the ULK1-Atg13-FIP200 complex required for autophagy. *Mol Biol Cell.* 20:1981-1991.
- Hosokawa, N., T. Sasaki, S. Iemura, T. Natsume, T. Hara, and N. Mizushima. 2009b. Atg101, a novel mammalian autophagy protein interacting with Atg13. *Autophagy.* 5:973-979.
- Huang, J., and B.D. Manning. 2008. The TSC1-TSC2 complex: a molecular switchboard controlling cell growth. *Biochem J.* 412:179-190.
- Huang, W.P., S.V. Scott, J. Kim, and D.J. Klionsky. 2000. The itinerary of a vesicle component, Aut7p/Cvt5p, terminates in the yeast vacuole via the autophagy/Cvt pathways. *J Biol Chem.* 275:5845-5851.
- Huotari, J., and A. Helenius. 2011. Endosome maturation. *Embo J.* 30:3481-3500.
- Hurley, J.H. 2010. The ESCRT complexes. *Critical reviews in biochemistry and molecular biology.* 45:463-487.
- Hurley, J.H., and S.D. Emr. 2006. The ESCRT complexes: structure and mechanism of a membrane-trafficking network. *Annual review of biophysics and biomolecular structure.* 35:277-298.

- Hurley, J.H., and P.I. Hanson. 2010. Membrane budding and scission by the ESCRT machinery: it's all in the neck. *Nat Rev Mol Cell Biol.* 11:556-566.
- Ichimura, Y., T. Kirisako, T. Takao, Y. Satomi, Y. Shimonishi, N. Ishihara, N. Mizushima, I. Tanida, E. Kominami, M. Ohsumi, T. Noda, and Y. Ohsumi. 2000. A ubiquitin-like system mediates protein lipidation. *Nature.* 408:488-492.
- Ikonomov, O.C., D. Sbrissa, K. Mlak, R. Deeb, J. Fligger, A. Soans, R.L. Finley, Jr., and A. Shisheva. 2003. Active PIKfyve associates with and promotes the membrane attachment of the late endosome-to-trans-Golgi network transport factor Rab9 effector p40. *J Biol Chem.* 278:50863-50871.
- Ikonomov, O.C., D. Sbrissa, and A. Shisheva. 2001. Mammalian cell morphology and endocytic membrane homeostasis require enzymatically active phosphoinositide 5-kinase PIKfyve. *J Biol Chem.* 276:26141-26147.
- Infante, R.E., M.L. Wang, A. Radhakrishnan, H.J. Kwon, M.S. Brown, and J.L. Goldstein. 2008. NPC2 facilitates bidirectional transfer of cholesterol between NPC1 and lipid bilayers, a step in cholesterol egress from lysosomes. *Proc Natl Acad Sci U S A.* 105:15287-15292.
- Inoki, K., Y. Li, T. Xu, and K.L. Guan. 2003. Rheb GTPase is a direct target of TSC2 GAP activity and regulates mTOR signaling. *Genes & development.* 17:1829-1834.
- Inoki, K., Y. Li, T. Zhu, J. Wu, and K.L. Guan. 2002. TSC2 is phosphorylated and inhibited by Akt and suppresses mTOR signalling. *Nat Cell Biol.* 4:648-657.
- Ioannou, Y.A. 2001. Multidrug permeases and subcellular cholesterol transport. *Nat Rev Mol Cell Biol.* 2:657-668.
- Ishihara, N., M. Hamasaki, S. Yokota, K. Suzuki, Y. Kamada, A. Kihara, T. Yoshimori, T. Noda, and Y. Ohsumi. 2001. Autophagosome requires specific early Sec proteins for its formation and NSF/SNARE for vacuolar fusion. *Mol Biol Cell.* 12:3690-3702.
- Itakura, E., C. Kishi, K. Inoue, and N. Mizushima. 2008. Beclin 1 forms two distinct phosphatidylinositol 3-kinase complexes with mammalian Atg14 and UVRAG. *Mol Biol Cell.* 19:5360-5372.
- Itakura, E., C. Kishi-Itakura, I. Koyama-Honda, and N. Mizushima. 2012a. Structures containing Atg9A and the ULK1 complex independently target depolarized mitochondria at initial stages of Parkin-mediated mitophagy. *J Cell Sci.* 125:1488-1499.
- Itakura, E., C. Kishi-Itakura, and N. Mizushima. 2012b. The hairpin-type tail-anchored SNARE syntaxin 17 targets to autophagosomes for fusion with endosomes/lysosomes. *Cell.* 151:1256-1269.
- Itakura, E., and N. Mizushima. 2009. Atg14 and UVRAG: mutually exclusive subunits of mammalian Beclin 1-PI3K complexes. *Autophagy.* 5:534-536.
- Jaber, N., Z. Dou, J.S. Chen, J. Catanzaro, Y.P. Jiang, L.M. Ballou, E. Selinger, X. Ouyang, R.Z. Lin, J. Zhang, and W.X. Zong. 2012a. Class III PI3K Vps34 plays an essential role in autophagy and in heart and liver function. *Proc Natl Acad Sci U S A.* 109:2003-2008.
- Jaber, N., Z. Dou, R.Z. Lin, J. Zhang, and W.X. Zong. 2012b. Mammalian PIK3C3/VPS34: The key to autophagic processing in liver and heart. *Autophagy.* 8.

- Jager, S., C. Bucci, I. Tanida, T. Ueno, E. Kominami, P. Saftig, and E.L. Eskelinen. 2004. Role for Rab7 in maturation of late autophagic vacuoles. *J Cell Sci.* 117:4837-4848.
- Jahreiss, L., F.M. Menzies, and D.C. Rubinsztein. 2008. The itinerary of autophagosomes: from peripheral formation to kiss-and-run fusion with lysosomes. *Traffic.* 9:574-587.
- Jeffries, T.R., S.K. Dove, R.H. Michell, and P.J. Parker. 2004. PtdIns-specific MPR pathway association of a novel WD40 repeat protein, WIPI49. *Mol Biol Cell.* 15:2652-2663.
- Johansen, T., and T. Lamark. 2011. Selective autophagy mediated by autophagic adapter proteins. *Autophagy.* 7:279-296.
- Johnson, E.E., J.H. Overmeyer, W.T. Gunning, and W.A. Maltese. 2006. Gene silencing reveals a specific function of hVps34 phosphatidylinositol 3-kinase in late versus early endosomes. *J Cell Sci.* 119:1219-1232.
- Jotwani, A., D.N. Richerson, I. Motta, O. Julca-Zevallos, and T.J. Melia. 2012. Approaches to the study of Atg8-mediated membrane dynamics in vitro. *Methods Cell Biol.* 108:93-116.
- Juhasz, G., J.H. Hill, Y. Yan, M. Sass, E.H. Baehrecke, J.M. Backer, and T.P. Neufeld. 2008. The class III PI(3)K Vps34 promotes autophagy and endocytosis but not TOR signaling in *Drosophila*. *J Cell Biol.* 181:655-666.
- Juhasz, G., and T.P. Neufeld. 2006. Autophagy: a forty-year search for a missing membrane source. *PLoS Biol.* 4:e36.
- Jung, C.H., C.B. Jun, S.H. Ro, Y.M. Kim, N.M. Otto, J. Cao, M. Kundu, and D.H. Kim. 2009. ULK-Atg13-FIP200 complexes mediate mTOR signaling to the autophagy machinery. *Mol Biol Cell.* 20:1992-2003.
- Kaesler, P.S., L. Deng, Y. Wang, I. Dulubova, X. Liu, J. Rizo, and T.C. Sudhof. 2011. RIM proteins tether Ca²⁺ channels to presynaptic active zones via a direct PDZ-domain interaction. *Cell.* 144:282-295.
- Kamada, Y., T. Funakoshi, T. Shintani, K. Nagano, M. Ohsumi, and Y. Ohsumi. 2000. Tor-mediated induction of autophagy via an Apg1 protein kinase complex. *J Cell Biol.* 150:1507-1513.
- Kang, S., J. Song, J. Kang, H. Kang, D. Lee, Y. Lee, and D. Park. 2005. Suppression of the alpha-isoform of class II phosphoinositide 3-kinase gene expression leads to apoptotic cell death. *Biochemical and biophysical research communications.* 329:6-10.
- Katso, R.M., O.E. Pardo, A. Palamidessi, C.M. Franz, M. Marinov, A. De Laurentiis, J. Downward, G. Scita, A.J. Ridley, M.D. Waterfield, and A. Arcaro. 2006. Phosphoinositide 3-Kinase C2beta regulates cytoskeletal organization and cell migration via Rac-dependent mechanisms. *Mol Biol Cell.* 17:3729-3744.
- Katzmann, D.J., C.J. Stefan, M. Babst, and S.D. Emr. 2003. Vps27 recruits ESCRT machinery to endosomes during MVB sorting. *J Cell Biol.* 162:413-423.
- Kaushik, S., and A.M. Cuervo. 2012. Chaperone-mediated autophagy: a unique way to enter the lysosome world. *Trends in cell biology.* 22:407-417.
- Kerr, M.C., J.S. Bennetts, F. Simpson, E.C. Thomas, C. Flegg, P.A. Gleeson, C. Wicking, and R.D. Teasdale. 2005. A novel mammalian retromer component, Vps26B. *Traffic.* 6:991-1001.

- Khalfan, W.A., and D.J. Klionsky. 2002. Molecular machinery required for autophagy and the cytoplasm to vacuole targeting (Cvt) pathway in *S. cerevisiae*. *Curr Opin Cell Biol.* 14:468-475.
- Kiel, J.A., K.B. Rechinger, I.J. van der Klei, F.A. Salomons, V.I. Titorenko, and M. Veenhuis. 1999. The Hansenula polymorpha PDD1 gene product, essential for the selective degradation of peroxisomes, is a homologue of *Saccharomyces cerevisiae* Vps34p. *Yeast.* 15:741-754.
- Kiffin, R., C. Christian, E. Knecht, and A.M. Cuervo. 2004. Activation of chaperone-mediated autophagy during oxidative stress. *Mol Biol Cell.* 15:4829-4840.
- Kihara, A., Y. Kabeya, Y. Ohsumi, and T. Yoshimori. 2001a. Beclin-phosphatidylinositol 3-kinase complex functions at the trans-Golgi network. *EMBO Rep.* 2:330-335.
- Kihara, A., T. Noda, N. Ishihara, and Y. Ohsumi. 2001b. Two distinct Vps34 phosphatidylinositol 3-kinase complexes function in autophagy and carboxypeptidase Y sorting in *Saccharomyces cerevisiae*. *J Cell Biol.* 152:519-530.
- Kim, E., P. Goraksha-Hicks, L. Li, T.P. Neufeld, and K.L. Guan. 2008. Regulation of TORC1 by Rag GTPases in nutrient response. *Nat Cell Biol.* 10:935-945.
- Kim, I., S. Rodriguez-Enriquez, and J.J. Lemasters. 2007. Selective degradation of mitochondria by mitophagy. *Archives of biochemistry and biophysics.* 462:245-253.
- Kimura, S., T. Noda, and T. Yoshimori. 2008a. Dynein-dependent movement of autophagosomes mediates efficient encounters with lysosomes. *Cell Struct Funct.* 33:109-122.
- Kimura, S., T. Noda, and T. Yoshimori. 2008b. Dynein-dependent movement of autophagosomes mediates efficient encounters with lysosomes. *Cell Struct Funct.* 33:109-122.
- Kirisako, T., M. Baba, N. Ishihara, K. Miyazawa, M. Ohsumi, T. Yoshimori, T. Noda, and Y. Ohsumi. 1999. Formation process of autophagosome is traced with Apg8/Aut7p in yeast. *J Cell Biol.* 147:435-446.
- Kirk, C.J., Morris, A.J., and Shears, S.B. . 1990. Peptide Hormone Action: A Practical Approach. Oxford Univ Pr.
- Klionsky, D.J. 2007. Autophagy: from phenomenology to molecular understanding in less than a decade. *Nat Rev Mol Cell Biol.* 8:931-937.
- Klionsky, D.J., J.M. Cregg, W.A. Dunn, Jr., S.D. Emr, Y. Sakai, I.V. Sandoval, A. Sibirny, S. Subramani, M. Thumm, M. Veenhuis, and Y. Ohsumi. 2003a. A unified nomenclature for yeast autophagy-related genes. *Dev Cell.* 5:539-545.
- Klionsky, D.J., J.M. Cregg, W.A. Dunn, Jr., S.D. Emr, Y. Sakai, I.V. Sandoval, A. Sibirny, S. Subramani, M. Thumm, M. Veenhuis, and Y. Ohsumi. 2003b. A unified nomenclature for yeast autophagy-related genes. *Dev Cell.* 5:539-545.
- Klionsky, D.J., A.M. Cuervo, W.A. Dunn, Jr., B. Levine, I. van der Klei, and P.O. Seglen. 2007. How shall I eat thee? *Autophagy.* 3:413-416.
- Klionsky, D.J., A.J. Meijer, and P. Codogno. 2005. Autophagy and p70S6 kinase. *Autophagy.* 1:59-60; discussion 60-51.
- Knaevelsrud, H., and A. Simonsen. 2010. Fighting disease by selective autophagy of aggregate-prone proteins. *FEBS Lett.* 584:2635-2645.

- Knaevelsrud, H., and A. Simonsen. 2012. Lipids in autophagy: Constituents, signaling molecules and cargo with relevance to disease. *Biochim Biophys Acta*. 1821:1133-1145.
- Knaevelsrud, H., K. Soreng, C. Raiborg, K. Haberg, F. Rasmuson, A. Brech, K. Liestol, T.E. Rusten, H. Stenmark, T.P. Neufeld, S.R. Carlsson, and A. Simonsen. 2013. Membrane remodeling by the PX-BAR protein SNX18 promotes autophagosome formation. *J Cell Biol*. 202:331-349.
- Kobayashi, T., M.H. Beuchat, J. Chevallier, A. Makino, N. Mayran, J.M. Escola, C. Lebrand, P. Cosson, T. Kobayashi, and J. Gruenberg. 2002. Separation and characterization of late endosomal membrane domains. *J Biol Chem*. 277:32157-32164.
- Kobayashi, T., M.H. Beuchat, M. Lindsay, S. Frias, R.D. Palmiter, H. Sakuraba, R.G. Parton, and J. Gruenberg. 1999. Late endosomal membranes rich in lysobisphosphatidic acid regulate cholesterol transport. *Nat Cell Biol*. 1:113-118.
- Kochl, R., X.W. Hu, E.Y. Chan, and S.A. Tooze. 2006. Microtubules facilitate autophagosome formation and fusion of autophagosomes with endosomes. *Traffic*. 7:129-145.
- Koga, H., M. Martinez-Vicente, E. Arias, S. Kaushik, D. Sulzer, and A.M. Cuervo. 2011. Constitutive upregulation of chaperone-mediated autophagy in Huntington's disease. *J Neurosci*. 31:18492-18505.
- Kokkonen, N., A. Rivinoja, A. Kauppila, M. Suokas, I. Kellokumpu, and S. Kellokumpu. 2004. Defective acidification of intracellular organelles results in aberrant secretion of cathepsin D in cancer cells. *J Biol Chem*. 279:39982-39988.
- Komada, M., and P. Soriano. 1999. Hrs, a FYVE finger protein localized to early endosomes, is implicated in vesicular traffic and required for ventral folding morphogenesis. *Genes & development*. 13:1475-1485.
- Komatsu, M., S. Waguri, T. Ueno, J. Iwata, S. Murata, I. Tanida, J. Ezaki, N. Mizushima, Y. Ohsumi, Y. Uchiyama, E. Kominami, K. Tanaka, and T. Chiba. 2005. Impairment of starvation-induced and constitutive autophagy in Atg7-deficient mice. *J Cell Biol*. 169:425-434.
- Kovacs, A.L., Z. Palfia, G. Rez, T. Vellai, and J. Kovacs. 2007. Sequestration revisited: integrating traditional electron microscopy, de novo assembly and new results. *Autophagy*. 3:655-662.
- Kovacs, A.L., A. Reith, and P.O. Seglen. 1982. Accumulation of autophagosomes after inhibition of hepatocytic protein degradation by vinblastine, leupeptin or a lysosomotropic amine. *Experimental cell research*. 137:191-201.
- Kraft, C., A. Deplazes, M. Sohrmann, and M. Peter. 2008. Mature ribosomes are selectively degraded upon starvation by an autophagy pathway requiring the Ubp3p/Bre5p ubiquitin protease. *Nat Cell Biol*. 10:602-610.
- Krick, R., R.A. Busse, A. Scacioc, M. Stephan, A. Janshoff, M. Thumm, and K. Kuhnel. 2012. Structural and functional characterization of the two phosphoinositide binding sites of PROPPINs, a beta-propeller protein family. *Proc Natl Acad Sci U S A*. 109:E2042-2049.
- Krick, R., S. Henke, J. Tolstrup, and M. Thumm. 2008. Dissecting the localization and function of Atg18, Atg21 and Ygr223c. *Autophagy*. 4:896-910.

- Krick, R., J. Tolstrup, A. Appelles, S. Henke, and M. Thumm. 2006. The relevance of the phosphatidylinositolphosphat-binding motif FRRGT of Atg18 and Atg21 for the Cvt pathway and autophagy. *FEBS letters*. 580:4632-4638.
- Ktistakis, N., P. Chandra, S. Walker, M. Manifava, P. Musiwaro, and E. Axe. 2009. Early events regulating autophagosome formation. *Autophagy*. 5:897-897.
- Kuma, A., M. Hatano, M. Matsui, A. Yamamoto, H. Nakaya, T. Yoshimori, Y. Ohsumi, T. Tokuhiya, and N. Mizushima. 2004. The role of autophagy during the early neonatal starvation period. *Nature*. 432:1032-1036.
- Kutateladze, T.G. 2010. Translation of the phosphoinositide code by PI effectors. *Nature chemical biology*. 6:507-513.
- Kwon, H.J., L. Abi-Mosleh, M.L. Wang, J. Deisenhofer, J.L. Goldstein, M.S. Brown, and R.E. Infante. 2009. Structure of N-terminal domain of NPC1 reveals distinct subdomains for binding and transfer of cholesterol. *Cell*. 137:1213-1224.
- Lam, S.M., and G. Shui. 2013. Lipidomics as a principal tool for advancing biomedical research. *Journal of genetics and genomics = Yi chuan xue bao*. 40:375-390.
- Lane, R.F., S.M. Raines, J.W. Steele, M.E. Ehrlich, J.A. Lah, S.A. Small, R.E. Tanzi, A.D. Attie, and S. Gandy. 2010. Diabetes-associated SorCS1 regulates Alzheimer's amyloid-beta metabolism: evidence for involvement of SorL1 and the retromer complex. *J Neurosci*. 30:13110-13115.
- Lane, R.F., P. St George-Hyslop, B.L. Hempstead, S.A. Small, S.M. Strittmatter, and S. Gandy. 2012. Vps10 family proteins and the retromer complex in aging-related neurodegeneration and diabetes. *J Neurosci*. 32:14080-14086.
- Lang, T., S. Reiche, M. Straub, M. Bredschneider, and M. Thumm. 2000. Autophagy and the cvt pathway both depend on AUT9. *J Bacteriol*. 182:2125-2133.
- Lee, J.A., A. Beigneux, S.T. Ahmad, S.G. Young, and F.B. Gao. 2007. ESCRT-III dysfunction causes autophagosome accumulation and neurodegeneration. *Curr Biol*. 17:1561-1567.
- Lee, J.H., W.H. Yu, A. Kumar, S. Lee, P.S. Mohan, C.M. Peterhoff, D.M. Wolfe, M. Martinez-Vicente, A.C. Massey, G. Sovak, Y. Uchiyama, D. Westaway, A.M. Cuervo, and R.A. Nixon. 2010. Lysosomal proteolysis and autophagy require presenilin 1 and are disrupted by Alzheimer-related PS1 mutations. *Cell*. 141:1146-1158.
- Lefevre, M. 1988. Localization of lipoprotein unesterified cholesterol in nondenaturing gradient gels with filipin. *Journal of lipid research*. 29:815-818.
- Leibiger, B., T. Moede, S. Uhles, C.J. Barker, M. Creveaux, J. Domin, P.O. Berggren, and I.B. Leibiger. 2010. Insulin-feedback via PI3K-C2alpha activated PKBalpha/Akt1 is required for glucose-stimulated insulin secretion. *Faseb J*. 24:1824-1837.
- Levine, B., and G. Kroemer. 2008. Autophagy in the pathogenesis of disease. *Cell*. 132:27-42.
- Lewin, T.M., C.G. Van Horn, S.K. Krisans, and R.A. Coleman. 2002. Rat liver acyl-CoA synthetase 4 is a peripheral-membrane protein located in two distinct subcellular organelles, peroxisomes, and mitochondrial-associated membrane. *Archives of biochemistry and biophysics*. 404:263-270.

- Li, W.W., J. Li, and J.K. Bao. 2012. Microautophagy: lesser-known self-eating. *Cell Mol Life Sci.* 69:1125-1136.
- Liang, C., J.S. Lee, K.S. Inn, M.U. Gack, Q. Li, E.A. Roberts, I. Vergne, V. Deretic, P. Feng, C. Akazawa, and J.U. Jung. 2008a. Beclin1-binding UVRAG targets the class C Vps complex to coordinate autophagosome maturation and endocytic trafficking. *Nature cell biology.* 10:776-787.
- Liang, C., J.S. Lee, K.S. Inn, M.U. Gack, Q. Li, E.A. Roberts, I. Vergne, V. Deretic, P. Feng, C. Akazawa, and J.U. Jung. 2008b. Beclin1-binding UVRAG targets the class C Vps complex to coordinate autophagosome maturation and endocytic trafficking. *Nat Cell Biol.* 10:776-787.
- Library, A.L. Vol. 2013. J.L.H.a.R.J. Weselake., editor.
- Linassier, C., L.K. MacDougall, J. Domin, and M.D. Waterfield. 1997. Molecular cloning and biochemical characterization of a *Drosophila* phosphatidylinositol-specific phosphoinositide 3-kinase. *Biochem J.* 321 (Pt 3):849-856.
- Lindmo, K., and H. Stenmark. 2006. Regulation of membrane traffic by phosphoinositide 3-kinases. *J Cell Sci.* 119:605-614.
- Liou, W., H.J. Geuze, M.J. Geelen, and J.W. Slot. 1997. The autophagic and endocytic pathways converge at the nascent autophagic vacuoles. *J Cell Biol.* 136:61-70.
- Liscum, L. 2000. Niemann-Pick type C mutations cause lipid traffic jam. *Traffic.* 1:218-225.
- Lloyd-Evans, E., and F.M. Platt. 2010. Lipids on trial: the search for the offending metabolite in Niemann-Pick type C disease. *Traffic.* 11:419-428.
- Lohner, K. 1996. Is the high propensity of ethanolamine plasmalogens to form non-lamellar lipid structures manifested in the properties of biomembranes? *Chemistry and physics of lipids.* 81:167-184.
- Longatti, A., C.A. Lamb, M. Razi, S. Yoshimura, F.A. Barr, and S.A. Tooze. 2012. TBC1D14 regulates autophagosome formation via Rab11- and ULK1-positive recycling endosomes. *J Cell Biol.* 197:659-675.
- Longatti, A., and S.A. Tooze. 2009. Vesicular trafficking and autophagosome formation. *Cell death and differentiation.* 16:956-965.
- Lu, N., Q. Shen, T.R. Mahoney, L.J. Neukomm, Y. Wang, and Z. Zhou. 2012. Two PI 3-kinases and one PI 3-phosphatase together establish the cyclic waves of phagosomal PtdIns(3)P critical for the degradation of apoptotic cells. *PLoS Biol.* 10:e1001245.
- Lu, Q., P. Yang, X. Huang, W. Hu, B. Guo, F. Wu, L. Lin, A.L. Kovacs, L. Yu, and H. Zhang. 2011. The WD40 repeat PtdIns(3)P-binding protein EPG-6 regulates progression of omegasomes to autophagosomes. *Dev Cell.* 21:343-357.
- Lv, L., D. Li, D. Zhao, R. Lin, Y. Chu, H. Zhang, Z. Zha, Y. Liu, Z. Li, Y. Xu, G. Wang, Y. Huang, Y. Xiong, K.L. Guan, and Q.Y. Lei. 2011. Acetylation targets the M2 isoform of pyruvate kinase for degradation through chaperone-mediated autophagy and promotes tumor growth. *Mol Cell.* 42:719-730.
- Ma, L., Z. Chen, H. Erdjument-Bromage, P. Tempst, and P.P. Pandolfi. 2005. Phosphorylation and functional inactivation of TSC2 by Erk implications for tuberous sclerosis and cancer pathogenesis. *Cell.* 121:179-193.
- Ma, X.M., and J. Blenis. 2009. Molecular mechanisms of mTOR-mediated translational control. *Nat Rev Mol Cell Biol.* 10:307-318.

- MacDougall, L.K., J. Domin, and M.D. Waterfield. 1995. A family of phosphoinositide 3-kinases in *Drosophila* identifies a new mediator of signal transduction. *Curr Biol.* 5:1404-1415.
- Maday, S., K.E. Wallace, and E.L. Holzbaur. 2012. Autophagosomes initiate distally and mature during transport toward the cell soma in primary neurons. *J Cell Biol.* 196:407-417.
- Maffucci, T., A. Brancaccio, E. Piccolo, R.C. Stein, and M. Falasca. 2003. Insulin induces phosphatidylinositol-3-phosphate formation through TC10 activation. *Embo J.* 22:4178-4189.
- Maffucci, T., F.T. Cooke, F.M. Foster, C.J. Traer, M.J. Fry, and M. Falasca. 2005. Class II phosphoinositide 3-kinase defines a novel signaling pathway in cell migration. *J Cell Biol.* 169:789-799.
- Makide, K., H. Kitamura, Y. Sato, M. Okutani, and J. Aoki. 2009. Emerging lysophospholipid mediators, lysophosphatidylserine, lysophosphatidylthreonine, lysophosphatidylethanolamine and lysophosphatidylglycerol. *Prostaglandins & other lipid mediators.* 89:135-139.
- Mandelkow, E.M., and E. Mandelkow. 2012. Biochemistry and cell biology of tau protein in neurofibrillary degeneration. *Cold Spring Harbor perspectives in medicine.* 2:a006247.
- Manning, B.D., A.R. Tee, M.N. Logsdon, J. Blenis, and L.C. Cantley. 2002. Identification of the tuberous sclerosis complex-2 tumor suppressor gene product tuberlin as a target of the phosphoinositide 3-kinase/akt pathway. *Mol Cell.* 10:151-162.
- Mari, M., J. Griffith, E. Rieter, L. Krishnappa, D.J. Klionsky, and F. Reggiori. 2010. An Atg9-containing compartment that functions in the early steps of autophagosome biogenesis. *J Cell Biol.* 190:1005-1022.
- Martinez-Vicente, M., Z. Tallozy, E. Wong, G. Tang, H. Koga, S. Kaushik, R. de Vries, E. Arias, S. Harris, D. Sulzer, and A.M. Cuervo. 2010. Cargo recognition failure is responsible for inefficient autophagy in Huntington's disease. *Nat Neurosci.* 13:567-576.
- Massey, A.C., S. Kaushik, G. Sovak, R. Kiffin, and A.M. Cuervo. 2006. Consequences of the selective blockage of chaperone-mediated autophagy. *Proc Natl Acad Sci U S A.* 103:5805-5810.
- Masters, C.L., and K. Beyreuther. 2006. Pathways to the discovery of the Abeta amyloid of Alzheimer's disease. *Journal of Alzheimer's disease : JAD.* 9:155-161.
- Matsunaga, K., E. Morita, T. Saitoh, S. Akira, N.T. Ktistakis, T. Izumi, T. Noda, and T. Yoshimori. 2010. Autophagy requires endoplasmic reticulum targeting of the PI3-kinase complex via Atg14L. *J Cell Biol.* 190:511-521.
- Matsunaga, K., T. Saitoh, K. Tabata, H. Omori, T. Satoh, N. Kurotori, I. Maejima, K. Shirahama-Noda, T. Ichimura, T. Isobe, S. Akira, T. Noda, and T. Yoshimori. 2009. Two Beclin 1-binding proteins, Atg14L and Rubicon, reciprocally regulate autophagy at different stages. *Nature cell biology.* 11:385-396.
- Matsuura, A., M. Tsukada, Y. Wada, and Y. Ohsumi. 1997. Apg1p, a novel protein kinase required for the autophagic process in *Saccharomyces cerevisiae*. *Gene.* 192:245-250.

- Maxfield, F.R., and I. Tabas. 2005. Role of cholesterol and lipid organization in disease. *Nature*. 438:612-621.
- Maxfield, F.R., and G. van Meer. 2010. Cholesterol, the central lipid of mammalian cells. *Curr Opin Cell Biol*. 22:422-429.
- Maxfield, F.R., and D. Wustner. 2002. Intracellular cholesterol transport. *J Clin Invest*. 110:891-898.
- Mayer, A., and W. Wickner. 1997. Docking of yeast vacuoles is catalyzed by the Ras-like GTPase Ypt7p after symmetric priming by Sec18p (NSF). *J Cell Biol*. 136:307-317.
- Mayer, C., J. Zhao, X. Yuan, and I. Grummt. 2004. mTOR-dependent activation of the transcription factor TIF-IA links rRNA synthesis to nutrient availability. *Genes & development*. 18:423-434.
- McBride, H.M., V. Rybin, C. Murphy, A. Giner, R. Teasdale, and M. Zerial. 1999. Oligomeric complexes link Rab5 effectors with NSF and drive membrane fusion via interactions between EEA1 and syntaxin 13. *Cell*. 98:377-386.
- McGough, I.J., and P.J. Cullen. 2011. Recent advances in retromer biology. *Traffic*. 12:963-971.
- McLeod, I.X., X. Zhou, Q.J. Li, F. Wang, and Y.W. He. 2011. The class III kinase Vps34 promotes T lymphocyte survival through regulating IL-7Ralpha surface expression. *J Immunol*. 187:5051-5061.
- Melendez, A., Z. Talloczy, M. Seaman, E.L. Eskelinen, D.H. Hall, and B. Levine. 2003. Autophagy genes are essential for dauer development and life-span extension in *C. elegans*. *Science*. 301:1387-1391.
- Mesmin, B., and F.R. Maxfield. 2009. Intracellular sterol dynamics. *Biochim Biophys Acta*. 1791:636-645.
- Meunier, F.A., S.L. Osborne, G.R. Hammond, F.T. Cooke, P.J. Parker, J. Domin, and G. Schiavo. 2005. Phosphatidylinositol 3-kinase C2alpha is essential for ATP-dependent priming of neurosecretory granule exocytosis. *Mol Biol Cell*. 16:4841-4851.
- Mijaljica, D., M. Prescott, and R.J. Devenish. 2011. Microautophagy in mammalian cells: revisiting a 40-year-old conundrum. *Autophagy*. 7:673-682.
- Mizushima, N. 2007. Autophagy: process and function. *Genes & development*. 21:2861-2873.
- Mizushima, N., and M. Komatsu. 2011. Autophagy: renovation of cells and tissues. *Cell*. 147:728-741.
- Mizushima, N., B. Levine, A.M. Cuervo, and D.J. Klionsky. 2008. Autophagy fights disease through cellular self-digestion. *Nature*. 451:1069-1075.
- Mizushima, N., T. Noda, T. Yoshimori, Y. Tanaka, T. Ishii, M.D. George, D.J. Klionsky, M. Ohsumi, and Y. Ohsumi. 1998. A protein conjugation system essential for autophagy. *Nature*. 395:395-398.
- Mizushima, N., A. Yamamoto, M. Hatano, Y. Kobayashi, Y. Kabeya, K. Suzuki, T. Tokuhisa, Y. Ohsumi, and T. Yoshimori. 2001. Dissection of autophagosome formation using Apg5-deficient mouse embryonic stem cells. *J Cell Biol*. 152:657-668.
- Mizushima, N., T. Yoshimori, and Y. Ohsumi. 2003. Role of the Apg12 conjugation system in mammalian autophagy. *Int J Biochem Cell Biol*. 35:553-561.

- Mizushima, N., T. Yoshimori, and Y. Ohsumi. 2011. The role of Atg proteins in autophagosome formation. *Annu Rev Cell Dev Biol.* 27:107-132.
- Mobius, W., E. van Donselaar, Y. Ohno-Iwashita, Y. Shimada, H.F. Heijnen, J.W. Slot, and H.J. Geuze. 2003. Recycling compartments and the internal vesicles of multivesicular bodies harbor most of the cholesterol found in the endocytic pathway. *Traffic.* 4:222-231.
- Monastyrska, I., C. He, J. Geng, A.D. Hoppe, Z. Li, and D.J. Klionsky. 2008. Arp2 links autophagic machinery with the actin cytoskeleton. *Mol Biol Cell.* 19:1962-1975.
- Monastyrska, I., E. Rieter, D.J. Klionsky, and F. Reggiori. 2009. Multiple roles of the cytoskeleton in autophagy. *Biological reviews of the Cambridge Philosophical Society.* 84:431-448.
- Moreau, K., B. Ravikumar, M. Renna, C. Puri, and D.C. Rubinsztein. 2011. Autophagosome precursor maturation requires homotypic fusion. *Cell.* 146:303-317.
- Morel, E., Z. Chamoun, Z.M. Lasiecka, R.B. Chan, R.L. Williamson, C. Vetanovetz, C. Dall'armi, S. Simoes, K.S. Point Du Jour, B.D. McCabe, S.A. Small, and G. Di Paolo. 2013. Phosphatidylinositol-3-phosphate regulates sorting and processing of amyloid precursor protein through the endosomal system. *Nat Commun.* 4:2250.
- Morishita, H., S. Eguchi, H. Kimura, J. Sasaki, Y. Sakamaki, M.L. Robinson, T. Sasaki, and N. Mizushima. 2013. Deletion of autophagy-related 5 (Atg5) and Pik3c3 genes in the lens causes cataract independent of programmed organelle degradation. *J Biol Chem.* 288:11436-11447.
- Muhammad, A., I. Flores, H. Zhang, R. Yu, A. Staniszewski, E. Planel, M. Herman, L. Ho, R. Kreber, L.S. Honig, B. Ganetzky, K. Duff, O. Arancio, and S.A. Small. 2008. Retromer deficiency observed in Alzheimer's disease causes hippocampal dysfunction, neurodegeneration, and Abeta accumulation. *Proc Natl Acad Sci U S A.* 105:7327-7332.
- Musiwaro, P., M. Smith, M. Manifava, S.A. Walker, and N.T. Ktistakis. 2013. Characteristics and requirements of basal autophagy in HEK 293 cells. *Autophagy.* 9:1407-1417.
- Nair, U., Y. Cao, Z. Xie, and D.J. Klionsky. 2010. Roles of the lipid-binding motifs of Atg18 and Atg21 in the cytoplasm to vacuole targeting pathway and autophagy. *J Biol Chem.* 285:11476-11488.
- Nair, U., A. Jotwani, J. Geng, N. Gammoh, D. Richerson, W.L. Yen, J. Griffith, S. Nag, K. Wang, T. Moss, M. Baba, J.A. McNew, X. Jiang, F. Reggiori, T.J. Melia, and D.J. Klionsky. 2011. SNARE proteins are required for macroautophagy. *Cell.* 146:290-302.
- Nakatogawa, H., Y. Ichimura, and Y. Ohsumi. 2007. Atg8, a ubiquitin-like protein required for autophagosome formation, mediates membrane tethering and hemifusion. *Cell.* 130:165-178.
- Nara, A., N. Mizushima, A. Yamamoto, Y. Kabeya, Y. Ohsumi, and T. Yoshimori. 2002. SKD1 AAA ATPase-dependent endosomal transport is involved in autolysosome formation. *Cell Struct Funct.* 27:29-37.

- Nemazanyy, I., B. Blaauw, C. Paolini, C. Caillaud, F. Protasi, A. Mueller, T. Proikas-Cezanne, R.C. Russell, K.L. Guan, I. Nishino, M. Sandri, M. Pende, and G. Panasyuk. 2013. Defects of Vps15 in skeletal muscles lead to autophagic vacuolar myopathy and lysosomal disease. *EMBO molecular medicine*. 5:870-890.
- Ng, S.K., S.Y. Neo, Y.W. Yap, R.K. Karuturi, E.S. Loh, K.H. Liao, and E.C. Ren. 2009. Ablation of phosphoinositide-3-kinase class II alpha suppresses hepatoma cell proliferation. *Biochemical and biophysical research communications*. 387:310-315.
- Nicot, A.S., H. Fares, B. Payrastre, A.D. Chisholm, M. Labouesse, and J. Laporte. 2006. The phosphoinositide kinase PIKfyve/Fab1p regulates terminal lysosome maturation in *Caenorhabditis elegans*. *Mol Biol Cell*. 17:3062-3074.
- Nielsen, E., S. Christoforidis, S. Uttenweiler-Joseph, M. Miaczynska, F. Dewitte, M. Wilm, B. Hoflack, and M. Zerial. 2000. Rabenosyn-5, a novel Rab5 effector, is complexed with hVPS45 and recruited to endosomes through a FYVE finger domain. *J Cell Biol*. 151:601-612.
- Nisar, S., E. Kelly, P.J. Cullen, and S.J. Mundell. 2010. Regulation of P2Y1 receptor traffic by sorting Nexin 1 is retromer independent. *Traffic*. 11:508-519.
- Nishida, Y., S. Arakawa, K. Fujitani, H. Yamaguchi, T. Mizuta, T. Kanaseki, M. Komatsu, K. Otsu, Y. Tsujimoto, and S. Shimizu. 2009. Discovery of Atg5/Atg7-independent alternative macroautophagy. *Nature*. 461:654-658.
- Nixon, R.A. 2007. Autophagy, amyloidogenesis and Alzheimer disease. *J Cell Sci*. 120:4081-4091.
- Nixon, R.A., J. Wegiel, A. Kumar, W.H. Yu, C. Peterhoff, A. Cataldo, and A.M. Cuervo. 2005. Extensive involvement of autophagy in Alzheimer disease: an immunoelectron microscopy study. *J Neuropathol Exp Neurol*. 64:113-122.
- Nixon, R.A., and D.S. Yang. 2011. Autophagy failure in Alzheimer's disease-locating the primary defect. *Neurobiol Dis*. 43:38-45.
- Nobukuni, T., M. Joaquin, M. Rocco, S.G. Dann, S.Y. Kim, P. Gulati, M.P. Byfield, J.M. Backer, F. Natt, J.L. Bos, F.J. Zwartkruis, and G. Thomas. 2005. Amino acids mediate mTOR/raptor signaling through activation of class 3 phosphatidylinositol 3OH-kinase. *Proc Natl Acad Sci U S A*. 102:14238-14243.
- Noda, N.N., H. Kumeta, H. Nakatogawa, K. Satoo, W. Adachi, J. Ishii, Y. Fujioka, Y. Ohsumi, and F. Inagaki. 2008. Structural basis of target recognition by Atg8/LC3 during selective autophagy. *Genes Cells*. 13:1211-1218.
- Noda, T., J. Kim, W.P. Huang, M. Baba, C. Tokunaga, Y. Ohsumi, and D.J. Klionsky. 2000. Apg9p/Cvt7p is an integral membrane protein required for transport vesicle formation in the Cvt and autophagy pathways. *J Cell Biol*. 148:465-480.
- Noda, T., K. Matsunaga, N. Taguchi-Atarashi, and T. Yoshimori. 2010. Regulation of membrane biogenesis in autophagy via PI3P dynamics. *Semin Cell Dev Biol*.
- Norris, F.A., R.C. Atkins, and P.W. Majerus. 1997. The cDNA cloning and characterization of inositol polyphosphate 4-phosphatase type II. Evidence for conserved alternative splicing in the 4-phosphatase family. *J Biol Chem*. 272:23859-23864.

- Norris, F.A., and P.W. Majerus. 1994. Hydrolysis of phosphatidylinositol 3,4-bisphosphate by inositol polyphosphate 4-phosphatase isolated by affinity elution chromatography. *J Biol Chem.* 269:8716-8720.
- Novikoff, A.B. 1959. The proximal tubule cell in experimental hydronephrosis. *The Journal of biophysical and biochemical cytology.* 6:136-138.
- Novikoff, A.B., and E. Essner. 1962. Cytolysosomes and mitochondrial degeneration. *J Cell Biol.* 15:140-146.
- Obara, K., T. Noda, K. Niimi, and Y. Ohsumi. 2008a. Transport of phosphatidylinositol 3-phosphate into the vacuole via autophagic membranes in *Saccharomyces cerevisiae*. *Genes Cells.* 13:537-547.
- Obara, K., and Y. Ohsumi. 2008. Dynamics and function of PtdIns(3)P in autophagy. *Autophagy.* 4:952-954.
- Obara, K., and Y. Ohsumi. 2011. PtdIns 3-Kinase Orchestrates Autophagosome Formation in Yeast. *J Lipids.* 2011:498768.
- Obara, K., T. Sekito, K. Niimi, and Y. Ohsumi. 2008b. The Atg18-Atg2 complex is recruited to autophagic membranes via phosphatidylinositol 3-phosphate and exerts an essential function. *J Biol Chem.* 283:23972-23980.
- Obara, K., T. Sekito, and Y. Ohsumi. 2006. Assortment of phosphatidylinositol 3-kinase complexes--Atg14p directs association of complex I to the pre-autophagosomal structure in *Saccharomyces cerevisiae*. *Mol Biol Cell.* 17:1527-1539.
- Ogawa, M., Y. Yoshikawa, T. Kobayashi, H. Mimuro, M. Fukumatsu, K. Kiga, Z. Piao, H. Ashida, M. Yoshida, S. Kakuta, T. Koyama, Y. Goto, T. Nagatake, S. Nagai, H. Kiyono, M. Kawalec, J.M. Reichhart, and C. Sasakawa. 2011. A Tecpr1-dependent selective autophagy pathway targets bacterial pathogens. *Cell host & microbe.* 9:376-389.
- Ohsumi, Y., and N. Mizushima. 2004. Two ubiquitin-like conjugation systems essential for autophagy. *Semin Cell Dev Biol.* 15:231-236.
- Oram, J.F. 2002. ATP-binding cassette transporter A1 and cholesterol trafficking. *Current opinion in lipidology.* 13:373-381.
- Orsi, A., M. Razi, H.C. Dooley, D. Robinson, A.E. Weston, L.M. Collinson, and S.A. Tooze. 2012. Dynamic and transient interactions of Atg9 with autophagosomes, but not membrane integration, are required for autophagy. *Mol Biol Cell.* 23:1860-1873.
- Panaretou, C., J. Domin, S. Cockcroft, and M.D. Waterfield. 1997. Characterization of p150, an adaptor protein for the human phosphatidylinositol (PtdIns) 3-kinase. Substrate presentation by phosphatidylinositol transfer protein to the p150.Ptdins 3-kinase complex. *J Biol Chem.* 272:2477-2485.
- Pankiv, S., E.A. Alemu, A. Brech, J.A. Bruun, T. Lamark, A. Overvatn, G. Bjorkoy, and T. Johansen. 2010. FYCO1 is a Rab7 effector that binds to LC3 and PI3P to mediate microtubule plus end-directed vesicle transport. *J Cell Biol.* 188:253-269.
- Pankiv, S., T.H. Clausen, T. Lamark, A. Brech, J.A. Bruun, H. Outzen, A. Overvatn, G. Bjorkoy, and T. Johansen. 2007. p62/SQSTM1 binds directly to Atg8/LC3 to facilitate degradation of ubiquitinated protein aggregates by autophagy. *J Biol Chem.* 282:24131-24145.

- Parekh, V.V., L. Wu, K.L. Boyd, J.A. Williams, J.A. Gaddy, D. Olivares-Villagomez, T.L. Cover, W.X. Zong, J. Zhang, and L. Van Kaer. 2013. Impaired autophagy, defective T cell homeostasis, and a wasting syndrome in mice with a T cell-specific deletion of Vps34. *J Immunol.* 190:5086-5101.
- Park, J., Y. Kim, S. Lee, J.J. Park, Z.Y. Park, W. Sun, H. Kim, and S. Chang. 2010. SNX18 shares a redundant role with SNX9 and modulates endocytic trafficking at the plasma membrane. *J Cell Sci.* 123:1742-1750.
- Pentchev, P.G., M.E. Comly, H.S. Kruth, M.T. Vanier, D.A. Wenger, S. Patel, and R.O. Brady. 1985. A defect in cholesterol esterification in Niemann-Pick disease (type C) patients. *Proc Natl Acad Sci U S A.* 82:8247-8251.
- Petiot, A., J. Faure, H. Stenmark, and J. Gruenberg. 2003. PI3P signaling regulates receptor sorting but not transport in the endosomal pathway. *J Cell Biol.* 162:971-979.
- Petiot, A., E. Ogier-Denis, E.F. Blommaert, A.J. Meijer, and P. Codogno. 2000. Distinct classes of phosphatidylinositol 3'-kinases are involved in signaling pathways that control macroautophagy in HT-29 cells. *J Biol Chem.* 275:992-998.
- Pinckard, R.N., R.S. Farr, and D.J. Hanahan. 1979. Physicochemical and functional identity of rabbit platelet-activating factor (PAF) released in vivo during IgE anaphylaxis with PAF released in vitro from IgE sensitized basophils. *J Immunol.* 123:1847-1857.
- Pirola, L., M.J. Zvelebil, G. Bulgarelli-Leva, E. Van Obberghen, M.D. Waterfield, and M.P. Wymann. 2001. Activation loop sequences confer substrate specificity to phosphoinositide 3-kinase alpha (PI3Kalpha). Functions of lipid kinase-deficient PI3Kalpha in signaling. *J Biol Chem.* 276:21544-21554.
- Polson, H.E., J. de Lartigue, D.J. Rigden, M. Reedijk, S. Urbe, M.J. Clague, and S.A. Tooze. 2010. Mammalian Atg18 (WIPI2) localizes to omegasome-anchored phagophores and positively regulates LC3 lipidation. *Autophagy.* 6.
- Pons, V., C. Ustunel, C. Rolland, E. Torti, R.G. Parton, and J. Gruenberg. 2012. SNX12 role in endosome membrane transport. *PLoS One.* 7:e38949.
- Posor, Y., M. Eichhorn-Gruenig, D. Puchkov, J. Schoneberg, A. Ullrich, A. Lampe, R. Muller, S. Zarbakhsh, F. Gulluni, E. Hirsch, M. Krauss, C. Schultz, J. Schmoranzler, F. Noe, and V. Haucke. 2013. Spatiotemporal control of endocytosis by phosphatidylinositol-3,4-bisphosphate. *Nature.*
- Potter, C.J., L.G. Pedraza, and T. Xu. 2002. Akt regulates growth by directly phosphorylating Tsc2. *Nat Cell Biol.* 4:658-665.
- Proikas-Cezanne, T., and P. Codogno. 2011. Beclin 1 or not Beclin 1. *Autophagy.* 7:671-672.
- Proikas-Cezanne, T., S. Ruckerbauer, Y.D. Stierhof, C. Berg, and A. Nordheim. 2007. Human WIPI-1 puncta-formation: a novel assay to assess mammalian autophagy. *FEBS letters.* 581:3396-3404.
- Proikas-Cezanne, T., S. Waddell, A. Gaugel, T. Frickey, A. Lupas, and A. Nordheim. 2004. WIPI-1alpha (WIPI49), a member of the novel 7-bladed WIPI protein family, is aberrantly expressed in human cancer and is linked to starvation-induced autophagy. *Oncogene.* 23:9314-9325.

- Prosser, D.C., D. Tran, A. Schooley, B. Wendland, and J.K. Ngsee. 2010. A novel, retromer-independent role for sorting nexins 1 and 2 in RhoG-dependent membrane remodeling. *Traffic*. 11:1347-1362.
- Puri, C., M. Renna, C.F. Bento, K. Moreau, and D.C. Rubinsztein. 2013. Diverse autophagosome membrane sources coalesce in recycling endosomes. *Cell*. 154:1285-1299.
- Querfurth, H.W., and F.M. LaFerla. 2010. Alzheimer's disease. *The New England journal of medicine*. 362:329-344.
- Raiborg, C., B. Bremnes, A. Mehlum, D.J. Gillooly, A. D'Arrigo, E. Stang, and H. Stenmark. 2001. FYVE and coiled-coil domains determine the specific localisation of Hrs to early endosomes. *J Cell Sci*. 114:2255-2263.
- Raiborg, C., K.O. Schink, and H. Stenmark. 2013. Class III phosphatidylinositol 3-kinase and its catalytic product PtdIns3P in regulation of endocytic membrane traffic. *The FEBS journal*. 280:2730-2742.
- Raiborg, C., and H. Stenmark. 2009. The ESCRT machinery in endosomal sorting of ubiquitylated membrane proteins. *Nature*. 458:445-452.
- Ravikumar, B., A. Acevedo-Arozena, S. Imarisio, Z. Berger, C. Vacher, C.J. O'Kane, S.D. Brown, and D.C. Rubinsztein. 2005. Dynein mutations impair autophagic clearance of aggregate-prone proteins. *Nature genetics*. 37:771-776.
- Ravikumar, B., K. Moreau, L. Jahreiss, C. Puri, and D.C. Rubinsztein. 2010a. Plasma membrane contributes to the formation of pre-autophagosomal structures. *Nature cell biology*. 12:747-757.
- Ravikumar, B., S. Sarkar, J.E. Davies, M. Futter, M. Garcia-Arencibia, Z.W. Green-Thompson, M. Jimenez-Sanchez, V.I. Korolchuk, M. Lichtenberg, S. Luo, D.C. Massey, F.M. Menzies, K. Moreau, U. Narayanan, M. Renna, F.H. Siddiqi, B.R. Underwood, A.R. Winslow, and D.C. Rubinsztein. 2010b. Regulation of mammalian autophagy in physiology and pathophysiology. *Physiological reviews*. 90:1383-1435.
- Raymond, C.K., I. Howald-Stevenson, C.A. Vater, and T.H. Stevens. 1992. Morphological classification of the yeast vacuolar protein sorting mutants: evidence for a prevacuolar compartment in class E vps mutants. *Mol Biol Cell*. 3:1389-1402.
- Razidlo, G.L., D. Katafiasz, and G.S. Taylor. 2011. Myotubularin regulates Akt-dependent survival signaling via phosphatidylinositol 3-phosphate. *J Biol Chem*. 286:20005-20019.
- Reaves, B.J., N.A. Bright, B.M. Mullock, and J.P. Luzio. 1996. The effect of wortmannin on the localisation of lysosomal type I integral membrane glycoproteins suggests a role for phosphoinositide 3-kinase activity in regulating membrane traffic late in the endocytic pathway. *J Cell Sci*. 109 (Pt 4):749-762.
- Reczek, D., M. Schwake, J. Schroder, H. Hughes, J. Blanz, X. Jin, W. Brondyk, S. Van Patten, T. Edmunds, and P. Saftig. 2007. LIMP-2 is a receptor for lysosomal mannose-6-phosphate-independent targeting of beta-glucocerebrosidase. *Cell*. 131:770-783.
- Reggiori, F., and D.J. Klionsky. 2005. Autophagosomes: biogenesis from scratch? *Curr Opin Cell Biol*. 17:415-422.

- Reggiori, F., I. Monastyrska, T. Shintani, and D.J. Klionsky. 2005. The actin cytoskeleton is required for selective types of autophagy, but not nonspecific autophagy, in the yeast *Saccharomyces cerevisiae*. *Mol Biol Cell*. 16:5843-5856.
- Robinson, J.S., D.J. Klionsky, L.M. Banta, and S.D. Emr. 1988. Protein sorting in *Saccharomyces cerevisiae*: isolation of mutants defective in the delivery and processing of multiple vacuolar hydrolases. *Mol Cell Biol*. 8:4936-4948.
- Rogaeva, E., Y. Meng, J.H. Lee, Y. Gu, T. Kawarai, F. Zou, T. Katayama, C.T. Baldwin, R. Cheng, H. Hasegawa, F. Chen, N. Shibata, K.L. Lunetta, R. Pardossi-Piquard, C. Bohm, Y. Wakutani, L.A. Cupples, K.T. Cuenco, R.C. Green, L. Pinessi, I. Rainero, S. Sorbi, A. Bruni, R. Duara, R.P. Friedland, R. Inzelberg, W. Hampe, H. Bujo, Y.Q. Song, O.M. Andersen, T.E. Willnow, N. Graff-Radford, R.C. Petersen, D. Dickson, S.D. Der, P.E. Fraser, G. Schmitt-Ulms, S. Younkin, R. Mayeux, L.A. Farrer, and P. St George-Hyslop. 2007. The neuronal sortilin-related receptor SORL1 is genetically associated with Alzheimer disease. *Nature genetics*. 39:168-177.
- Roggo, L., V. Bernard, A.L. Kovacs, A.M. Rose, F. Savoy, M. Zetka, M.P. Wymann, and F. Muller. 2002. Membrane transport in *Caenorhabditis elegans*: an essential role for VPS34 at the nuclear membrane. *EMBO J*. 21:1673-1683.
- Rojas, R., S. Kametaka, C.R. Haft, and J.S. Bonifacino. 2007. Interchangeable but essential functions of SNX1 and SNX2 in the association of retromer with endosomes and the trafficking of mannose 6-phosphate receptors. *Mol Cell Biol*. 27:1112-1124.
- Rosenbaum, A.I., and F.R. Maxfield. 2011. Niemann-Pick type C disease: molecular mechanisms and potential therapeutic approaches. *Journal of neurochemistry*. 116:789-795.
- Rozycka, M., Y.J. Lu, R.A. Brown, M.R. Lau, J.M. Shipley, and M.J. Fry. 1998. cDNA cloning of a third human C2-domain-containing class II phosphoinositide 3-kinase, PI3K-C2gamma, and chromosomal assignment of this gene (PIK3C2G) to 12p12. *Genomics*. 54:569-574.
- Rubinsztein, D.C., P. Codogno, and B. Levine. 2012a. Autophagy modulation as a potential therapeutic target for diverse diseases. *Nat Rev Drug Discov*. 11:709-730.
- Rubinsztein, D.C., T. Shpilka, and Z. Elazar. 2012b. Mechanisms of autophagosome biogenesis. *Curr Biol*. 22:R29-34.
- Rudge, S.A., D.M. Anderson, and S.D. Emr. 2004. Vacuole size control: regulation of PtdIns(3,5)P2 levels by the vacuole-associated Vac14-Fig4 complex, a PtdIns(3,5)P2-specific phosphatase. *Mol Biol Cell*. 15:24-36.
- Rusinol, A.E., Z. Cui, M.H. Chen, and J.E. Vance. 1994. A unique mitochondria-associated membrane fraction from rat liver has a high capacity for lipid synthesis and contains pre-Golgi secretory proteins including nascent lipoproteins. *J Biol Chem*. 269:27494-27502.
- Rusten, T.E., L.M. Rodahl, K. Pattni, C. Englund, C. Samakovlis, S. Dove, A. Brech, and H. Stenmark. 2006. Fab1 phosphatidylinositol 3-phosphate 5-kinase controls trafficking but not silencing of endocytosed receptors. *Mol Biol Cell*. 17:3989-4001.

- Rusten, T.E., and H. Stenmark. 2006. Analyzing phosphoinositides and their interacting proteins. *Nature methods*. 3:251-258.
- Rusten, T.E., T. Vaccari, K. Lindmo, L.M. Rodahl, I.P. Nezis, C. Sem-Jacobsen, F. Wendler, J.P. Vincent, A. Brech, D. Bilder, and H. Stenmark. 2007. ESCRTs and Fab1 regulate distinct steps of autophagy. *Curr Biol*. 17:1817-1825.
- Rutherford, A.C., C. Traer, T. Wassmer, K. Pattni, M.V. Bujny, J.G. Carlton, H. Stenmark, and P.J. Cullen. 2006. The mammalian phosphatidylinositol 3-phosphate 5-kinase (PIKfyve) regulates endosome-to-TGN retrograde transport. *J Cell Sci*. 119:3944-3957.
- Saftig, P., and J. Klumperman. 2009. Lysosome biogenesis and lysosomal membrane proteins: trafficking meets function. *Nat Rev Mol Cell Biol*. 10:623-635.
- Sahu, R., S. Kaushik, C.C. Clement, E.S. Cannizzo, B. Scharf, A. Follenzi, I. Potolicchio, E. Nieves, A.M. Cuervo, and L. Santambrogio. 2011. Microautophagy of cytosolic proteins by late endosomes. *Dev Cell*. 20:131-139.
- Sakai, Y., A. Koller, L.K. Rangell, G.A. Keller, and S. Subramani. 1998. Peroxisome degradation by microautophagy in *Pichia pastoris*: identification of specific steps and morphological intermediates. *J Cell Biol*. 141:625-636.
- Saksena, S., J. Sun, T. Chu, and S.D. Emr. 2007. ESCRTing proteins in the endocytic pathway. *Trends in biochemical sciences*. 32:561-573.
- Sancak, Y., L. Bar-Peled, R. Zoncu, A.L. Markhard, S. Nada, and D.M. Sabatini. 2010. Ragulator-Rag complex targets mTORC1 to the lysosomal surface and is necessary for its activation by amino acids. *Cell*. 141:290-303.
- Sancak, Y., T.R. Peterson, Y.D. Shaul, R.A. Lindquist, C.C. Thoreen, L. Bar-Peled, and D.M. Sabatini. 2008. The Rag GTPases bind raptor and mediate amino acid signaling to mTORC1. *Science*. 320:1496-1501.
- Sato, T.K., T. Darsow, and S.D. Emr. 1998. Vam7p, a SNAP-25-like molecule, and Vam3p, a syntaxin homolog, function together in yeast vacuolar protein trafficking. *Mol Cell Biol*. 18:5308-5319.
- Saucedo, L.J., X. Gao, D.A. Chiarelli, L. Li, D. Pan, and B.A. Edgar. 2003. Rheb promotes cell growth as a component of the insulin/TOR signalling network. *Nat Cell Biol*. 5:566-571.
- Scarlatti, F., R. Maffei, I. Beau, P. Codogno, and R. Ghidoni. 2008. Role of non-canonical Beclin 1-independent autophagy in cell death induced by resveratrol in human breast cancer cells. *Cell Death Differ*. 15:1318-1329.
- Scheuner, D., C. Eckman, M. Jensen, X. Song, M. Citron, N. Suzuki, T.D. Bird, J. Hardy, M. Hutton, W. Kukull, E. Larson, E. Levy-Lahad, M. Viitanen, E. Peskind, P. Poorkaj, G. Schellenberg, R. Tanzi, W. Wasco, L. Lannfelt, D. Selkoe, and S. Younkin. 1996. Secreted amyloid beta-protein similar to that in the senile plaques of Alzheimer's disease is increased in vivo by the presenilin 1 and 2 and APP mutations linked to familial Alzheimer's disease. *Nature medicine*. 2:864-870.
- Schu, P.V., K. Takegawa, M.J. Fry, J.H. Stack, M.D. Waterfield, and S.D. Emr. 1993. Phosphatidylinositol 3-kinase encoded by yeast VPS34 gene essential for protein sorting. *Science*. 260:88-91.

- Schwarz, D.G., C.T. Griffin, E.A. Schneider, D. Yee, and T. Magnuson. 2002. Genetic analysis of sorting nexins 1 and 2 reveals a redundant and essential function in mice. *Mol Biol Cell*. 13:3588-3600.
- Scott, R.C., O. Schuldiner, and T.P. Neufeld. 2004. Role and regulation of starvation-induced autophagy in the Drosophila fat body. *Dev Cell*. 7:167-178.
- Seaman, M.N. 2004. Cargo-selective endosomal sorting for retrieval to the Golgi requires retromer. *J Cell Biol*. 165:111-122.
- Seaman, M.N. 2005. Recycle your receptors with retromer. *Trends Cell Biol*. 15:68-75.
- Seaman, M.N. 2012. The retromer complex - endosomal protein recycling and beyond. *J Cell Sci*. 125:4693-4702.
- Seaman, M.N., J.M. McCaffery, and S.D. Emr. 1998. A membrane coat complex essential for endosome-to-Golgi retrograde transport in yeast. *J Cell Biol*. 142:665-681.
- Seet, L.F., and W. Hong. 2006. The Phox (PX) domain proteins and membrane traffic. *Biochim Biophys Acta*. 1761:878-896.
- Shin, H.W., M. Hayashi, S. Christoforidis, S. Lacas-Gervais, S. Hoepfner, M.R. Wenk, J. Modregger, S. Uttenweiler-Joseph, M. Wilm, A. Nystuen, W.N. Frankel, M. Solimena, P. De Camilli, and M. Zerial. 2005. An enzymatic cascade of Rab5 effectors regulates phosphoinositide turnover in the endocytic pathway. *J Cell Biol*. 170:607-618.
- Shpilka, T., H. Weidberg, S. Pietrokovski, and Z. Elazar. 2011. Atg8: an autophagy-related ubiquitin-like protein family. *Genome biology*. 12:226.
- Simonsen, A., H.C. Birkeland, D.J. Gillooly, N. Mizushima, A. Kuma, T. Yoshimori, T. Slagsvold, A. Brech, and H. Stenmark. 2004. Alfy, a novel FYVE-domain-containing protein associated with protein granules and autophagic membranes. *J Cell Sci*. 117:4239-4251.
- Simonsen, A., J.M. Gaullier, A. D'Arrigo, and H. Stenmark. 1999. The Rab5 effector EEA1 interacts directly with syntaxin-6. *J Biol Chem*. 274:28857-28860.
- Simonsen, A., R. Lippe, S. Christoforidis, J.M. Gaullier, A. Brech, J. Callaghan, B.H. Toh, C. Murphy, M. Zerial, and H. Stenmark. 1998. EEA1 links PI(3)K function to Rab5 regulation of endosome fusion. *Nature*. 394:494-498.
- Simonsen, A., and S.A. Tooze. 2009. Coordination of membrane events during autophagy by multiple class III PI3-kinase complexes. *J Cell Biol*. 186:773-782.
- Singh, R., and A.M. Cuervo. 2011. Autophagy in the cellular energetic balance. *Cell Metab*. 13:495-504.
- Singh, R., and A.M. Cuervo. 2012. Lipophagy: connecting autophagy and lipid metabolism. *Int J Cell Biol*. 2012:282041.
- Singh, R., S. Kaushik, Y. Wang, Y. Xiang, I. Novak, M. Komatsu, K. Tanaka, A.M. Cuervo, and M.J. Czaja. 2009. Autophagy regulates lipid metabolism. *Nature*. 458:1131-1135.
- Small, S.A. 2008. Retromer sorting: a pathogenic pathway in late-onset Alzheimer disease. *Arch Neurol*. 65:323-328.
- Small, S.A., and S. Gandy. 2006. Sorting through the cell biology of Alzheimer's disease: intracellular pathways to pathogenesis. *Neuron*. 52:15-31.

- Small, S.A., K. Kent, A. Pierce, C. Leung, M.S. Kang, H. Okada, L. Honig, J.P. Vonsattel, and T.W. Kim. 2005. Model-guided microarray implicates the retromer complex in Alzheimer's disease. *Annals of neurology*. 58:909-919.
- Smith, L.D., E.S. Hickman, R.V. Parry, J. Westwick, and S.G. Ward. 2007. PI3Kgamma is the dominant isoform involved in migratory responses of human T lymphocytes: effects of ex vivo maintenance and limitations of non-viral delivery of siRNA. *Cellular signalling*. 19:2528-2539.
- Soccio, R.E., and J.L. Breslow. 2004. Intracellular cholesterol transport. *Arteriosclerosis, thrombosis, and vascular biology*. 24:1150-1160.
- Sou, Y.S., S. Waguri, J. Iwata, T. Ueno, T. Fujimura, T. Hara, N. Sawada, A. Yamada, N. Mizushima, Y. Uchiyama, E. Kominami, K. Tanaka, and M. Komatsu. 2008. The Atg8 conjugation system is indispensable for proper development of autophagic isolation membranes in mice. *Mol Biol Cell*. 19:4762-4775.
- Srivastava, S., L. Di, O. Zhdanova, Z. Li, S. Vardhana, Q. Wan, Y. Yan, R. Varma, J. Backer, H. Wulff, M.L. Dustin, and E.Y. Skolnik. 2009. The class II phosphatidylinositol 3 kinase C2beta is required for the activation of the K+ channel KCa3.1 and CD4 T-cells. *Mol Biol Cell*. 20:3783-3791.
- Stack, J.H., D.B. DeWald, K. Takegawa, and S.D. Emr. 1995. Vesicle-mediated protein transport: regulatory interactions between the Vps15 protein kinase and the Vps34 PtdIns 3-kinase essential for protein sorting to the vacuole in yeast. *J Cell Biol*. 129:321-334.
- Stack, J.H., and S.D. Emr. 1994. Vps34p required for yeast vacuolar protein sorting is a multiple specificity kinase that exhibits both protein kinase and phosphatidylinositol-specific PI 3-kinase activities. *J Biol Chem*. 269:31552-31562.
- Stack, J.H., P.K. Herman, P.V. Schu, and S.D. Emr. 1993. A membrane-associated complex containing the Vps15 protein kinase and the Vps34 PI 3-kinase is essential for protein sorting to the yeast lysosome-like vacuole. *Embo J*. 12:2195-2204.
- Stahelin, R.V., D. Karathanassis, K.S. Bruzik, M.D. Waterfield, J. Bravo, R.L. Williams, and W. Cho. 2006. Structural and membrane binding analysis of the Phox homology domain of phosphoinositide 3-kinase-C2alpha. *J Biol Chem*. 281:39396-39406.
- Stefkova, J., R. Poledne, and J.A. Hubacek. 2004. ATP-binding cassette (ABC) transporters in human metabolism and diseases. *Physiological research / Academia Scientiarum Bohemoslovaca*. 53:235-243.
- Stein, M.P., Y. Feng, K.L. Cooper, A.M. Welford, and A. Wandinger-Ness. 2003. Human VPS34 and p150 are Rab7 interacting partners. *Traffic*. 4:754-771.
- Stenmark, H., and R. Aasland. 1999. FYVE-finger proteins--effectors of an inositol lipid. *J Cell Sci*. 112 (Pt 23):4175-4183.
- Stenmark, H., R. Aasland, B.H. Toh, and A. D'Arrigo. 1996. Endosomal localization of the autoantigen EEA1 is mediated by a zinc-binding FYVE finger. *J Biol Chem*. 271:24048-24054.
- Stocker, H., T. Radimerski, B. Schindelholz, F. Wittwer, P. Belawat, P. Daram, S. Breuer, G. Thomas, and E. Hafen. 2003. Rheb is an essential regulator of S6K in controlling cell growth in Drosophila. *Nat Cell Biol*. 5:559-565.

- Stromhaug, P.E., T.O. Berg, M. Fengsrud, and P.O. Seglen. 1998. Purification and characterization of autophagosomes from rat hepatocytes. *Biochem J.* 335 (Pt 2):217-224.
- Stromhaug, P.E., F. Reggiori, J. Guan, C.W. Wang, and D.J. Klionsky. 2004. Atg21 is a phosphoinositide binding protein required for efficient lipidation and localization of Atg8 during uptake of aminopeptidase I by selective autophagy. *Mol Biol Cell.* 15:3553-3566.
- Sun, Q., W. Fan, K. Chen, X. Ding, S. Chen, and Q. Zhong. 2008. Identification of Barkor as a mammalian autophagy-specific factor for Beclin 1 and class III phosphatidylinositol 3-kinase. *Proc Natl Acad Sci U S A.* 105:19211-19216.
- Sun, Q., W. Westphal, K.N. Wong, I. Tan, and Q. Zhong. 2010. Rubicon controls endosome maturation as a Rab7 effector. *Proc Natl Acad Sci U S A.* 107:19338-19343.
- Suzuki, K., T. Kirisako, Y. Kamada, N. Mizushima, T. Noda, and Y. Ohsumi. 2001. The pre-autophagosomal structure organized by concerted functions of APG genes is essential for autophagosome formation. *Embo J.* 20:5971-5981.
- Suzuki, K., Y. Kubota, T. Sekito, and Y. Ohsumi. 2007. Hierarchy of Atg proteins in pre-autophagosomal structure organization. *Genes Cells.* 12:209-218.
- Suzuki, K., and R.D. Terry. 1967. Fine structural localization of acid phosphatase in senile plaques in Alzheimer's presenile dementia. *Acta neuropathologica.* 8:276-284.
- Tabas, I. 2002. Consequences of cellular cholesterol accumulation: basic concepts and physiological implications. *J Clin Invest.* 110:905-911.
- Tabata, K., K. Matsunaga, A. Sakane, T. Sasaki, T. Noda, and T. Yoshimori. 2010. Rubicon and PLEKHM1 negatively regulate the endocytic/autophagic pathway via a novel Rab7-binding domain. *Mol Biol Cell.* 21:4162-4172.
- Taguchi-Atarashi, N., M. Hamasaki, K. Matsunaga, H. Omori, N.T. Ktistakis, T. Yoshimori, and T. Noda. 2010. Modulation of local PtdIns3P levels by the PI phosphatase MTMR3 regulates constitutive autophagy. *Traffic.* 11:468-478.
- Takahashi, Y., D. Coppola, N. Matsushita, H.D. Cuaing, M. Sun, Y. Sato, C. Liang, J.U. Jung, J.Q. Cheng, J.J. Mule, W.J. Pledger, and H.G. Wang. 2007. Bif-1 interacts with Beclin 1 through UVRAG and regulates autophagy and tumorigenesis. *Nature cell biology.* 9:1142-1151.
- Takeshige, K., M. Baba, S. Tsuboi, T. Noda, and Y. Ohsumi. 1992. Autophagy in yeast demonstrated with proteinase-deficient mutants and conditions for its induction. *J Cell Biol.* 119:301-311.
- Tanida, I., T. Ueno, and E. Kominami. 2008. LC3 and Autophagy. *Methods in molecular biology.* 445:77-88.
- Tee, A.R., B.D. Manning, P.P. Roux, L.C. Cantley, and J. Blenis. 2003. Tuberous sclerosis complex gene products, Tuberin and Hamartin, control mTOR signaling by acting as a GTPase-activating protein complex toward Rheb. *Curr Biol.* 13:1259-1268.
- Terry, R.D., N.K. Gonatas, and M. Weiss. 1964. The ultrastructure of the cerebral cortex in Alzheimer's disease. *Transactions of the American Neurological Association.* 89:12.

- Teter, S.A., and D.J. Klionsky. 2000. Transport of proteins to the yeast vacuole: autophagy, cytoplasm-to-vacuole targeting, and role of the vacuole in degradation. *Semin Cell Dev Biol.* 11:173-179.
- Thiam, A.R., R.V. Farese Jr, and T.C. Walther. 2013. The biophysics and cell biology of lipid droplets. *Nat Rev Mol Cell Biol.* 14:775-786.
- Thies, W., and L. Bleiler. 2013. 2013 Alzheimer's disease facts and figures. *Alzheimer's & dementia : the journal of the Alzheimer's Association.* 9:208-245.
- Thompson, L.M., C.T. Aiken, L.S. Kaltenbach, N. Agrawal, K. Illes, A. Khoshnan, M. Martinez-Vincente, M. Arrasate, J.G. O'Rourke, H. Khashwji, T. Lukacsovich, Y.Z. Zhu, A.L. Lau, A. Massey, M.R. Hayden, S.O. Zeitlin, S. Finkbeiner, K.N. Green, F.M. LaFerla, G. Bates, L. Huang, P.H. Patterson, D.C. Lo, A.M. Cuervo, J.L. Marsh, and J.S. Steffan. 2009. IKK phosphorylates Huntingtin and targets it for degradation by the proteasome and lysosome. *J Cell Biol.* 187:1083-1099.
- Thoresen, S.B., N.M. Pedersen, K. Liestol, and H. Stenmark. 2010. A phosphatidylinositol 3-kinase class III sub-complex containing VPS15, VPS34, Beclin 1, UVRAG and BIF-1 regulates cytokinesis and degradative endocytic traffic. *Experimental cell research.* 316:3368-3378.
- Thumm, M., R. Egner, B. Koch, M. Schlumpberger, M. Straub, M. Veenhuis, and D.H. Wolf. 1994. Isolation of autophagocytosis mutants of *Saccharomyces cerevisiae*. *FEBS Lett.* 349:275-280.
- Tian, S., J. Lin, J. Jun Zhou, X. Wang, Y. Li, X. Ren, W. Yu, W. Zhong, J. Xiao, F. Sheng, Y. Chen, C. Jin, S. Li, Z. Zheng, and B. Xia. 2010. Beclin 1-independent autophagy induced by a Bcl-XL/Bcl-2 targeting compound, Z18. *Autophagy.* 6:1032-1041.
- Titorenko, V.I., I. Keizer, W. Harder, and M. Veenhuis. 1995. Isolation and characterization of mutants impaired in the selective degradation of peroxisomes in the yeast *Hansenula polymorpha*. *J Bacteriol.* 177:357-363.
- Tooze, J., M. Hollinshead, T. Ludwig, K. Howell, B. Hoflack, and H. Kern. 1990. In exocrine pancreas, the basolateral endocytic pathway converges with the autophagic pathway immediately after the early endosome. *J Cell Biol.* 111:329-345.
- Tsukada, M., and Y. Ohsumi. 1993. Isolation and characterization of autophagy-defective mutants of *Saccharomyces cerevisiae*. *FEBS Lett.* 333:169-174.
- Ueno, T., D. Munro, and E. Kominami. 1991. Membrane markers of endoplasmic reticulum preserved in autophagic vacuolar membranes isolated from leupeptin-administered rat liver. *J Biol Chem.* 266:18995-18999.
- Urbe, S., I.G. Mills, H. Stenmark, N. Kitamura, and M.J. Clague. 2000. Endosomal localization and receptor dynamics determine tyrosine phosphorylation of hepatocyte growth factor-regulated tyrosine kinase substrate. *Mol Cell Biol.* 20:7685-7692.
- van der Goot, F.G., and J. Gruenberg. 2006. Intra-endosomal membrane traffic. *Trends Cell Biol.* 16:514-521.
- van Meer, G., D.R. Voelker, and G.W. Feigenson. 2008. Membrane lipids: where they are and how they behave. *Nat Rev Mol Cell Biol.* 9:112-124.

- Vanhaesebroeck, B., J. Guillermet-Guibert, M. Graupera, and B. Bilanges. 2010. The emerging mechanisms of isoform-specific PI3K signalling. *Nat Rev Mol Cell Biol.* 11:329-341.
- Vanhaesebroeck, B., S.J. Leever, K. Ahmadi, J. Timms, R. Katso, P.C. Driscoll, R. Woscholski, P.J. Parker, and M.D. Waterfield. 2001. Synthesis and function of 3-phosphorylated inositol lipids. *Annu Rev Biochem.* 70:535-602.
- Vardarajan, B.N., S.Y. Bruesegem, M.E. Harbour, R. Inzelberg, R. Friedland, P. St George-Hyslop, M.N. Seaman, and L.A. Farrer. 2012. Identification of Alzheimer disease-associated variants in genes that regulate retromer function. *Neurobiology of aging.* 33:2231 e2215-2231 e2230.
- Velikkakath, A.K., T. Nishimura, E. Oita, N. Ishihara, and N. Mizushima. 2012. Mammalian Atg2 proteins are essential for autophagosome formation and important for regulation of size and distribution of lipid droplets. *Mol Biol Cell.* 23:896-909.
- Vergne, I., and V. Deretic. 2010. The role of PI3P phosphatases in the regulation of autophagy. *FEBS Lett.* 584:1313-1318.
- Vergne, I., E. Roberts, R.A. Elmaoued, V. Tosch, M.A. Delgado, T. Proikas-Cezanne, J. Laporte, and V. Deretic. 2009. Control of autophagy initiation by phosphoinositide 3-phosphatase Jumpy. *Embo J.* 28:2244-2258.
- Visnjic, D., J. Curic, V. Crljen, D. Batinic, S. Volinia, and H. Banfic. 2003. Nuclear phosphoinositide 3-kinase C2beta activation during G2/M phase of the cell cycle in HL-60 cells. *Biochim Biophys Acta.* 1631:61-71.
- Volinia, S., R. Dhand, B. Vanhaesebroeck, L.K. MacDougall, R. Stein, M.J. Zvelebil, J. Domin, C. Panaretou, and M.D. Waterfield. 1995. A human phosphatidylinositol 3-kinase complex related to the yeast Vps34p-Vps15p protein sorting system. *EMBO J.* 14:3339-3348.
- Walkley, S.U., and M.T. Vanier. 2009. Secondary lipid accumulation in lysosomal disease. *Biochim Biophys Acta.* 1793:726-736.
- Walther, T.C., and R.V. Farese, Jr. 2012. Lipid droplets and cellular lipid metabolism. *Annu Rev Biochem.* 81:687-714.
- Wang, K., Z. Yang, U. Nair, K. Mao, X. Liu, and D.J. Klionsky. 2012. Phosphatidylinositol 4-kinases are required for autophagic membrane trafficking. *J Biol Chem.*
- Wang, Y., K. Yoshioka, M.A. Azam, N. Takuwa, S. Sakurada, Y. Kayaba, N. Sugimoto, I. Inoki, T. Kimura, T. Kuwaki, and Y. Takuwa. 2006. Class II phosphoinositide 3-kinase alpha-isoform regulates Rho, myosin phosphatase and contraction in vascular smooth muscle. *Biochem J.* 394:581-592.
- Wassmer, T., N. Attar, M.V. Bujny, J. Oakley, C.J. Traer, and P.J. Cullen. 2007. A loss-of-function screen reveals SNX5 and SNX6 as potential components of the mammalian retromer. *J Cell Sci.* 120:45-54.
- Wassmer, T., N. Attar, M. Harterink, J.R. van Weering, C.J. Traer, J. Oakley, B. Goud, D.J. Stephens, P. Verkade, H.C. Korswagen, and P.J. Cullen. 2009. The retromer coat complex coordinates endosomal sorting and dynein-mediated transport, with carrier recognition by the trans-Golgi network. *Dev Cell.* 17:110-122.
- Watanabe, Y., T. Kobayashi, H. Yamamoto, H. Hoshida, R. Akada, F. Inagaki, Y. Ohsumi, and N.N. Noda. 2012. Structure-based Analyses Reveal Distinct

- Binding Sites for Atg2 and Phosphoinositides in Atg18. *J Biol Chem.* 287:31681-31690.
- Webber, J.L., and S.A. Tooze. 2010a. Coordinated regulation of autophagy by p38alpha MAPK through mAtg9 and p38IP. *EMBO J.* 29:27-40.
- Webber, J.L., and S.A. Tooze. 2010b. New insights into the function of Atg9. *FEBS Lett.* 584:1319-1326.
- Weidberg, H., E. Shvets, and Z. Elazar. 2011. Biogenesis and cargo selectivity of autophagosomes. *Annu Rev Biochem.* 80:125-156.
- Weidberg, H., E. Shvets, T. Shpilka, F. Shimron, V. Shinder, and Z. Elazar. 2010. LC3 and GATE-16/GABARAP subfamilies are both essential yet act differently in autophagosome biogenesis. *EMBO J.* 29:1792-1802.
- Wen, P.J., S.L. Osborne, I.C. Morrow, R.G. Parton, J. Domin, and F.A. Meunier. 2008. Ca²⁺-regulated pool of phosphatidylinositol-3-phosphate produced by phosphatidylinositol 3-kinase C2alpha on neurosecretory vesicles. *Mol Biol Cell.* 19:5593-5603.
- Wenk, M.R. 2005. The emerging field of lipidomics. *Nat Rev Drug Discov.* 4:594-610.
- Wenk, M.R. 2010. Lipidomics: new tools and applications. *Cell.* 143:888-895.
- Wheeler, M., and J. Domin. 2006. The N-terminus of phosphoinositide 3-kinase-C2beta regulates lipid kinase activity and binding to clathrin. *Journal of cellular physiology.* 206:586-593.
- Wiczner, B.M., and G. Thomas. 2012. Phospholipase D and mTORC1: nutrients are what bring them together. *Sci Signal.* 5:pe13.
- Willinger, T., and R.A. Flavell. 2012. Canonical autophagy dependent on the class III phosphoinositide-3 kinase Vps34 is required for naive T-cell homeostasis. *Proc Natl Acad Sci U S A.* 109:8670-8675.
- Willnow, T.E., and O.M. Andersen. 2013. Sorting receptor SORLA - a trafficking path to avoid Alzheimer disease. *J Cell Sci.* 126:2751-2760.
- Willnow, T.E., C.M. Petersen, and A. Nykjaer. 2008. VPS10P-domain receptors - regulators of neuronal viability and function. *Nature reviews. Neuroscience.* 9:899-909.
- Wing, S.S., H.L. Chiang, A.L. Goldberg, and J.F. Dice. 1991. Proteins containing peptide sequences related to Lys-Phe-Glu-Arg-Gln are selectively depleted in liver and heart, but not skeletal muscle, of fasted rats. *Biochem J.* 275 (Pt 1):165-169.
- Wong, E., and A.M. Cuervo. 2010. Autophagy gone awry in neurodegenerative diseases. *Nat Neurosci.* 13:805-811.
- Worby, C.A., and J.E. Dixon. 2002. Sorting out the cellular functions of sorting nexins. *Nat Rev Mol Cell Biol.* 3:919-931.
- Xie, Z., and D.J. Klionsky. 2007. Autophagosome formation: core machinery and adaptations. *Nat Cell Biol.* 9:1102-1109.
- Xie, Z., U. Nair, and D.J. Klionsky. 2008. Atg8 controls phagophore expansion during autophagosome formation. *Mol Biol Cell.* 19:3290-3298.
- Xu, L., D. Salloum, P.S. Medlin, M. Saqcena, P. Yellen, B. Perrella, and D.A. Foster. 2011. Phospholipase D mediates nutrient input to mammalian target of rapamycin complex 1 (mTORC1). *J Biol Chem.* 286:25477-25486.

- Xu, Z., W. Farver, S. Kodukula, and J. Storch. 2008. Regulation of sterol transport between membranes and NPC2. *Biochemistry*. 47:11134-11143.
- Yamamoto, A., M.L. Cremona, and J.E. Rothman. 2006. Autophagy-mediated clearance of huntingtin aggregates triggered by the insulin-signaling pathway. *J Cell Biol*. 172:719-731.
- Yamamoto, A., Y. Tagawa, T. Yoshimori, Y. Moriyama, R. Masaki, and Y. Tashiro. 1998. Bafilomycin A1 prevents maturation of autophagic vacuoles by inhibiting fusion between autophagosomes and lysosomes in rat hepatoma cell line, H-4-II-E cells. *Cell Struct Funct*. 23:33-42.
- Yamamoto, H., S. Kakuta, T.M. Watanabe, A. Kitamura, T. Sekito, C. Kondo-Kakuta, R. Ichikawa, M. Kinjo, and Y. Ohsumi. 2012. Atg9 vesicles are an important membrane source during early steps of autophagosome formation. *J Cell Biol*. 198:219-233.
- Yan, Y., and J.M. Backer. 2007. Regulation of class III (Vps34) PI3Ks. *Biochem Soc Trans*. 35:239-241.
- Yang, H. 2006. Nonvesicular sterol transport: two protein families and a sterol sensor? *Trends Cell Biol*. 16:427-432.
- Yang, Z., and D.J. Klionsky. 2010. Eaten alive: a history of macroautophagy. *Nature cell biology*. 12:814-822.
- Yetukuri, L., K. Ekroos, A. Vidal-Puig, and M. Oresic. 2008. Informatics and computational strategies for the study of lipids. *Molecular bioSystems*. 4:121-127.
- Yla-Anttila, P., H. Vihinen, E. Jokitalo, and E.L. Eskelinen. 2009. 3D tomography reveals connections between the phagophore and endoplasmic reticulum. *Autophagy*. 5:1180-1185.
- Yoon, M.S., G. Du, J.M. Backer, M.A. Frohman, and J. Chen. 2011. Class III PI-3-kinase activates phospholipase D in an amino acid-sensing mTORC1 pathway. *J Cell Biol*. 195:435-447.
- Yoshioka, K., N. Sugimoto, N. Takuwa, and Y. Takuwa. 2007. Essential role for class II phosphoinositide 3-kinase alpha-isoform in Ca²⁺-induced, Rho- and Rho kinase-dependent regulation of myosin phosphatase and contraction in isolated vascular smooth muscle cells. *Molecular pharmacology*. 71:912-920.
- Yoshioka, K., K. Yoshida, H. Cui, T. Wakayama, N. Takuwa, Y. Okamoto, W. Du, X. Qi, K. Asanuma, K. Sugihara, S. Aki, H. Miyazawa, K. Biswas, C. Nagakura, M. Ueno, S. Iseki, R.J. Schwartz, H. Okamoto, T. Sasaki, O. Matsui, M. Asano, R.H. Adams, N. Takakura, and Y. Takuwa. 2012. Endothelial PI3K-C2alpha, a class II PI3K, has an essential role in angiogenesis and vascular barrier function. *Nature medicine*. 18:1560-1569.
- Young, A.R., E.Y. Chan, X.W. Hu, R. Kochl, S.G. Crawshaw, S. High, D.W. Hailey, J. Lippincott-Schwartz, and S.A. Tooze. 2006. Starvation and ULK1-dependent cycling of mammalian Atg9 between the TGN and endosomes. *J Cell Sci*. 119:3888-3900.
- Yu, L., C.K. McPhee, L. Zheng, G.A. Mardones, Y. Rong, J. Peng, N. Mi, Y. Zhao, Z. Liu, F. Wan, D.W. Hailey, V. Oorschot, J. Klumperman, E.H. Baehrecke, and M.J. Lenardo. 2010. Termination of autophagy and reformation of lysosomes regulated by mTOR. *Nature*. 465:942-946.

- Yu, W.H., A.M. Cuervo, A. Kumar, C.M. Peterhoff, S.D. Schmidt, J.H. Lee, P.S. Mohan, M. Mercken, M.R. Farmery, L.O. Tjernberg, Y. Jiang, K. Duff, Y. Uchiyama, J. Naslund, P.M. Mathews, A.M. Cataldo, and R.A. Nixon. 2005. Macroautophagy—a novel Beta-amyloid peptide-generating pathway activated in Alzheimer's disease. *J Cell Biol.* 171:87-98.
- Zavodszky, E., M. Vicinanza, and D.C. Rubinsztein. 2013. Biology and trafficking of ATG9 and ATG16L1, two proteins that regulate autophagosome formation. *FEBS Lett.* 587:1988-1996.
- Zeng, X., J.H. Overmeyer, and W.A. Maltese. 2006. Functional specificity of the mammalian Beclin-Vps34 PI 3-kinase complex in macroautophagy versus endocytosis and lysosomal enzyme trafficking. *J Cell Sci.* 119:259-270.
- Zervas, M., K. Dobrenis, and S.U. Walkley. 2001. Neurons in Niemann-Pick disease type C accumulate gangliosides as well as unesterified cholesterol and undergo dendritic and axonal alterations. *J Neuropathol Exp Neurol.* 60:49-64.
- Zhang, Y., X. Gao, L.J. Saucedo, B. Ru, B.A. Edgar, and D. Pan. 2003a. Rheb is a direct target of the tuberous sclerosis tumour suppressor proteins. *Nat Cell Biol.* 5:578-581.
- Zhang, Y., C. Yu, J. Liu, T.A. Spencer, C.C. Chang, and T.Y. Chang. 2003b. Cholesterol is superior to 7-ketocholesterol or 7 alpha-hydroxycholesterol as an allosteric activator for acyl-coenzyme A:cholesterol acyltransferase 1. *J Biol Chem.* 278:11642-11647.
- Zhong, Y., Q.J. Wang, X. Li, Y. Yan, J.M. Backer, B.T. Chait, N. Heintz, and Z. Yue. 2009. Distinct regulation of autophagic activity by Atg14L and Rubicon associated with Beclin 1-phosphatidylinositol-3-kinase complex. *Nature cell biology.* 11:468-476.
- Zhou, X., L. Wang, H. Hasegawa, P. Amin, B.X. Han, S. Kaneko, Y. He, and F. Wang. 2010. Deletion of PIK3C3/Vps34 in sensory neurons causes rapid neurodegeneration by disrupting the endosomal but not the autophagic pathway. *Proc Natl Acad Sci U S A.* 107:9424-9429.
- Zhu, J.H., C. Horbinski, F. Guo, S. Watkins, Y. Uchiyama, and C.T. Chu. 2007. Regulation of autophagy by extracellular signal-regulated protein kinases during 1-methyl-4-phenylpyridinium-induced cell death. *Am J Pathol.* 170:75-86.
- Zoncu, R., A. Efeyan, and D.M. Sabatini. 2011. mTOR: from growth signal integration to cancer, diabetes and ageing. *Nat Rev Mol Cell Biol.* 12:21-35.